STATISTICAL NONRECURSIVE SPATIAL-TEMPORAL FOCAL PLANE PROCESSING FOR BACKGROUND CLUTTER SUPPRESSION AND TARGET DETECTION.

Baruch Even-or

NAVAL POSTGRADUATE SCHOOL
Monterey, California

THESIS

STATISTICAL NONRECURSIVE SPATIAL-TEMPORAL FOCAL PLANE PROCESSING FOR BACKGROUND CLUTTER SUPPRESSION AND TARGET DETECTION

by

Baruch Even-or

March 1979

Thesis Advisor: T. F. Tao

Approved for public release; distribution unlimited.

T18958

UNCLASSIFIED

SECURITY CLASSIFICATION OF THIS PAGE (When Data Entered)

REPORT DOCUMENTATION PAGE		READ INSTRUCTIONS BEFORE COMPLETING FORM
1. REPORT NUMBER	2. GOVT ACCESSION NO.	3. RECIPIENT'S CATALOG NUMBER
4. TITLE (and Subtitle) Statistical Nonrecursive Spatial-Temporal Focal Plane Processing for Background Clutter Suppression and Target Detection		5. TYPE OF REPORT & PERIOD COVERED Ph.D. Thesis; March 1979 6. PERFORMING ORG. REPORT NUMBER
7. AUTHOR(s) Baruch Even-or		8. CONTRACT OR GRANT NUMBER(s)
9. PERFORMING ORGANIZATION NAME AND ADDRESS Naval Postgraduate School Monterey, California 93940		10. PROGRAM ELEMENT, PROJECT, TASK AREA & WORK UNIT NUMBERS
11. CONTROLLING OFFICE NAME AND ADDRESS Naval Postgraduate School Monterey, California 93940		12. REPORT DATE March 1979 13. NUMBER OF PAGES
14. MONITORING AGENCY NAME & ADDRESS(if different from Controlling Office) Naval Postgraduate School Monterey, California 93940		15. SECURITY CLASS. (of this report) Unclassified 15a. DECLASSIFICATION/ DOWNGRADING SCHEDULE

16. DISTRIBUTION STATEMENT (of this Report)

Approved for public release; distribution unlimited.

17. DISTRIBUTION STATEMENT (of the abstract entered in Block 20, if different from Report)

18. SUPPLEMENTARY NOTES

19. KEY WORDS (Continue on reverse side if necessary and identify by block number)

Statistical nonrecursive spatial-temporal filtering
Focal plane processing

20. ABSTRACT (Continue on reverse side if necessary and identify by block number)

Advanced surveillance and weapon guidance systems using new mosaic sensor arrays and large scale integration (LSI) electronic data processors on the same focal plane require detection of weak targets deeply buried in background clutter noise by many tens of db's. This investigation reports on the focal plane processing techniques to accomplish these heretofore unachievable goals.

Five focal plane processing algorithms are developed consisting

DD FORM 1 JAN 73 1473 EDITION OF 1 NOV 65 IS OBSOLETE
S/N 0102-014-6601

UNCLASSIFIED

SECURITY CLASSIFICATION OF THIS PAGE (When Data Entered)

of nonrecursive statistical spatial-temporal filters for clutter suppression followed by thresholding for initialization of target detection. These filters are based on either the minimization of mean square error criterion (for MMSE filters) or the maximization of signal to noise ratio criterion (for matched filters). Two are nonadaptive spatial filters and two are nonadaptive spatial-temporal filters. The fifth type is an adaptive spatial filter based on the minimization of mean square error criterion.

These filters have been investigated analytically and by computer simulation using computer generated images containing correlated clutter noises modeled by Markov processes and also real world infrared images. Using an infrared image in the red spike spectral band, a single frame statistical spatial filter can suppress the clutter by 27 db. A five frame sequential statistical spatial-temporal filter was found to have a clutter suppression of 87 db.

Approved for public release; distribution unlimited

Statistical Nonrecursive Spatial-Temporal Focal Plane Processing for Background Clutter Suppression and Target Detection

by

Baruch Even-or
Lieutenant Commander, Israeli Navy
B.S., Technion Israel Institute of Technology, 1969
M.S., Naval Postgraduate School, 1977

Submitted in partial fulfillment of the
requirements for the degree of

DOCTOR OF PHILOSOPHY

from the

NAVAL POSTGRADUATE SCHOOL
March 1979

ABSTRACT

Advanced surveillance and weapon guidance systems using new mosaic sensor arrays and large scale integration (LSI) electronic data processors on the same focal plane require detection of weak targets deeply buried in background clutter noise by many tens of db's. This investigation reports on the focal plane processing techniques to accomplish these heretofore unachievable goals.

Five focal plane processing algorithms are developed consisting of nonrecursive statistical spatial-temporal filters for clutter suppression followed by thresholding for initialization of target detection. These filters are based on either the minimization of mean square error criterion (for MMSE filters) or the maximization of signal to noise ratio criterion (for matched filters). Two are nonadaptive spatial filters and two are nonadaptive spatial-temporal filters. The fifth type is an adaptive spatial filter based on the minimization of mean square error criterion.

These filters have been investigated analytically and by computer simulation using computer generated images containing correlated clutter noises modeled by Markov processes and also real world infrared images. Using an infrared image in the red spike spectral band, a single frame statistical spatial filter can suppress the clutter by 27 db. A five frame sequential statistical spatial-temporal filter was found to have a clutter suppression of 87 db.

TABLE OF CONTENTS

I. INTRODUCTION---------- 9

A. MOSAIC FOCAL PLANE AND SMART SENSOR DEVELOPMENTS---------- 9

B. REQUIREMENTS OF NEW FOCAL PLANE PROCESSING------ 10

C. FOCAL PLANE PROCESSING TECHNIQUES FOR BACK-GROUND CLUTTER SUPPRESSION AND TARGET DETECTION- 12

D. FOCAL PLANE PROCESSING TECHNIQUES DEVELOPED IN THIS THESIS---------- 16

II. BASIC CONCEPT AND PROCEDURES OF NONRECURSIVE STATISTICAL FOCAL PLANE PROCESSING---------- 23

A. INTRODUCTION---------- 23

B. BASIC CONCEPT OF NONRECURSIVE STATISTICAL FILTERS FOR CLUTTER SUPPRESSION---------- 24

C. CONFIGURATION OF NONRECURSIVE FILTERS---------- 26

D. PRINCIPLE OF STATISTICAL FILTER DESIGN---------- 33

E. IMAGES USED IN ANALYZING AND TESTING OF THE STATISTICAL FOCAL PLANE PROCESSING---------- 34

III. SINGLE FRAME FOCAL PLANE PROCESSING FOR CLUTTER SUPPRESSION - NONRECURSIVE STATISTICAL SPATIAL FILTERS---------- 37

A. INTRODUCTION---------- 37

B. CONFIGURATION OF TWO DIMENSIONAL NONRECURSIVE SPATIAL FILTERS---------- 38

C. NONRECURSIVE SPATIAL MMSE FILTER---------- 42

D. NONRECURSIVE SPATIAL MATCHED FILTERS---------- 57

E. SUMMARY---------- 66

IV. MULTIPLE FRAMES FOCAL PLANE PROCESSING FOR CLUTTER SUPPRESSION - NONRECURSIVE STATISTICAL TEMPORAL FILTER AND SPATIAL-TEMPORAL FILTERS-------- 67

A. INTRODUCTION---------- 67

B. NONSTATISTICAL TEMPORAL FILTERS - FRAME DIFFERENCING---------- 69

C. STATISTICAL SEQUENTIAL SPATIAL-TEMPORAL FILTERS---------- 74

D. AN EFFECTIVE WAY OF HARDWARE IMPLEMENTATION OF SEQUENTIAL SPATIAL-TEMPORAL FILTER---------- 88

E. COMPUTER SIMULATION PROCEDURE FOR EVALUATING SEQUENTIAL SPATIAL-TEMPORAL FILTERS---------- 89

F. SUMMARY---------- 92

V. TARGET DETECTION IN FOCAL PLANE PROCESSING---------- 93

A. INTRODUCTION---------- 93

B. PREDETECTION FOCAL PLANE PROCESSING FOR CLUTTER SUPPRESSION---------- 94

C. TARGET DETECTION IN FOCAL PLANE PROCESSING------ 99

D. SUMMARY----------110

VI. PROPERTIES AND PERFORMANCE OF NONADAPTIVE STATISTICAL FOCAL PLANE PROCESSING - NON-RECURSIVE FILTERS FOR CLUTTER SUPPRESSION FOLLOWED BY THRESHOLDING FOR TARGET DETECTION-------111

A. INTRODUCTION----------111

B. ORGANIZATION OF COMPUTER SIMULATED STUDIES------112

C. SINGLE FRAME PROCESSING I - NONRECURSIVE SPATIAL MMSE FILTER FOLLOWED BY THRESHOLDING----116

D. MATCHED FRAME PROCESSING II - NONRECURSIVE SPATIAL MATCHED FILTER FOLLOWED BY THRESHOLDING----------128

E. SUBOPTIMAL SPATIAL FILTERS----------138

F. MULTIPLE FRAME PROCESSING - NONRECURSIVE SEQUENTIAL SPATIAL-TEMPORAL FILTER FOLLOWED BY THRESHOLDING----------142

VII. ADAPTIVE SPATIAL FILTER I - STATIONARY CLUTTER STATISTICS----------154

A. INTRODUCTION----------154

B. ADAPTIVE WIENER FILTER----------154

C. ADAPTIVE ALGORITHM BASED ON STEEPEST DESCENT----156

D. TWO DIMENSIONAL ADAPTIVE FILTERING CONSIDERATIONS----------160

E. COMPUTER SIMULATION RESULTS----------181

F. SUMMARY----------196

VIII. ADAPTIVE SPATIAL FILTER II - NONSTATIONARY CLUTTER STATISTICS----------198

A. INTRODUCTION----------198

B. THEORETICAL DEVELOPMENT AND PRACTICAL CONSIDERATIONS----------198

C. COMPUTER SIMULATION RESULTS----------200

D. SUMMARY----------233

IX. SUMMARY AND CONCLUSIONS----------234

A. SUMMARY----------234

B. CONCLUSION----------238

APPENDIX A: GENERATION (MODELING) OF TWO-DIMENSIONAL RANDOM FIELDS----------241

APPENDIX B: BAYES CRITERION----------256

APPENDIX C: DERIVATION OF ADAPTIVE FILTER ALGORITHM-------264

BIBLIOGRAPHY----------282

INITIAL DISTRIBUTION LIST----------285

ACKNOWLEDGEMENTS

The author expresses his deep appreciation to Dr. T. F. Tao for his guidance in this study and his aid in the clear presentation of the study concepts.

The author also expresses his gratitude to the Ph.D. Committee members for their assistance in accomplishing this study and the degree requirements.

I. INTRODUCTION

A. MOSAIC FOCAL PLANE AND SMART SENSOR DEVELOPMENTS

The enormous impact of integrated circuit technologies on baseband electronics is well known. Revolutionary advances of LSI (large scale integration) and VLSI (very large scale integration) devices are making high performance computer and signal processing capabilities available at lower cost with lighter weight, less power consumption and higher reliability. Their impact on military systems will be tremendous and far-reaching.

In recent years, IC technologies have also been making important changes in high frequency electronics throughout the microwave and optical bands. In optical detection technologies, thousands and hundreds of thousands of optical and infrared detectors can be made in the not too distant future on one chip by IC batch processing in the form of what is generally known as "mosaic detector array" or "mosaic focal plane array" [1]. The availability of such a large number of detectors on the same focal plane has inspired new modes of optical detection, such as the time-delayed-integration scanning [2], staring [3], and step-staring [3] modes which offer better detection performance. Combined with LSI computers or signal processors on the same focal plane, complex tasks can now be carried out at or near the focal plane by

what are called "smart sensors."[1] This equipment is intelligent, small, light, comsumes little power and is not expensive. It is certain that these smart sensors are going to make significant improvements to many surveillance, reconnaissance and guidance systems.

This thesis deals with an image processing, or more specifically, a "focal plane processing" problem which is created by these new "mosaic focal plane" and "smart sensor" developments. It will be explained in the next section.

B. REQUIREMENTS OF NEW FOCAL PLANE PROCESSING

With the new-found computing and signal processing capabilities which will be mounted next to the detector array in the near future, very ambitious focal plane processing objectives have been formulated. In front of the mosaic detector array, computer controlled adaptive optics and programmable optical filters are being developed. On the mosaic detector focal plane, sophisticated "on chip" signal processing operations such as time-delayed integration [2], a.c. coupling [4], differentiation [5], multiplexing [6], convolutional read-out and others are being investigated. After, or during, the read-out, image processing operations of sampled analog signals can be carried out. If digital focal plane processing is used, signal formating, sample and hold and analog to digital conversion must be performed.

---

[1] "Smart sensors" session in SPIE 1979 East Symposium to be held in Washington, D.C. April 17-18, 1979.

For military applications of surveillance, reconnaissance and guidance, focal plane processing objectives include the basic signal manipulations described above and other predetection steps, such as background clutter suppression, target enhancement and thresholding for initialization of target detection. Following this, there are many post-thresholding focal plane processing steps such as target linking, tracking, track assembly, track association, trajectory estimation, target discrimination, target recognition, and many others. This thesis is concerned with the predetection steps of background clutter suppression and thresholding for initialization of target detection.

In visible imaging systems, the contrast between targets and background is usually high. The target signal to noise ratio is often quite adequate. Therefore, focal plane processing operations of visible images can directly deal with target signals and background noise in most cases without any preprocessing to improve the signal to noise ratio. However, in infrared imaging systems, the contrasts between targets and backgrounds are much smaller. Target signals are often a very small fraction of the incoming signal which consists of a large amount of background clutter noise and other white noise. All infrared imaging systems must deal with the clutter problem. The need of suppressing background clutter and detecting targets buried in clutter certainly is not unique in these new mosaic focal plane arrays. However, the

requirements of clutter suppression and target detection are now much more demanding because of the improved performance of mosaic focal plane sensors processors and much more ambitious system goals. In new surveillance and guidance systems, it is sometimes required to detect weak targets deeply buried in clutter by many ten's of db's. Old processing techniques used to separate targets from clutter are simply not adequate to meet these requirements. New processing techniques using spatial, temporal and spectral characteristics of both the targets and clutter must be developed. These techniques are different from most of the well known image processing techniques in two major aspects:

- They deal with image signals of very low signal to noise ratio. Furthermore, the dominant noise component is due to clutter and is correlated rather than white.
- The signals of interest are usually point targets, line targets and targets of different shapes instead of pictorial details of the image.

Therefore, they are called "focal plane processing" in this thesis instead of the widely used name of "image processing" which usually concerns pictures, photographs, TV pictures, etc.

C. FOCAL PLANE PROCESSING TECHNIQUES FOR BACKGROUND CLUTTER SUPPRESSION AND TARGET DETECTION

Clutter suppression and target detection are not unique problems for mosaic focal plane processing. Similar types

of problems exist in radar and sonar processing and have been extensively investigated [7,8]. Effective processing algorithms for clutter suppression and thresholding for target detection have been well developed. However, there are significant differences between mosaic focal plane systems and radar and sonar systems so that most of the developed processing algorithms either are not applicable or must be modified if they are to be used for imaging systems. The major differences are the following:

1. Imaging systems are mostly passive. Therefore, processing algorithms based on Doppler shift or the signal waveform cannot be applied to passive optical systems.

2. Image signals are three dimensional, which includes two dimensional spatial variations on a single image frame and one dimensional temporal variations on several frames of images. Radar and sonar signals are mostly one dimensional with temporal variations. Therefore, radar and sonar processing algorithms must be modified if they are applicable to mosaic focal plane problems.

In spite of these differences, the concepts of most signal processing approaches can be applied to the new problems. In the following, several processing approaches for target enhancement and detection are listed.

When signal to noise ratio is above unity, thresholding can be applied to separate true targets from background noise. The threshold level can be determined from several different

considerations; for example, based on a constant false alarm rate (CFAR), or on a given probability of detection, or on a given probability of tracking, etc.

If the signal to noise ratio is low, as in many practical situations, prethresholding signal processing steps must be employed to suppress the noise and enhance the target, if possible, so that the signal to noise ratio will be adequate for thresholding. Some of these processing approaches are based on the following concepts:

- Summing - Time integration
- Differencing - pulse canceller
- Filtering:
  - Based on time domain knowledge - correlator
  - Based on frequency domain knowledge - frequency domain filter

Other approaches are statistical, based on the following procedures:

- Statistical processing:
  - Maximization of signal to noise ratio - statistical matched filter
  - Minimization of mean square error
    - Kalman filter
    - Wiener filter, MMSE filter
  - Maximization of likelihood filter

The principles of some of these signal processing approaches have been extended and applied to the focal plane processing

problems by other investigators for background clutter suppression. Some are deterministic processing, based on the following concepts:

Deterministically Designed Focal Plane Processing:

Single frame processing - Spatial filters:

Masking - First order, Second order (Laplacian), Fourth order [9]

Summing - Time-delayed integration [2]

Multiple frame processing - Temporal filters:

Summing - Multiple frame integration

Differencing - Frame to frame differencing, Non-recursive Second differencing, Third differencing, etc. [10]

Filtering - Recursive digital high pass filters based on the knowledge of frequency characteristics of the clutter [11] Active band pass filters.

Several statistically designed processing approaches have also been investigated.

Statistically Designed Focal Plane Processing:

Single frame processing:

Spatial Kalman filter [12,13]

Spatial MMSE filter [14]

Multiple frame processing - Temporal filter

Maximum likelihood filter [15]

Although quite a few processing algorithms are listed above, only the deterministic single frame spatial filters and the multiple frame differencing filters have been substantially developed. All other processing approaches have only received preliminary investigation. None of these filters have shown

enough clutter suppression capabilities to enable detection of weak targets more than 70 db below clutter.

D. FOCAL PLANE PROCESSING TECHNIQUES DEVELOPED IN THIS THESIS

The objective of this thesis investigation was to develop statistical processing algorithms for background clutter suppression. This is accomplished in several phases. First, design procedures are developed for two types of nonrecursive spatial filters. These concepts are then extended to three dimensions by adding a temporal filter. Several aspects of target detection are also addressed, with special consideration given to cases involving non-Gaussian probability densities. Adaptive filter algorithms are also developed for situations involving unknown and non-stationary statistics of background clutter noise. Analytical results and computer simulation studies demonstrate the feasibility of the filter algorithms proposed. The following paragraphs describe in more detail the development of the processing techniques.

In Chapter II the basic structure of nonrecursive spatial and/or temporal filters is introduced. The spatial filters, which may be adaptive, utilize image signals in the neighborhood of the "estimation pixel" to suppress clutter and enhance target intensity at the estimation pixel. Further improvement is obtained by also processing spatially filtered data from adjacent image frames.

Expressions for the filter coefficients are derived in Chapter III for two criteria which have been previously used in one-dimensional statistical processing filters [16]: minimization of mean square error (MMSE) and maximization of output signal to noise ratio (matched filter). Statistical nonrecursive spatial filters based on the MMSE criterion have been studied before for image restoration and for improvement of signal to noise ratio against white noise [23-25]. The design of these filters, however, is carried out using spatial frequency domain techniques, or equivalent. Such filters have not been very useful in practical applications because of the large size, e.g., larger than 10 x 10, required to achieve meaningful improvement [25]. Furthermore, a nonrecursive spatial filter tends to blur the edges of an object [17]. The concept of using nonrecursive statistical spatial filters for suppression of correlated noise was originated by Bar Yehoshua [14] who developed a design procedure in the spatial domain using the MMSE criterion. Bar Yehoshua developed the special application of statistical nonrecursive spatial filters for enhancement of point/line target signal to noise ratio in the presence of spatially correlated noise. He showed that spatial filters as small as 3 x 3 pixels are effective in the suppression of spatially correlated noise. Furthermore, his design procedure in the spatial domain is well suited for hardware implementation because the rather complex two dimensional transformation operations required in spatial frequency

domain design procedures are unnecessary. Chapter III reviews Bar Yehoshua's work and extends the concept to nonrecursive spatial matched filters. Other related work is contained in [17]. The matched filter for the enhancement of point and line targets described here is applicable to correlated, as well as white, noise. In addition, a new explicit design procedure is presented. This thesis extends Bar Yehoshua's concept in three directions. In this chapter, a different design criterion based on the maximization of signal to noise ratio is developed for the second type of nonrecursive spatial filter--matched filter. Again, spatial matched filters are not new [17,18]. The contribution of this study is in the development of its new application to the enhancement of point/line target to noise ratio in two dimensional and three dimensional images of very low signal to noise ratio, and in the design procedure in spatial and temporal domains instead of the spatial frequency and temporal frequency used by most other workers. Extensions in two other directions will be described in Chapter IV and Chapter VII.

In Chapter IV, two nonadaptive multiple frame processing approaches for clutter suppression are developed. They are the nonrecursive sequential spatial-temporal filters designed again by two statistical criteria similar to those in Chapter III which lead to the spatial-temporal MMSE filters and the spatial-temporal matched filters. Temporal filters which use several frames of image designed by either deterministic

or statistical information are not new [17]. However, the combinations of spatial and temporal filters using statistical information of several frames of image for achieving substantial enhancement of signal to noise ratio has not been reported before. This thesis investigates a special type of multiple frame processing consisting of sequential application of a spatial filter followed by a temporal filter using several frames. It is shown analytically that the clutter suppression of the spatial filter and of the temporal filter are multiplicative (or additive, if they are expressed in terms of db).

In Chapter V, the thresholding problem for initialization of target detection is investigated. The concept of thresholding for detection has been well developed for radar systems [8]. The extension of the thresholding operation to two dimensional problems has not been extensively investigated for cases where the probability density functions are not Gaussian. In this chapter, a procedure for setting the threshold based on the assumption of a Gaussian distribution is applied to computer generated images whose probability density functions are Gaussian. In addition, a new procedure for setting threshold level based on a constant false alarm rate criterion without the assumption of a Gaussian probability density function is also developed.

In Chapter VI, the four nonadaptive statistical filters developed for clutter suppression are combined with thresholding as the nonadaptive focal plane processing algorithm studied in this thesis. Their properties and performance are quantitatively studied by computer simulation using two types of images. The first type consists of computer generated images which contain targets and two random noise components. One noise component is uncorrelated, or "white" Gaussian noise. The other noise component is correlated, or "colored" noise modeled by two Markov processes--first order and second order [14,19]. These correlated noises are used to simulate background clutter. In these computer generated images, the statistical properties of the correlated noise are known "a priori." The second type of image is a set of twenty frames of real world infrared images. Here, correlated noise in both spatial and temporal domains is not known "a priori." Practical filter design procedures are developed which first "learn" the statistics from the real world image, then design a filter using the techniques developed in Chapters III and IV. Using single frames of these real world images, clutter suppression of up to 27 db has been achieved by spatial filtering alone. Using five frames, clutter suppression of up to 87 db has been achieved by sequential spatial-temporal filters. These large clutter suppression values based on computer simulated tests on real world infrared images are

the most important testimony of the practical usefulness of the statistical focal plane processing algorithms developed in this thesis.

In Chapters VII and VIII, adaptive design procedures are developed to further extend the concept of clutter suppression using the nonrecursive spatial filter. No "a priori" knowledge of the statistical properties of the clutter is needed to design the filter. The adaptive procedure automatically corrects the filter coefficients iteratively toward the optimal values to yield the minimum error between the target estimate and a selected desired response. The concept of one dimensional adaptive filters based on the least mean square error criterion has been very well developed by Widrow, McCool, et al. [20-22]. This thesis extends the basic concept to two dimensions and also develops the following new techniques to improve the performance of the adaptive spatial filter:

1. Derivation of desired responses corresponding to various types of targets of interest.

2. An "automatic gain control" procedure which yields constant misadjustment for varying statistical properties of the clutter, prevents overflow and assures adaptive convergence.

3. Dividing an image into small subimage zones to carry out filter adaptations if the statistical properties of the image are both "nonstationary" and unknown a priori.

Simulation results are given in both Chapters VII and VIII which demonstrate the efficacy of the proposed design procedures.

Chapter IX contains a summary of the results developed in this thesis and conclusions.

II. BASIC CONCEPT AND PROCEDURES OF NONRECURSIVE STATISTICAL FOCAL PLANE PROCESSING

A. INTRODUCTION

Focal plane processing has a wide range of objectives such as optical filtering, sensing, multiplexing, signal formating, background clutter suppression, thresholding, target tracking, target discrimination, target recognition, and many others. This thesis is only concerned with background clutter suppression and thresholding. They are two old problems taking on new urgency and demanding requirements due to the recent developments of "mosaic focal plane arrays" and "smart sensors."

The thresholding process is not significantly different from that developed for radar. However, clutter suppression algorithms will be drastically different from those developed for radar and for old infrared systems using only a small number of detectors. New focal plane processing techniques capable of suppressing clutter by several ten's of db's are urgently needed to meet demanding requirements of new surveillance and guidance systems.

Five nonrecursive statistical focal plane processing algorithms are developed in this thesis for clutter suppression. These are followed by a thresholding step to initiate the target detection process. Although differing in detailed

implementation, they share the same basic concept and filter configurations. The main difference lies in the design of their filter coefficients. They will be presented in this chapter. An appreciation of the common underlying concept will help to place in proper perspective the detailed developments of all five statistical filters in the following chapters.

B. BASIC CONCEPT OF NONRECURSIVE STATISTICAL FILTERS FOR CLUTTER SUPPRESSION

One of the major objectives of focal plane processing developed in this thesis is background clutter suppression. In infrared mosaic focal plane array systems, clutter originates from thermal radiations in the background scene in the field of view of the sensor system. Since the background scene has well defined spatial shapes and temperature distributions, the background clutter noise in the image must have well defined spatial shapes or structures also which may be contaminated by scattering through the atmosphere, distortion through the optical and electronic components, and different noise sources. In other words, the clutter noise is a random signal with well defined spatial structure for a given scene. This information on the clutter noise is useful in helping to achieve its suppression. However, the important concept of the statistical filter is the assertion that although the spatial structure of the background clutter varies with the scene, the statistical characteristics of the spatial structure

over a large area may be described by well defined statistical characterizations such as the correlation matrix, autocorrelation function or power spectral density. If this is true, a spatial filter can be designed to use the signals around a selected pixel or over its neighborhood to process the signal at that pixel. Since background clutter has well defined statistical spatial behavior while the target of interest only dwells in one pixel, or several pixels of well defined location, signals in the neighborhood can be properly used to suppress the spatially related background clutter and thus raise the target signal out of the clutter. This is the basic concept of the statistical spatial filter for clutter suppression. The filter can be designed by performing a statistical estimation of the target signal, using one of several criteria. They will be explained in a later section.

The statistical correlation concept in the spatial domain can be extended to the temporal domain also. If successive frames of images are fairly well registered, with small amounts of drift and jitter in between frames, it is reasonable to expect that the signals are correlated in temporal domain. If this is true, a temporal filter can be designed that will use the signals at the same pixel location of successive frames of images to process the signal at one of the frames for suppression of the temporally correlated clutter.

In summary, if background clutter sources are related (in the statistical sense) either spatially in a single frame

or temporally over several frames, signals in both the spatial and temporal neighborhood can be used together to process the signal at the selected pixel for suppressing the clutter. These unprocessed signals are multiplied by the filter coefficients and summed together to provide the processed signal at the selected pixel. Therefore, it is a "nonrecursive" filter operation. The filter configuration will be described in the following section.

C. CONFIGURATION OF NONRECURSIVE FILTERS

1. Nonadaptive Nonrecursive Filters

In the previous section, the concept of nonrecursive filtering using unprocessed signals in the neighborhood around a selected pixel, to be called the "estimation pixel," was introduced. The purpose of such a filter is to suppress the background clutter by performing a statistical estimation of the target signal at that pixel. The neighborhood area where the filtering is carried out is called the "search box." The location of the "estimation pixel" is usually inside the "search box" but can also be outside. For symmetrical clutter characteristics, it is best to have the "estimation pixel" in the middle of the search box. However, it must be moved toward the edges of the search box when the estimation pixel is located at the edge of an image because there is no signal outside the image.

In summary, unprocessed signals in a search box are used to process the signal at only one "estimation pixel" inside the search box. The estimation pixel is then scanned throughout the image. This filter configuration is further described in two cases shown in Fig. 2-1 and 2-2 for a spatial filter and a spatial-temporal filter respectively.

Let $X^T \stackrel{D}{=}$ unprocessed signal $= S^T + N^T$ (2-1)

$S^T \stackrel{D}{=}$ targets of interest $= [s_1, s_2, s_i, \ldots s_I]$ (2-2)

$N^T \stackrel{D}{=}$ sum of all noise components including uncorrelates "white" noise and correlated "colored" noise $= [n_1, n_2, n_i, \ldots n_I]$ (2-3)

where $i = 1,2,\ldots I$ and I is the total number of pixels in the search box.

CASE I - Spatial Filter (Fig. 2-1)

A nonrecursive spatial filter is described by a set of filter coefficients, or weighting coefficients, over the area of a "search box." The set of filter coefficients is represented by a vector W. The intensity of the unprocessed signals in the search box, represented by the vector X, are multiplied by the weighting coefficients, (the vector "W") corresponding to the same pixel location in the same search box and summed together to give the output intensity at the estimation pixel, y, that is,

$$y = W^T \cdot X$$

The filter coefficients are designed by different criteria to be described in the following section. Spatial-filtering using

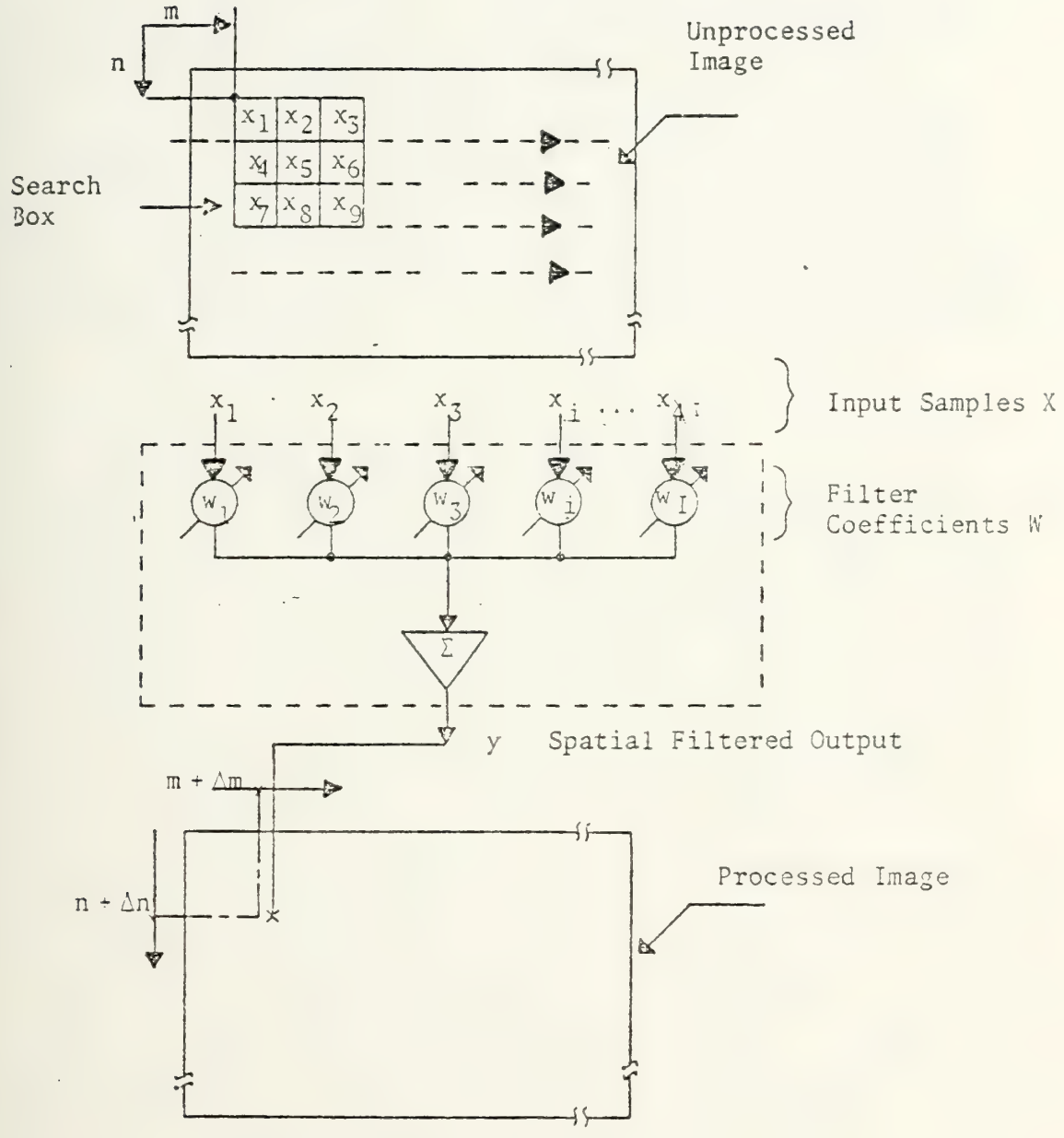

Figure 2-1 Configuration of Nonadaptive Two Dimensional Nonrecursive Spatial Filter

one search box will yield a processed signal, called the "estimation signal," of only one pixel, the "estimation pixel." The search box is then moved, following the scanning of the "estimation pixel" throughout the image.

This thesis concentrates on a search box size of 3 by 3 pixels. Therefore, nine filter coefficients are required. The estimation pixel is usually the center pixel. It is moved to the middle of one edge or one corner sometimes, as explained above.

CASE II - Spatial-Temporal Filter (Fig. 2-2)

In general, a three dimensional nonrecursive filter is described by a set of filter coefficients, W, over the volume of a "search box" which consists of several frames of a two dimensional box. For example, in a 3x3x5 search box, a 3x3 search box is used in five successive frames of the image. Altogether, W consists of 45 coefficients. However, the spatial-temporal filters developed in this thesis are the special case which consists of sequentially applying a spatial filter, first on one frame of image, then followed by a temporal filter, W_K, using several successive frames of images. For example, consider a sequential 3x3 spatial filter followed by a five frame temporal filter. The spatial filter is implemented by the same procedure described in Case I. For the five frame temporal filter, signals at the same pixel location from five successive frames are multiplied by the temporal

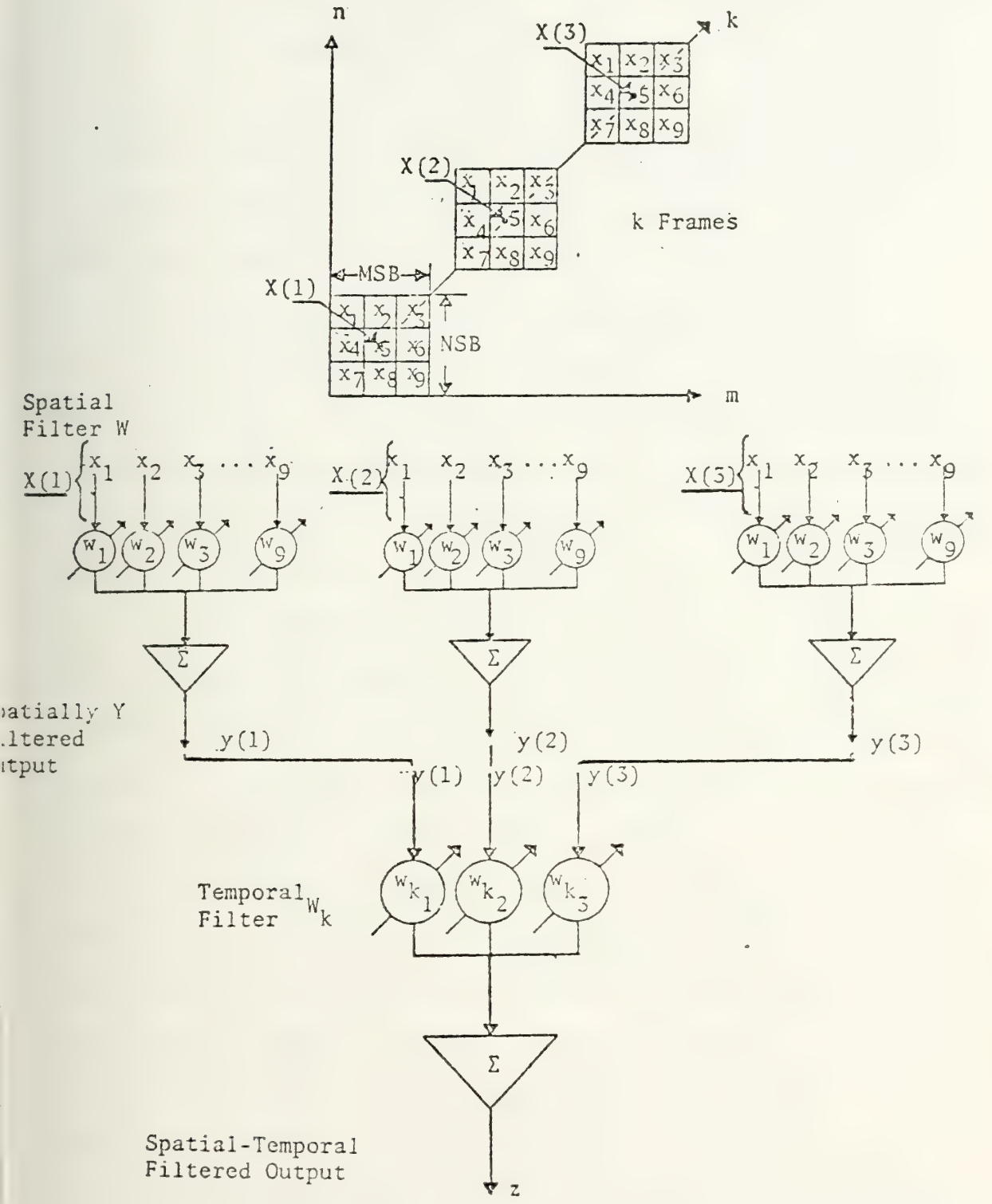

Figure 2-2 Configuration of Nonadaptive Three Dimensional Nonrecursive Sequential Spatial-Temporal Filter

filter coefficients and summed together. Therefore, instead of 45 filter coefficients for the general three dimensional filters, the sequential spatial-temporal filters have only 14 filter coefficients. The first nine coefficients are for the spatial filter. The last five coefficients are for the five frame temporal filter.

2. Adaptive Nonrecursive Filters (Fig. 2-3)

In this thesis, only an adaptive spatial filter is developed. Its configuration is an extension of the spatial filter configuration shown in Fig. 2-1. The concept of adaptation is based on the one dimensional adaptive filter originally developed by B. Widrow [20,21,22].

In the adaptive filter, there is an automatic correction procedure for adapting the filter coefficients by using a feedback loop shown in Fig. 2-3. The search box and operation of an adaptive spatial filter are still the same as that of the nonadaptive spatial filter. However, the output of the spatial filter is now compared with a desired reference signal, d_j, by a subtraction operation. The error of this comparison is multiplied by an adaptive loop gain, μ, and the unprocessed signal at a pixel to yield a correction term for the filter coefficient corresponding to that pixel. This adaptive correction is carried out by scanning the search box over an "adaptation area." Therefore, in the adaptive filter case there are three image areas:

The given image area,

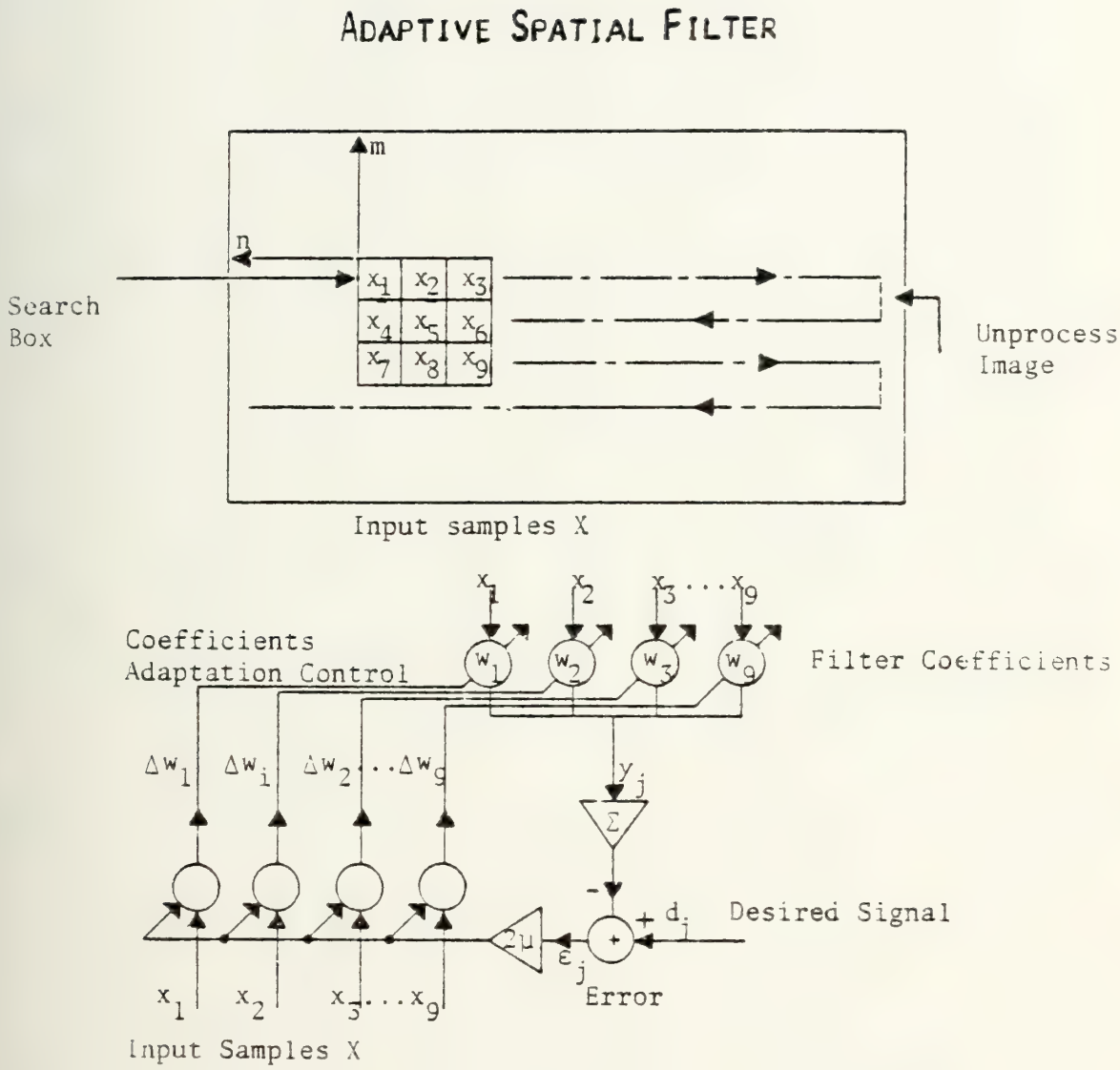

Figure 2-3 Configuration of Adaptive Two Dimensional Nonrecursive Spatial Filter

The spatial filter area - search box area,

The adaptation area - which is in general larger than the search box area; for example, 8x8 for a search box of 3x3.

D. PRINCIPLE OF STATISTICAL FILTER DESIGN

In section C, configurations of all five statistical filters are shown in three different types: Figures 2-1, 2-2 and 2-3. The common principle behind them is to "sum" the "weighted" signals in the neighborhood of the "estimation pixel." The neighborhood is defined in a general sense to include both spatial neighborhood and temporal neighborhood. Once the configuration is chosen, the only parameters remaining to describe the filter are the weighting coefficients. They are designed by several different criteria.

Two criteria are used in this thesis.

1. Criterion I - Minimization of Mean Square Error

In this criterion, a desired result is selected. For example, in the nonadaptive spatial filter case, the objective of spatial filtering is to estimate the target, s. However, the output of the filter only provides an estimate of the target, $y = \hat{s}$. Therefore, there is an error, $e = \hat{s} - s$. Its mean square value is $E(e^2)$. The filter coefficients, W, are designed by minimization of the mean squared error. This filter is called "spatial MMSE" filter or "spatial Wiener filter" [14,18,23,24,25,26].

A similar procedure is developed for the temporal MMSE filter and the spatial-temporal MMSE filter.

2. Criterion II - Maximization of Signal to Noise Ratio [27,28,29]

In this criterion, the objective is to maximize the output signal to noise ratio. The filter designed by this criterion is called the "spatial matched filter."

A similar procedure is developed for the temporal matched filter and the spatial-temporal matched filter.

E. IMAGES USED IN ANALYZING AND TESTING OF THE STATISTICAL FOCAL PLANE PROCESSING

Two dimensional infrared images containing a background scene and different targets have been collected in the past using infrared scanners and radiometers. Although they provide some information on the background and target, they are found inadequate because these instruments typically use only a few detectors. They are scanning instruments with relatively large instantaneous fields of view and fairly broad spectral bands. Many of them are not in spectral bands suitable for target detection in the new surveillance systems. Therefore, there is an acute lack of standard background scenes needed for developing and testing new focal plane processing algorithms to be used in these new high performance surveillance and guidance systems using smart sensors.

In this thesis, a set of real world infrared images of twenty frames with relative drift of 10% pixel each frame, selected by a responsible agency, was made available.[2]

---

[2] M. Schlesinger, Aerospace Corporation., private communication.

They are used extensively in testing both the spatial filters and spatial-temporal filters. The performance results are the most convincing evidence of the usefulness of this research because the test is based on real world infrared images.

However, to carry out detailed research of this statistical focal plane processing, a wide variety of images with varying parameters is needed. Since there is simply no such supply of real world images taken by the new mosaic focal planes, it was necessary to develop a theoretical model for the background clutter. If it can be proven valid, different test images can be generated on a computer readily by simply varying the appropriate parameters.

For this purpose, contaminated images have been generated by using the following models. A contaminated image consists of three components.

1. Target

It is described by its spatial shape, its movement between frames and its intensity. The intensity is described either deterministically by S, as defined by eq. 2-2, or statistically by a mean μ_T and variance σ_T^2.

2. Random Noise

There are two types. The first type is Gaussian uncorrelated, or "white" noise described by its mean μ_{UN} and variance σ_{UN}^2. The second type is Gaussian correlated, or "colored" noise - modeled by two Markov processes [Appendix A].

° A first order Markov process described by its auto-correlation function.

$$R = \sigma_{CN}^2 \rho_H^{|m|} \rho_V^{|n|}$$

where σ_{CN}^2 = variance

ρ_H = horizontal correlation factor

ρ_V = vertical correlation factor

m = horizontal coordinate of image

n = vertical coordinate of image.

° A second order Markov process described by its auto-correlation function.

$$R = \sigma_{CN}^2 \rho_H^{|m|} \rho_V^{|n|} \cos(\beta_H m) \cos(\beta_V n)$$

where β_H = horizontal spatial frequency

β_V = vertical spatial frequency.

III. SINGLE FRAME FOCAL PLANE PROCESSING FOR CLUTTER SUPPRESSION - NONRECURSIVE STATISTICAL SPATIAL FILTERS

A. INTRODUCTION

In this chapter, two statistical spatial filters which use only one frame of an image are developed. One is designed by minimizing a mean square error criterion. This type of filter is called "MMSE" filter, which is more commonly known as a Wiener filter. It provides an "optimal" estimate of the target signal and will be developed in Section C. The second type is designed by maximizing the output signal to noise ratio criterion and is commonly known as the matched filter. It will be developed in Section D.

These two statistical design procedures can be equally well applied to focal plane processing using several frames of images in the form of three dimensional spatial-temporal or temporal-spatial filters. They will be developed in the next chapter.

Both the spatial filters developed in this chapter and the spatial-temporal filters developed in the next chapter will be evaluated by using two types of images. One type is computer generated images containing correlated noise modeled by a Markov process to simulate background clutter. The other type is a real world infrared image. The results from both simulated and real world scenes are presented together in Chapter VI.

B. CONFIGURATION OF TWO DIMENSIONAL NONRECURSIVE SPATIAL FILTERS

Although the design criteria of two statistical spatial filters developed in this chapter are different, they share the same filter configurations as shown in Fig. 3-1. Therefore, the filter configuration and operation procedure will be described before their individual design criteria are presented in the next two sections.

In these spatial filters, signals in the neighborhood of a selected pixel of interest are used together to help the processing of signals at that pixel. The selected neighborhood is called a "search box." As explained in Chapter II and the previous section, the objective is to suppress the background clutter by performing an estimation of the target signal at that pixel, using its neighborhing signals and the knowledge of their statistical spatial correlation properties. This is carried out by designing a set of weighting coefficients, or filter coefficients, W. For every pixel in the search box, a weighting coefficient is assigned. Signals of all pixels, X, in the search box are multiplied by their corresponding filter coefficients, W, and summed together to give an "optimal" estimate of the target intensity at the "estimation pixel," which can be anywhere inside the search box. It could also be located outside the search box although this is not developed in this thesis. In general, the location of the "estimation pixel" is in, or close to, the middle of the search box

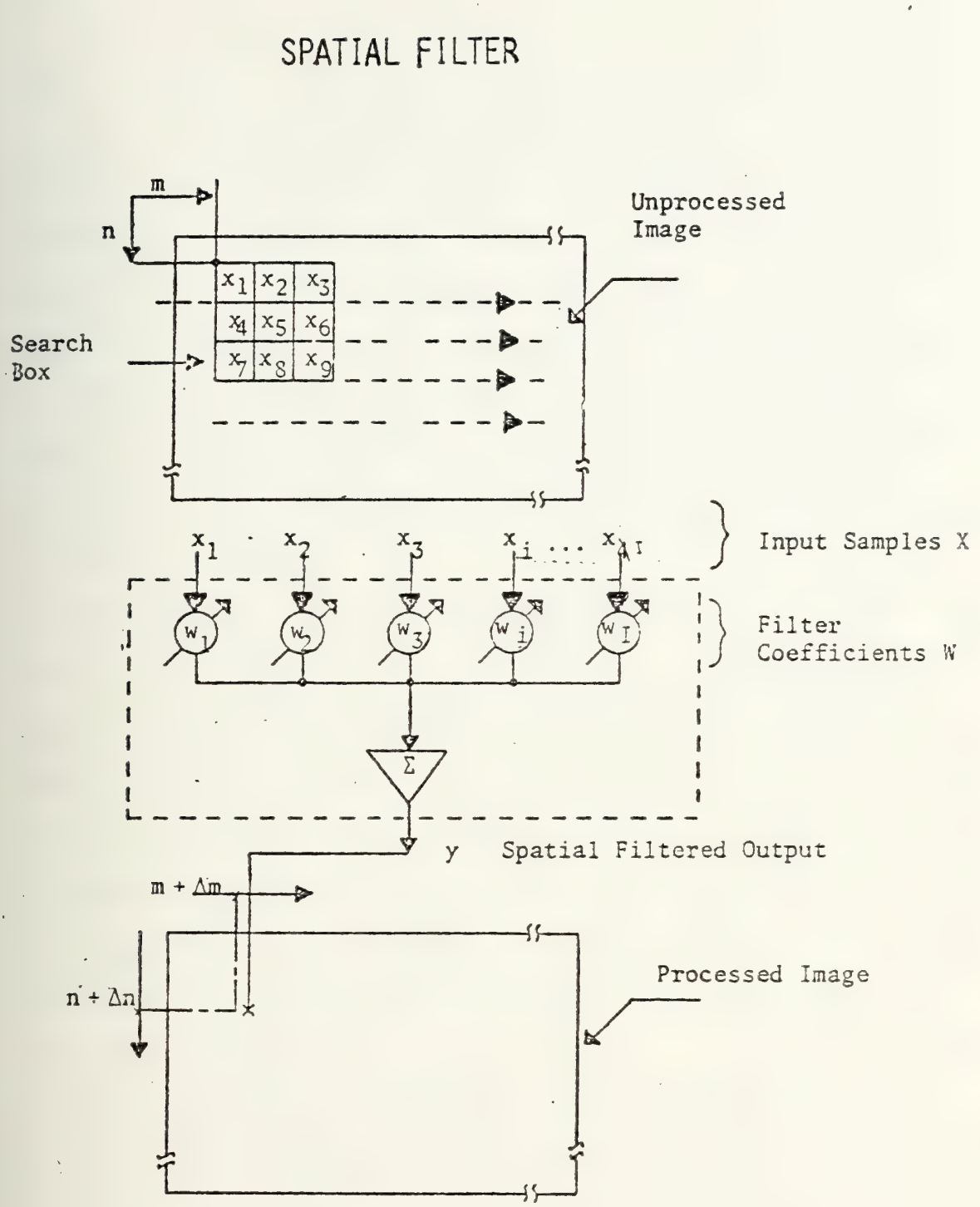

Figure 3-1 Configuration of Nonadaptive Two Dimensional Nonrecursive Spatial Filter

because common sense suggested that spatial behaviors in all directions around the estimation pixel should be used to reveal the spatial behavior of background clutter and to help achieve their suppression. However, there are situations where signals in certain parts of the neighborhood do not exist; for example, when the estimation pixel is located at the edge of an image. In these cases, it is not possible to have the estimation pixel in the middle of the filter. Instead, it must be off to the side, as will be shown later by several examples.

The size and shape of the search box can also vary. Only square shaped search boxes are developed in this thesis because the correlation properties in vertical and horizontal directions are assumed to be quite close. On the other hand, the concept and design procedure developed in this thesis can be easily extended to non-square-shaped search boxes if needed; for example, if the correlation properties in the vertical direction are significantly different from those in the horizontal direction.

The size of the search box depends on the correlation property of the background clutter and on the size of the targets of interest. If the spatial correlation of the clutter is strong, there is no need to go beyond a few neighboring pixels to determine the correlation properties. Therefore, a small search box is sufficient to accomplish an effective suppression of background clutter. On the other hand, if

the spatial correlation of clutter is weak, one needs further away neighboring pixels to obtain the correlation properties properly and a larger search box is needed. In this thesis, a 3x3 search box is developed almost exclusively because it was found that the correlation properties of several real world infrared images are quite strong. In terms of a correlation factor, on a scale from 0 to 1 corresponding to no correlation (white noise) to perfect correlation (deterministic), the real world images examined in this thesis indicated a range of values above 0.8. On the other hand, the concept and design procedure developed in this thesis can be easily extended to large sizes such as 4x4, 5x5, etc.

In summary, nonrecursive spatial filters developed in this chapter consist of a search box for every pixel of interest in the image, called the "estimation pixel." Because secondary signals in the search box are used to estimate the target at the estimation pixel, target estimation pixel can be moved to any part of the image or scanned to cover any selected corner of the image. In this thesis, a raster scan of the estimation pixel is used to cover the whole image. When the estimation pixel is at the corner or along the edges of the image, it cannot be located in the middle of the search box. On the other hand, whenever possible it will be located in the center. For every search box, signals of all pixels are weighted and summed to give an estimate of the target intensity at only one pixel inside the box, the estimation pixel.

The weighting coefficients are designed using different criteria. Two of these design procedures are presented in the next two sections.

C. NONRECURSIVE SPATIAL MMSE FILTER

1. Principle of Optimal Estimation

The objective of the spatial MMSE filter is to give a processed signal $Y = f_Y(m_o,n_o)$ which will be the "optimal" estimate of the target of interest, $S = f_S(m_o,n_o)$ where (m_o,n_o) are the indices of the estimation pixel. The criterion for "optimality" is the "minimum mean square error" (MMSE), sometimes known as the Wiener filter. The theoretical derivation of the MMSE filter is well known and more detailed information can be found in the following references:

- Reference 18 states the general MMSE criteria.
- Reference 23 describes an image restoration technique using spatial frequency domain design technique.
- Reference 24 describes an image enhancement technique based on the MMSE algorithm using, again, spatial frequency domain design method, requiring efficient transformation techniques.
- Reference 25 describes in detail the spatial domain derivation algorithm for the MMSE filter considering some implementation methods in the frequency domain.
- Reference 26 describes the linear algebraic image restoration method in general, and the least squares technique including the Wiener filter formulation in particular. The design equations, both in spatial and spatial frequency domain, are presented.

A practical method of implementation of spatial Wiener filter for suppression of correlated noise and enhancement of point and line target was suggested in Ref. 14. This design method will be further extended here and in Chapter IV, which presents multiple plane spatial temporal filtering. The design procedure is presented in the following paragraphs.

[Step I] Description of Unprocessed Image:

The unprocessed signal of the whole image X is given by a two dimensional array shown in Fig. 3-2(a).

$$X \triangleq \begin{bmatrix} x_{11} & x_{21} & \cdots & x_{MMAX\ 1} \\ x_{12} & x_{22} & & x_{MMAX\ 2} \\ \vdots & & & \\ x_{1\ NMAX} & & & x_{MMAX,NMAX} \end{bmatrix} = S + N \qquad (3\text{-}3.1)$$

where

X = intensity of unprocessed signal (3-3.1(a))

S = target signal of interest (3-3.1(b))

N = sum of all noise sources (3-3.1(c))

MMAX - number of horizontal pixels in the image

NMAX - number of vertical pixels in the image.

The original signals inside the spatial filter search box are given by a smaller two dimensional array.

$$X = \begin{bmatrix} x_{m,n} & x_{m+1,n} & \cdots & x_{m+MSB,n} \\ x_{m,n+1} & x_{m+1,n+1} & & x_{m+MSB,n+1} \\ \vdots & & & \\ x_{m,NSB} & x_{m+1,NSB} & & x_{m+MSB,n+NSB} \end{bmatrix} \qquad (3\text{-}3.2)$$

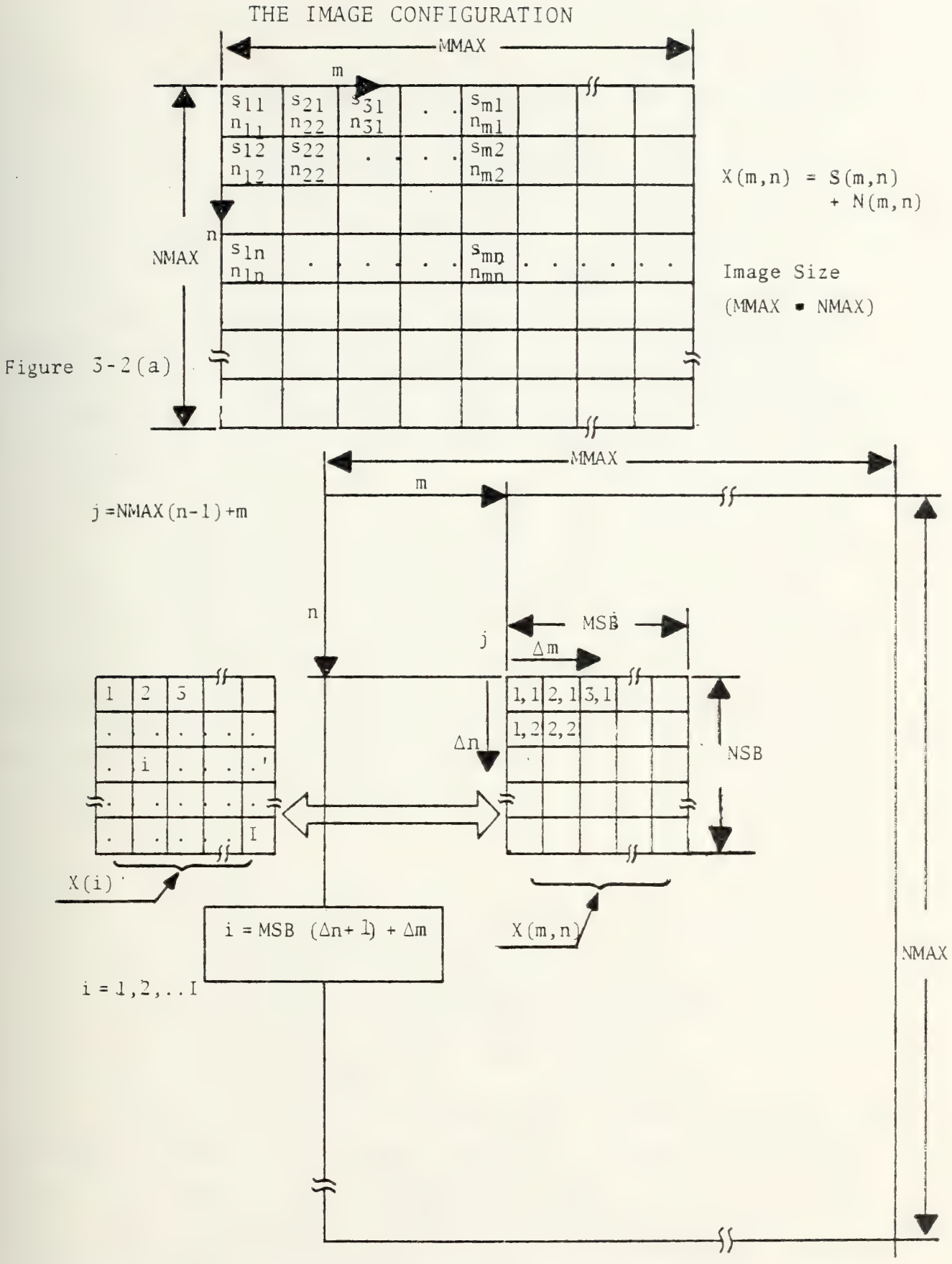

Figure 3-2(a) Coordinate System for the Image
(b) Coordinate System for the Spatial Filter

where m = horizontal pixel number of the upper left corner of the search box

n = vertical pixel number of the upper left corner of the search box

MSB - horizontal size of the search box

NSB = vertical size of the search box.

In this thesis, a new search box coordinate system is used for pixels inside the search box. They are referenced with respect to the upper left corner pixel (m,n) and described, shown in Fig. 3-2(b) by

$$X = \begin{bmatrix} x_1, x_2, & \cdots & x_{MSB} \\ x_{MSB+1} & & x_{2MSB} \\ \vdots & & \\ x & \cdots & x_{MSB \cdot NSB} \end{bmatrix} \qquad (3\text{-}3.3)$$

This two dimensional array is further simplified by using a one dimensional vector representation.

$$X^T \triangleq [x_1, x_2, \ldots x_i, \ldots x_I] \qquad (3\text{-}3.4)$$

where $i = MSB \cdot (\Delta n - 1) + \Delta m$

Δ_m = Horizontal pixel location in search box with respect to top row

Δ_n = Vertical pixel location in search box with respect to left-most column

I = MSB NSB - total number of pixels in the search box

The objective of the spatial MMSE filter is to give the optimal estimate of the target signal of interest at the estimation pixel (MES,NES) by summing all weighted signals in the search box. (MES,NES) is the location in the search box coordinate system. In the one dimensional vector representation, the weighting coefficients are also described by a vector W as shown in Fig. 3-2(c).

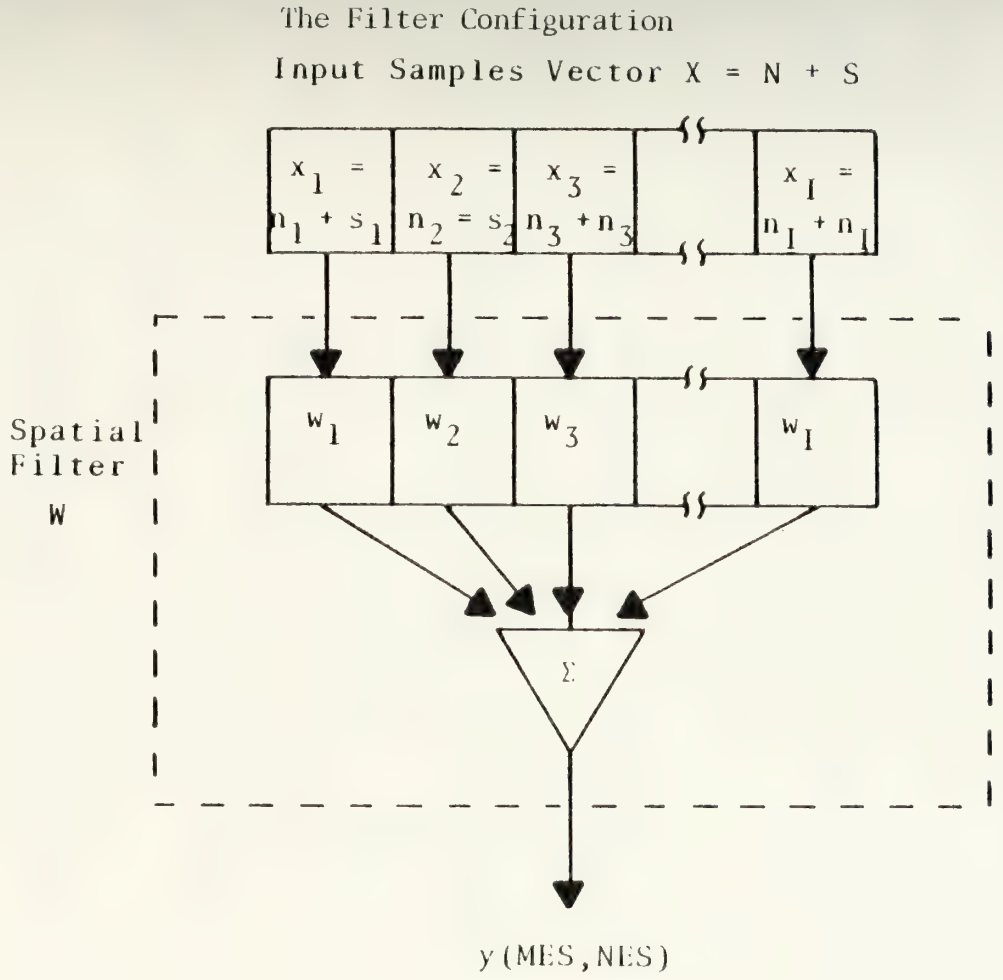

Figure 3-2(c) Operations of Nonrecursive Spatial Filter.

$$W^T \overset{D}{=} [w_1, w_2, \cdots w_{ES}, \cdots w_I] \qquad (3\text{-}3.5)$$

where w_{ES} = filter coefficient at the estimation pixel (MES,NES).

[Step II] Filtered Image and Mean Square Error:

The output of the filter is:

$$y = X^T \cdot W = \hat{s} \qquad (3\text{-}3.6)$$

where $\hat{s}$ = estimate of the target signal at the estimation pixel (MES,NES).

Let us define the estimation error as

$$e(MES,NES) = s(MES,NES) - \hat{s}(MES,NES) \qquad (3\text{-}3.7)$$

The mean square error is then the expectation value

$$E[e^2(MES,NES)] = E\{[s(MES,NES) - \hat{s}(MES,NES)]\}$$

$$= E\{[s(MES,NES) - X^T \cdot W]^2\} \qquad (3\text{-}3.8)$$

[Step III] Minimization of Mean Square Errors:

To minimize (3-3.8), it is differentiated with respect to W and is then equated to zero.

$$\frac{\partial}{\partial W} E[e^2(MES,NES)] = E\{-X \cdot 2[s(MES,NES) - X^T \cdot W]\}$$

$$= E\{-X \cdot 2\, e\} = 0 \qquad (3\text{-}3.9)$$

Equation (3-3.9) shows that the estimation error is orthogonal to the unprocessed signal X. Further simplification of (3-3.9) gives:

$$E[X \cdot s(MES,NES)] = E[X \cdot X^T \cdot W] = E[X \cdot X^T] \cdot W \qquad (3\text{-}3.10)$$

which is the equation for designing the filter coefficient W.

Let us define

$$P \overset{D}{=} E[X \cdot s(MES, NES)] \qquad (3\text{-}3.11)$$

= cross correlation between the unprocessed image signal X and the target signal of interest.

$$R_{XX} \triangleq E[X \cdot X^T] = \begin{bmatrix} E(x_1, x_1) & E(x_1, x_2) & \cdots & E(x_1, x_I) \\ E(x_2, x_1) & E(x_2, x_2) & \cdots & E(x_2, x_I) \\ \vdots & & & \\ E(x_I, x_1) & \cdots & \cdots & E(x_I, x_I) \end{bmatrix} \qquad (3\text{-}3.12)$$

= correlation matrix of the unprocessed image signal.

[Step IV] Equation of Filter Design:

Equation (3-3.10) is now expressed as:

$$R_{XX} \cdot W = P$$

or

$$\boxed{W = R_{XX}^{-1} \cdot P} \qquad (3\text{-}3.13)$$

It is a set of I simultaneous linear equations used to solve for the weighting coefficients, or filter coefficients, of the two dimensional spatial MMSE filter for target estimation.

In many practical applications, we assume that the target signal S and the noise N are uncorrelated. If we further assume that the mean of the noise is zero, then

$$R_{XX} = R_{SS} + R_{NN} \tag{3-3.14}$$

where R_{SS} = correlation matrix of the target signal

R_{NN} = covariance matrix of the noise.

The filter coefficients (3-3.13) are given by:

$$\boxed{W_{WF} = (R_{NN} + R_{SS})^{-1}.P} \tag{3-3.15}$$

The subscript WF stands for "Wiener Filter."

2. Design Procedure for Spatial MMSE Filter [Ref. 1]

To design a spatial MMSE filter, a three step procedure is used. The first step is to calculate the statistical properties of the targets R_{SS} and P. The second step is to calculate the statistical property of the background clutter noise R_{NN}. The last step is to calculate the filter coefficients by solving (3-3.15). They will be explained in more detail in the following.

[Step I] Calculations of Statistical Properties of the Targets R_{SS} and P: [14]

The calculation of R_{SS} and P are relatively straightforward. They depend on the type of target signal. Once the target signal of interest is given, as shown by several examples of point target and line targets in Fig. 3-3, R_{SS} and P are calculated by the following expressions:

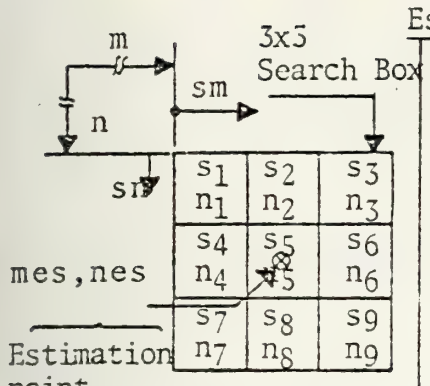

3-3.1. Estimation Point in Center of Search Box

Estimation Point Location

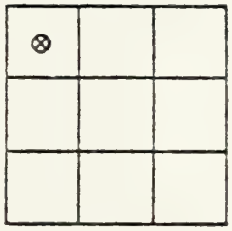

3-3.2. Estimation Point at Upper Left Corner of of Search Box

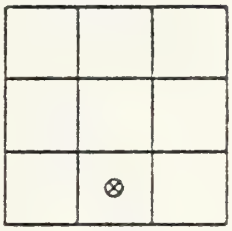

3-3.3. Estimation Point at Lower Center Location of Search Box.

Fig. 3-3.1,2,3. Three Possible Estimation Point Locations in Search Box (out of 9 Possibilities in a 3x3 Search Box).

Point Target Relative Required Location

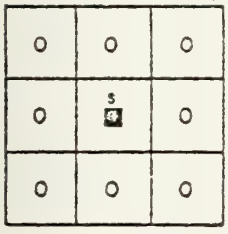

Fig. 3-3.4. Point Target Required Location with Respect to the Search Box in Fig. 3-3.1.

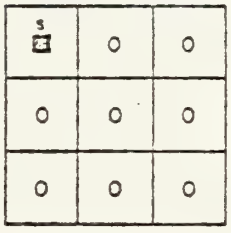

Fig. 3-3.5. Point Target Required Location with Respect to the Search Box in Fig. 3-3.2.

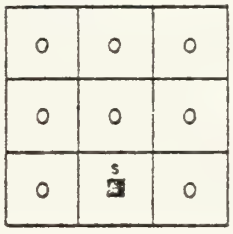

Fig. 3-3.6. Point Target Required Location with Respect to the Search Box in Fig. 3-3.3.

Examples of Line Targets Relative Required Location

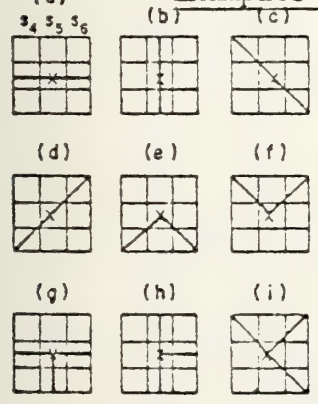

Fig. 3-3.7

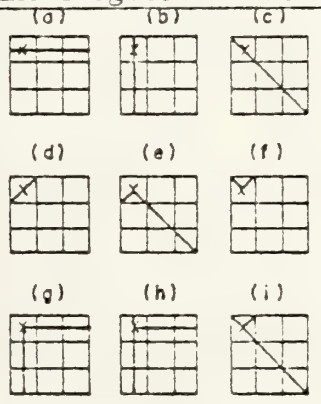

Fig. 3-3.8

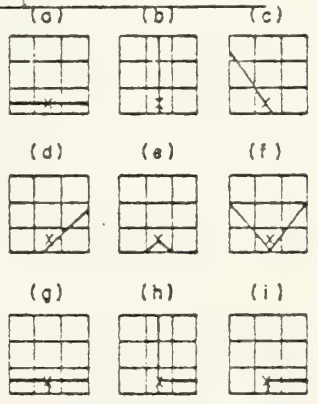

Fig. 3-3.9

Some target configuration with respect to search box

Figure 3-3 Examples of Different Estimation Pixel Locations and Different Target Types

$$R_{SS} = \begin{bmatrix} E(s_1,s_1) & E(s_1,s_2) & \cdots & E(s_1,s_9) \\ E(s_2,s_1) & E(s_2,s_2) & \cdots & E(s_2,s_9) \\ \vdots & & & \\ E(s_9,s_1) & \cdots & \cdots & E(s_9,s_9) \end{bmatrix} \qquad (3\text{-}3\text{-}16)$$

$$P = \begin{bmatrix} E(s_5,x_1) \\ E(s_5,x_2) \\ \vdots \\ E(s_5,x_9) \end{bmatrix} = \begin{bmatrix} E(s_5,s_1) \\ E(s_5,s_2) \\ \vdots \\ E(s_5,s_9) \end{bmatrix} \qquad (3\text{-}3\text{-}17)$$

Notice that s_5 is the signal at the E.P. for a 3x3 search box.

Two special cases will be presented. The first case is for point targets and for a central estimation pixel. Under those conditions, $s_5 = T$, and all other s's are zero.

$$R_{SS} = \begin{bmatrix} 0 & 0 & 0 & 0 & 0 & 0 & 0 & 0 & 0 \\ 0 & 0 & & & \cdot & & & & 0 \\ 0 & & & & \cdot & & & & \\ 0 & & & & \cdot & & & & \\ 0 & \cdots & \cdots & \cdots & T^2 & \cdots & \cdots & \cdots & \\ 0 & & & & \cdot & & & & \\ 0 & & & & \cdot & & & & \\ 0 & & & & \cdot & & & & \\ 0 & 0 & \cdots & \cdots & 0 & \cdots & \cdots & \cdots & 0 \end{bmatrix} \qquad (3\text{-}3.18)$$

$$P = \begin{bmatrix} 0 \\ 0 \\ 0 \\ 0 \\ T^2 \\ 0 \\ 0 \\ 0 \\ 0 \end{bmatrix} \qquad (3\text{-}3.19)$$

where T = intensity of the point target.

The second case is for a horizontal line target, as shown in Fig. 3-3.7(a), and for a central estimation pixel. Under these conditions, s_4, s_5 and s_6 are not zero; all other s's are zero.

$$R_{SS} = \begin{bmatrix} 0 & 0 & 0 & 0 & 0 & 0 & 0 & 0 & 0 \\ 0 & & & & & & & & 0 \\ 0 & & & & & & & & 0 \\ 0 & & & E(s_4s_4) & E(s_4s_5) & E(s_4s_6) & & & 0 \\ 0 & & & E(s_5s_4) & E(s_5s_5) & E(s_5s_6) & & & 0 \\ 0 & & & E(s_5s_4) & E(s_6s_5) & E(s_6s_6) & & & 0 \\ 0 & & & & & & & & 0 \\ 0 & & & & & & & & 0 \\ 0 & 0 & 0 & 0 & 0 & 0 & 0 & 0 & 0 \end{bmatrix} \qquad (3\text{-}3.20)$$

$$P = \begin{bmatrix} 0 \\ 0 \\ 0 \\ E(s_5s_4) \\ E(s_5s_5) \\ E(s_5s_6) \\ 0 \\ 0 \\ 0 \end{bmatrix} \qquad (3\text{-}3\text{-}21)$$

The amplitude of the line target s_4, s_5, s_6 can be either deterministic or statistical. In many applications, a deterministic target amplitude is considered. If the interest is only in the location of the targets, $s_4 = s_5 = s_6 = \text{constant}$. If the amplitude of the target signal is known, s_4, s_5, and s_6 will be proportional to its spatial variations.

Statistical amplitudes are useful in cases where a large number of targets are expected and their amplitudes are described statistically, for example, by a probability density function. This problem will be discussed further in Chapter V where a target detection procedure is developed.

Other types of targets can be handled in a similar manner.

[Step II] Calculation of R_{NN}:

Two procedures are used in this thesis to calculate the covariance matrix of the background clutter noise, depending on the type of images used in the analysis.

1. Computer Generated Images:

It is assumed that background clutters in real infrared images can be modeled by Markov processes. Their autocorrelation functions can be described by the following closed-form mathematical expressions:

First order Markov process:

$$Q(m,n) = \sigma_{CN}^2 \rho_H^{|m|} \rho_V^{|n|} \qquad (3\text{-}3.21)$$

Second order Markov process:

$$Q(m,n) = \sigma_{CN}^2 \rho_H^{|m|} \rho_V^{|n|} \cos(\beta_H m) \cos(\beta_V n) \qquad (3\text{-}3.22)$$

where σ_{CN}^2 = variance of correlated noise which is used to model the clutter.

ρ_H = horizontal correlation coefficient between two adjacent pixels.

ρ_V = vertical correlation coefficient between two adjacent pixels.

$\beta_H = \omega_m$ = horizontal spatial frequency (for 2nd order Markov process)

$\beta_V = \omega_n$ = vertical spatial frequency (for 2nd order Markov process)

These two dimensional correlated random noise sources can be simulated by a recursive procedure described in Appendix A to generate simulated background clutter images. For these images, R_{NN} can be calculated easily [14].

2. Real World Infrared Image:

If real world infrared images are given, their statistical characteristics must be calculated directly from the given images, using eq. (3-3.12) and then averaging it over a large number of pixels to obtain its expected value. It must be pointed out if the number of targets in the image is high, and their amplitudes are high, they will cause error in the calculation of the statistical properties of the clutter. The analysis of a real world infrared image was made by Captain D. Hilmers in his thesis research [30].

[Step III]. Design of Filter coefficients:

After the calculations of R_{SS}, P and R_{NN}, the filter coefficients are designed by solving eq. (3-3.15).

3. Figure of Merit for Clutter Suppression - Processing Gain

To evaluate the performance of the designed filter, the processing gain (PG) was selected as a figure of merit.

The PG definition is:

$$PG = \frac{\text{(Signal power/Noise power) At filter output}}{\text{(Signal power/Noise power) At filter input}} \qquad (3\text{-}3.23)$$

The PG is given by the following equations:

Input signal power at a given pixel $\stackrel{D}{=} s^2 = p_{S_i}$

Input noise power at a given pixel $\stackrel{D}{=} \sigma_N^2 + \mu_N^2 = p_{N_i}$

σ_N^2 is noise variance, defined by (3-3.22)

μ_N is noise mean

Output signal power at estimation pixel = $(S^T \cdot W)^2 = P_{S_o}$

where $\tilde{s}^T$ was defined by eq. (2-2) and $\tilde{w}$ by eq. (3-3.5).

Output noise power at estimation pixel =

$E[(N^T \cdot W)^2] = E[W^T \cdot N \cdot N^T \cdot W] = W^T \cdot E[N \cdot N^T] \cdot W = W^T \cdot R_{NN} \cdot W = p_{N_o}$

where R_{NN} defined by (3-3.13).

Therefore, the PG is:

$$PG = \frac{(p_{S_o}/p_{N_o})}{(p_{S_i}/p_{N_i})} = \frac{(S^T \cdot W)^2/(W^T \cdot R_{NN} \cdot W)}{s^2/(\sigma_N^2 + \mu_N^2)} \qquad (3\text{-}3.24)$$

where σ_N and μ_N were presented in Section II.E.2.

For a point target and zero mean noise, the PG will become:

$$PG = \frac{s^2 \cdot w^2(MES,NES)/\ \sigma_N^2\, W^T \cdot R_{NN}^{\rho} \cdot W}{s^2/(\sigma_N^2)} = \frac{w^2(MES,NES)}{W^T \cdot R_{NN}^{\rho} \cdot W} \qquad (3\text{-}3.25)$$

where $R_{NN} \stackrel{\Delta}{=} \sigma_N^2 \cdot R_{NN}^{\rho}$ and $w(MES,NES)$ is the filter coefficient at the estimation pixel.

4. Results of Computer Simulation

Properties of nonrecursive spatial MMSE filters and their performances in clutter suppression and target detection, when combined with the thresholding process, are investigated by computer simulation. Two types of images were used. One is a computer generated image containing spatially correlated noise represented by Markov models to simulate background clutter. The other is a real world infrared image.

The search box size is limited to a 3x3 square. Point targets are used in most of the computer simulation. The estimation pixel is usually in the center of the 3x3 box. It is moved to the side of the 3x3 only when the estimation pixel is along the edges of the image.

Investigation of the filters is carried out over a range of input conditions:

SNRI = Input power signal to noise ratio

= -21 db to 0 db

= Correlation factor = 0.999 to 0.4.

For target detection, a probability of false alarm (P_{FA}) in the range of 10^{-1} to 10^{-5} is selected as a parameter.

The computer simulation results are presented in Chapter VI where both single frame spatial filter results and multiple frame spatial-temporal filter results are presented together. Two types of presentations are used. The first

type is quantitative and does not use two dimensional pictures. Filter properties such as filter coefficients will be presented as functions of input signal to noise ratio and correlation factor. Filter performance, such as processing gain for clutter suppression and probability of detection for target detection, is related to input signal to noise ratio while the correlation factor and probability of false alarm are selected as parameters. The second type of presentation is pictorial and uses two dimensional images. Computer printouts using nine gray levels are used to present the unprocessed image, processed image after the application of spatial filter and images after further processing by thresholding.

D. NONRECURSIVE SPATIAL MATCHED FILTERS

1. Principle of Maximizing Signal to Noise Ratio [Ref. 27-29]

The objective of the spatial matched filter is to give a processed signal, $Y = f_Y(m_o,n_o)$ which will provide the maximum output target signal to total noise ratio. The filter design procedure is presented in the following paragraphs and is an extension to two dimensions based on the theoretical derivation of Appelbaum [29].

[Step I] Unprocessed Image:

The configuration of the nonrecursive spatial matched filter is the same as that of the MMSE filter. The description of unprocessed image and filters is the same also as presented in Section B.1.

$$X^T = [x_1, x_2, \ldots x_I] \tag{3-4.1}$$

$$X = S + N \tag{3-4.2}$$

The filter is described by

$$W = [w_1, w_2, \ldots w_I] \tag{3-4.3}$$

[Step II] Filtered Image and Output Signal to Noise Ratio:

The output of the filter is

$$y = X^T \cdot W \tag{3-4.4}$$

y contains two components:

$$y = v_S + v_N \tag{3-4.5}$$

where v_S = output signal voltage = $S^T \cdot W$ (3-4.6)

v_N = output noise voltage = $N^T \cdot W$ (3-4.7)

The output signal power is $|v_S|^2$. The output noise power is the expected value of $|v_n|^2$:

$$P_n = E[v_n \cdot v_n] = E[|N^T \cdot W|^2] = E[W^{T*} N^* N^T W]$$

$$= W^{T*} E[N^* N^T] W$$

$$= W^{T*} R_{NN} \cdot W \tag{3-4.8}$$

(the superscript * refers to the complex conjugate wherever a superscripted variable is complex; otherwise the * can be ignored)

where R_{NN} is the covariance matrix of the noise given by

$$R_{NN} = \begin{bmatrix} E(N_1N_1) & E(N_1N_2) & \ldots & E(N_1N_I) \\ E(N_2N_1) & E(N_2N_2) & \ldots & E(N_2N_I) \\ \vdots & & & \\ E(N_IN_1) & \ldots & \ldots & E(N_IN_I) \end{bmatrix} \tag{3-4.9}$$

assuming N has a zero mean. The output power signal to noise ratio is:

$$SNR_{out} = \frac{|v_S|^2}{W^T * R_{NN} \cdot W} \qquad (3\text{-}4.10)$$

The matched filter coefficients can be designed by maximizing (3-4.10). However, a more effective way to derive the matched filter design equation is to diagonalize the matrix R_{NN}.

[Step III] Diagonalize Output Signal to Noise Ratio:

Let A = the linear unitary transformation which diagonalizes the matrix R_{NN} which is equivalent to decorrelating the input clutter noise, i.e.,

$$A^* R_{NN} A^T = I \quad \text{and} \quad R_{NN}^{-1} = (A^T \cdot A^*) \qquad (3\text{-}4.11)$$

The new filter configuration is shown in Fig. 3-4. The resultant transformed input signal and noise are:

$$S' = A \cdot S \qquad (3\text{-}4.12)$$

$$N' = A \cdot N \qquad (3\text{-}4.13)$$

Let W' be the new transformed filter, then the output signal and noise voltages are

$$v_S = W'^T \cdot S' = W'^T \cdot A \cdot S \qquad (3\text{-}4.14)$$

$$v_N = W'^T \cdot N' = W'^T \cdot A \cdot N \qquad (3\text{-}4.15)$$

Comparison of (3-4.13) and (3-4.14) with (3-4.6) and (3-4.7), the relation between W and W' can be found as

$$W = A^T \cdot W' = W' A^T \qquad (3\text{-}4.16)$$

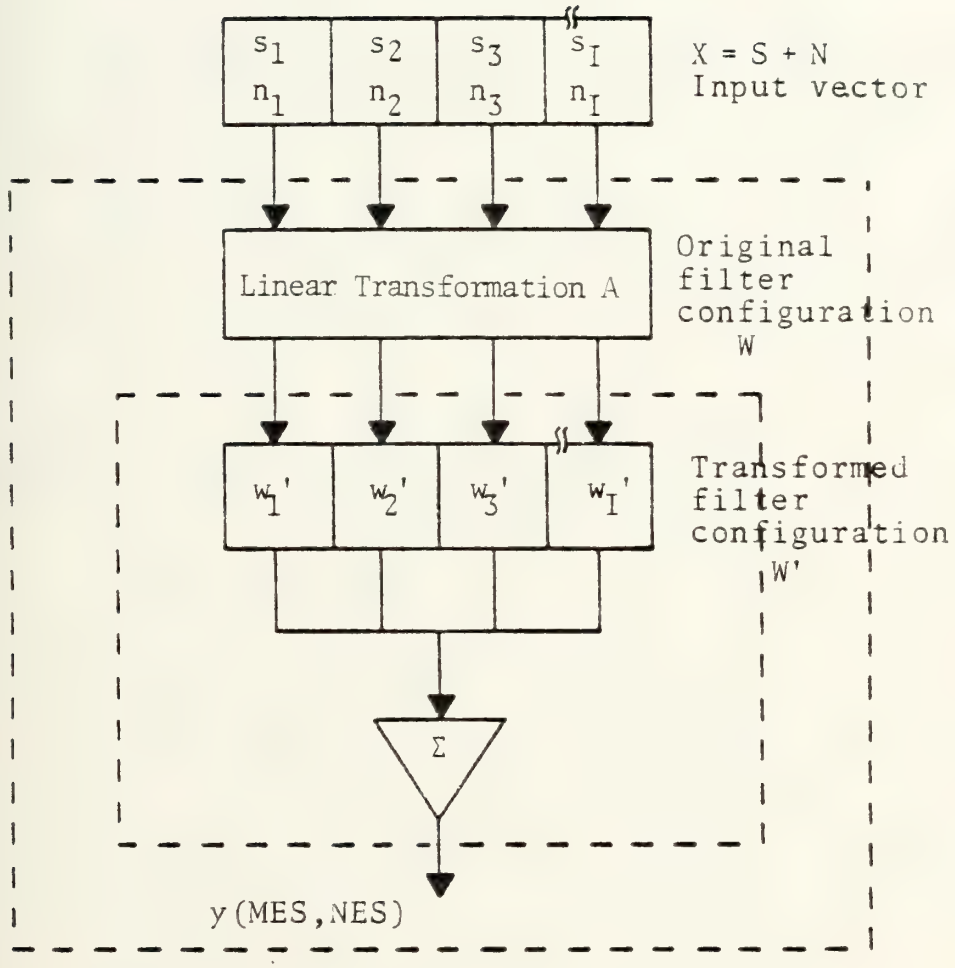

Figure 3-4 Original and Transformed Filter Configurations Used in the Derivation of Spatial Matched Filter Design Equation

The output noise power after the transformation is

$$P_n = E[|W'^T \cdot N'|^2] = E[W'^{*T} N'^* N'^T W']$$

$$= W'^{*T} E[N'^* N'^T] W' \qquad (3\text{-}4.17)$$

Since the transformation A diagonalized the R_{NN} and decorrelates the noise

$$E[N'^{*T} N'] = I \qquad (3\text{-}4.18)$$

and

$$P_n = W'^{*T} W' \qquad (3\text{-}4.19)$$

The output signal power after the transformation is

$$P_S = |v_S'|^2 \qquad (3\text{-}4.20)$$

Therefore, the output signal to noise ratio is

$$SNR_{out} = \frac{|v_S'|^2}{W'^{*T} W'} \qquad (3\text{-}4.21)$$

[Step IV] Equation of Matched Filter Design:

The design equation for the spatial matched filter is obtained by finding the maximum value for $(SNR)_{out}$. To accomplish this, the Cauchy Schwarz inequality is applied to [3-4.14).

$$|v_S|^2 \leq |W'^T|^2 |S'|^2 \qquad (3\text{-}4.22)$$

where

$$|W'|^2 = W'^{*T} W' \qquad (3\text{-}4.23)$$

$$|S'|^2 = |S'^{*T}||S'| \qquad (3\text{-}4.24)$$

$$\therefore (SNR)_{out} = \frac{|v_S|^2}{W'^{*T} W'} \leq |S'|^2 \qquad (3\text{-}4.25)$$

Therefore, the maximum output SNR is

$$(SNR)_{max} = |S'|^2 \tag{3-4.26}$$

It will be shown in the following that the special filter

$$W' = cS'^* \tag{3-4.27}$$

where c = an arbitrarily selected constant

will provide the maximum $(SNR)_{output}$. For this filter

$$v_S = cS'^T S' = c|S'|^2$$

$$p_n = c^2|S'|^2$$

$$(SNR)_{out} = \frac{|v_S|^2}{p_n} = |S'|^2 = (SNR)_{max}.$$

Thus, it has been shown that the special filter, $W' = cS'$, is the matched filter after the transformation of A. The matched filter itself is expressed by:

$$W_{MF} = A^T W' = A^T \cdot c \cdot S'^* = A^T \cdot c\ A^* S^*$$

$$= c\ A^T \cdot A^* S^*$$

Using the definition of (3-4.11)

$$\boxed{W_{MF} = c\ R_{NN}^{-1} \cdot S^*} \tag{3-4.28}$$

This is the design equation for the nonrecursive spatial matched filter. Using this matched filter, the maximum signal to noise ratio is:

$$SNR_{max} = S^T R_{NN}^{-1} S^* \tag{3-4.29}$$

It is worthwhile to note that the maximum output signal to noise ratio depends only on the target signal and clutter noise characteristics. In active systems, such as radar and communication systems, the signals can be designed to yield very high SNR. On the other hand, in passive systems, such as passive infrared and optical surveillance systems, the target signal can not be designed. The maximum SNR is given by (3-4.29).

2. Design Procedure of Spatial Matched Filter

To design a nonrecursive spatial matched filter, a procedure somewhat similar to that of the nonrecursive spatial MMSE filter is used. This is readily clear by comparing their design equations.

For MMSE filter: (Wiener filter) $$W_{WF} = (R_{NN} + R_{SS})^{-1} P \qquad (3\text{-}3.15)$$

For matched filter: $$W_{MF} = cR_{NN}^{-1} \cdot S^* \qquad (3\text{-}4.28)$$

A three step procedure is also used.

[Step I] Selection of c and Calculation of S*:

Although the selection of c is arbitrary from the viewpoint of matched filter design, its selection is important since its value will affect the threshold setting for target detection. This will be discussed in more detail in Chapter VI. In general, the value of c is chosen so that the filter coefficient corresponding to the estimation pixel is normalized to unity.

The determination of S* is very simple. Two examples will be given. For a point target as in Fig. 3-3.1.

$$S^{*T} = [0\ 0\ 0\ 0\ S\ 0\ 0\ 0\ 0].$$

For a horizontal line target as in Fig. 3-3.7(a).

$$S^{*T} = [0\ 0\ 0\ S\ S\ S\ 0\ 0\ 0]$$

where S = amplitude of target

Other types of targets can be handled in similar ways.

[Step II] Calculation of R_{NN}:

This is exactly the same as described in section B.2.

[Step III] Calculation of Filter Coefficients:

The filter coefficients are calculated by solving equation (3-4.28).

3. Processing Gain

The processing gain (PG) of the matched filter is derived in a way similar to the derivation in section B.3., using equation (3-3.24) as a generalized PG equation. For a point target, equation (3-3.25) can be used to determine the PG. When the constant c in the matched filter is selected as suggested in D.2., the PG of point target will simply become:

$$PG = \frac{1}{W^T \cdot R_{NN}^{\rho} \cdot W}$$

For a point target, assuming noise with zero mean, the P.G. can be shown to be independent of input SNR. Defining $S^T \triangleq s[0\ 0\ ..\ 1\ ..\ 0] = s \cdot S_I^T$ and $R_{NN}^{-1} \triangleq \frac{1}{\sigma^2} R_{NN\rho}^{-1}$ and substituting these definitions into eq. (3-4.29) yields:

$$PG = \frac{SNR_{(output)}}{SNR_{(input)}} = \frac{SNR_{max}}{SNR_{(input)}} = \frac{s^2 S_I^T \cdot R_{NN}^{-1} S_I}{s^2/\sigma^2} =$$

$$S_I^T R_{NN\rho}^{-1} S_I$$

This last expression of P.G. is independent of signal and noise power and depending only on the correlation factor of the correlated noise and the target location in the search box.

4. Results of Computer Simulation

Properties of nonrecursive spatial matched filters and their performance in clutter suppression and target detection when combined with the thresholding process were also investigated using computer simulation.

The items of investigation in terms of search box size, background clutter characteristics, target types, filter coefficients, performance figures of merits, are the same as in cases of nonrecursive spatial MMSE filters. They have been described in Section C.4. and will not be repeated here.

E. SUMMARY

Two types of statistical spatial filters were discussed in this chapter: the spatial MMSE filter and the spatial

matched filter. Both filters offer some signal processing advantages.

The MMSE filter, designed to minimize the mean square error, will offer the best spatial estimate of a given target.

The matched filter, designed to maximize output signal to noise ratio, will result in the best enhancement of SNR suitable for detection purposes.

It turns out that for the detection of a point target, both the MMSE and the matched filter offer the same processing gain. This will be shown in Chapter VI.

In general, the type of filter to be selected will be determined by the practical processing requirements for a given problem. For target enhancement and restoration techniques which require accurate estimation of the target's shape and intensity, the Wiener filter is preferred. For target detection requirements which allow distortion of target's shape and intensity, the matched filter is preferred.

IV. MULTIPLE FRAMES FOCAL PLANE PROCESSING FOR CLUTTER SUPPRESSION - NONRECURSIVE STATISTICAL TEMPORAL FILTER AND SPATIAL-TEMPORAL FILTERS

A. INTRODUCTION

If an imaging system can be stabilized or tracked to follow a scene, several successive frames of images can be used for various image processing purposes. Signals from multiple frames of images can be used in several ways. The simplest way is to use one pixel from each frame; signals of the same pixel from successive frames are used together in what amounts to temporal processing. A more involved way is to use several pixels from each frame; for example, signals from nine pixels in a 3x3 search box as developed in Chapter III are used together with signals of the same search box location from consecutive frames in what amounts to a combined spatial-temporal processing.

In this thesis, an intermediate process is developed. A spatial filter is first used to process several successive frames of images individually. Then, single pixels from each of these frames already processed by the spatial filters are used together to perform a temporal filtering. The spatial filters are designed by statistical criteria as presented in Chapter III. The temporal filter will be designed in a similar manner, using the same principle - that if the temporal noise is correlated, it can be suppressed by a

nonrecursive temporal filter designed either by a minimization of mean square error criterion or by a maximization of signal to noise ratio criterion. The objective of these temporal filters is the same as other focal plane processing techniques developed in this thesis, namely, signals from single frame and/or multiple frames of images are processed to suppress the background clutter so that weak targets buried in them can be pulled above the noise, thus enabling a threshold to be applied to initiate the target detection process.

In Section B, a class of nonstatistical, multiple frame focal plane processing techniques, called "frame differencing" techniques, are first presented. An analysis is then made of their effects on the statistical properties of the images. These nonstatistical techniques will be compared with the performance of statistical temporal filters developed in this thesis. In Section C, three dimensional statistical filters using multiple frames of images are developed. Specifically, a sequential combination of several spatial filters and one temporal filter is developed. In Section D, an accumulative implementation of the nonrecursive temporal filter is suggested which may simplify the memory requirements in hardware implementation. In Section E, computer procedures for investigation of these multiple frame, focal plane processing algorithms are described for both simulated images with prescribed statistical properties and real world images without a priori knowledge of their statistical properties.

However, the simulated results will not be presented in this chapter. They will be presented in Chapter VI, which includes the simulated results for both the single frame spatial filters and the multiple frame spatial-temporal filters.

B. NONSTATISTICAL TEMPORAL FILTERS - FRAME DIFFERENCING

1. Introduction

Multiple frame processing has been actively developed in the past few years for space surveillance applications, especially for those systems in which the image sensors platform is stabilized to cover the same area for certain periods of time. These systems are generally known as the staring, or step-staring, systems. In these systems, there is a great deal of correlation of background clutter among consecutive frames of images. A simple subtraction of two neighboring frames should eliminate completely, in principle, all background clutter. This is most effective in revealing those weak targets which are moving and do not dwell in the same pixel between two frames. However, in real world situations, sensor systems cannot be perfectly stabilized. Also, not all background clutter is stationary. An example is clouds which move. Consequently, simple subtraction of two neighboring frames is not adequate in many practical applications. More involved subtraction processes using

several frames of image have been developed. They are commonly known as the "Frame Differencing" methods [10].

"Single Differencing" using two frames =

$$F_1 - F_2$$

"Double Differencing" using three frames:

$$F_1 - 2F_2 + F_3 = (F_1 - F_2) - (F_2 - F_3)$$

"Third Differencing" using four frames:

$$F_1 - 3F_2 + 3F_3 - F_4 = (F_1 - 2F_2 + F_3) - (F_2 - 2F_3 + F_4)$$

"Fourth Differencing" using five frames:

$$F_1 - 4F_2 + 6F_3 - 4F_4 + F_5 = (F_1 - 3F_2 + 3F_3 - F_4) - (F_2 - 3F_3 + 3F_4 - F_5)$$

etc.

where F_i refers to the signal from the same pixel from the "i"th frame.

These "frame differencing" methods were developed from the simple concept that "non-moving" clutter can be cancelled out by frame to frame subtraction. The weighting factors for individual frames are fixed and are independent of the specific nature of the images. Since the statistical temporal filters to be developed in this chapter are designed according to the specific statistical properties of a given set of images, a statistical analysis of the standard "frame differencing" techniques will be made so that they can be compared with the statistical temporal filters developed in this chapter.

2. Statistical Analysis of First Differencing Technique

Since the same pixel location is used in "frame differencing" techniques, its coordinate (m,n) will not be used in the following analysis. Instead, a number k is used to describe the "k"th frame. In the following analysis, special attention is given to the jitter problem which is modeled by a random noise component from frame to frame, i.e.,

$$x(k+1) = \alpha x(k) + \beta n(0,1) \qquad (4\text{-}1)$$

where α,β are two constants

$n(0,1)$ = a Gaussian noise component of zero mean and unity variance

$x(k)$ = background clutter level at a given pixel in the k-th frame

$x(k+1)$ = background clutter level at that pixel in the (k+1)-th frame

In eq. (4-1) it is assumed that the noise intensity at a pixel in the (k+1) frame is proportional to the intensity in the same pixel at frame (k) with proportionally constant α. The second term in eq. (4-1) represents the noise added to that pixel due to the sensor jitter.

The constants α,β can be rewritten in different forms compatible with the notation used in the Markov model in Appendix A.

$$x(k+1) = \rho_K x(k) + \sigma_K \sqrt{1-\rho_K^2}\, n(0,1) \qquad (4\text{-}2)$$

where $\alpha = \rho_K$ = temporal correlation factor

$\beta = \sigma_K \sqrt{1-\rho_K^2}$

σ_K = temporal standard deviation.

In the following, the statistical properties of the first differencing method will be derived.

Let $z(k)$ = first differenced signal

$$= x(k) - x(k+1)$$

$$= (1-\rho_K)\, x(k) - \sigma_K\sqrt{1-\rho_K}^{\,2} \cdot n(0,1) \qquad (4\text{-}3)$$

The mean of $z(k)$ is zero since $\bar{x}(k) = \bar{x}(k-1)$, (4-4)

where the symbol $\bar{x}$ is the expected value of x, $E(x)$, taken by averaging over the two dimensional image. The variance of $z(k)$ is

$$E[z^2(k)] = E[(1-\rho_K)^2 x(k)^2 + \sigma_K^2(1-\rho_K^2)\, n^2(0,1)$$

$$+ 2(1-\rho_K)x(k)\sigma_K\sqrt{1-\rho_K}^{\,2}\, n(0,1)]$$

$$= (1-\rho_K)^2\sigma_X^2 + \sigma_K^2(1-\rho_K^2)\sigma_n^2 + E[X(K)n(0,1)]\cdot\text{constant}$$

The last term is zero because $x(k)$ and $n(0,1)$ are assumed to be uncorrelated and since $n(0,1)$ has zero mean.

$$E[z^2(k)] = \sigma_X^2(1-\rho_K)^2 + \sigma_K^2(1-\rho_K^2)\sigma_n^2 .$$

Since the variance of $n(0,1)$ is unity,

$$E[z^2(k)] = \sigma_X^2(1-\rho_K)^2 + \sigma_K^2(1-\rho_K^2) \qquad (4\text{-}5)$$

where σ_K^2 = temporal variance

σ_X^2 = variance in one frame

when $\sigma_X = \sigma_K = \sigma$

$$E[z^2(k)] = \sigma^2\, w(1-\rho) \qquad (4\text{-}6)$$

3. Figure of Merit for Frame Differencing - Processing Gain

A figure of merit, "processing gain," is defined to describe the performance of frame differencing. The same definition is used for processing gain for all filter techniques developed in this thesis.

$$PG = \frac{(S/N)_0^2}{(S/N)_i^2} \tag{4-7}$$

where $(S/N)_0^2 \triangleq$ output power signal to noise ratio

$(S/N)_i^2 \triangleq$ input power signal to noise ratio.

The "signals" considered in this thesis are point target signals. In this chapter, it is assumed that these point target signals move at least one pixel from one frame to the next.

Let S_1^2 = signal power in the first frame pixel = S^2

S_2^2 = signal power in the same pixel in the second frame

= 0 because the target has moved away

$\therefore S_{out}^2$ = output signal power = $S_1^2 - S_2^2 = S^2$

S_{input}^2 = input signal power = $S_1^2 = S^2$

The input noise power is

$$N_i^2 = \sigma_X^2 + \mu_X^2$$

where σ_X^2 = input noise variance

μ_X^2 = input noise mean power

The output noise power is

$$N_0^2 = E[z^2] = \sigma_X^2(1-\rho_X)^2 + \sigma_K^2(1-\rho_K)^2$$

with zero mean as shown by (4-5)

Therefore, the processing gain is

$$PG = \frac{(S/N)_o^2}{(S/N)_i^2} = \frac{\dfrac{S^2}{\sigma_X^2(1-\rho_K)^2 + \sigma_K^2(1-\rho^2)}}{\dfrac{S^2}{\sigma_X^2 + \mu_X^2}}$$

$$PG = \frac{1+\left(\dfrac{\mu_X}{\sigma_X}\right)^2}{(1-\rho_K)^2 + \left(\dfrac{\sigma_K}{\sigma_X}\right)^2 (1-\rho_K^2)} \qquad (4-8)$$

For the special case of $\sigma_K = \sigma_X = \sigma$

$$PG = \frac{1 + \left(\dfrac{\mu_X}{\sigma}\right)^2}{2(1-\rho_K)} \qquad (4-9)$$

This "first differencing" processing gain will be used in section C.2 when it is compared with the processing gain of statistical spatial-temporal filters.

C. STATISTICAL SEQUENTIAL SPATIAL-TEMPORAL FILTERS

In this section, a three dimensional statistical filter is developed. It consists of a sequential application of several spatial filters to successive frames of images followed by a temporal filter using these processed images. In contrast, another three dimensional filter processing signals from several frames of image all at once will be presented in the next section, D.

1. Filter Configuration

The configuration of the sequential spatial-temporal filter is presented in Fig. 4-1. Its operation is described as follows: K frames of images consist of point targets contaminated by background noise.

Step I - Spatial Filters for K Frames:

The detailed design procedure for spatial filters have been presented in Chapter III. The highlights of their operation will be repeated here for completeness of the description of sequential spatial-temporal filters.

[Unprocessed Signal]

A two dimensional array of unprocessed signals in a selected search box around the estimation pixel (m,n) is taken from each frame.

$$X(m,n) = X_j = \begin{bmatrix} x_{11}, x_{12}, \cdots x_{1,MSB} \\ x_{21}, x_{22}, \cdots x_{2,MSB} \\ \vdots \\ x_{NSB,1}, \cdots x_{NSB,MSB} \end{bmatrix} \qquad (4\text{-}10)$$

This two dimensional array of data is represented by a one dimensional vector.

$$X = X_j = [x_1, x_2, \ldots x_i \ldots x_I] \qquad (4\text{-}11)$$

$$j = MMAX(n-1) + m$$

$$n = 1, \ldots NMAX$$

$$m = 1, \ldots MMAX$$

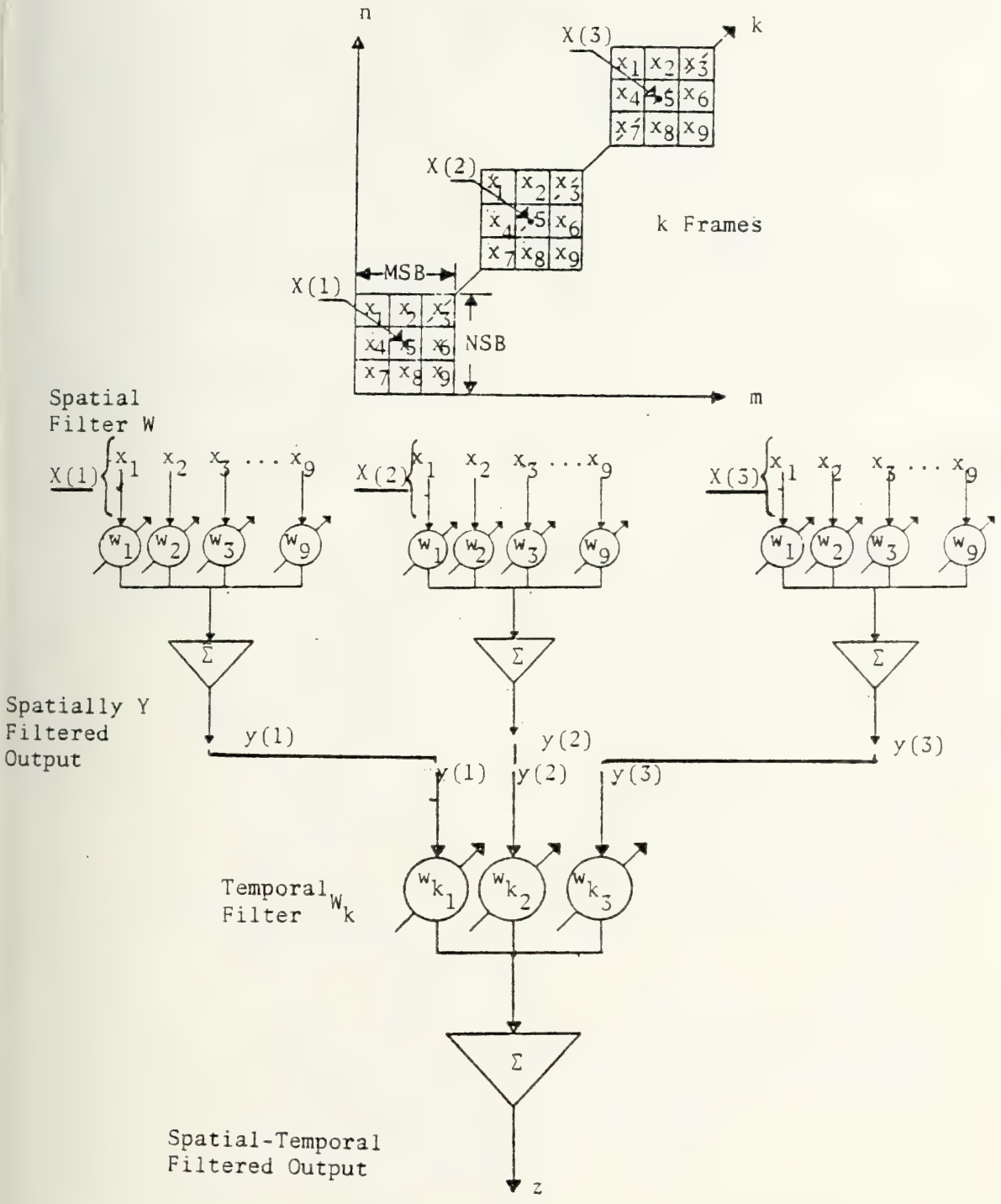

Figure 4-1 Configuration of Nonadaptive Three Dimensional Nonrecursive Sequential Spatial-Temporal Filter

$$i = MSB\cdot(\Delta n-1) + \Delta m$$

$$\Delta n = 1,\ldots,NSB$$

$$\Delta m = 1,\ldots,MSB$$

$$I = NSB\cdot MSB$$

as presented in Fig. 4-2.

The unprocessed signal X contains target signals

$$S = [s_1, s_2, \cdots, s_I] \tag{4-12}$$

and clutter noise

$$N = [n_1, n_2, \cdots, n_I] \tag{4-13}$$

[Spatial Filter]

A linear two dimensional filter is described by a two dimensional array of weighting coefficients

$$W(m,n) = \begin{bmatrix} w_{11}, w_{12}, \cdots, w_{1,MSB} \\ w_{21}, w_{22}, \cdots, w_{2,MSB} \\ \vdots \\ w_{NSB,1} \cdots, w_{NSB,MSB} \end{bmatrix} \tag{4-14}$$

It can be described also by a one dimensional vector

$$W = W(i) = [w_1\ w_2, \cdots, w_I] \tag{4-15}$$

These filter coefficients can be designed either by the minimization of mean square error criteria or by the maximization of signal to noise ratio criteria.

[Spatial-Filter Output]

The output of the spatial filter is

$$y(m,n) = y = W\cdot X^T \tag{4-16}$$

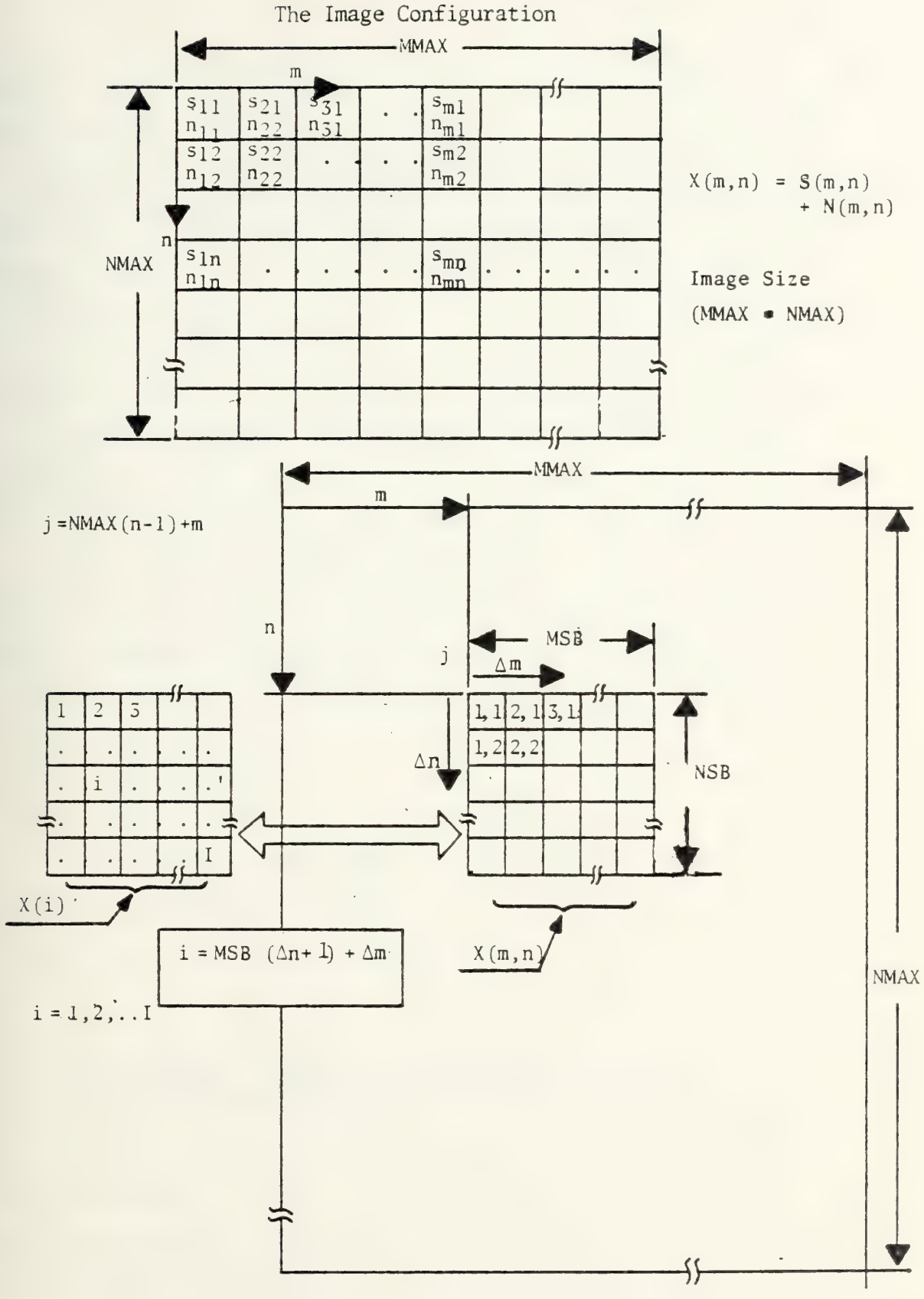

Figure 4-2(a) Coordinate System for the Image
(b) Coordinate System for the Spatial Filter

Step II - Temporal Filter:

[Input Signal]

Filtered signals at the same pixel location (m,n) of K frames are put together to form the input signal to the temporal filter.

$$Y = [y_1, y_2, \cdots, y_K] \tag{4-17}$$

[Temporal Filter]

A linear one dimensional filter is described by a one dimensional vector.

$$W_K = W_K(m,n) = [w_{K1}, w_{K2}, \cdots, w_{KK}] \tag{4-18}$$

The filter coefficients are designed by the same procedures used for spatial filters by following either the minimization of mean square error criterion or the maximization of signal to noise ratio criterion.

[Combined Spatial-Temporal Filter Output]

The final processed signal at pixel (m,n) after the sequential application of K spatial filters and one temporal filter using K frames is described by

$$z(m,n) = Y \cdot W_K^T \tag{4-19}$$

2. Statistical Analysis of Two Frame Sequential Spatial-Temporal Filter

A statistical analysis of the two frame sequential spatial-temporal filter will be analyzed first so that it can be compared with the result of the nonstatistical first differencing method analyzed in Section B.

The analysis of the more general K frame sequential spatial-temporal filters will be presented in the next section.

a. Statistical Model of Two Frame Single Differencing:

The outputs from the spatial filtering are described by:

$$y(1) = X(1)\cdot W^T \quad \text{where } X(1) \text{ denotes } X \text{ of frame (1)}$$

$$y(2) = X(2)\cdot W^T \quad \text{where } X(2) \text{ denotes } X \text{ of frame (2)}$$

In matrix form, they are

$$Y^T = \begin{bmatrix} y(1) \\ y(2) \end{bmatrix} = \left[\begin{array}{c|c} W & 0 \\ \hline 0 & W \end{array}\right] \left[\begin{array}{c} X^T(1) \\ \hline X^T(2) \end{array}\right] \tag{4-20}$$

To calculate the noise power of the final output, the covariance of the spatial filtered image, R_{YY}, is needed. Using (4-20):

$$R_{YY} = E[Y^T \cdot Y]$$

$$= \left[\begin{array}{c|c} W & 0 \\ \hline 0 & W \end{array}\right] \left[\begin{array}{c} X^T(1) \\ \hline X^T(2) \end{array}\right] \left[\begin{array}{c} X(1) \\ \hline X(2) \end{array}\right] \left[\begin{array}{c|c} W^T & 0 \\ \hline 0 & W^T \end{array}\right]$$

$$= \left[\begin{array}{c|c} W & 0 \\ \hline 0 & W \end{array}\right] \left[\begin{array}{c|c} R_{XX}(1,1) & R_{XX}(1,2) \\ \hline R_{XX}(2,1) & R_{XX}(2,2) \end{array}\right] \left[\begin{array}{c|c} W^T & 0 \\ \hline 0 & W^T \end{array}\right] \tag{4-21}$$

where $R_{XX}(i,j) = E[X^T(i)X(j)]$ = covariance of [X] (4-22)

It is assumed that both X and Y have zero mean and that frame (1) and frame (2) statistical properties are the same. Therefore:

$$R_{XX}(1,1) = R_{XX}(2,2) = R \tag{4-23}$$

Using the first order Markov model, as in section IV.B.2, (4-2) the temporal statistical characteristics are:

$$X^T(2) = \rho_K I \cdot X^T(1) + I \cdot \sigma_K \sqrt{1 - \rho_K^2}\, n(0,1) \qquad (4\text{-}24)$$

where I is the unity matrix.

Multiplying (4-24) by X(1) and taking the expected value yields:

$$E[X^T(2) \cdot X(1)] = E\{[\rho_K I\, X^T(1) + I\, \sigma_K \sqrt{1-\rho_K^2}\, n(0,1)]X(1)\}$$

$$R_{XX}(2,1) = \rho_K \cdot E[X^T(1)X(1)] + I\ \sigma_K \sqrt{1-\rho_K^2}\, n(0,1)X(1) \qquad (4\text{-}25)$$

The second term is zero since n is Gaussian with zero mean and is not correlated with X(1). Therefore,

$$R_{XX}(2,1) = R_{XX}(1,2) = \rho_K E[X^T(1)X(1)] = \rho_K R_{XX} \qquad (4\text{-}26)$$

Substituting back into (4-21),

$$R_{YY} = \left[\begin{array}{c|c} W & 0 \\ \hline 0 & W \end{array}\right] \left[\begin{array}{c|c} R_{XX} & \rho_K R_{XX} \\ \hline \rho_K R_{XX} & R_{XX} \end{array}\right] \left[\begin{array}{c|c} W^T & 0 \\ \hline 0 & W^T \end{array}\right]$$

$$= \left[\begin{array}{c|c} W\ R_{XX}\ W^T & \rho_K W\ R_{XX}\ W^T \\ \hline \rho_K W\ R_{XX}\ W^T & W\ R_{XX}\ W^T \end{array}\right] \qquad (4\text{-}27)$$

$W\ R_{XX}\ W^T = \sigma_Y^2$ is the noise variance of spatial filtered images since

$$\sigma_Y^2 = E[y \cdot y] = E[(WX^T)(WX^T)] = E[W \cdot X^T \cdot X \cdot W^T]$$

$$= W \cdot E[X^T \cdot X] \cdot W^T = W \cdot R_{XX} W^T$$

Therefore,

$$R_{YY} = \begin{bmatrix} \sigma_Y^2 & \rho_K \sigma_Y^2 \\ \rho_K \sigma_Y^2 & \sigma_Y^2 \end{bmatrix} = \sigma_Y^2 \cdot \begin{bmatrix} 1 & \rho_K \\ \rho_K & 1 \end{bmatrix} \qquad (4\text{-}28)$$

b. Statistical Analysis of Two Frame Single Differencing

The temporal filter W_K used in this analysis is the simple first differencing operation, so that the temporal filtered output is:

$$W_K = [1, -1]$$

$$z = [1, -1] \cdot \begin{bmatrix} y(1) \\ y(2) \end{bmatrix} = y(1) - y(2) = W_K Y^T \qquad (4\text{-}29)$$

The variance of z is:

$$z^2 = E[z^2] = E[W_K \cdot Y^T \cdot Y \cdot W_K^T] = W_K E[Y^T \cdot Y] W_K^T \qquad (4\text{-}30)$$

Substituting (4-28) into (4-30) will yield:

$$\sigma_z^2 = W_K \cdot R_{YY} \cdot W_K^T = [1, -1] \sigma_Y^2 \begin{bmatrix} 1 & \rho_K \\ \rho_K & 1 \end{bmatrix} \begin{bmatrix} 1 \\ -1 \end{bmatrix}$$

$$= \sigma_Y^2 2(1 - \rho_K) \qquad (4\text{-}31)$$

It can be shown that the same result is true for a sequential filter by applying first the temporal differencing followed by the spatial filtering.

c. Processing Gain

It will be assumed again that the target signals are point targets which move at least one pixel from one frame to the next, so that

$$s(1) = s$$

$$s(2) = 0$$

as in IV.B.3.

Therefore,

$$s_{in} = s$$

$$s_{out} = s(1) - s(2) = s$$

The input noise power is given by

$$N_{in}^2 = \sigma_X^2 \quad \text{assuming X has zero mean.}$$

The output noise power is given by (4-31).

Finally, the processing gain is:

$$PG = \frac{\frac{s^2}{\sigma_Y^2 2(1-\rho_K)}}{\frac{s^2}{\sigma_X^2}} \quad \frac{\sigma_X^2}{\sigma_Y^2 2(1-\rho_K)}$$

$$= \frac{\sigma_X^2}{\sigma_Y^2} \frac{1}{2(1-\rho_K)} = \frac{1}{W R_{XX}^{\rho} W^T} \cdot \frac{1}{2(1-\rho_K)}$$

= (PG of spatial filter)·(PG of first temporal differencing) (4-32)

using the relation $R_{XX} = \sigma_X^2 R_{XX}^{\rho}$.

(4-32) shows that the processing gain of the sequential spatial-temporal differencing is a product of two individual

processing gains whereas the temporal differencing alone possesses only the PG related to the second term in eq. (4-32).

3. Statistical Analysis of K Frame Sequential Spatial-Temporal Filter

In this section, a more general K frame sequential spatial-temporal filter is analyzed. In this case, the temporal filter used is designed by a statistical process instead of the nonstatistical "first differencing" temporal filter used in the previous section.

a. Statistical Analysis of Spatial Filters of Different Frames

The input temporal signal from K successive frames is described by spatially filtered output Y where:

$$Y = [y_1, y_2, \cdots y_K]$$

which results from applying spatial filters to K frames of unprocessed signal X.

$$\begin{matrix} y(1) \\ y(2) \\ \vdots \\ y(K) \end{matrix} = \begin{bmatrix} W & 0 & 0 & 0 & X^T(1) \\ 0 & W & & 0 & \vdots \\ & & W & & \vdots \\ 0 & & & W & X^T(K) \end{bmatrix} \qquad (4\text{-}33)$$

or,

$$Y^T = \tilde{W}\,\tilde{X}^T \qquad (4\text{-}34)$$

Again, the covariance of Y is needed for calculating the noise power of the images processed by the spatial filters.

If we assume Y has zero mean,

$$R_{YY} =$$

$$\text{Covariance } [Y] = E[Y^T \cdot Y] = E[\tilde{W} \cdot \tilde{X}^T \cdot \tilde{X} \cdot \tilde{W}^T]$$

$$= \tilde{W} \cdot E[\tilde{X}^T \cdot \tilde{X}] \tilde{W}^T \qquad (4\text{-}35)$$

$$= \tilde{W}\, \tilde{R}_{XX}\, \tilde{W}^T$$

The same first order Markov model is used for the correlation of two successive frames.

$$X^T(K) = \rho_K\, I\, X^T(K-1) + I\, \sigma_K \sqrt{(1-\rho_K{}^2)}\, n(0,1)$$

Therefore, similar to eqs. (4-25) and (4-26),

$$E[X^T(K) \cdot X(K-1)] = \rho_K\, R_{XX} \qquad (4\text{-}36)$$

Similarly, it can be shown that

$$E[X^T(K)\, X\,(K-2)] = \rho_K{}^2\, R_{XX}$$

In general,

$$E[X^T(K)\, X\,(K-j)] = \rho_K{}^j\, R_{XX} \qquad (4\text{-}37)$$

Substituting (4-37) into (4-35) and using the following two relations -

$$R_{YY} = \tilde{W} \cdot \begin{bmatrix} R_{XX} & \rho_K R_{XX} & \rho_K{}^2 R_{XX} & \cdots & \rho_K{}^{K-1} R_{XX} \\ \rho_K R_{XX} & R_{XX} & \rho_K R_{XX} & & \rho_K{}^{K-2} R_{XX} \\ \vdots & & & & \\ \rho_K{}^{K-1} R_{XX} & \cdots & \cdots & & R_{XX} \end{bmatrix} \cdot \tilde{W}^T \qquad (4\text{-}38)$$

and

$$\sigma_Y{}^2 = W \cdot R_{XX} W^T = \text{variance of spatial filtered image.}$$

$$R_{YY} = \sigma_Y^2 \begin{bmatrix} 1 & \rho_K & \rho_K^2 & \cdots & \rho_K^{K-1} \\ \rho_K & 1 & \rho_K & \cdots & \rho_K^{K-2} \\ \vdots & & & & \\ \rho_K^{K-1} & \cdots & \cdots & \cdots & 1 \end{bmatrix}$$

or

$$R_{YY} = \sigma_Y^2 R_{YY}^{\rho K} \tag{4-38}$$

b. Statistical Analysis of Temporal Filters

Similar to the spatial filter cases in Chapter III, two statistical criteria can be applied to design the temporal filter.

If the minimization of mean square error criterion is used,

$$W_K = [R_{YYK}]^{-1} P_K \tag{4-39}$$

where $R_{YYK} = R_{NNK} + R_{SSK}$

R_{NNK} = covariance $[N_K]$

R_{SSK} = covariance $[S_K]$

$P_K = E[Y \cdot S_K]$

As before, target signal and clutter noise are assumed to be uncorrelated.

If the maximization of signal to noise ratio criterion is used,

$$W_K = C[R_{NNK}]^{-1} S_K^* \tag{4-40}$$

where C = selected constant

S_K = target signal vector in the same pixel along K frames

$= [s_{K1}, s_{K2}, \cdot\cdot s_{Kk}, \cdot\cdot s_{KK}]$ where k = 1, 2, ... K

The final output of the sequential spatial-temporal filter is

$$z = Y \cdot W_K^T$$

The noise output power of z is given by

$$\sigma_z^2 = W_K \cdot R_{YY} \cdot W_K^T = W_K \cdot R_{YY}^{\rho k} \cdot W_K^T \sigma_Y^2 \qquad (4\text{-}41)$$

c. Processing Gain

Assuming again that the target signals move at least one pixel from one frame to the next -

$$s_{out} = W_K \cdot S_K$$

where $S_K = [0,0,...s,000..]$ for a moving point target.

In most applications of point target detection,

$s_{out} = S = s_{in}$

N_{in}^2 = one frame input noise power = σ_X^2

N_{out}^2 = output noise power after multiple frame filtering = σ^2

$$PG = \frac{(S/N)^2_{out}}{(S/N)^2_{in}} = \frac{\frac{S^2}{\sigma_z^2}}{\frac{S^2}{\sigma_X^2}} = \frac{\sigma_X^2}{\sigma_z^2} \qquad (4\text{-}42)$$

where $\sigma_z^2 = W_K \cdot R_{YY} \cdot W_K^T = \sigma_Y^2 \cdot W_K \cdot R_{YY}^{\rho k} \cdot W_K^T$

$$\sigma_Y^2 = W \cdot R_{XX} W^T = \sigma_X^2 \cdot W \cdot R_{XX}^{\rho k} \cdot W^T$$

$$\therefore \sigma_z^2 = \sigma_X^2 [W \cdot R_{XX}^{\rho} \cdot W^T][W_K \cdot R_{YY}^{\rho k} \cdot W_K^T]$$

Finally,

$$PG = \frac{1}{(W \cdot R_{XX}^{\rho} \cdot W^T)} \cdot \frac{1}{(W_K \cdot R_{YY}^{\rho k} \cdot W_K^T)} \qquad (4\text{-}43)$$

= (PG of spatial filter)(PG of temporal filter)

D. AN EFFECTIVE WAY OF HARDWARE IMPLEMENTATION OF SEQUENTIAL SPATIAL-TEMPORAL FILTER

In the previous section, a special class of a three dimensional spatial-temporal filter was developed in which nonrecursive spatial filtering and nonrecursive temporal filter were carried out sequentially. They are described by the following operations.

$$\left.\begin{aligned} y(1) &= \sum_{i=1}^{I} x(i,1)w(i,1) = X(1)\, W^T \\ y(2) &= \sum_{i=1}^{I} x(i,2)w(i,2) = X(2)\, W^T \\ &\vdots \\ y(K) &= \sum_{i=1}^{I} x(i,K)w(i,K) = X(K)\, W^T \end{aligned}\right\} \quad \text{Spatial}$$

$$z = \sum_{k=1}^{K} y(k)\, w_K(k) = Y\, W_K^T \quad \text{Temporal}$$

In general form,

$$z = \sum_{k=1}^{K} w_K(k) \sum_{m=1}^{MSB} \sum_{n=1}^{NSB} w(m,n)x(m,n)$$

This type of nonrecursive processing requires the memory of all K frames of image data.

It might be possible to implement this type of three dimensional filter by only using one frame of memory and updating its signals in a recursive manner as follows:

$$z(k) = z(k-1) + w_K(k) \sum_{m=1}^{MSB} \sum_{n=1}^{NSB} w(m,n)x(m,n)$$

This approach of combining a recursive implementation of nonrecursive temporal filter with nonrecursive spatial filter could be used when the temporal filter is designed by other criteria, such as by the Kalman filter approach, instead of the MMSE filter and matched filter approaches developed in this thesis. This recursive approach is suggested as a method to be developed in possible future work.

E. COMPUTER SIMULATION PROCEDURE FOR EVALUATING SEQUENTIAL SPATIAL-TEMPORAL FILTERS

The three dimensional sequential spatial-temporal filters have been evaluated by computer simulation using two types of images:

a. Simulated images using Markov model clutter noise

b. A real world infrared image.

The results will be presented in detail in Chapter VI. In the following, software procedures for evaluation of these two types of images will be presented.

1. Markov Model Simulated Images

The following steps are used.

a. Generate a two dimensional stochastic field with specified statistical properties to simulate the background clutter (Appendix A).

b. Add a set of targets in the clutter to form an image.

c. Generate K frames of images with specified temporal statistical properties.

d. Design spatial filter and then temporal filters according to either MMSE or matched filter criteria, optimized to the assumed clutter statistics and target characteristics.

e. Apply sequentially the spatial filter and temporal filter to suppress the clutter and to enhance the targets and evaluate the processing gain.

f. Calculate a threshold setting according to a specified probability of false alarm assuming that the probability density function of the filtered image is Gaussian.

g. Apply the threshold to separate targets from residual clutter.

2. Real World Infrared Images of Background Clutter

Because the statistical properties are inherent in the images, no computer simulated clutter is needed. The following steps are used.

a. Read the k-th frame, calculate its statistical spatial properties such as mean, variance, probability density function and covariance matrix. The exact calculation method is presented in Ref. [30].

b. Design statistical spatial filters according to either the MMSE filter criterion or the matched filter criterion.

c. Add a set of targets to the given infrared images.

d. Apply the spatial filter, evaluate the processing gain, and store the processed k-th frame. The detailed procedure can be found in Ref. [30].

e. Repeat steps (a) to (d) for all the K frames.

f. Calculate the statistical temporal properties of selected pixel locations from all K frames of spatially filtered data.

g. Design a statistical temporal filter according to either the MMSE filter criterion or the matched filter criterion.

h. Apply the temporal filter, calculate the mean and the variance of the filtered image and evaluate the processing gain.

i. Calculate a threshold setting for a specified probability of false alarm using the method to be described in Chapter V because the probability density function is generally non-Gaussian.

j. Apply the threshold to separate targets, false alarms from residual clutter noise.

F. SUMMARY

Three dimensional focal plane processing methods are very effective in background clutter suppression because the processing gains of spatial and temporal filters are multiplicative. A combination of spatial and temporal filtering should always improve the total processing gain. Furthermore, if the temporal clutter noise is highly correlated, which usually is true if the drift and/or jitter between successive frames is small, the processing gain of a temporal filter is usually higher than that of the spatial filters. An example will be presented in Section F of Chapter VI.

In this chapter, the configuration, design procedure and performance analysis of nonstatistical "frame differencing" temporal filters developed elsewhere [10] were first presented, followed by the sequential statistical spatial-temporal filters developed in this thesis. It was found that the sequential spatial temporal filtering technique, when applied on real IR images, offers indeed superior processing gain compared to either spatial filtering or frame differencing.

V. TARGET DETECTION IN FOCAL PLANE PROCESSING

A. INTRODUCTION

In most infrared images, targets are deeply buried in noise which consists of strong background clutter noise and other random noise. The targets can be as weak as 70 to 80 db below clutter. Predetection processing must be used to suppress the clutter to the point that "target" signal to "clutter" noise ratio is adequate for target detection. This was discussed in Chapters III and IV.

Target detection usually consists of several steps. The first step is "thresholding" which is the subject of this chapter. This is used to separate targets from noise remaining after the predetection processing. Since both target signals and noise after filtering are statistical quantities, it is generally difficult to clearly separate targets from noise except in rare occasions when the signal to noise ratio is very high. In most cases, the intensities of targets and noise overlap. Any selection of threshold will miss some targets and include some noise (false alarms). There is always a compromise between a complete detection of targets by using a low threshold at the expense of including many false alarms, and a complete elimination of false alarms by using a high threshold but at the expense of missing many of the targets. Two figures of merit are normally defined to

describe the false alarm and target detection. They are the probability of false alarm (P_{FA}) and probability of detection (P_D).

A target detection process involves five types of related information:

1. The PDF of filtered targets and noise (PDF is probability density function)
2. Signal to noise ratio - SNR
3. Threshold level
4. P_{FA}
5. P_D

Their relationships to detection have been very well developed in radar, sonar and elsewhere [31-33]. In this chapter, the one dimensional detection procedure is extended in a straightforward way to two dimensions for application to focal plane processing problems.

B. PREDETECTION FOCAL PLANE PROCESSING FOR CLUTTER SUPPRESSION

Clutter suppression is one of the most important processing steps before the thresholding for target detection. Statistical spatial filter and spatial-temporal filters have been developed in Chapters III and IV respectively. Their important steps and statistical descriptions will be reviewed and summarized in this section.

1. Statistical Properties of Unprocessed Image

The unprocessed image data taken from a two dimensional detector array of $\Delta m \times \Delta n$ pixels are described by:

$$X = \begin{matrix} x_{11}, x_{21} \cdots x_{MSB,1} \\ \vdots \qquad\qquad \vdots \\ x_{1,NSB} \cdots x_{MSB,NSB} \end{matrix}$$

In this study, this two dimensional array is written as a one dimensional vector for ease of programming in processing software.

$$X = X(i) = [x_1, x_2, \ldots x_I] \tag{5-1}$$

where $i = MSB \cdot (\Delta n - 1) + \Delta m$ $\quad \Delta m = 1, 2, \ldots . MSB$, $\Delta n = 1, 2, \ldots . NSB$

This transformation was previously presented in Fig. 3-2. The unprocessed image is considered to be the sum of target signals

$$S = S(i) = [s_1, s_2, \ldots, s_I] \tag{5-2}$$

and background clutter noise

$$N = N(i) = [n_1, n_2, \ldots, n_I] \tag{5-3}$$

Target signals can be either deterministic or statistical. It is assumed that their spatial shapes are deterministic such as point target or line targets of various orientations. Their intensity amplitudes may be deterministic or statistical with Gaussian probability density functions assumed. Deterministic targets are described by the vector -

$$S = [s_1, s_2, \ldots, s_I]$$

Statistical targets are described by several statistical characteristics:

$$\text{Mean vector} = \mu_S = [\mu_{S1}, \mu_{S2}, \cdots \mu_{SI}] \tag{5-4}$$

$$\text{Covariance matrix} = R_{SS} = E[(S^T - \mu_S^T)(S - \mu_S)] \tag{5-5}$$

$$\text{Variance} = \sigma_S^2 \tag{5-6}$$

$$\text{Autocorrelation function} = Q_S \tag{5-7}$$

The background clutter is statistical and described by the following characteristics:

$$\text{Mean vector} = \mu_N = [\mu_{N1}, \mu_{N2}, \cdots \mu_{NI}] \tag{5-8}$$

$$\text{Covariance matrix} = R_{NN} = E[(N^T - \mu_N^T)(N - \mu_N)] \tag{5-9}$$

$$\text{Variance} = \sigma_N^2 \tag{5-10}$$

$$\text{Autocorrelation function} = Q_N \tag{5-11}$$

In computer simulated images, the clutter noise is described by either the first order or the second order Markov models described in Appendix A, and the PDF is assumed to be Gaussian.

2. Single Frame Processing - Nonrecursive Statistical Spatial Filters

Two nonrecursive statistical linear spatial filters were developed to process the image signal X.

The filter is described by its filter coefficient vector:

$$W = [w_1, w_2, \cdots w_I] \tag{5-12}$$

The coefficients can be designed by two criteria. A minimization of mean square error led to the spatial MMSE (or Wiener) filter. A maximization of output signal to noise ratio led to the spatial matched filter.

The filtered output is described by:

$$y = X\ W^T \tag{5-13}$$

which contains both the filtered target signal y_S and filtered clutter noise y_N.

The filtered statistical targets are described by the following statistical characteristics:

$$\text{Mean} = \mu_{Y_S} = \mu_S \cdot W^T \tag{5-14}$$

$$\text{Variance} = \sigma^2_{Y_S} = W \cdot R_{SS} \cdot W^T \tag{5-15}$$

The filtered deterministic targets are simply described by their intensities.

$$y_S = S \cdot W^T \tag{5-16}$$

The filtered clutter noise is described by the following statistical characteristics:

$$\text{Mean} = \mu_{Y_N} = \sum_1^I w(i)\mu_N(i) = \mu_N \cdot W^T \tag{5-17}$$

$$\text{Variance} = \sigma^2_{Y_N} \tag{5-18}$$

$$= E[(y_N - \mu_{Y_N})^T (Y - \mu_{Y_N})] = E[W(N-\mu_N)^T (N-\mu_N) W^T]$$

$$= W\ E[(N - \mu_N)^T (N - \mu_N)] W^T$$

$$= W\ R_{NN}\ W^T$$

3. Multiple Frame Processing - Nonrecursive Statistical Spatial-Temporal Filters

In multiple frame processing, a one dimensional temporal filter W_K is added to the two dimensional spatial filters W. In this thesis, spatial filtering is performed first on several frames of images. It is then followed by temporal filtering of the spatial-filtered images using signals from the same pixel location from several consecutive frames. This set of time-varying signals is described by the vector

$$Y_K = [y_1, y_2, \cdots y_K] \tag{5-19}$$

Y_K consists of target signals -

$$S_K = [s_{K1}, s_{K2}, \cdots s_{KK}] \tag{5-20}$$

and correlated temporal noise -

$$N_K = [n_{K1}, n_{K2}, \cdots n_{KK}] \tag{5-21}$$

In the computer simulations reported later, only the first order Markov model is used for correlated temporal noise. The temporal filter is described by:

$$W_K = [w_{K1}, w_{K2}, \cdots w_{KK}] \tag{5-22}$$

The output spatial-temporal filtered image is described by:

$$z = Y_K \cdot W_K^T \tag{5-23}$$

Again, z also has its target components and clutter noise components.

The spatial-temporal filtered target signals are described by:

$$\text{The signal intensity} = z_S = S_K \cdot W_K^T \qquad (5\text{-}24)$$

for deterministic targets. For statistical targets, they are described by:

$$\text{Mean} = \mu z_S = \mu Y_K \cdot W_K^T \qquad (5\text{-}25)$$

$$\text{Variance} = \sigma^2 z_S = W_K \cdot R_{SSK} \cdot W_K^T \qquad (5\text{-}26)$$

C. TARGET DETECTION IN FOCAL PLANE PROCESSING

Two methods of calculating threshold level are investigated.

1) CFAR (constant false alarm rate)

2) Bayes criteria.

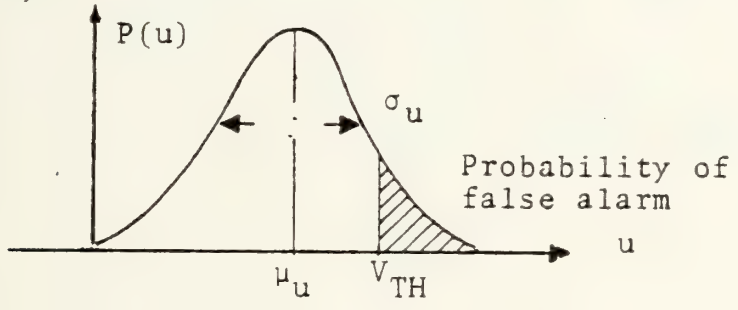

Figure 5-1

1. CFAR

In the CFAR approach, the threshold level = V_{TH} is selected such that P_{FA} is constant. It is important in many practical military applications because a system will operate for a long time without any target being present, facing mostly background clutter noise. It is important to know

the expected false alarm rate and keep it constant. Two methods of setting V_{TH} will be presented.

a. Gaussian PDF Case

When the PDF of the filtered noise (denoted by P(u)) is Gaussian, as shown in figure 5-1, the threshold level V_{TH} can be calculated analytically as follows:

$$P_{FA} = \int_{V_{TH}}^{\infty} P(u)du = \int_{-\infty}^{\infty} P(u)du - \int_{-\infty}^{V_{TH}} P(u)du \quad (5\text{-}27)$$

as shown in Fig. 5-1 by the shaded area.

u denotes noise variable

$\mu_u = E[u]$

$\sigma_u^2 = E[(u-\mu_u)^2]$.

Since P(u) is a PDF, the first term is 1. The second term is the normal cumulative distribution function F(u) which is tabulated or can be computed using standard computer routines.

$$\therefore P_{FA} = 1 - F\left(\frac{V_{TH} - \mu_u}{\sigma_u}\right)$$

This threshold equation is:

$$V_{TH} = \sigma_u \cdot F^{-1}(1 - P_{FA}) + \mu_u \quad (5\text{-}28)$$

σ_u can be found from σ_u^2 which is the variance of the filtered noise given by (5-18) for the spatial filter case and by (5-26) for the spatial-temporal filter case. μ_u is the mean of the filtered noise given by (5-17) for the spatial filter case and by (5-25) for the spatial-temporal filter case.

In many practical cases, the mean of the filtered noise is approximately zero. Therefore the threshold level,

$$V_{TH} = K \cdot \sigma_u \qquad (5\text{-}29)$$

is proportional to the standard deviation of the filtered noise for a specified P_{FA}. For CFAR requirements, the setting of V_{TH} is equivalent to finding the constant K.

b. Non-Gaussian PDF Case

In real world situations, it was found that the PDF of clutter intensity is usually non-Gaussian. A typical example is shown in Fig. 5-2 which contains normalized histograms of real world infrared scene.

Fig. 5-2(a) -"APDF" of unprocessed image ("APDF" is approximated PDF)
Fig. 5-2(b) -"APDF" of spatial-filtered image
Fig. 5-2(c) -"APDF" of spatial-temporal filtered image.

The "APDF" is achieved by evaluation of each pixel intensity and counting all pixels with approximately the same intensity so as to achieve the histogram. The histogram is then normalized so that the total area under the curve becomes 1 so as to yield the approximated PDF.

It can be seen that the mean of the filtered scene can be approximated by zero, and also that none of these "APDFs" are Gaussian.

For these cases, a numerical algorithm is developed to set the threshold for a specified P_{FA}, or CFAR. The basic assumptions are the following:

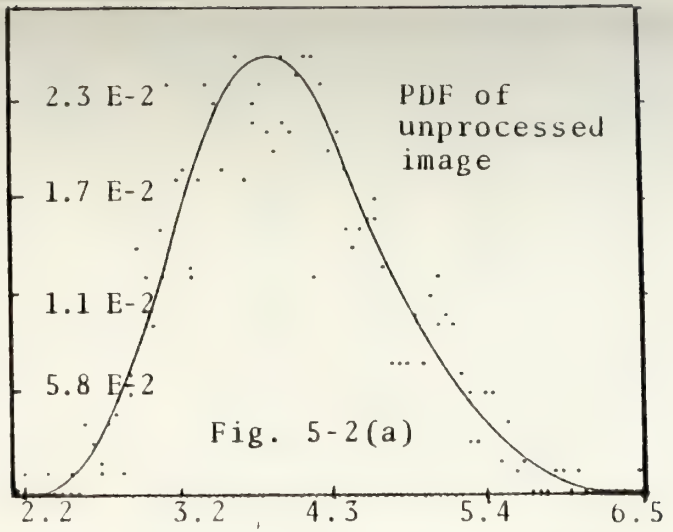

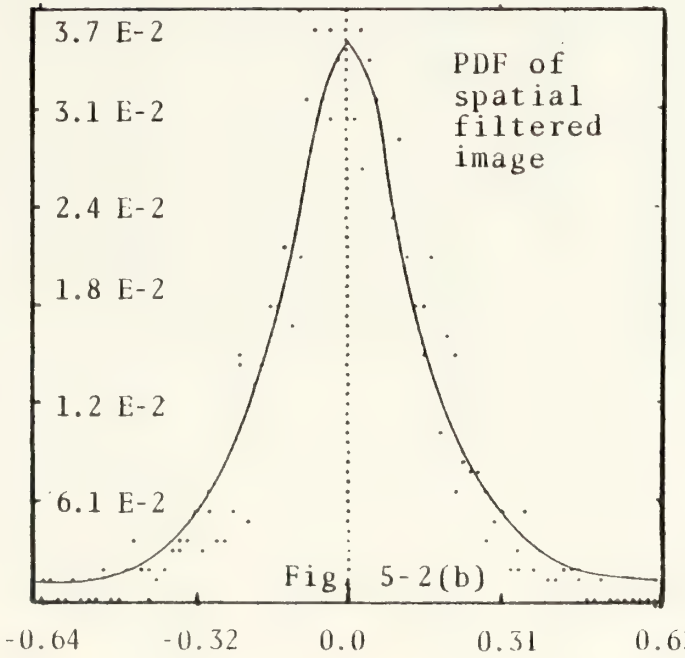

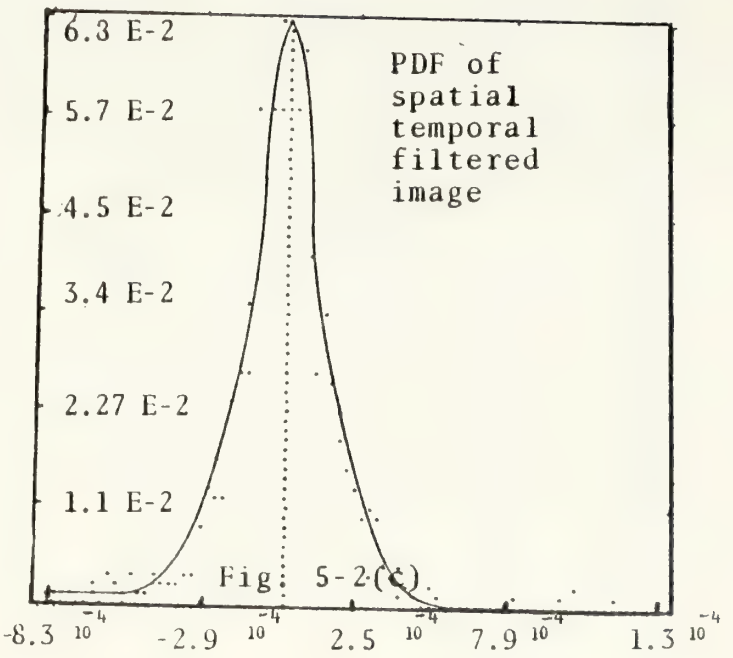

Figure 5-2
Typical Histograms of Clutter Intensity
(Hand fitted curve is added to the histogram to indicate an approximate PDF)

a) The "APDF" of filtered image is available but cannot be expressed in terms of an explicit analytical function.

b) The mean of the filtered image is zero.

c) Similar to the Gaussian PDF case, the threshold level is given by:

$$V_{TH} = K \cdot \sigma_u \quad (\sigma_u \text{ is standard deviation of filtered image})$$

K is to be determined by a computational procedure whose flow chart is shown in Fig. 5-3(a)(b). The false alarm rate can be shown to be indeed constant for a given K considering the following:

$$P_{FA} = \int_{V_{TH}}^{\infty} p(u)du \tag{5-30}$$

where $p(u)$ is any given PDF. The threshold level is selected to be

$$V_{TH} = K \cdot \sigma \tag{5-31}$$

where

$$\sigma^2 = \int_{-\infty}^{+\infty} u^2 p(u) \cdot du = C_1 \text{ (assuming u has zero mean)} \tag{5-32}$$

If we select C_2 so that $\sigma = \sqrt{C_1} = C_2$ and substitute eq. (5-23) into eq. (5-22), the P_{FA} for a given K is:

$$P_{FA}\Big|_{K=\text{constant}} = \int_{K \cdot C_2}^{+\infty} p(u)du = \text{constant} = C_3 \tag{5-33}$$

Eq. (5-25) shows that for a given K, P_{FA} is constant, yielding the CFAR algorithm. In general, P_{FA} is a function of K and can be expressed as $P_{FA}(K)$.

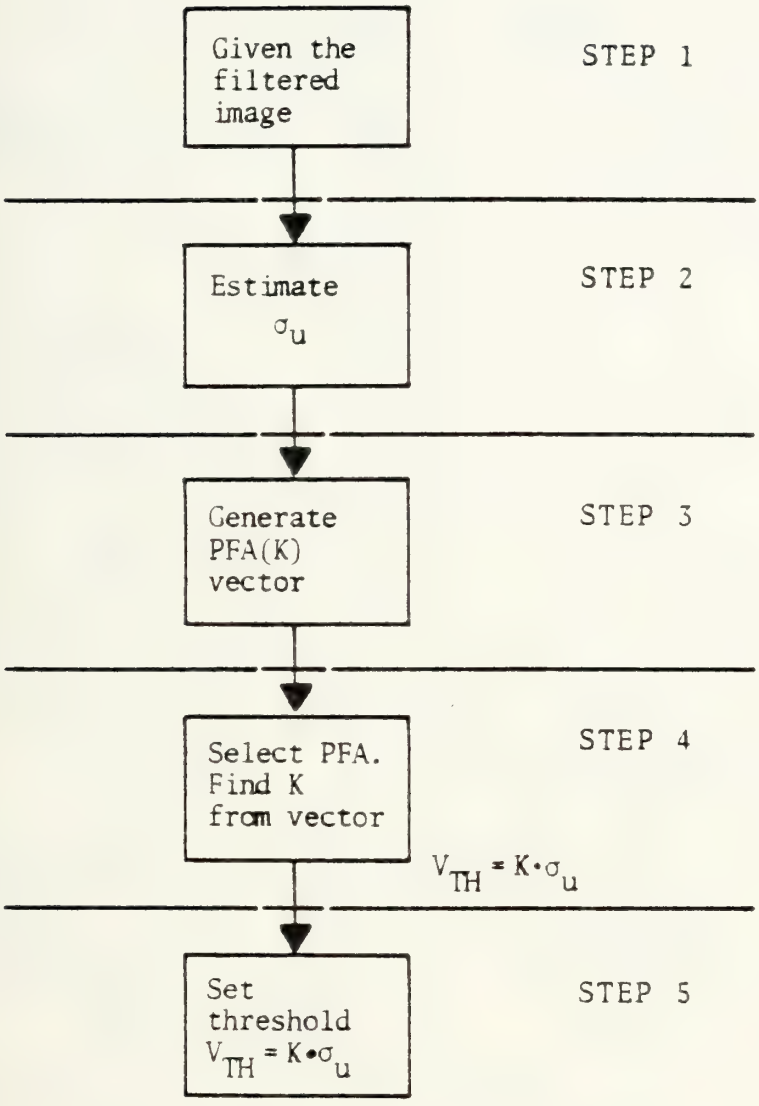

Figure 5-3(a) Procedure for Setting Threshold in Cases of Non-Gaussian Probability Density Function

STEP #3

Flow chart of the generation of vector PFA(K)

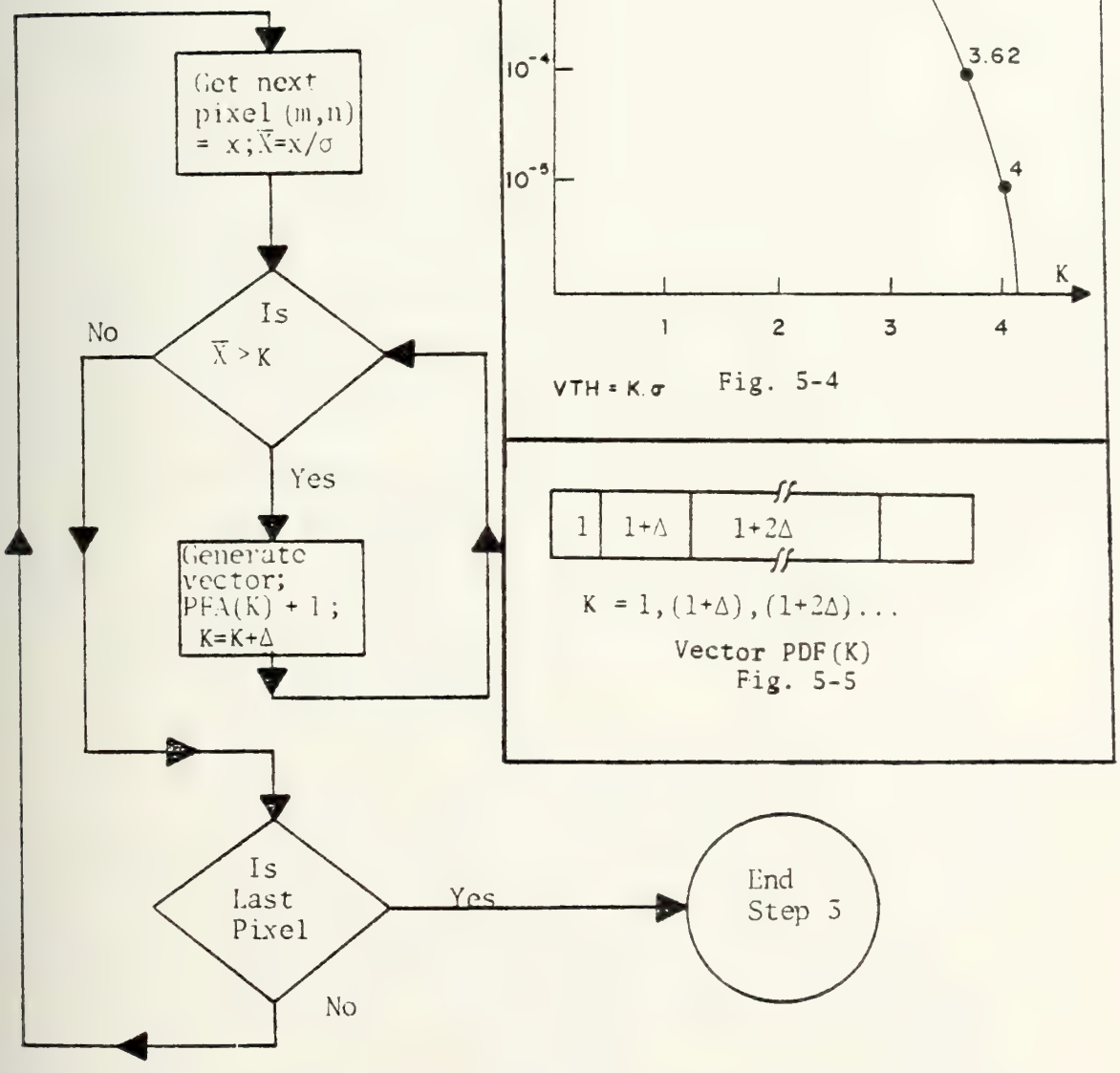

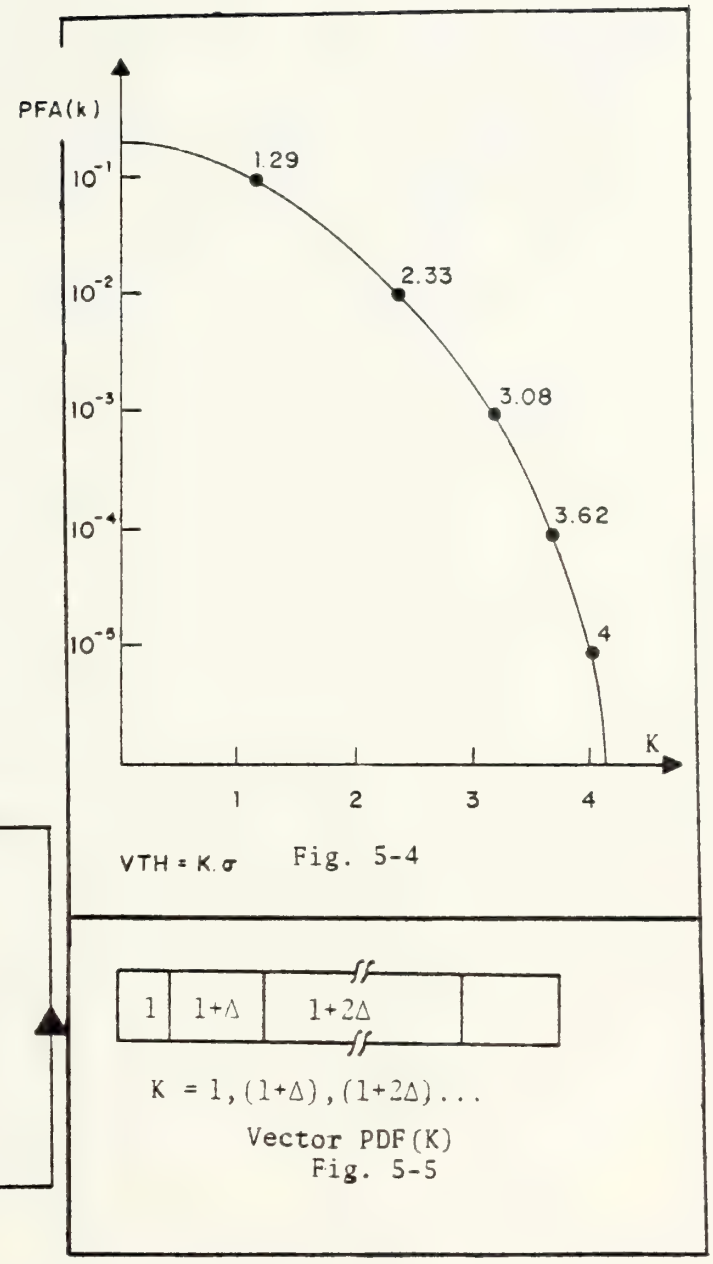

Figure 5-3(b) Flow Chart for Generating PFA versus K Curve Used in Setting Threshold

The only nontrivial step in this flow chart is step 3 where we generate a vector (or table look up) which relates K to P_{FA} [vector $P_{FA}(K)$] for a given σ_u and unknown PDF. Figure 5-4 is a typical plot of such a table look up for Gaussian PDF. In Fig. 5-5, the vector $P_{FA}(K)$ will contain data similar to Fig. 5-4 but for the unknown PDF. To perform step 4, a P_{FA} has to be specified and then the vector $P_{FA}(K)$ will be searched (left to right) to find the first K to yield $P_{FA} \leq P_{FA}$ (specified).

2. Bayes Criterion

Bayes criterion is another method of threshold setting based on a priori knowledge of the target as well as the noise. The basic disadvantage of this method, compared with the CFAR approach, is the requirement to specify the target, background clutter and their statistical properties. However, if this information is already available, the Bayes criterion can be useful. Otherwise, the CFAR approach is more useful. The Bayes criterion is described in detail in Appendix B.

3. Probability of Detection

a. Introduction

If the probability density function (PDF) of the target and also the noise are known, the probability of detection (P_d) can be calculated in a straightforward manner. It should be emphasized that the clutter noise considered in the calculation of P_d is, in most cases, not the unfiltered

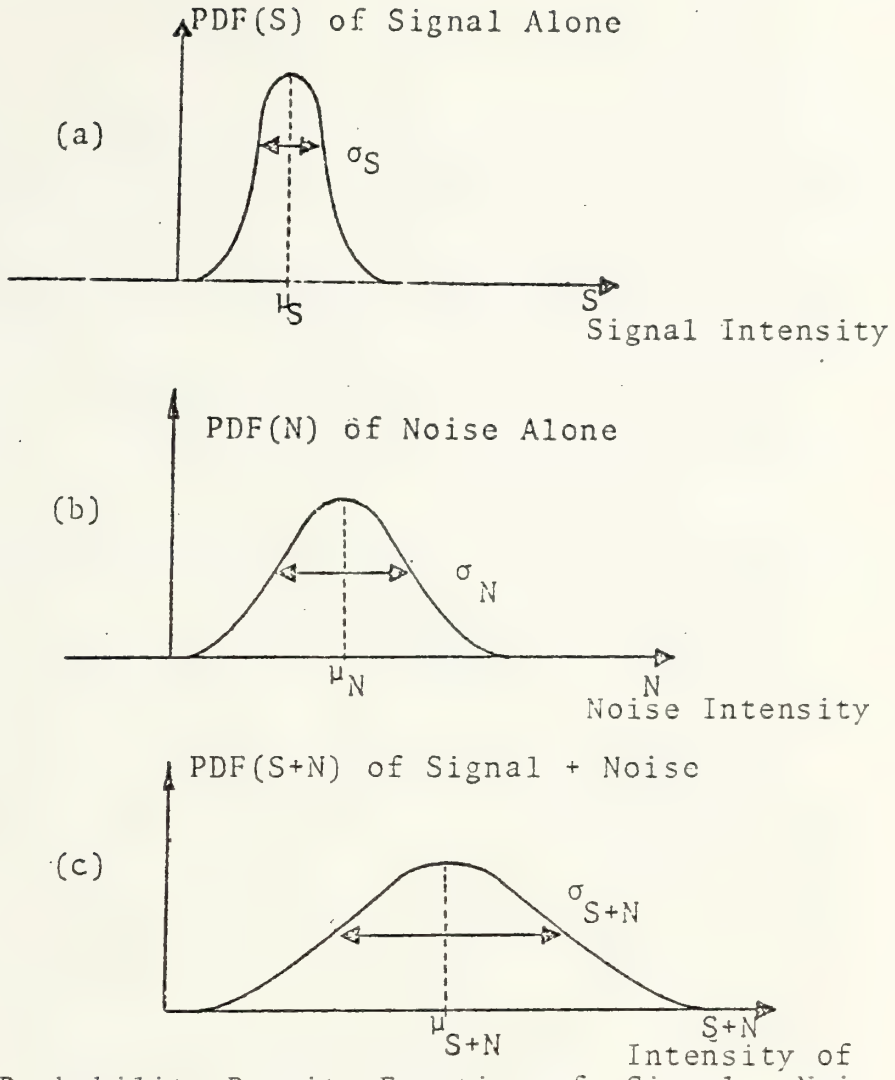

Figure 5-9 Probability Density Function of Signal + Noise
(a) Target Signals
(b) Noise
(c) Targets and Noise

Fig. 5-10

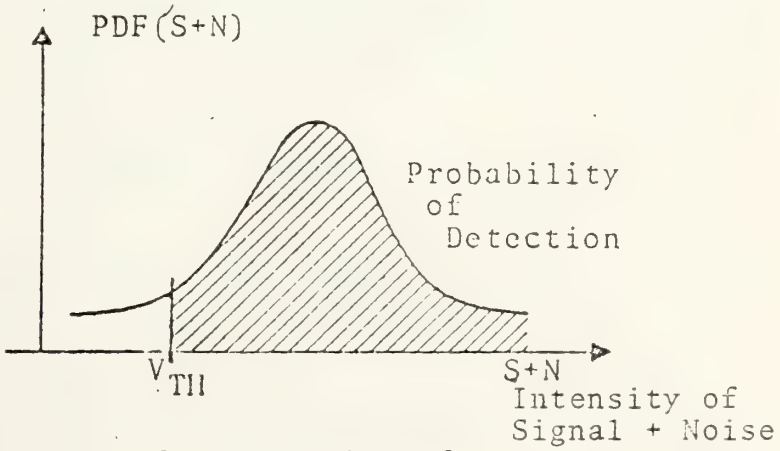

Figure 5-10 Calculation of Probability of Detection

clutter, but the filtered clutter noise. Because in the unfiltered condition intensities of targets are usually only a small fraction of the clutter intensity, the threshold should not be applied at this stage. Only in limited cases is target intensity sufficiently higher than the clutter so that a threshold can be applied without any predetection processing.

Two methods of calculating the P_d are implemented in this thesis. The first method is analytical and only applies to the special cases when the PDF is either Gaussian or can be explicitly described by mathematical expressions. The second method is numerical and is applicable to any case, regardless of whether or not the PDF can be described by well known functions. This method is implemented in the computer simulation by counting the detected targets and comparing their number with the number of inserted targets.

b. Gaussian PDF Case

If the PDF of the clutter noise is Gaussian, the PDF of the processed clutter by any linear filter is also Gaussian, as shown in Fig. 5-9(b). Target signals considered in this thesis can be either deterministic or statistical, as shown in Fig. 5-9(a). Assuming the signal and noise are uncorrelated, then

$$PDF_{(S+N)} = PDF_{(S)} * PDF_{(N)} \text{ is also Gaussian} \qquad (5\text{-}34)$$

where * denotes convolution. A typical result is shown in Fig. 5-9(c). The resultant statistical properties are:

$$\mu_{S+N} = \mu_S + \mu_N \quad = \text{mean of signal + noise}$$
$$\sigma_{S+N}^2 = \sigma_S^2 + \sigma_N^2 \quad = \text{variance of signal + noise} \tag{5-35}$$

The mean and the variance have been calculated in Chapter V, section B.

For a selected threshold V_{TH}, the probability of detection is given by the shaded area in Fig. 5-10 and can be determined by the following integration:

$$P_d = \int_{V_{TH}}^{\infty} \frac{1}{\sqrt{2\pi}\,\sigma_{S+N}} \exp\left[-\frac{1}{2}\left(\frac{x-\mu_{S+N}}{\sigma_{S+N}}\right)^2\right] dx$$

$$= \int_{-\infty}^{\infty} N(\mu_{S+N}, \sigma_{S+N})\, d(S+N) - \int_{-\infty}^{V_{TH}} N(\mu_{S+N}, \sigma_{S+N})\, d(S+N)$$

$$P_d = 1 - F\left(\frac{V_{TH} - \mu_{S+N}}{\sigma_{S+N}}\right) \tag{5-36}$$

where $F(X) = \int_{-\infty}^{X} N(0,1)\, dn$

= normal cumulative distribution function.

F(X) can be easily evaluated by using the error function routine available in most computer libraries because

$$\text{erf}(X) = 2F(\sqrt{2}x) - 1 \tag{5-37}$$

c. Non-Gaussian PDF Case, P_d

If the PDF of the unprocessed clutter noise is other than Gaussian, the PDF of the processed clutter is generally not Gaussian. The processed clutters PDF can be obtained wither analytically or by a best fit algorithm, and

the PDF of the processed signal plus clutter can be obtained as well. Denoting the PDF of clutter as P(N) and the PDF of signal plus clutter as P(S+N), the resulting probability of detection is given by $P_d = \int_{V_{TH}}^{\infty} P(S+N)d(S\_N)$.

D. SUMMARY

Three major steps in target detection are discussed in this chapter. First, the probability density function (PDF) of both filtered image and target signals are determined. Next, based on the PDF, a threshold can be calculated for any specified probability of false alarm. Third, from the threshold, the probability of detection can also be calculated using the known PDF.

If the PDF of filtered clutter noise is Gaussian, both the threshold and P_d can be theoretically determined. Otherwise, they must be numerically calculated using the known PDF. Typical results based on computer simulations will be presented in Chapter VI where predetection processing using statistical spatial filters and temporal-spatial filters for clutter suppression will be combined with thresholding for target detection. Both computer simulated images containing Markov model clutter noise and a real world infrared background image will be used to test the results of focal plane processing.

VI. PROPERTIES AND PERFORMANCE OF NONADAPTIVE STATISTICAL FOCAL PLANE PROCESSING - NONRECURSIVE FILTERS FOR CLUTTER SUPPRESSION FOLLOWED BY THRESHOLDING FOR TARGET DETECTION

A. INTRODUCTION

Focal plane processing consists of many steps. It is started at the optical detectors. After detection, multiplexing and signal conditioning, the first two steps are clutter suppression and thresholding. Following these, image enhancement techniques may be used to improve the shapes and features of targets, linking procedures may be used to connect moving point targets from many frames to form tracks in what is sometimes known as the "track association" or "track assembly" processing, trajectory estimation techniques may be used to determine the dynamics such as velocity and acceleration of the targets, pattern recognition and discrimination techniques may be used to obtain more information on the targets. All of these additional processing techniques can be used to distinguish true targets from false alarms. However, this thesis is concerned only with the first two steps - background clutter suppression and thresholding.

In previous chapters, the principles and design procedures for four focal plane processing procedures have been developed.

° For background clutter suppression:

Chapter III - Single frame focal plane processing:

MMSE filters

Matched filters

Chapter IV - Multiple frame focal plane processing:

MMSE filters

Matched filters

° For initiation of target detection:

Chapter V - Thresholding

In this chapter, quantitative results of these focal plane processing procedures will be investigated and analyzed in more detail. The organization of results of computer simulated analysis and tests are described in the following section.

B. ORGANIZATION OF COMPUTER SIMULATED STUDIES

1. Types of Focal Plane Processing Procedures

Four focal plane processing procedures have been developed, as listed above. Two are spatial filters which use one frame of an image. Two are spatial-temporal filters which use several frames of images. Each of these filters is followed by a thresholding step.

The important features of these filters are:

a. For spatial filters:

° 3x3 search box

° Estimation point is in the center of the box in most cases. It is moved to the edge or corner of the search box when the estimation point is along the edges or corners of an image.

° Point targets are considered in almost all cases.

b. For temporal filters:

° One pixel from three or five successive frames.

° Estimation point is in the middle of successive frames. Example: second frame for a 3 frame temporal filter, third frame for a 5 frame temporal filter.

° Point targets are considered which move at least one pixel from one frame to the next.

2. Types of Images Used in Computer Simulation

Two classes of images are used.

a. Computer Generated Images

Unprocessed images are generated by computer simulation and contain three components:

(1) Targets - Mostly point targets, described by their locations and intensity.

(2) Uncorrelated random noise is described by its mean, which is usually zero, and variance σ_{UN}^2.

(3) Correlated random noise - Two types of Markov processes are used to describe correlated random noise. The detailed theoretical model analysis is presented in Appendix A.

First order: $Q(m,n) = \sigma_{CN}^2 \rho_H^{|m|} \rho_V^{|n|}$

Second order: $Q(m,n) = \sigma_{CN}^2 \rho_H^{|m|} \rho_V^{|n|} \cos(\beta_H \cdot m) \cos(\beta_V \cdot n)$

It can be seen that three parameters are needed to describe the first order Markov model.

σ_{CN}^2 = variance of correlated noise

ρ_H = horizontal correlation factor

ρ_V = vertical correlation factor.

For the second order Markov model, two additional parameters are needed.

β_H = horizontal spatial frequency

β_V = vertical spatial frequency

b. Real World Infrared Image

Twenty successive frames of a real world infrared image in the medium wavelength infrared spectral band are used in the test of sequential spatial-temporal filters.

The target intensity and the unprocessed image are combined together and described by another very important parameter.

Input signal to noise ratio = SNRI

3. Properties and Performances Evaluated

The following properties and performance figures of merit are evaluated.

a. For Clutter Suppression:

(1) Filter coefficients as functions of input signal to noise ratio and correlation factors.

(2) Processing gain as functions of input signal to noise ratio and correlation factors.

(3) Spatial side-lobes after the application of spatial filters as functions of input signal to noise ratio.

b. For Threshold Detection:

(1) Threshold levels as functions of input signal to noise ratio, using the probability of false alarm (P_{FA}) as a parameter.

(2) Probability of detection as functions of input signal to noise ratio and probability of false alarm.

4. Sensitivity Analysis

All nonrecursive filters developed in this thesis use a common set of mathematical operations which is the summation of weighted and delayed signals. The differences among four nonadaptive filters developed in Chapters III and IV and adaptive filters to be developed in Chapters VII and VIII are in the criteria and design procedures of their filter coefficients. Therefore, there exists a real interest in using new sample analog tapped delay line devices which can efficiently carry out the nonrecursive filter operations at high speed because it is a pipelined and parallel processor. However, the disadvantage of sampled analog tapped delay line implementation is its lower accuracy. Therefore, a special

investigation is carried out by truncating and rounding-off the filter coefficients to simulate the lower accuracy of sampled analog implementation and investigating their effects on filter performance.

5. Suboptimal Filter Investigation

In practical applications the noise parameters that were used to design the filter coefficients might be inaccurate, resulting in a "suboptimal" filter. The suboptimal filter performance is investigated in this thesis by monitoring the PG of a given "suboptimal" filter while the background noise correlation factor ($\rho_H = \rho_V$) is changed from 0 to 1.

C. SINGLE FRAME PROCESSING I - NONRECURSIVE SPATIAL MMSE FILTER FOLLOWED BY THRESHOLDING

1. Introduction

An isotropic second order Markov process model is used to simulate the correlated spatial noise in this section. The spatial frequencies of the correlated noise are $\beta_H = \beta_V = \frac{\pi}{k} = 0.267$. The horizontal and vertical correlation factors are varied. The variance of the correlated noise is 1.0. The variance of the uncorrelated noise is 0.01. The target intensity is also varied and is described, together with the spatial noise, by the parameter "input signal to noise ratio" (SNRI).

2. Filter Coefficients

Since the unprocessed images contain only isotropic random noises and point targets, the filter coefficients are

centrally symmetrical. Of the nine filter coefficients, there are only three distinct values: center coefficient W_5, corner coefficient $W_1 = W_3 = W_7 = W_9$, and edge coefficient $W_2 = W_4 = W_6 = W_8$. They are presented in Fig. 6-1(a) and (b) as functions of input signal to noise ratio and for five different correlation factors, $\rho_H = \rho_V = \rho = 0.999$, 0.99, 0.9, 0.8 and 0.4. It should be pointed out that $\rho = 0$ corresponds to the uncorrelated random noise case and $\rho = 1$ corresponds to the deterministic case.

The following observations of their behaviors are made.

a. Symmetry

Filter coefficients have a central symmetry as described above.

b. Coefficient Values

All coefficient values are less than unity. They are easy to implement in hardware if sampled analog image processing is used by simply using a resistor potentiometer.

The sum of nine coefficients is very close to zero. This implies that this type of spatial filter will usually suppress the spatial mean of background noise. It can be considered as a "whitening" spatial filter.

c. Dependence on Correlation

As the correlation factor approaches unity, the filter coefficients change less and less as ρ varies and are also independent of input signal to noise ratio. In the limit

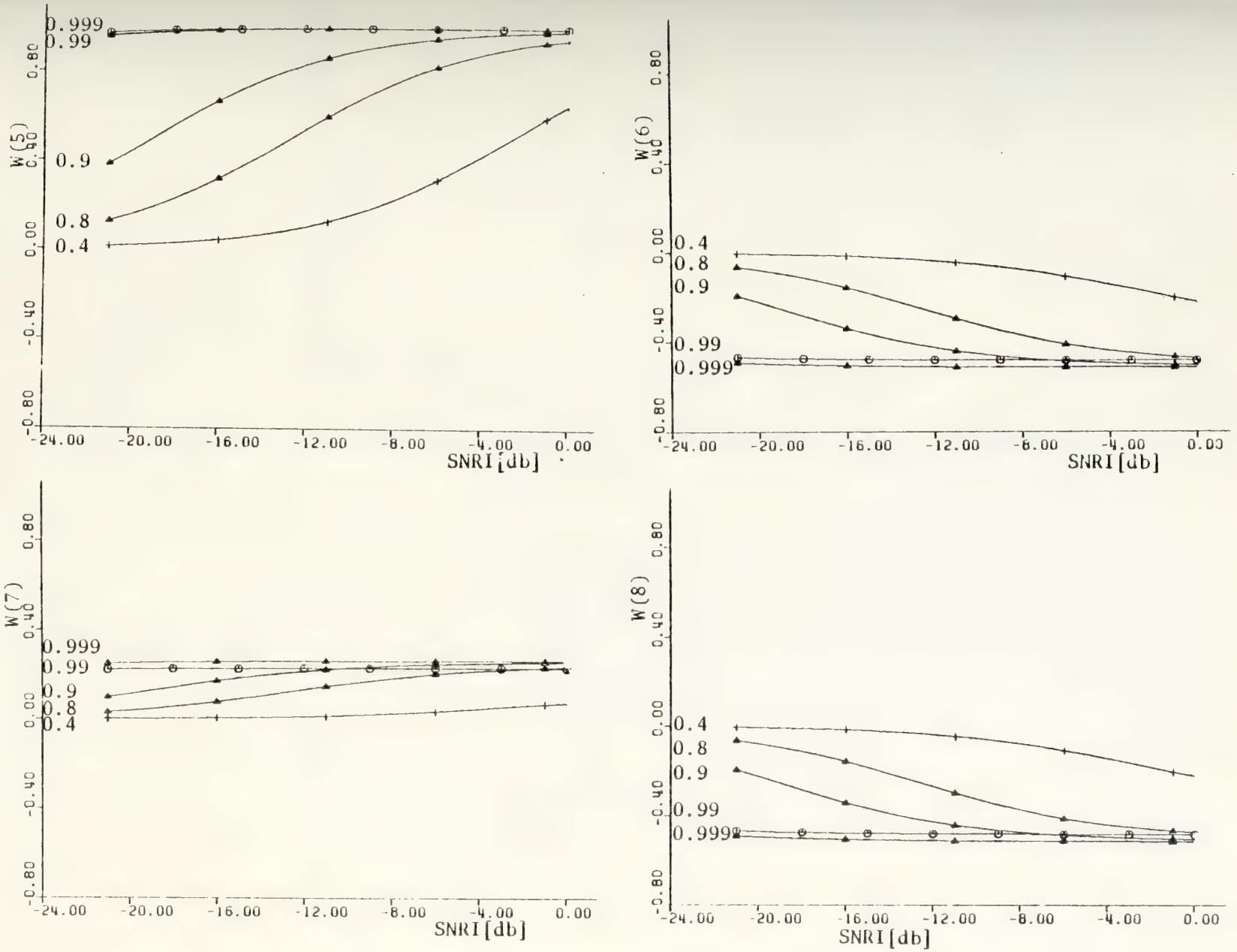

Wiener Filter Coefficients as a Function of Input SNR; $\rho_H = \rho_V$ = Parameter.

Figure 6-1(a)

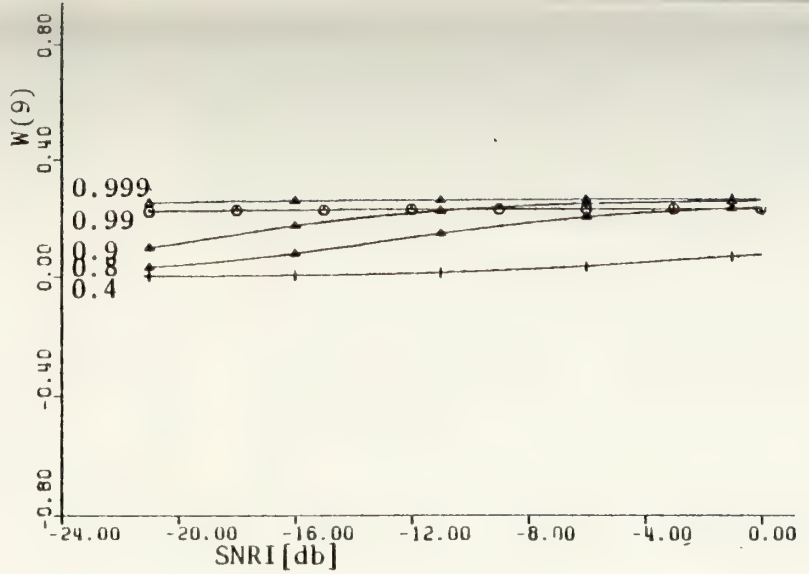

Wiener filter coefficients as a function of input SNRI; $\rho_H = \rho_V$ = Parameter

Figure 6-1(b)

W(1)	W(2)	W(3)
W(4)	W(5)	W(6)
W(7)	W(8)	W(9)

Filter coefficients configuration.

of $\rho = 1$, the filter coefficients approach the values of a spatial Laplacian mask in those cases when β_H and β_V are small (< 0.26).

The Laplacian mask for point target:	0.25	-0.5	0.25
	-0.5	1	-0.5
	0.25	-0.5	0.25

For high values of spatial frequencies, β_H and β_V (> 0.26), the filter coefficients are different than the Laplacian mask.

In the other direction, when ρ approaches zero all eight filter coefficients other than the middle coefficient are decreased. In the limit of $\rho = 0$, only the middle coefficient is non zero. This indicates that in the extreme case of uncorrelated spatial noise, there is no help provided by using neighboring signals to estimate a point target and to suppress the background noise because the noise is not correlated.

d. Dependence on Input Signal to Noise Ratio

Filter coefficient values become smaller as the input SNR is decreased. It can be understood because the MMSE filter is designed to give the optimal estimate of the target signal. When the noise is high, the filter tends to attenuate the noise by smaller coefficient values and to yield the estimation of the small target value.

3. Processing Gain

Processing gain of the spatial MMSE filter is presented in Fig. 6-2(a) as functions of input signal to noise ratio for different correlation factors and in Fig. 6-2(b) as functions of correlation factors. The following observations are made.

a. Dependence on Input Signal to Noise Ratio

The processing gain of spatial MMSE filter for point target estimation is independent of input SNR.

b. Dependence on Correlation

The processing gain is strongly dependent on the correlation factor. The higher the correlation, the larger processing gain can be achieved, but this will be affected by the intensity of uncorrelated noise components also in the image. For example, in this particular case, the PG of approximately 45 db is achieved for $\rho = 0.999$, as shown in Fig. 6-2(a). If the uncorrelated spatial noise is excluded, which is the case in Fig. 6-2(b) when $\rho \simeq 1$, the PG can be as high as 60 db. Unfortunately, uncorrelated noise always exists in real world images due to background shot noise, electronic noise, etc.

As approaches zero, the PG decreases. In the limit $\rho = 0$, PG = 1 which confirms the discussion in the last section on filter coefficients.

4. Threshold Level and Spatial Side Lobe Level

Threshold level and spatial side lobe level are related because if the threshold is set below the side lobe

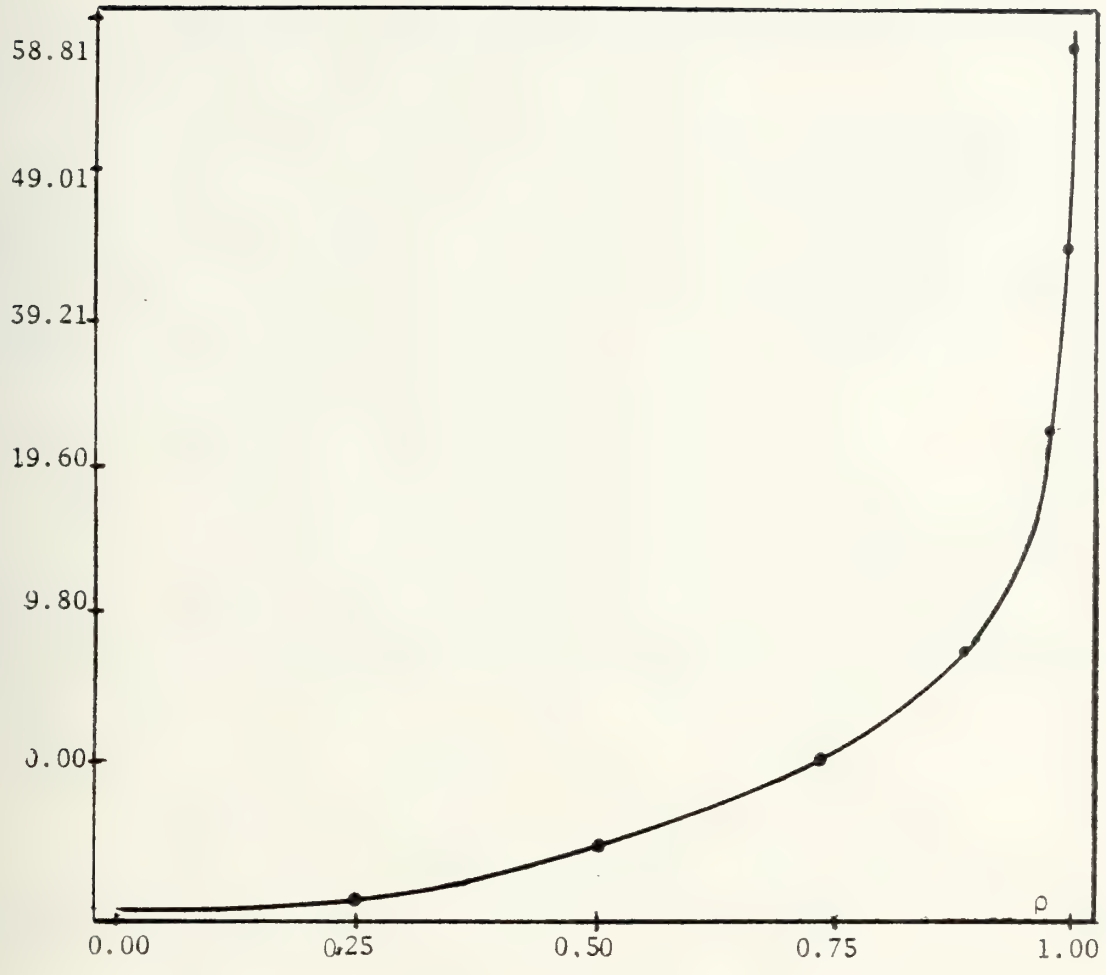

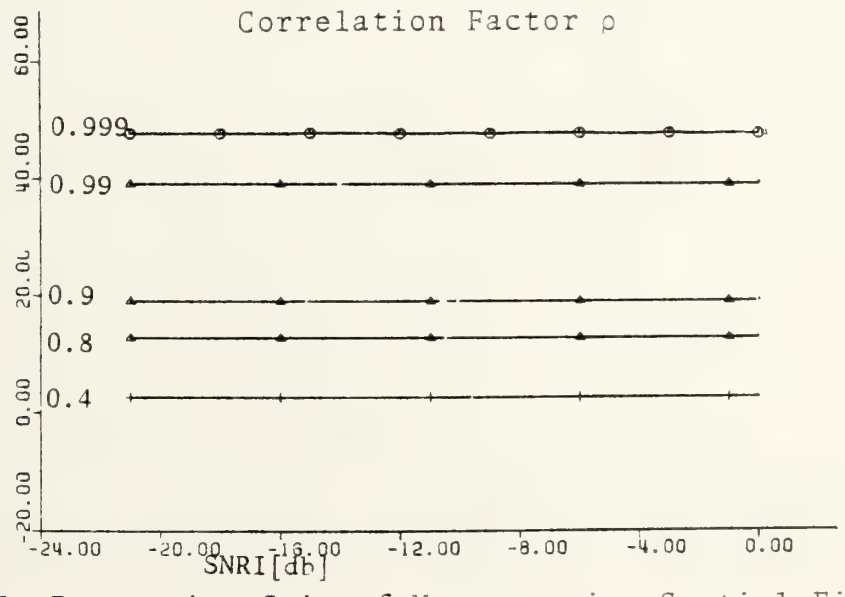

Figure 6-2. Processing Gain of Nonrecursive Spatial Filter as a Function of (a) Input Signal to Noise Ratio, (b) Correlation Factor

level, a false alarm will result. The spatial side lobe level is determined by multiplying the highest positive filter coefficient with the target level.

In Fig. 6-3(a), (b), threshold levels are plotted as functions of input SNR for several values of probability of false alarms from 10^{-1} to 10^{-5} and a given correlation factor. Curves are presented for $\rho = 0.99$, $\rho = 0.9$, $\rho = 0.8$, and $\rho = 0.4$. Two observations are made:

a. Dependence on Correlation

As ρ is increased, the threshold value can be lowered to achieve the same P_{FA}. This is because the processing gain of the spatial MMSE filter is better for higher ρ.

b. Dependence on P_{FA}

As P_{FA} is reduced, threshold value must be increased.

The spatial side lobe levels are presented in Fig. 6-3(a),(b) as well as functions of input signal to noise ratio. By comparing the threshold level plots and side lobe level plots corresponding to the case of $\rho = 0.9$ in Fig. 6-3(a), it can be seen that false alarms due to side lobes will occur for input SNR approximately above -4 db for threshold levels in the range $10^{-2} < P_{FA} < 10^{-1}$.

5. Probability of Detection

A set of figures (Fig. 6-4) is used to present the probability of detection, P_D, as functions of input SNR for

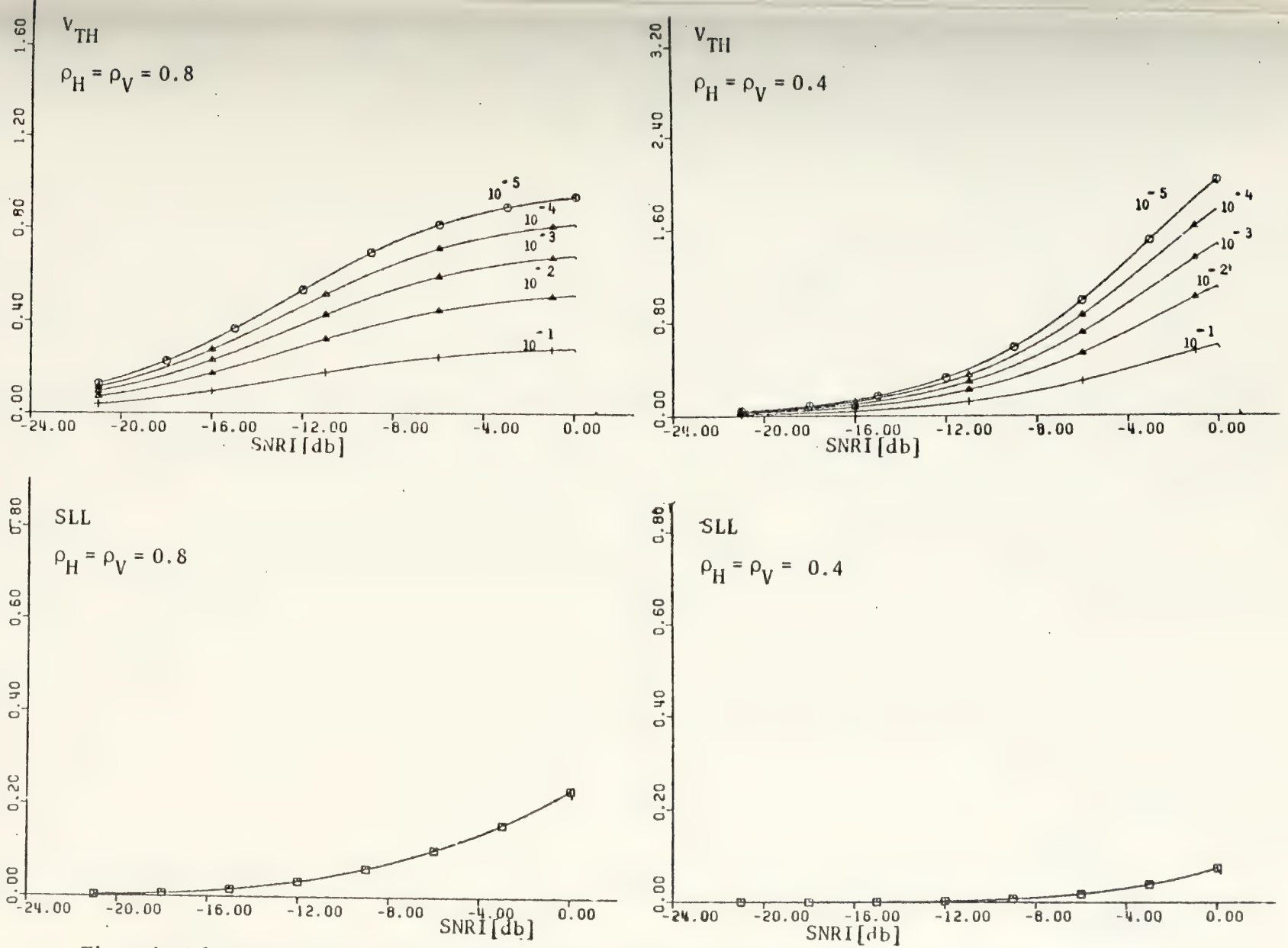

Threshold Level (V_{TH}) and Spatial Side Lobe Level (SLL) as a function of Input Signal to Noise Ratio in db (SNRI[db]) PFA = Parameter

Figure 6-3(a)

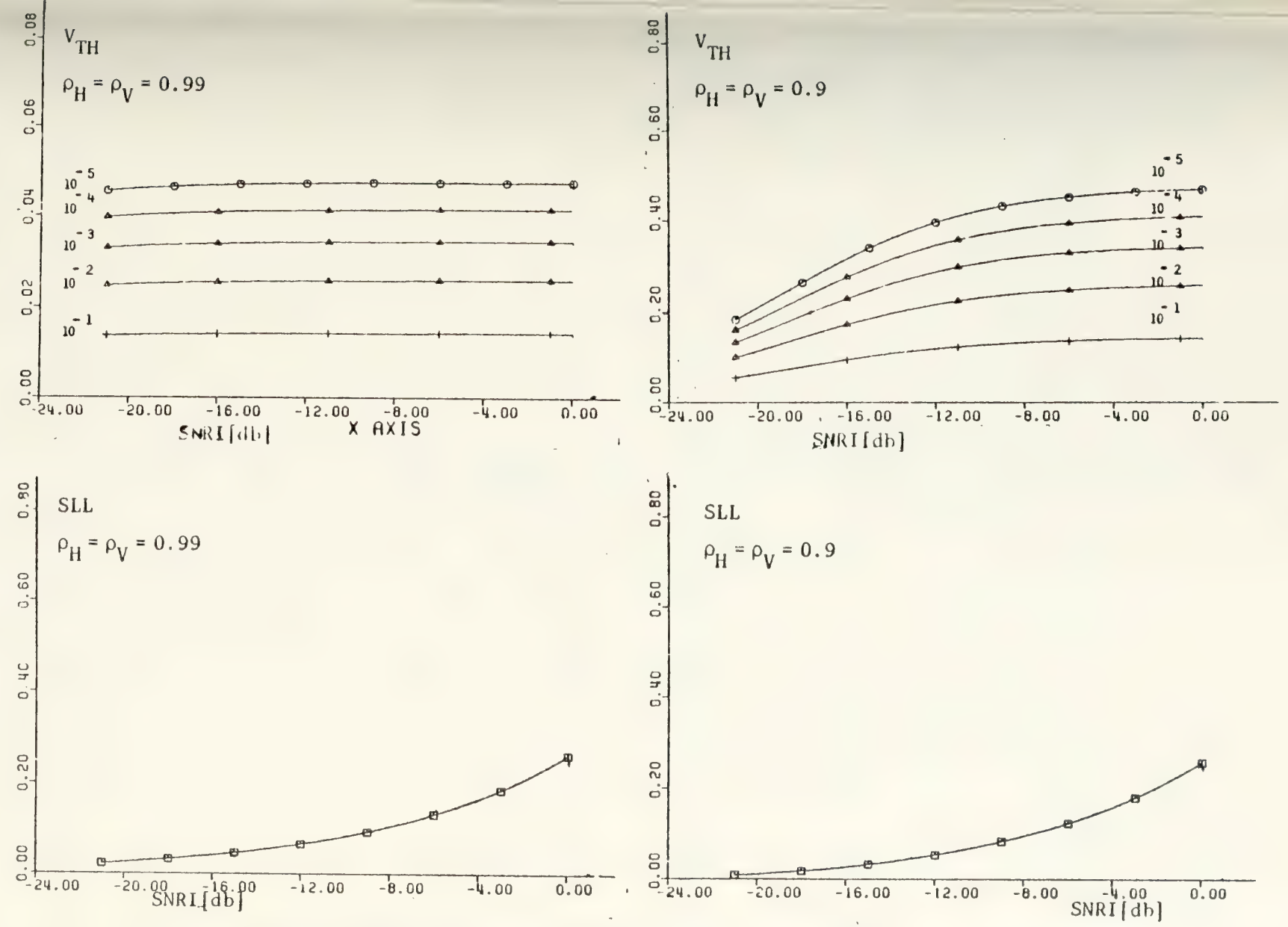

Threshold Level (V_{TH}) and Spatial Side Lobe Level (SLL) as a function of Input Signal to Noise Ratio in db (SNRI[db]) PFA = Parameter

Figure 6-3(b)

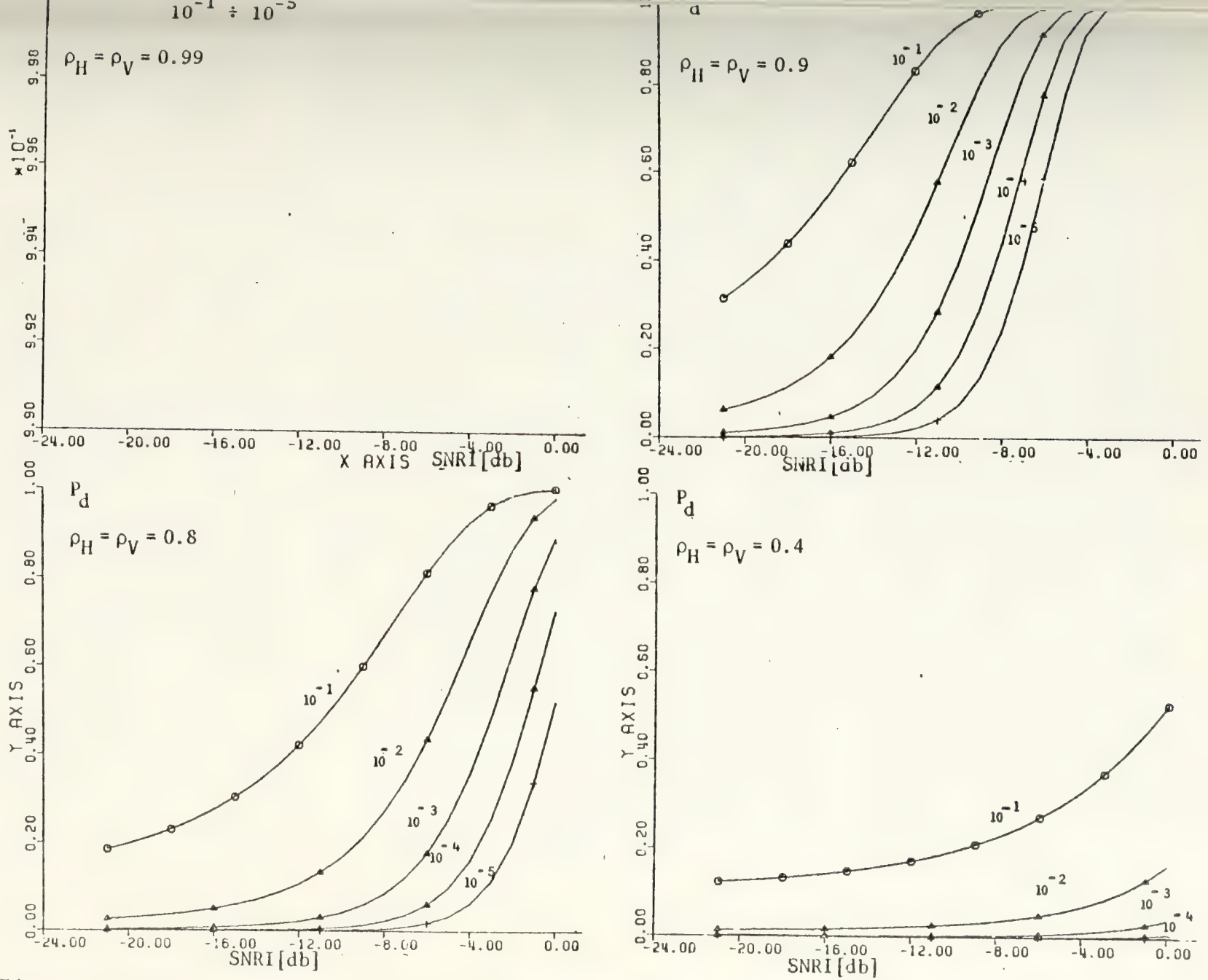

Fig.6-4 Probability of Detection as a Function of Input SNR; PFA = Parameter

several values of P_{FA} from 10^{-1} to 10^{-5}. Each figure is for a selected correlation factor, $\rho_H = \rho_V$.

It should be emphasized that the two figures of merit of PG and P_d must be used together in the evaluation of effectiveness of focal plane processing. Otherwise, misleading evaluation could result as demonstrated by the following example.

Consider a case of $\rho = 0.9$; the processing gain of a 3x3 spatial MMSE filter for point target estimation is 20 db. It could be interpreted that any target of input SNR better than -20 db, say -12 db, can be detected. However, the P_d plot in Fig. 6-4 reveals that for $P_{FA} = 10^{-3}$, the probability of detection of a weak target of -12 db is very low. P_d is less than 0.9 even for a stronger target of -7 db. Therefore, the capability of a focal plane processing process consisting of a spatial filter for clutter suppression (evaluated by PG) and thresholding (evaluated by P_d) must be correctly determined by using both PG and P .

6. Summary

Some highlights of the first type of focal plane processing which consists of spatial MMSE filtering and thresholding are:

a. The processing gain is strongly affected by correlation factor, relative intensity of white noise, types of targets, search box size and location of estimation pixel [Ref. 14].

b. Input SNR does not affect the processing gain but will influence the probability of detection.

D. SINGLE FRAME PROCESSING II - NONRECURSIVE SPATIAL MATCHED FILTER FOLLOWED BY THRESHOLDING

1. Introduction

The same unprocessed image used in the study of nonrecursive spatial MMSE filters is used in this section. There will be a great deal of similarities in the organization of presenting the results also.

2. Filter Coefficients

Figure 6-5(a),(b),(c) presents the filter coefficients as a function of input SNR for several isotropic correlation factors. Since point targets are being considered and only isotropic noises exist in the unprocessed image, the filter coefficients have again a central symmetry. Only three of the nine filter coefficients need to be presented - W(1), W(2) and W(5).

It can be seen that their values are not only very large but also have strong dependence on the input SNR. Both facts are inconvenient in hardware implementation. (It should be remembered that in spatial MMSE filters, the filter coefficients are all less than one and are independent of input SNR.) These difficulties with the matched filter can be removed by a proper choice of the constant C in the solution of the coefficient equation (3-4.28) to normalize the filter coefficient for the estimation pixel to unity. Figure 6-6(a),(b)

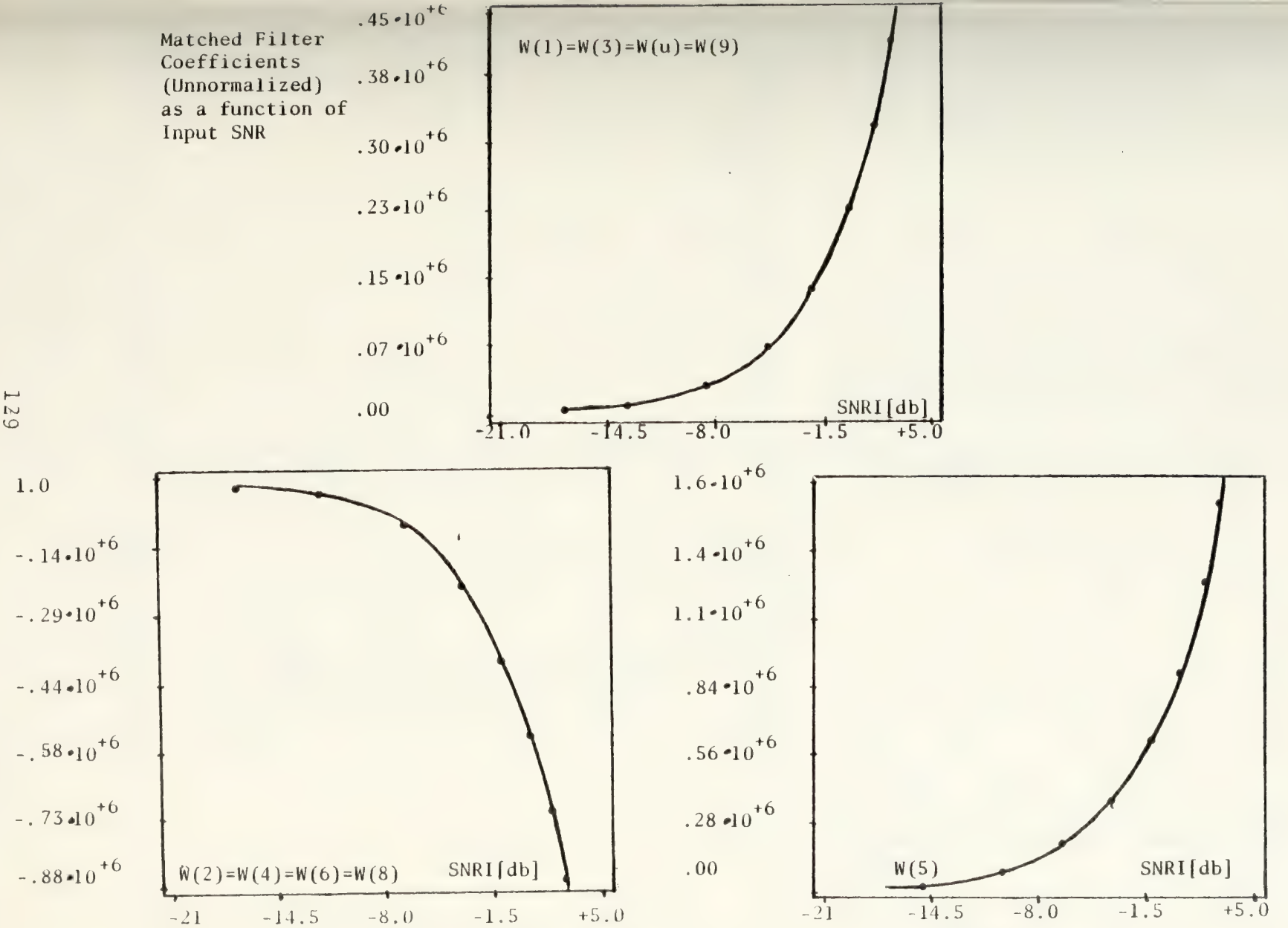

Figure 6-5 Unnormalized Matched Filter Coefficients as a Function of Input Signal to Noise Ratio.

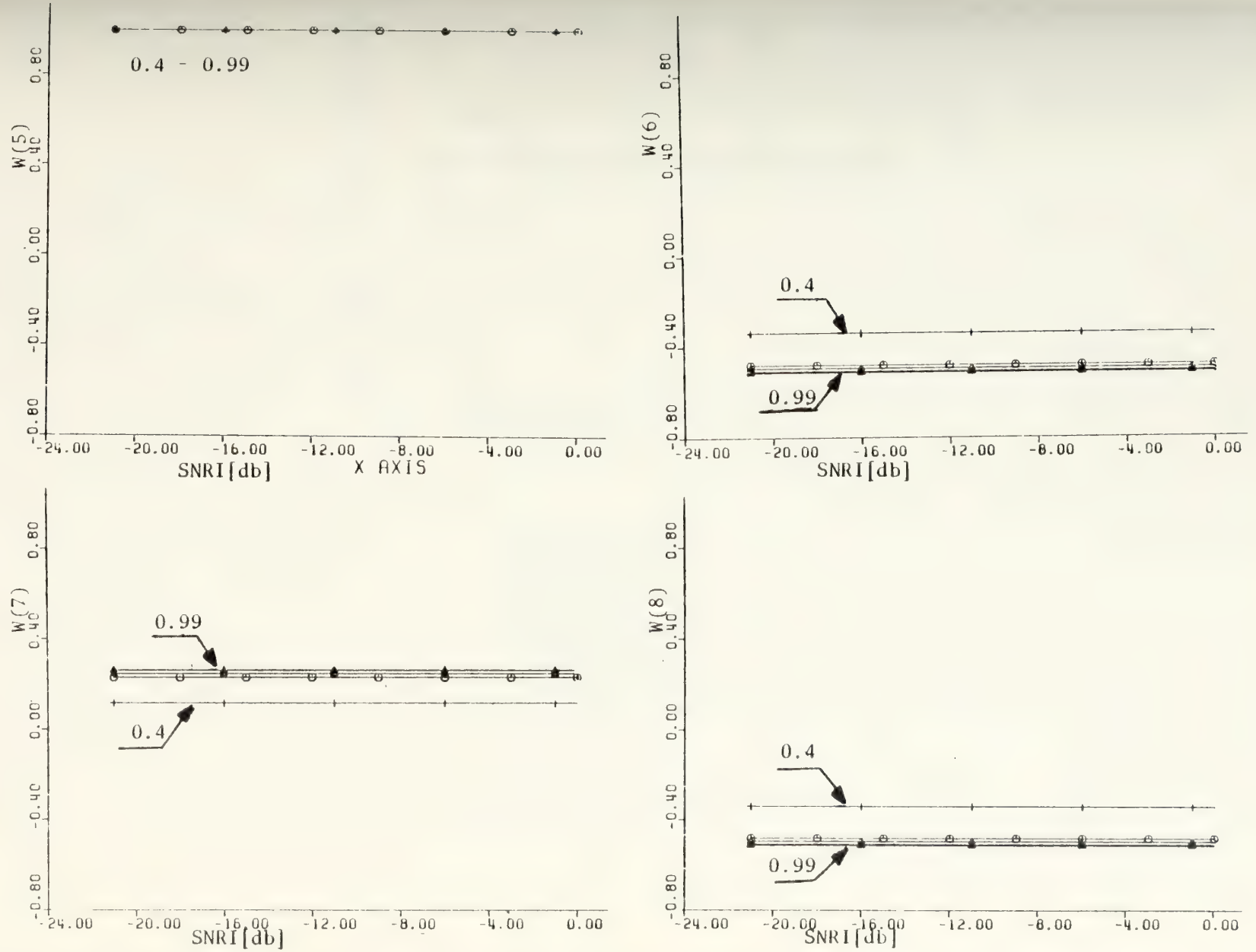

Fig. 6-6(a) Matched Filter Coefficients as a Function of Input SNR; $\rho_H = \rho_V$ = Parameter

Filter
Coefficient

Figure 6-6(b)

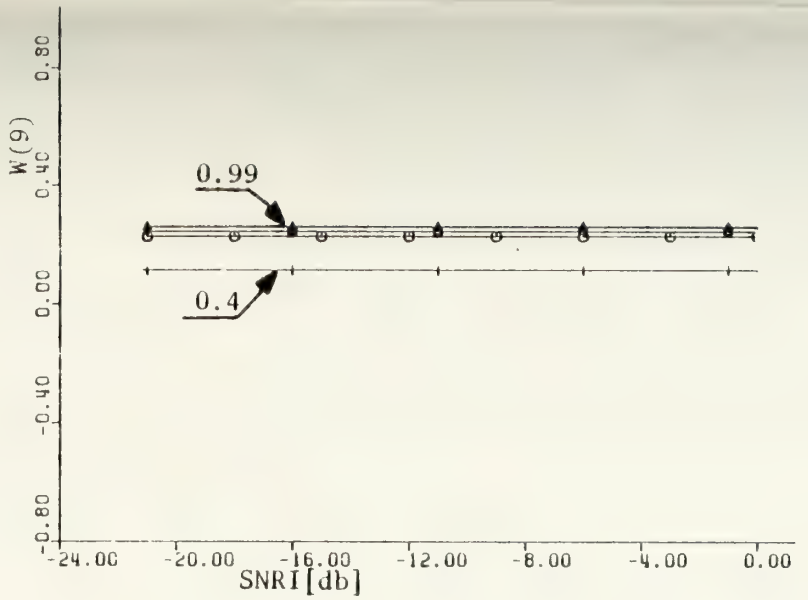

W(1)	W(2)	W(3)
W(4)	W(5)	W(6)
W(7)	W(8)	W(9)

Filter Coefficients Configurations

shows the dependence of filter coefficients after the normalization.

Other observations made for the MMSE filters also apply for the matched filters.

3. Processing Gain

The processing gain of the spatial matched filter for point target estimation is presented in Fig. 6-7 as a function of input signal to noise ratio for different isotropic correlation factors, $\rho_H = \rho_V$.

Again, the general observations obtained for the MMSE filters are also valid in the matched filter cases. In fact, by comparing Fig. 6-7 with Fig. 6-2(a), it is discovered that although the filter coefficients for these two filters are quite different, their processing gains are the same. This result can be justified by using the following reasoning. The MMSE filter is designed to suppress the noise and to yield the best estimate of the signal. The matched filter is designed not only to suppress the noise but also to enhance the signal. This second feature of the matched filter results usually in signal distortion in contrast to the MMSE filter which is designed to yield the best estimate of the signal. When the concerned signal is a point target, as in the above case, the normalized matched filter cannot affect the signal and therefore both matched filter and MMSE filter will only suppress the noise to the same extent, resulting in the same PG.

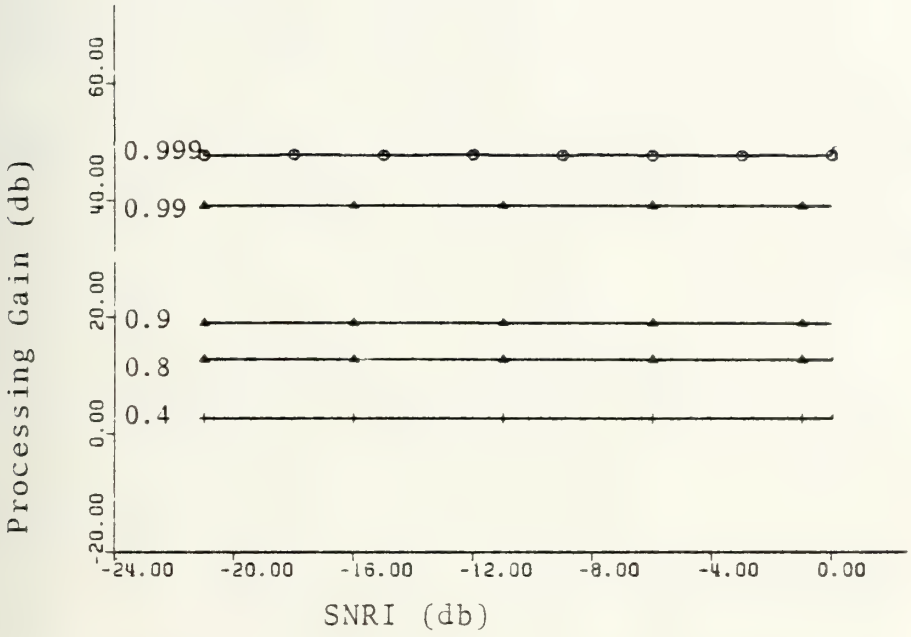

Figure 6-7 Processing Gain of Nonrecursive Spatial Matched Filter as a Function of Input Signal to Noise Ratio and Correlation Factor.

4. Threshold Level and Side-Lobe Level

Threshold levels are plotted in Fig. 6-7(a),(b) as functions of input SNR for several values of P_{FA} from 10^{-1} to 10^{-5} and a selected correlation factor. Several figures are presented for different ρ's.

Side lobe levels are also shown in Fig. 6-7(a),(b) as functions of input SNR.

Again, there are many similarities between the spatial matched filters and the spatial MMSE filters presented in the last section. It should be noted that the threshold level of the normalized matched filter does not vary with SNRI as it does for the MMSE filter.

5. Probability of Detection

The probability of detection is presented in Fig. 6-8 as functions of input SNR for several values of P_{FA} from 10^{-1} to 10^{-5}. Each figure is for a selected correlation factor.

6. Summary and Comparison with MMSE Filters

Comparing spatial matched filter results of this section and spatial MMSE filter results in the previous section, many similarities are observed. The only difference is in the filter coefficients. It must be pointed out that these observations are true only for point targets. For other targets, MMSE filters and matched filters will not be as similar as in the case of point targets. It is believed that for extended targets, the matched filters will offer more superior processing gain and probability of detection because

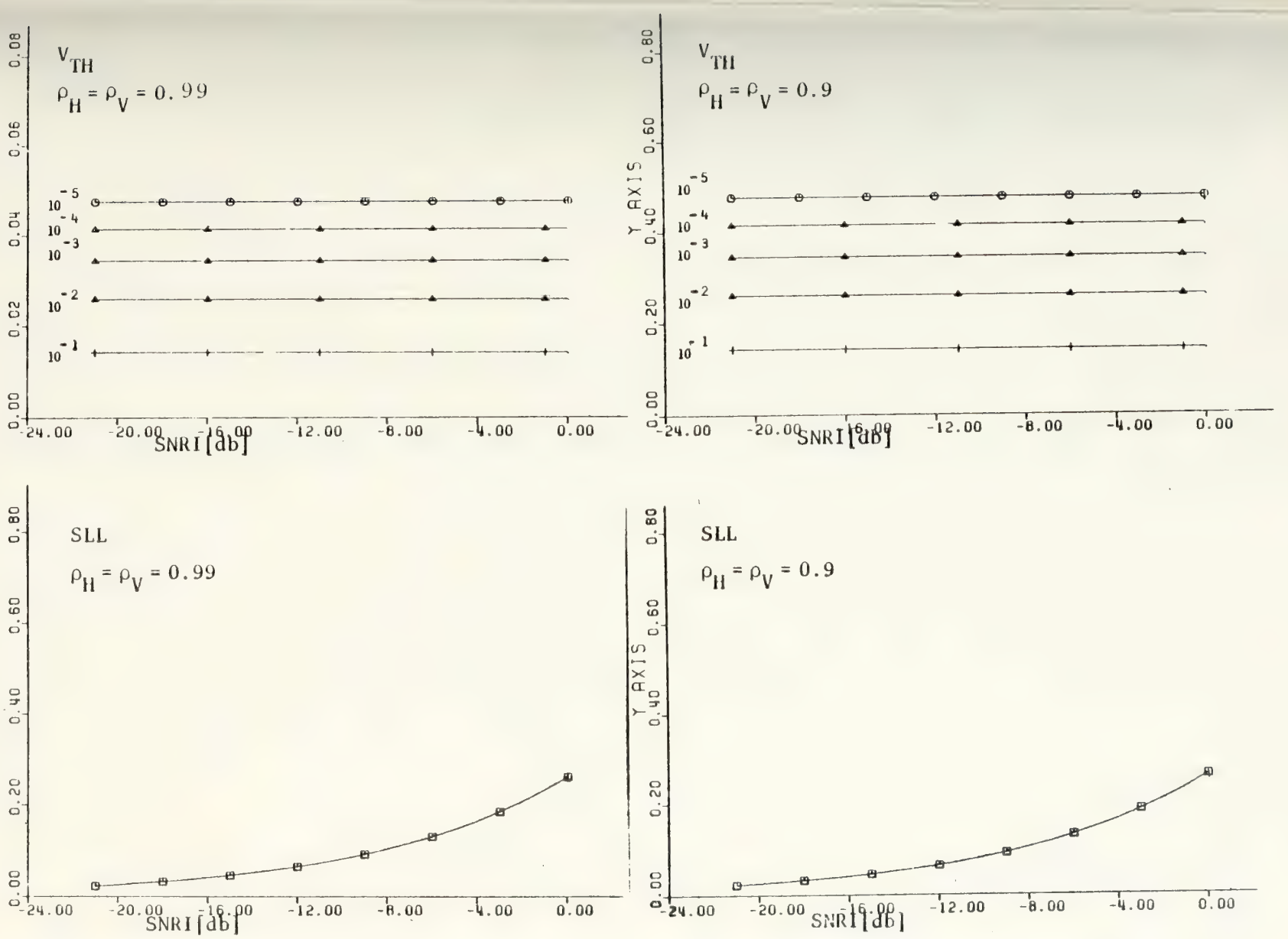

Fig. 6-7(a) Threshold Level (V_{TH}) and Spatial Side Lobe Level (SLL) as a Function of Input Signal to Noise Ratio in db (SNRI[db]); PFA = Parameter

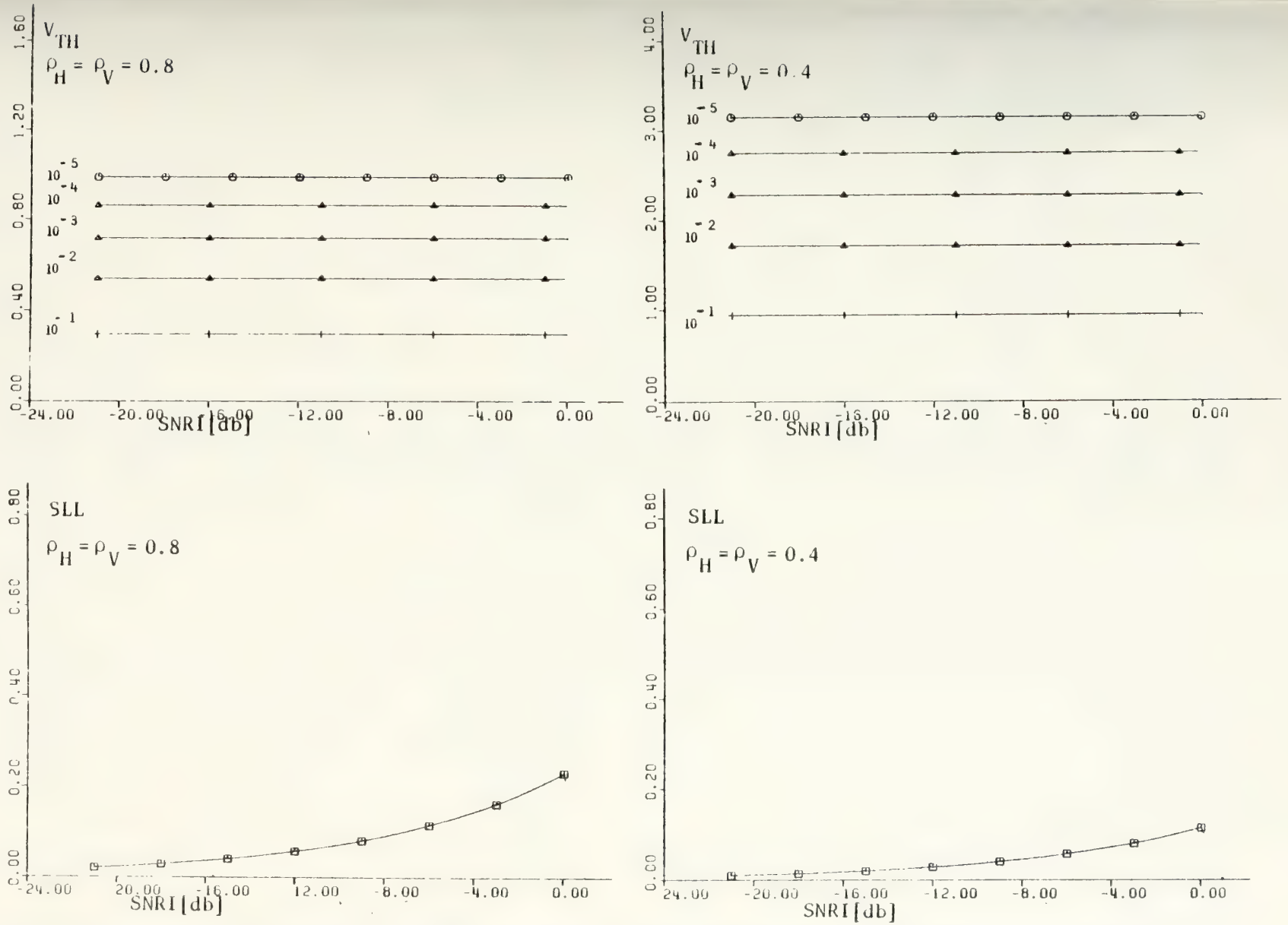

Fig. 6-7(b) Threshold Level (V_{TH}) and Spatial Side Lobe Level (SLL) as a Function of Input Signal to Noise Ratio in db (SNRI[db]); PFA = Parameter

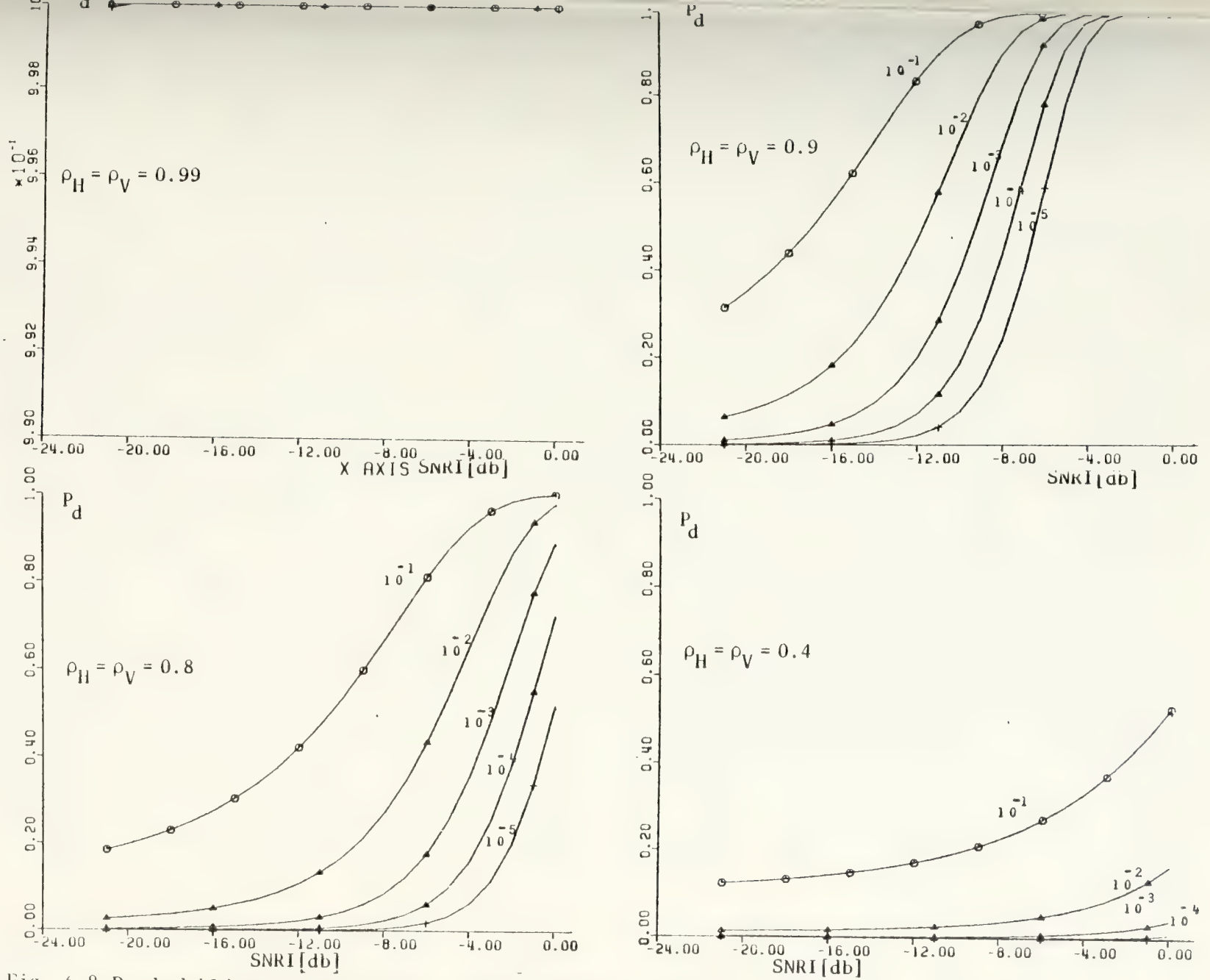

Fig. 6-8 Probability of Detection as a Function of Input SNR; PFA = Parameter

the matched filter is designed to enhance the target as well as suppressing the noise, as mentioned in VI.D.3.

E. SUBOPTIMAL SPATIAL FILTERS

1. Filter Coefficients Accuracy

When filter coefficients are inaccurate due to round-off error or other implementation constraints, the processing gain will deteriorate accordingly. Fig. 6-9 presents the deterioration in PG as a result of artificial coefficients round-off at a certain location after the decimal point. It is seen that round-off at the fourth place after the decimal point hardly affects the PG.

2. Suboptimal Filter Performances

When the correlation factor of the noise is expected to vary within the image, it is necessary to determine which is the best "suboptimal" filter. Figure 6-10 shows the resulting PG when a filter designed for a correlation factor of $\rho = 0.999$ is facing a correlation factor that varies from 0 to 1. Comparison of Fig. 6-10(a.1) with Fig. 6-9(a.1) reveals that the resulting deterioration in PG in various ρ's is from 0 to about 3 db. Figures 6-10(a.2),(a.3),(a.4) and (a.5) are similar to Fig. 6-10(a.1) with filters designed for $\rho = 0.99$, 0.9, 0.8 and 0.4 respectively.

The strongest deterioration in PG is noticed in the suboptimal filter related to $\rho = 0.4$ (Fig. 6-10(a.5)) and the least deterioration is noticed in the filter related to $\rho = 0.999$ (Fig. 6-10(a.1)).

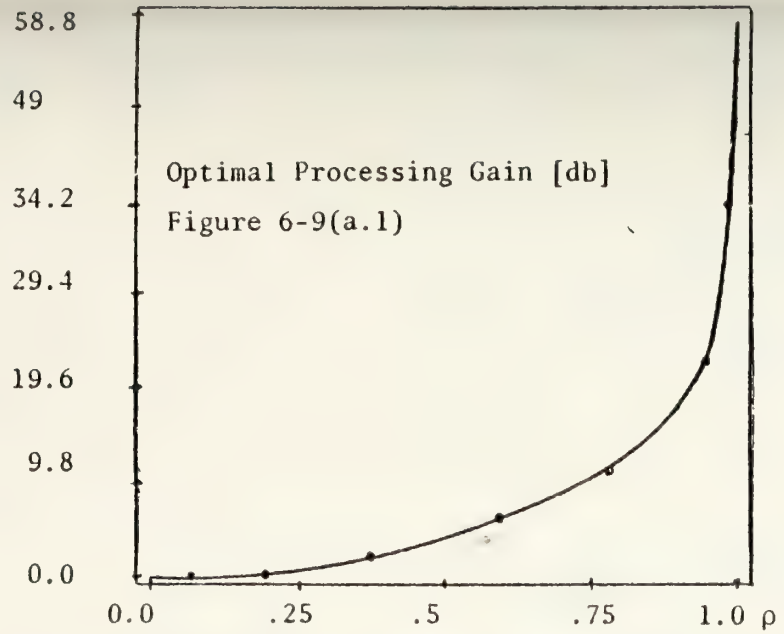

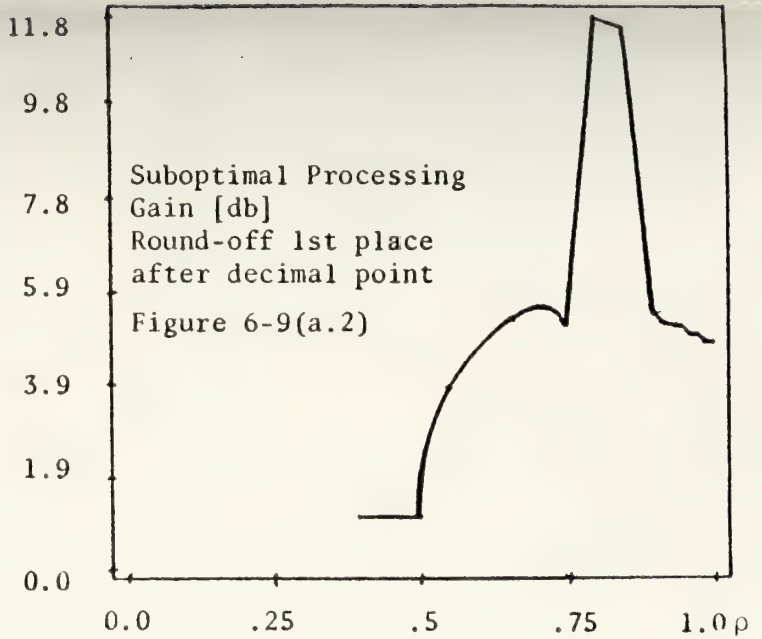

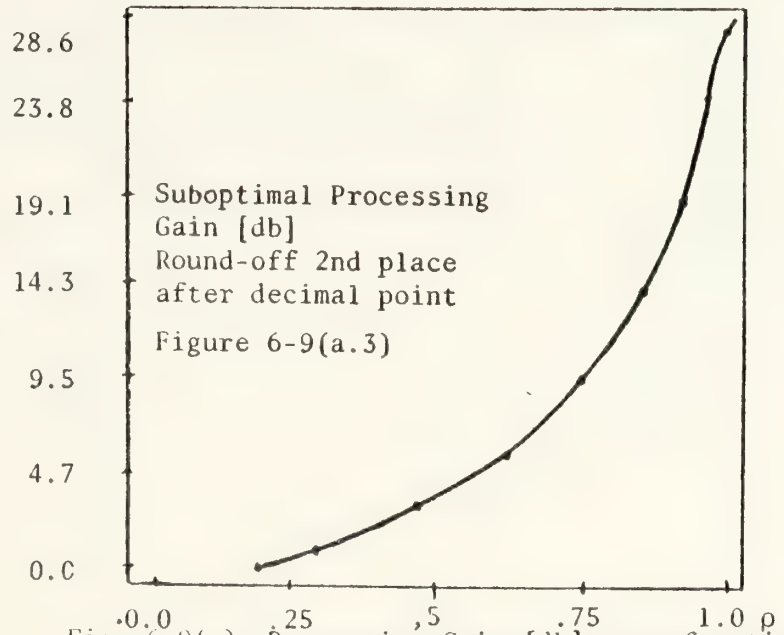

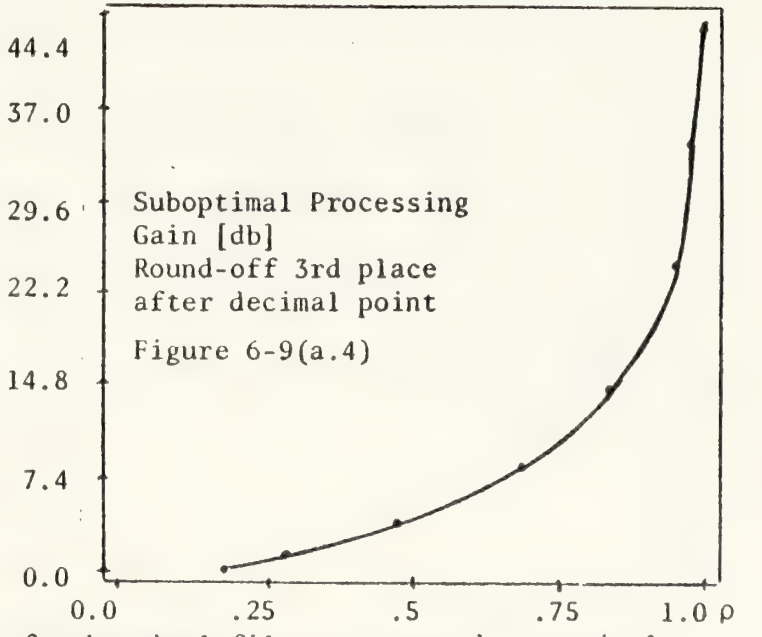

Fig. 6-9(a) Processing Gain [db] as a function of ρ - of suboptimal filters compared to optimal.

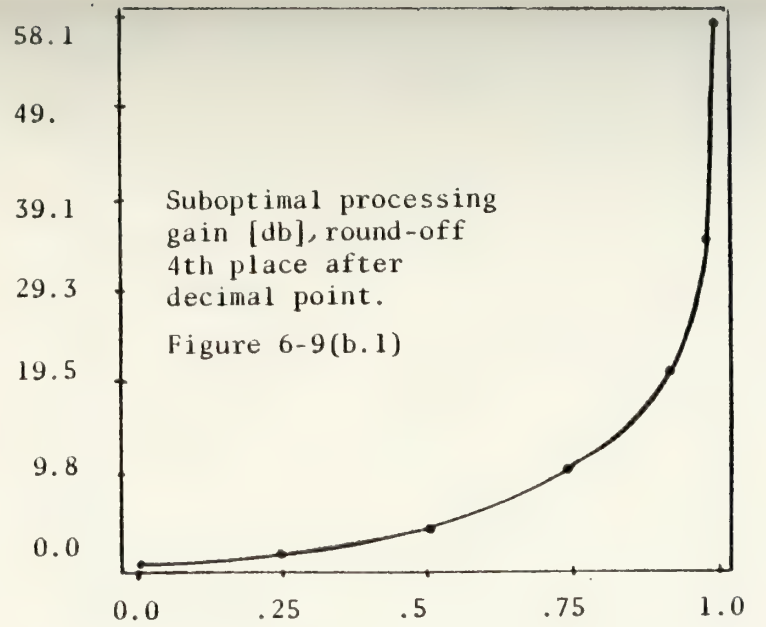

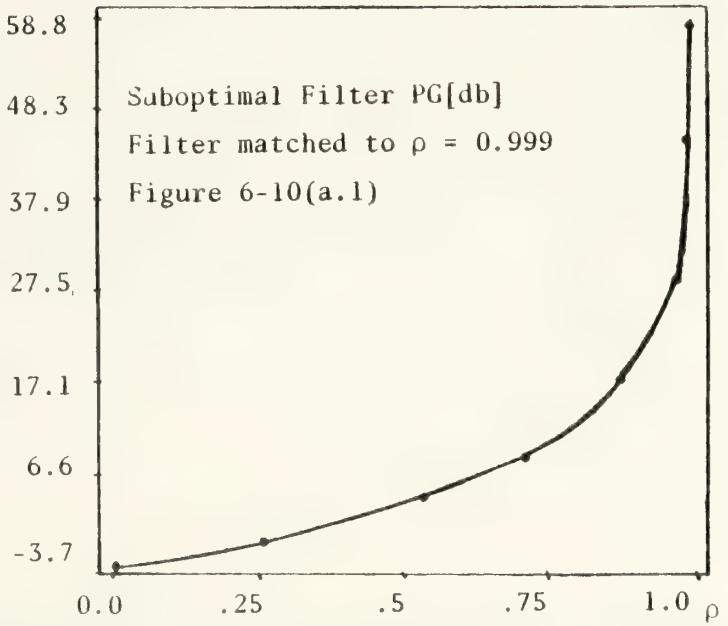

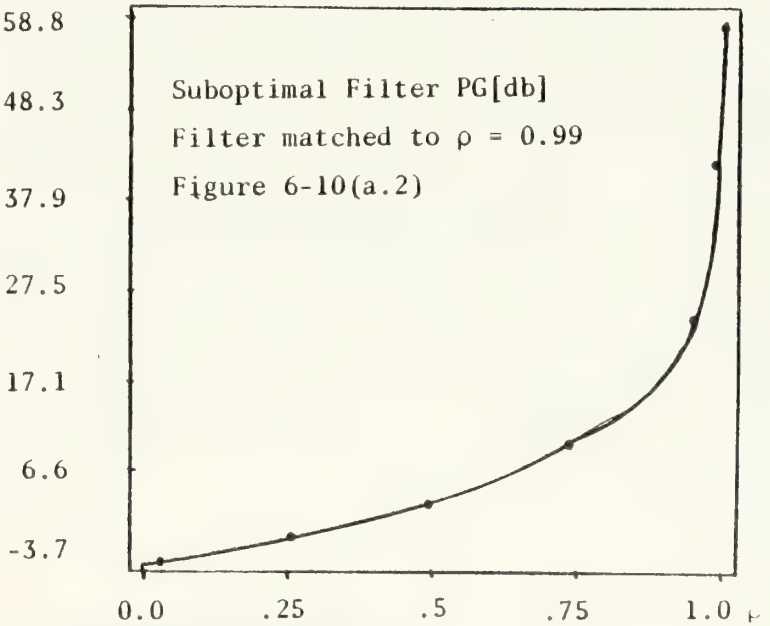

Fig.6-10(a) Processing Gain [db] as a function of ρ - of suboptimal filters.

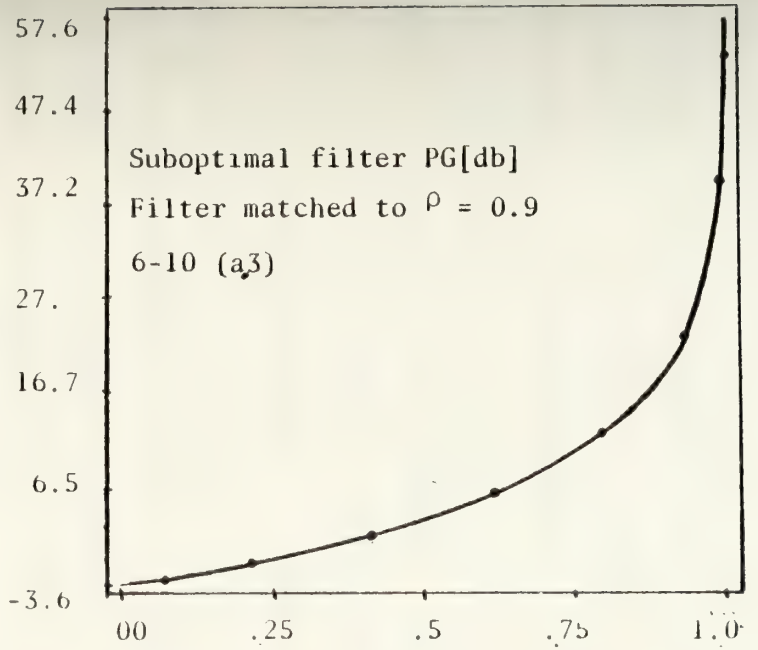

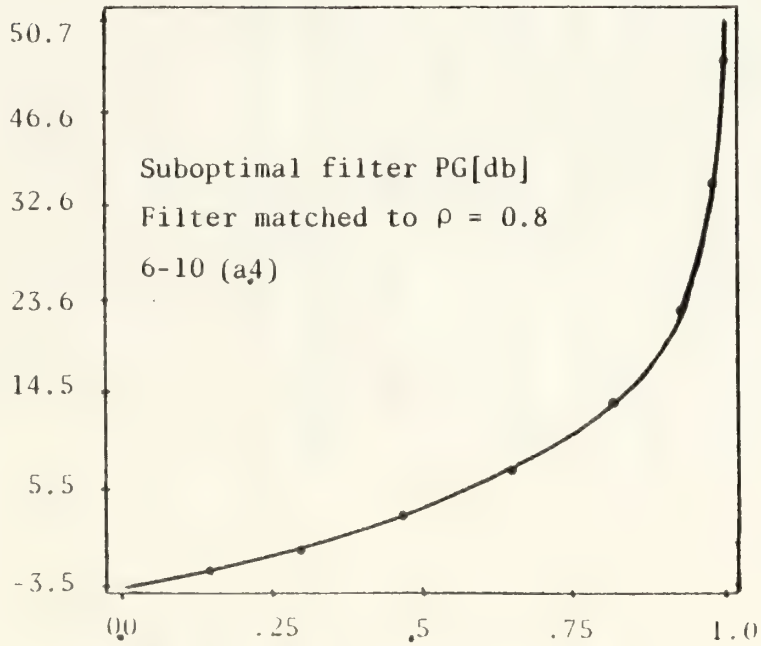

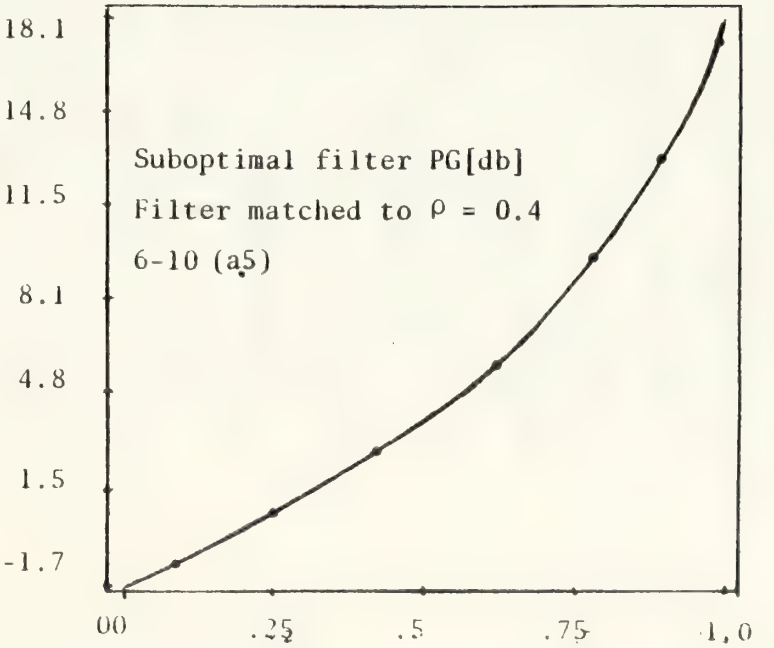

Fig. 6-10(b) Processing gain [db] as a function of ρ suboptimal filter.

Conclusion: The best suboptimal filter in this case was found to be the one designed for $\rho = 0.999$. Similar suboptimal studies should be performed to select the best "suboptimal" filter whenever noise statistics are expected to vary and when filter coefficients cannot be adapted on line.

F. MULTIPLE FRAME PROCESSING - NONRECURSIVE SEQUENTIAL SPATIAL-TEMPORAL FILTER FOLLOWED BY THRESHOLDING

1. Introduction

To evaluate three dimensional spatial-temporal focal plane processing, successive frames of images are needed. In Chapter IV, theoretical models based on Markov processes were used for correlated noises. In the spatial domain, both first order and second order Markov model correlated spatial noises are considered. Only first order Markov model was considered for the temporal correlated noise.

In this section, instead of using those computer generated images containing Markov model correlated noise, one set of real world infrared images of 32 x 32 pixels with constant drift of 10% of a pixel between frames is used to evaluate the performance of the sequential spatial-temporal filter followed by a thresholding. Except that it was originally taken by an ERIM[3] background measurement and subsequently modified by another group to include drift and several other modifications, no detailed information was given because

[3]ERIM is the Environmental Research Institute of Michigan

of the classified nature of the program which developed this scene as a standard test for focal plane processing algorithms.

In this section, statistical spatial filters are first designed for each frame to suppress clutter. The statistical spatial correlation properties of every frame of images are calculated separately and used in the filter design. Then, several frames of these spatially-filtered images are used together for the calculation of their temporal correlation properties which are used to design a temporal filter which will be applied to several frames of spatial-filtered images to give one frame of spatial-temporal filtered image. A threshold level is then determined from the PDF of the intensity of the filtered image and applied to initiate the target detection. These procedures were developed in another thesis by Captain D. Hilmers [30].

2. Spatial Filters and Their Performance

Figure 6-11 is a nine gray-level* computer overlay print of one frame of the real world infrared image. Figure 6-12 is a plot of its probability density function. The mean is found to be 4.03 and the variance is .45. Six moving targets of intensity 0.001, shown in Fig. 6-13, are added to this frame of image. This corresponds to an input signal to noise ratio of -72.3 db. The targets move down 1 pixel for each frame.

*Nine gray level: "blank" -, +, V, M, 0, θ, θ, ▒, ■

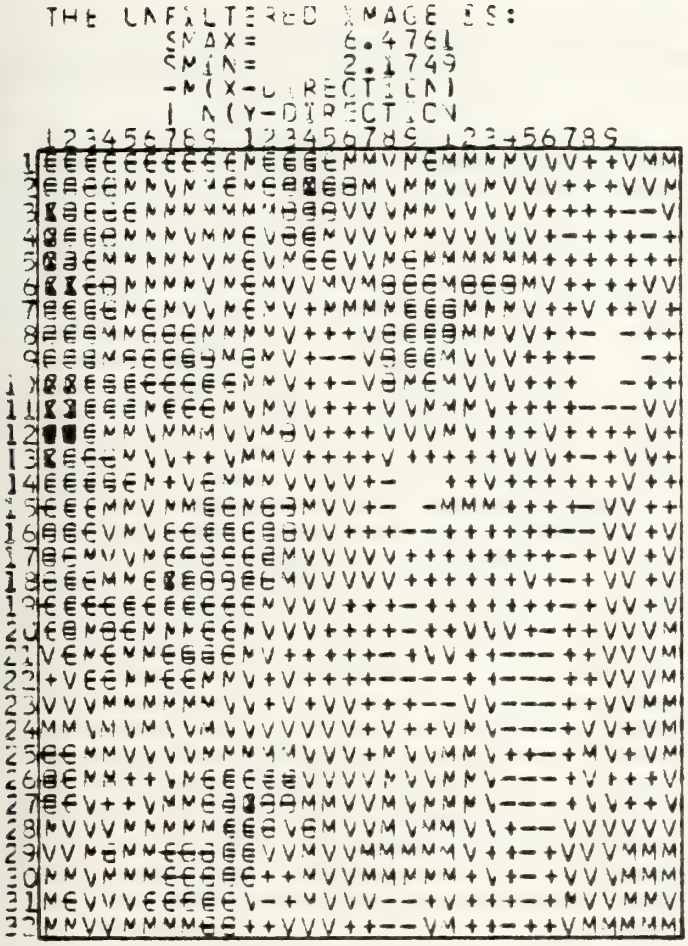

THE STATISTICS OF THE UNFILTERED IMAGE ARE:
MEAN= 4.33731
MEAN SQUARE= 16.75146
VARIANCE= 0.45103

Figure 6-11 9 Gray-level Computer Print of One Frame of 32 by 32 Pixels "Mill Creek" Infrared Image.

The Histogram of the Intensity of the Original Clutter Image Normalized so that the Area under the Curve is 1.0. [A hand fitted curve is added to indicate the shape of the PDF]

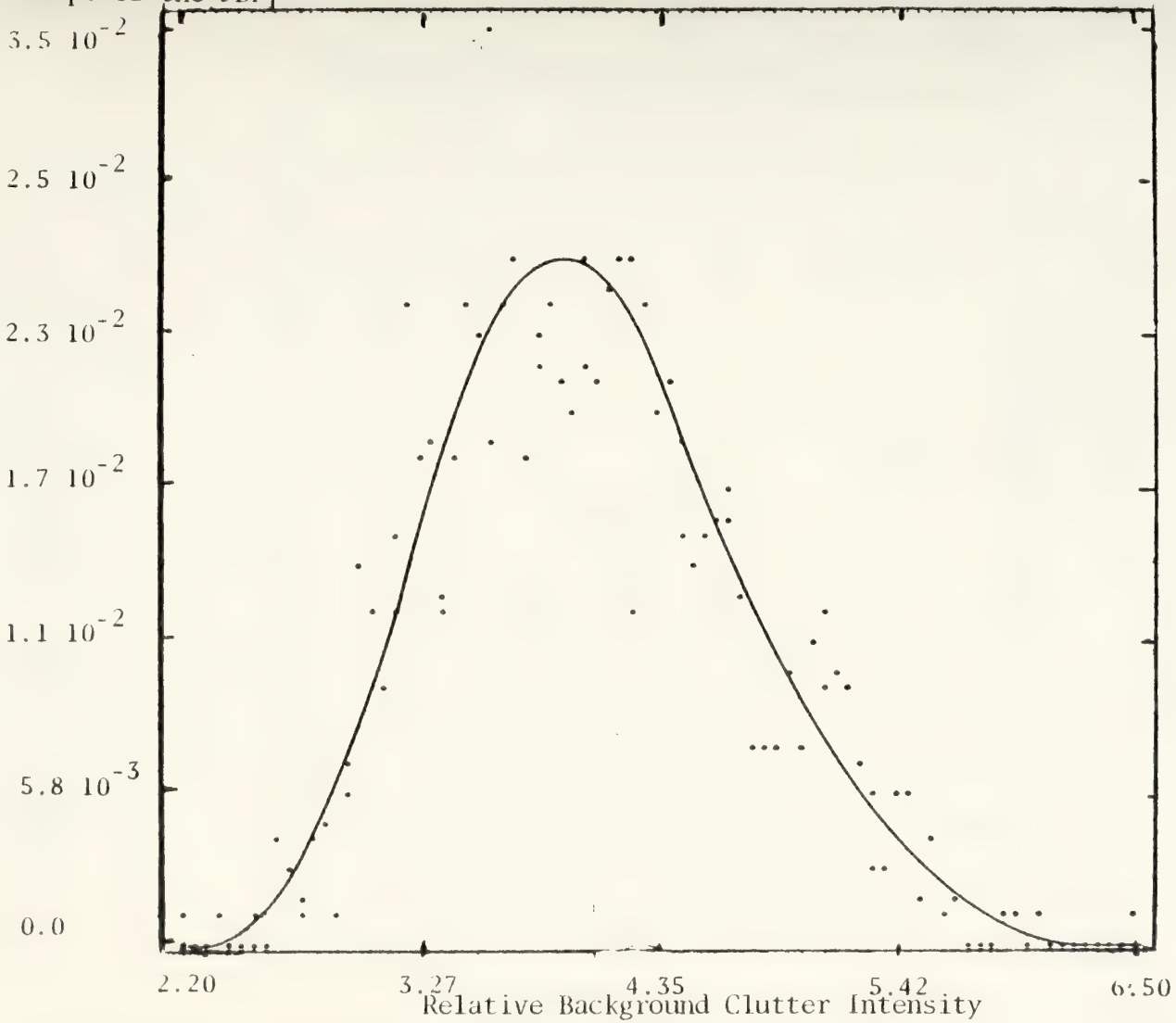

Figure 6-12 Histogram of Background Clutter Intensity of "Mill Creek" Image.

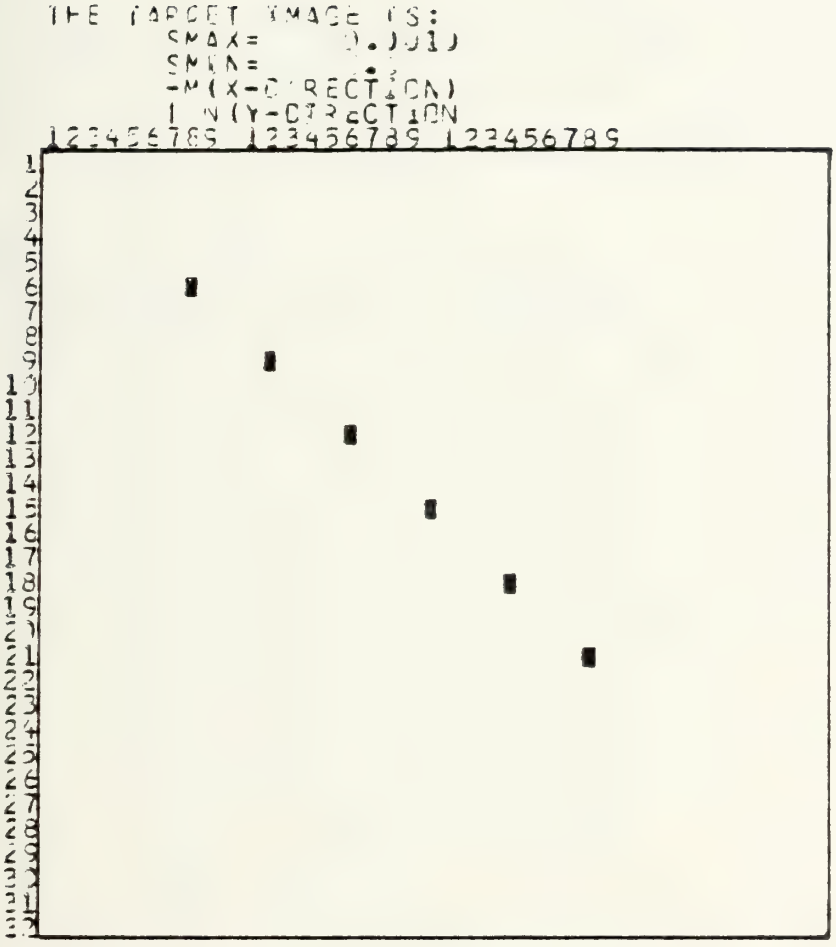

Figure 6-13 Six Moving Point Targets Added to the First Frame of "Mill Creek" Background Image.

At this low input SNR and for point targets there is no difference between the MMSE filter and the matched filter. A 3x3 spatial filter is designed and its filter coefficients are shown in Fig. 6-14. This spatial filter is then applied throughout this 32 x 32 image. The spatial-filtered image is shown in Fig. 6-14 with its new PDF shown in Fig. 6-15. It can be seen that the new PDF is somewhat symmetrical around zero intensity, indicating a zero mean.

3. Temporal Filter and Its Performance

Five consecutive spatial filter frames of images are filtered by a temporal matched filter whose coefficients are shown in Fig. 6-16. The resulting temporal filtered image is shown in Fig. 6-16 with its PDF shown in Fig. 6-17. The processing gains of both the spatial and temporal filters are also listed in Figs. 6-14 and 6-16 respectively. A threshold is then set to yield a P_{FA} of 10^{-3} and the resulting image is shown in Fig. 6-18. It should be recognized that the third frame is the "estimation frame" of this five frame temporal filter. Consequently, the targets in Fig. 6-18 appear 3 pixels down relative to their location in Fig. 6-13.

4. Conclusions

The spatial-temporal filtering method is a very useful technique for suppression of correlated clutter and detection of low signal level target. In the general case when K two dimensional frames of images are given, an optimal spatial-temporal filter can be designed for a given shaped target to

Spatial Filter Coefficients with Asymmetry Due to Anisotropy of Statistical Properties of the Real IR Image.

VECTOR- W

	1	2	3
1	0.266629	-0.453618	0.132261
2	-0.430767	1.000000	-0.463614
3	0.133065	-0.435073	0.284427

THE IMAGE AFTER SPATIAL FILTERING IS:

SMAX= 0.6257

SMIN= -0.6429

-M(X-DIRECTION)

| N(Y-DIRECTION)

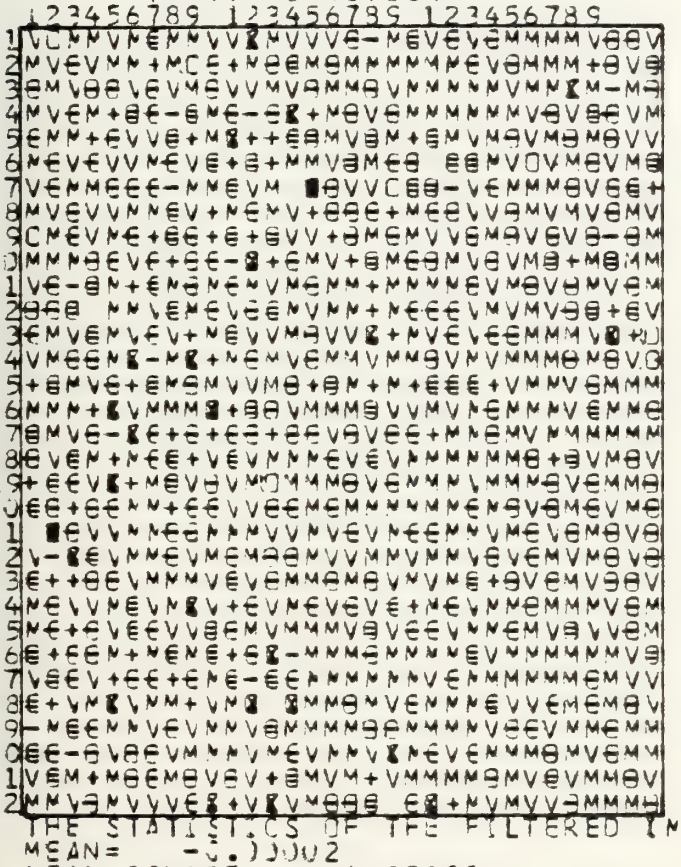

THE STATISTICS OF THE FILTERED IMAGE ARE:

MEAN= -0.0002

MEAN SQUARE= 0.02321

VARIANCE= 0.02821

THE PROCESSING GAIN OF THE FILTER= 27.73653 DB

Figure 6-14 Nine Gray-level Computer Print of Spatially Filtered First Frame of "Mill Creek" Image

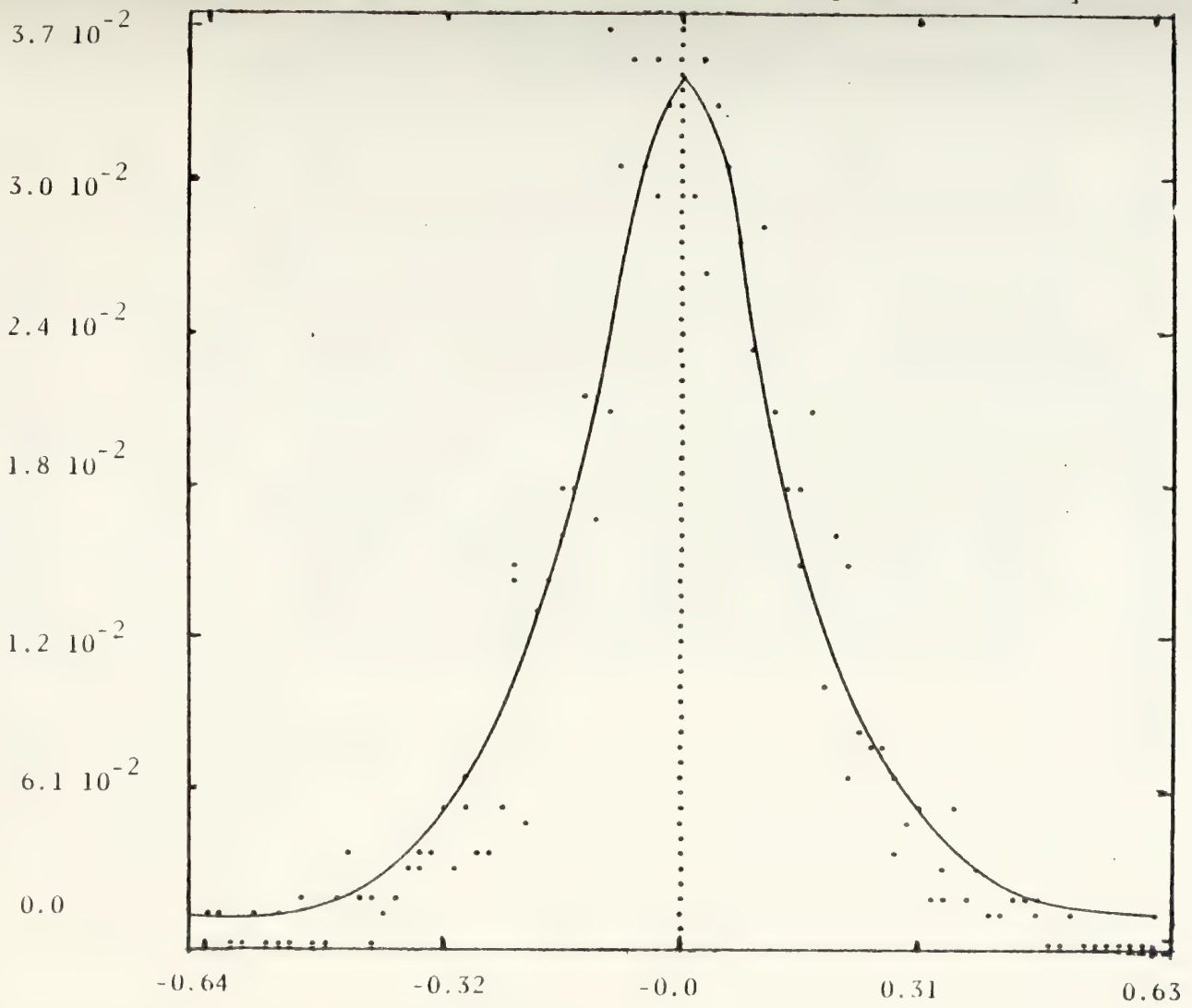

Figure 6-15 Histogram of Spatially Filtered First Frame of "mill Creek" Image Including Background Clutter and Added Point Targets.

The Spatially Temporally Filtered Image
and the Temporal Filter Coefficients

Temporal Filter Coefficients

Vector W_K

1	2	3	4	5
0.1776	-0.6771	1.0000	-0.6740	0.1753

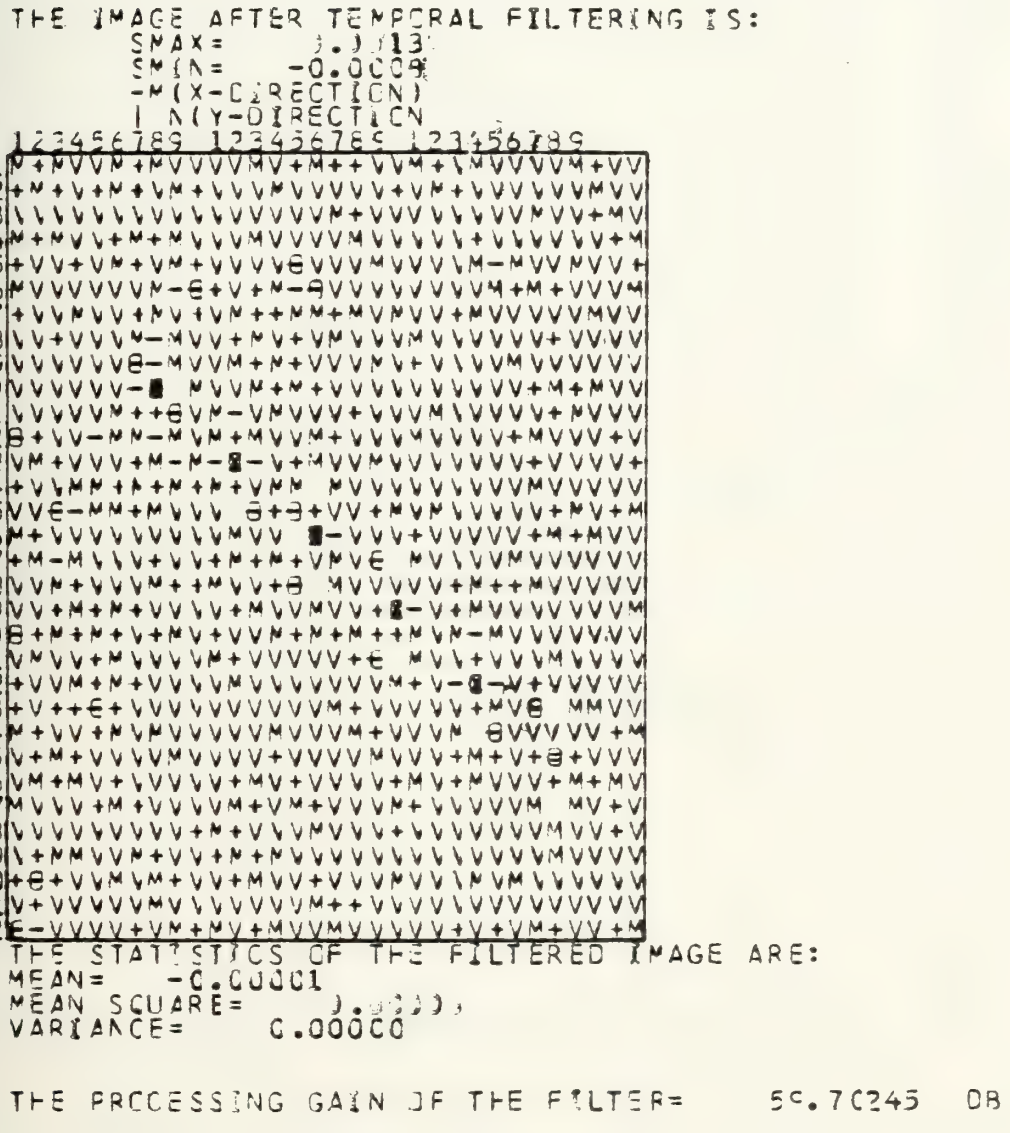

Figure 6-16 Nine Gray-level Computer Print of Spatially and Temporally Filtered Third Frame "Mill Creek" Image Including Background Clutter and Point Targets.

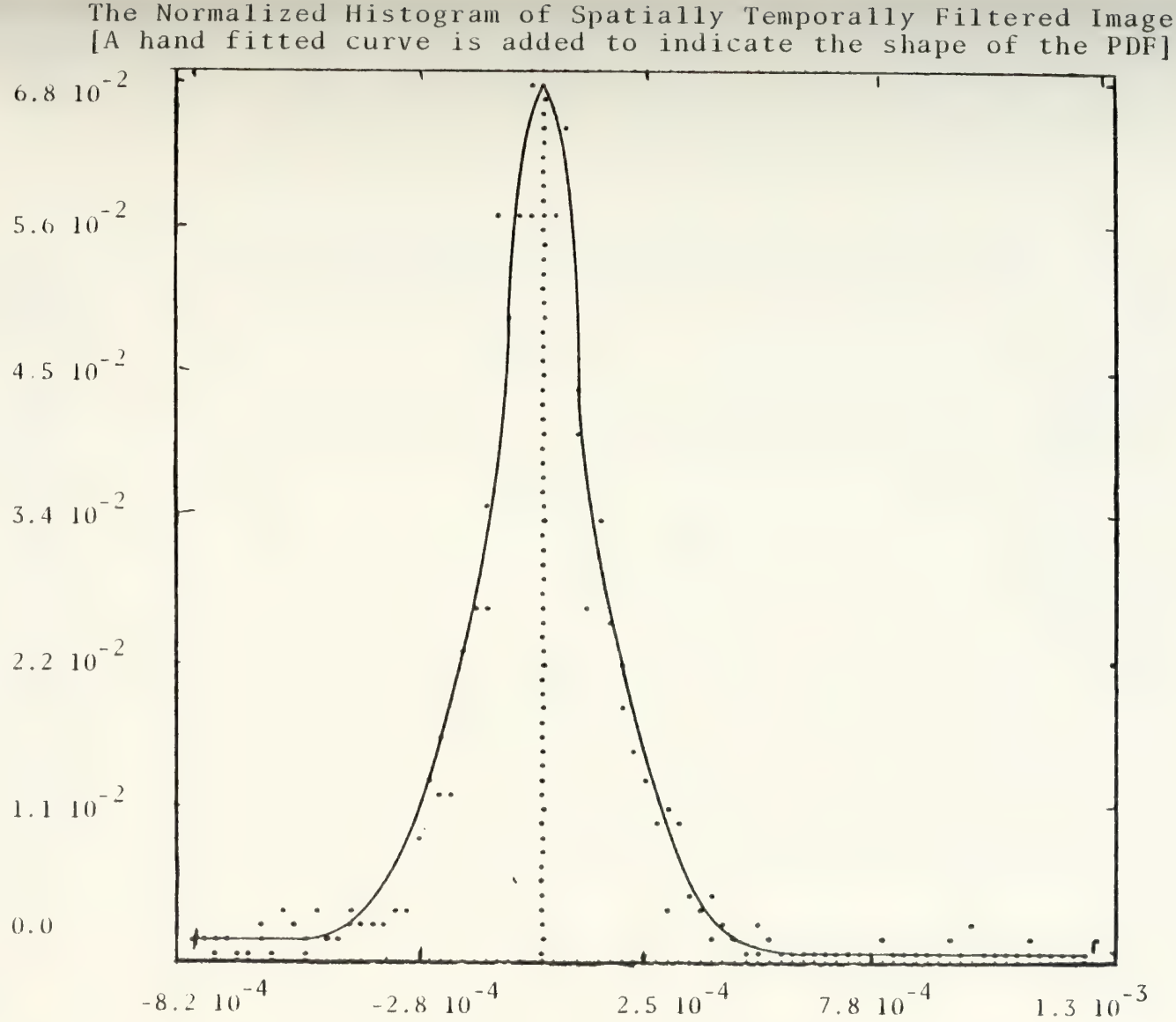

Figure 6-17 Histogram of Spatially and Temporally Filtered Third Frame of "Mill Creek" Image Including Background Clutter and Point Targets.

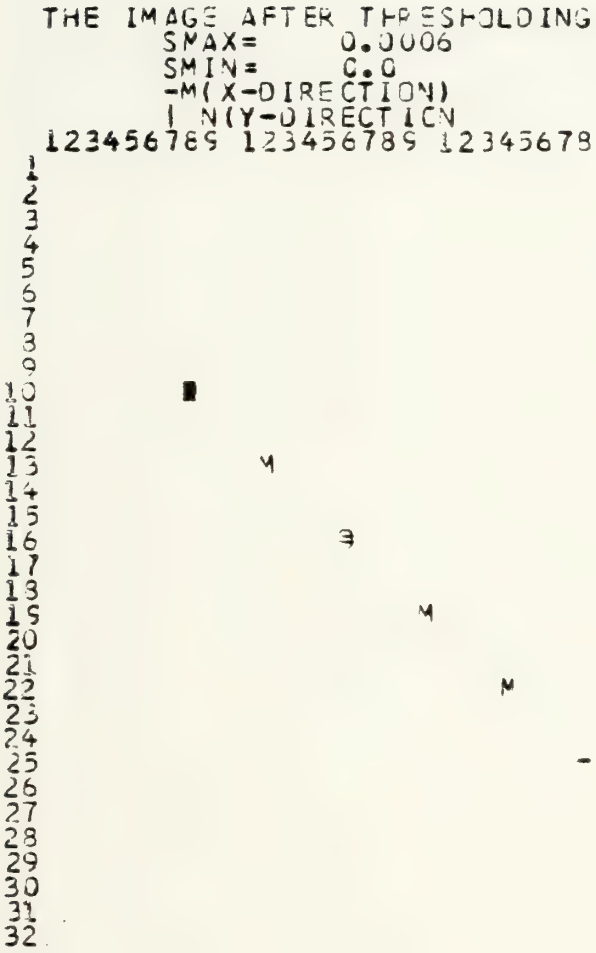

Figure 6-18 Nine Gray-level Computer Print of the Third Frame of "Mill Creek" Image after Spatial-Temporal Filtering and Thresholding.

achieve a certain processing goal. These goals and the resulting filter design method have to be evaluated for the particular application. In this chapter, a spatial temporal filter for the enhancement of moving point targets has been designed and tested using real IR clutter images. The results indicated that this type of filter can yield a processing gain as high as 60-70 db.

VII. ADAPTIVE SPATIAL FILTER I - STATIONARY CLUTTER STATISTICS

A. INTRODUCTION

In previous chapters, two types of filters were discussed: the two dimensional and three dimensional MMSE filters and matched filters, along with their design and implementation schemes. The performance of these filters was analyzed and presented. They both offer significant suppression of clutter noise when properly designed. The first problem we face when trying to design the filter is the unknown statistical properties of the noise. The second and more serious problem is the nonuniformities of the statistical properties of the noise. In other words, the noise is nonstationary.

In this chapter, a two dimensional adaptive filtering technique will be developed for cases where statistical properties of the noise are unknown but does not vary (stationary statistics). Extension to the nonstationary statistical properties of the image will be presented in Chapter VIII. An adaptive algorithm will be developed first for the Wiener filter, followed by a suggested modification to the matched filter.

B. ADAPTIVE WIENER FILTER

The requirement for this adaptive algorithm is to change the filter coefficients to minimize the mean square error as

fast as possible based on the clutter noise characteristic. The adaptation is achieved by utilizing the steepest descent algorithm together with a proper selection of required reference performance. Steepest descent is a well established technique for one dimensional adaptive filters. Extension of this technique to two dimensional adaptive filters will be presented in the following sections. An implementation scheme will be suggested along with simulation results and performance analysis.

It should be pointed out that there is another important difference from the previously developed one dimensional filters. Most one dimensional adaptive filters are designed to operate in a white noise environment with correlated target samples. In this study, instead of white noise, we are facing a highly correlated noise. On the other hand, targets are often uncorrelated. For example, point targets are uncorrelated in both x and y variables. Horizontal line targets are uncorrelated in the vertical direction.

There are two approaches to suppress the correlated noise.

1. The first approach is to treat the correlated noise as if it were a "signal" and try to predict (or estimate) its value in each pixel. Reference 34 demonstrates this basic concept utilizing an adaptive filtering technique. References 13 and 35 demonstrated again this concept by utilizing

a two dimensional Kalman filter rather than an adaptive filter.

2. The second approach is to treat the correlated noise as "noise," and to design an optimal noise suppression technique based on the statistical noise and target characteristics.

In this work, the second approach is taken by direct adaptation of the filter coefficients so as to minimize the mean square error between the target and the target estimate. This approach was selected since it seemed to be easier for practical implementation.

C. ADAPTIVE ALGORITHM BASED ON STEEPEST DESCENT

Steepest descent is an effective adaptation technique and was shown to be superior [21] to other adaptive methods when a reference input can be specified.

The analysis of this method is similar to the analysis of nonrecursive spatial filters presented in Chapter III. The input signal vector, X_j, is defined as

$$X_j^T = [x_{1_j}, x_{2_j} \ldots x_{i_j} \ldots x_{I_j}] \tag{7-1}$$

The filter coefficients are

$$W^T = [w_{1_j}, w_{2_j} \ldots w_{i_j} \ldots w_{I_j}] \tag{7-2}$$

The input signals are assumed to appear simultaneously on all input lines at discrete spatial locations indexed by the subscript j; j is the pixel number in the image as was

shown before in Fig. 4-2 where $j = NMAX\ (n-1) + m$; i is the index describing the location of the input samples in the search box as in Fig. 4-2 where $i = MSB * (n-1) + m$.

The input signals are multiplied by the nonrecursive filter coefficients $w_1, w_2 \ldots w_I$ and then summed together as shown in Fig. 7-1.

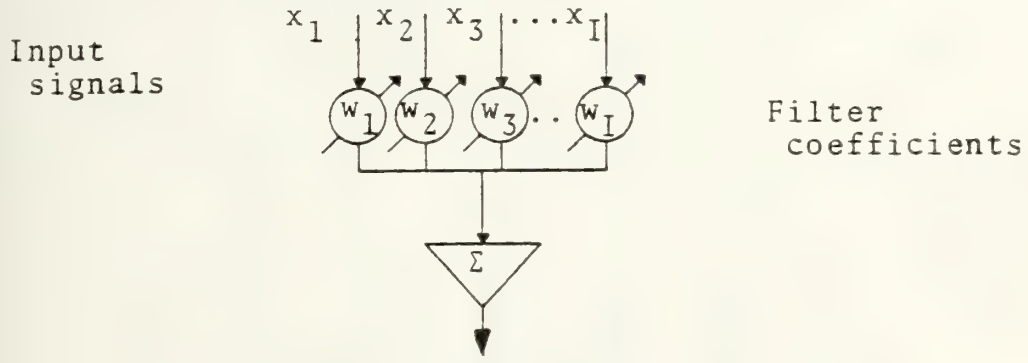

Figure 7-1

The general filtering configuration is given in Fig. 7-2.

In the following, an adaptive method will be presented to adapt the filter coefficients $W_1 \ldots W_n$ to achieve an optimal estimate of a known signal. It will be shown that at steady state the filter coefficient will approach the Wiener filter coefficients. A review of the adaptive filtering formulation based on references 21, 22 will be presented in Appendix C.

The algorithm derivation is based on the following model. At a given pixel, the output of the filter is

$$y_j = X_j^T \quad W = W^T X_j \qquad (7\text{-}3)$$

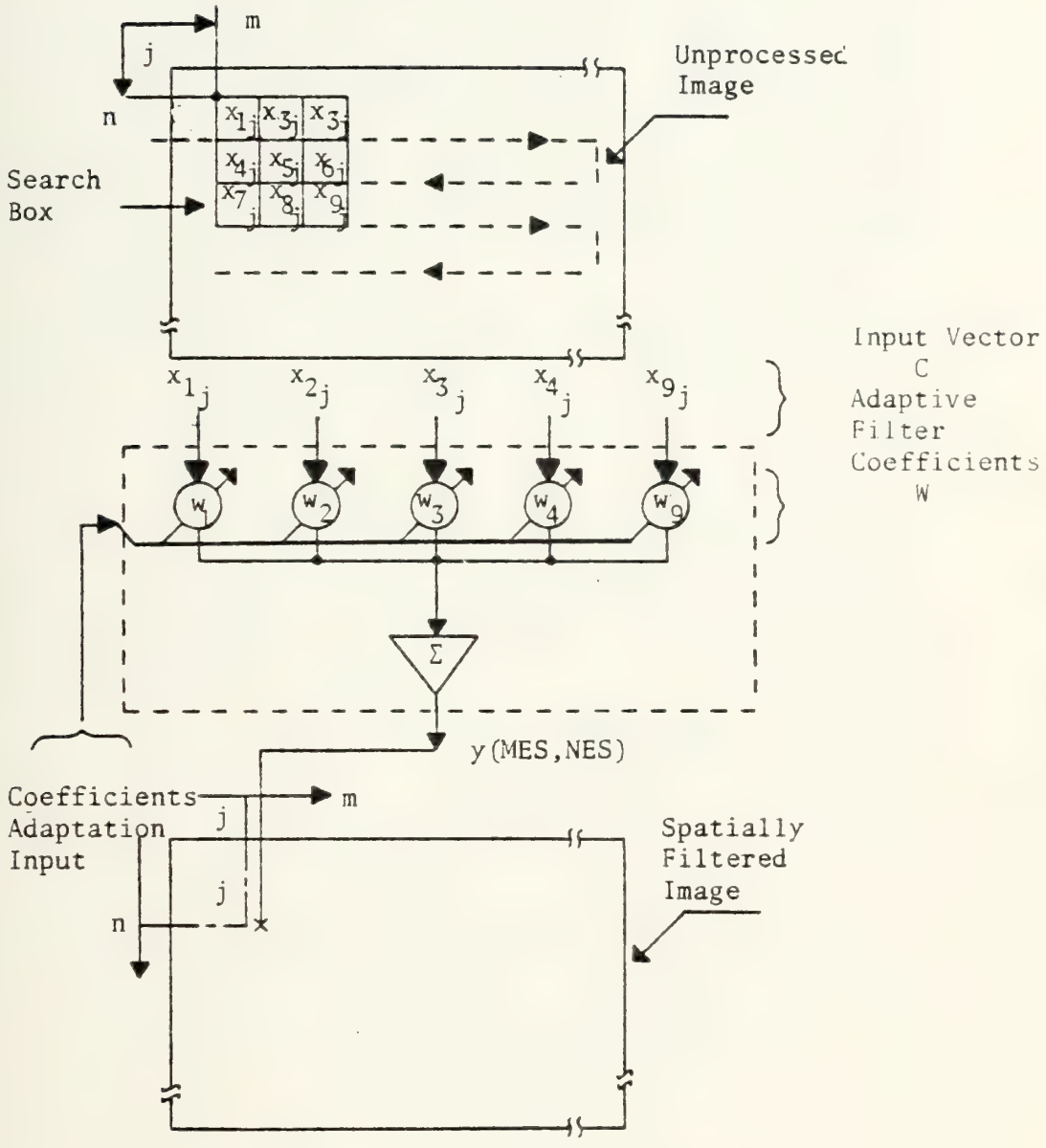

Figure 7-2 Configuration of Nonadaptive Two Dimensional Nonrecursive Spatial Filter.

Let us select a desirable reference performance, d_j, which we seek to achieve at the steady state. For example, in the case of point target detection (or estimation), we seek to achieve the best estimate of a point target while suppressing the background clutter noise as much as possible. Similarly, in case of line target detection (or estimation), we seek to achieve the best estimate of a given line while suppressing the clutter noise.

Let us define the error ε_j at pixel location j to be

$$\varepsilon_j = d_j - y_j = d_j - W^T X_j \qquad (7\text{-}4)$$

It is the purpose of the adaptive process to adjust the weighting coefficients of the linear adaptive filter to minimize the mean square error ε_j.

In this chapter we will make the assumption that the clutter noise is stationary. In the following chapter, a method will be suggested to deal with nonstationary clutters, where the statistical properties can be assumed to be stationary only within a small area. The detailed adaptation method and derivation are explained in Appendix C.

D. TWO DIMENSIONAL ADAPTIVE FILTERING CONSIDERATIONS

1. Introduction

In this section, "non-optimal" spatial filtering will be described to introduce the need for adaptive filtering. For this purpose, a composite simulated image is used which consists of four subimages simulated by computer and having four different statistical correlated noise characteristics as shown in Fig. 7-3.

Upper left quadrant:- 2nd order Markov model

$$\beta_H = 0.628$$
$$\beta_V = 0.063$$
$$\rho_H = \rho_V = 0.95$$

Upper right quadrant:- 2nd order Markov model

$$\beta_H = 0.063$$
$$\beta_V = 0.628$$
$$\rho_H = \rho_V = 0.95$$

Lower left quadrant:- 2nd order Markov model

$$\beta_H = 0.628$$
$$\beta_V = 0.628$$
$$\rho_H = \rho_V = 0.95$$

Lower right quadrant:- 1st order Markov process

$$\rho_H = 0.99$$
$$\rho_V = 0.30$$

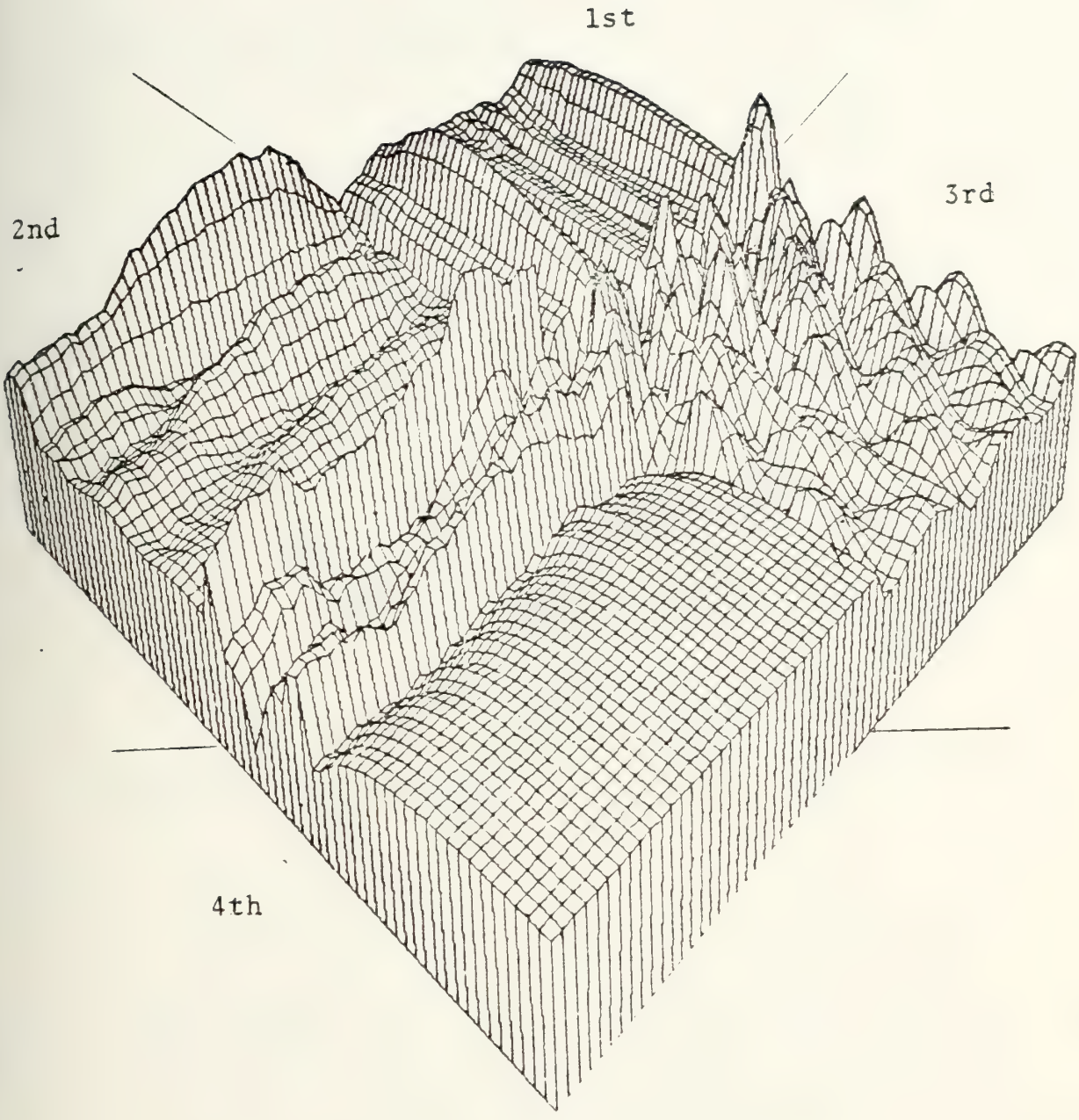

Figure 7-3 Three Dimensional Plot of Computer Generated Four Quadrants "Nonstationary" Clutter Image

Based on the statistical properties of each quadrant, optimal spatial MMSE filter can be designed as follows:

For upper left quadrant:

$$\begin{bmatrix} .3 & -.5 & .3 \\ -.6 & 1.0 & -.6 \\ .3 & -.5 & .3 \end{bmatrix}$$

For upper right quadrant:

$$\begin{bmatrix} .3 & -.6 & .3 \\ -.5 & 1.0 & -.5 \\ .3 & -.6 & .3 \end{bmatrix}$$

For lower left quadrant:

$$\begin{bmatrix} .36 & -.6 & .36 \\ -.6 & 1.0 & -.6 \\ .36 & -.6 & .36 \end{bmatrix}$$

For lower right quadrant:

$$\begin{bmatrix} .24 & -.487 & .24 \\ .499 & 1.0 & .499 \\ .243 & -.487 & .243 \end{bmatrix}$$

However, Fig. 7-4 shows the filtered image by using only one spatial MMSE filter optimally designed for the upper right quadrant but applied throughout the whole image. It should be pointed out that a threshold was applied after the spatial filtering to obtain Fig. 7-4. It can be seen that excellent "clutter noise" suppression was accomplished in the optimal

Filtered and Thresholded Image

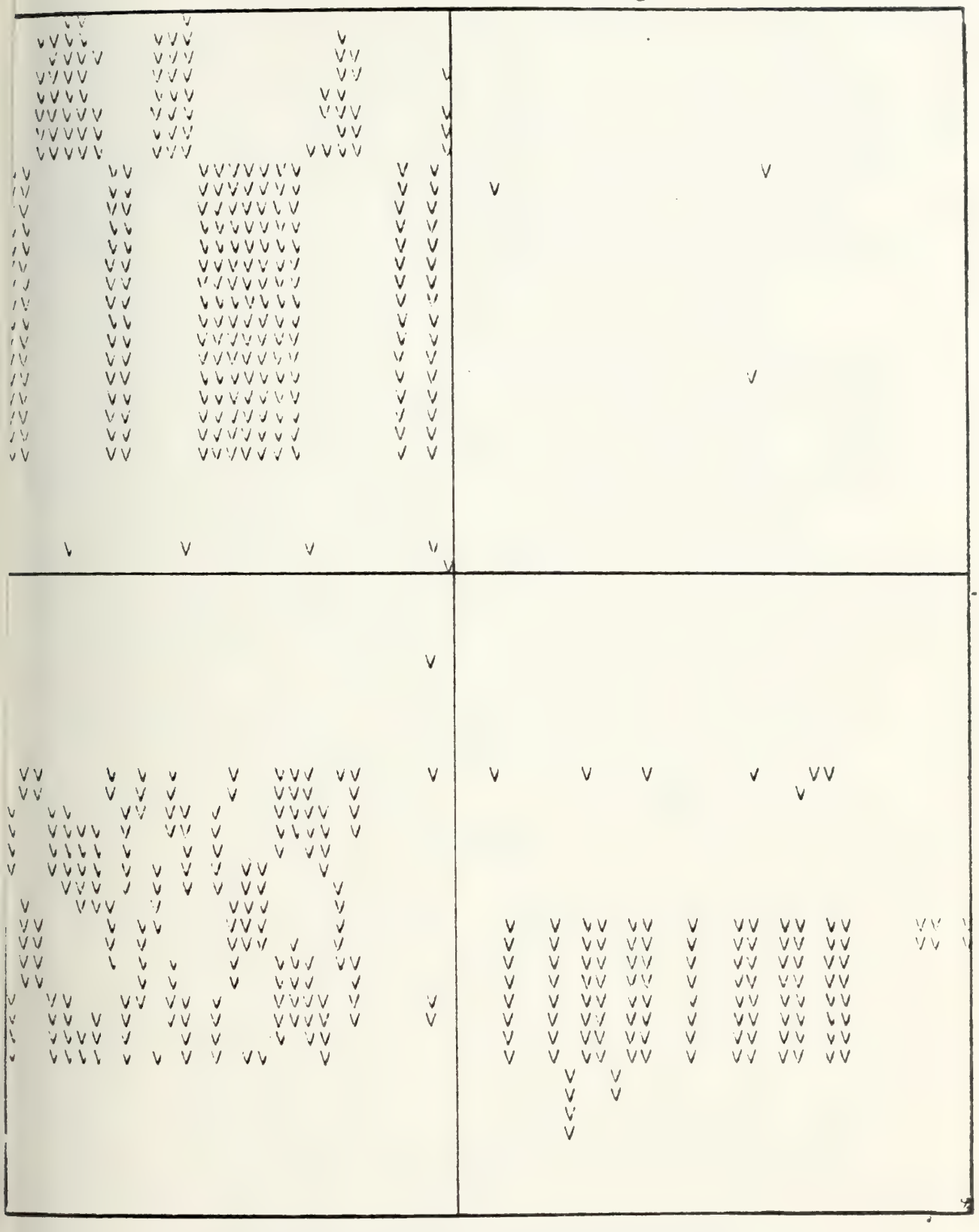

Probability of false alarm is 0.1462.

V ≡ false alarm]

Figure 7-4 Computer Print of Nonadaptively Filtered and Thresholded Four Quadrant "Nonstationary" Clutter Image.

filter quadrant. Considerable amount of clutter noise remained in the other three "suboptimal" filtered quadrants. It would be desirable if an adaptive algorithm can be developed so that the filter coefficients will be adaptively changed to new optimal values when the filter is moved into areas having different statistics.

An example of such an adaptive filter configuration is shown in Fig. 7-5. Similar to all other spatial filters developed in this thesis, it uses a 3x3 search box. Signals of all nine pixels in the box are weighted and summed to give an estimate of the target signal at the central pixel. However, there are two major differences. First, the weighting coefficients are adaptively changed by a feedback procedure as shown in Fig. 7-5. At the beginning, nonrecursive spatial filtering is carried out as described previously. The processed target signal, y_j, is now compared with the selected desirable reference target, d_j, by subtraction and produces an error signal, ε_j. This is then multiplied by the adaptive loop gain constant, μ, and then by the nine corresponding unprocessed signals, X, to process a correction weighting coefficient, ΔW_j, for its corresponding coefficient, W_j. The new filter coefficients, $W_j + \Delta W_j$, are used to perform a new step of spatial filtering and generate an additional set of corrections to the filter coefficient. Then the estimation pixel is moved one pixel, a new set of unprocessed

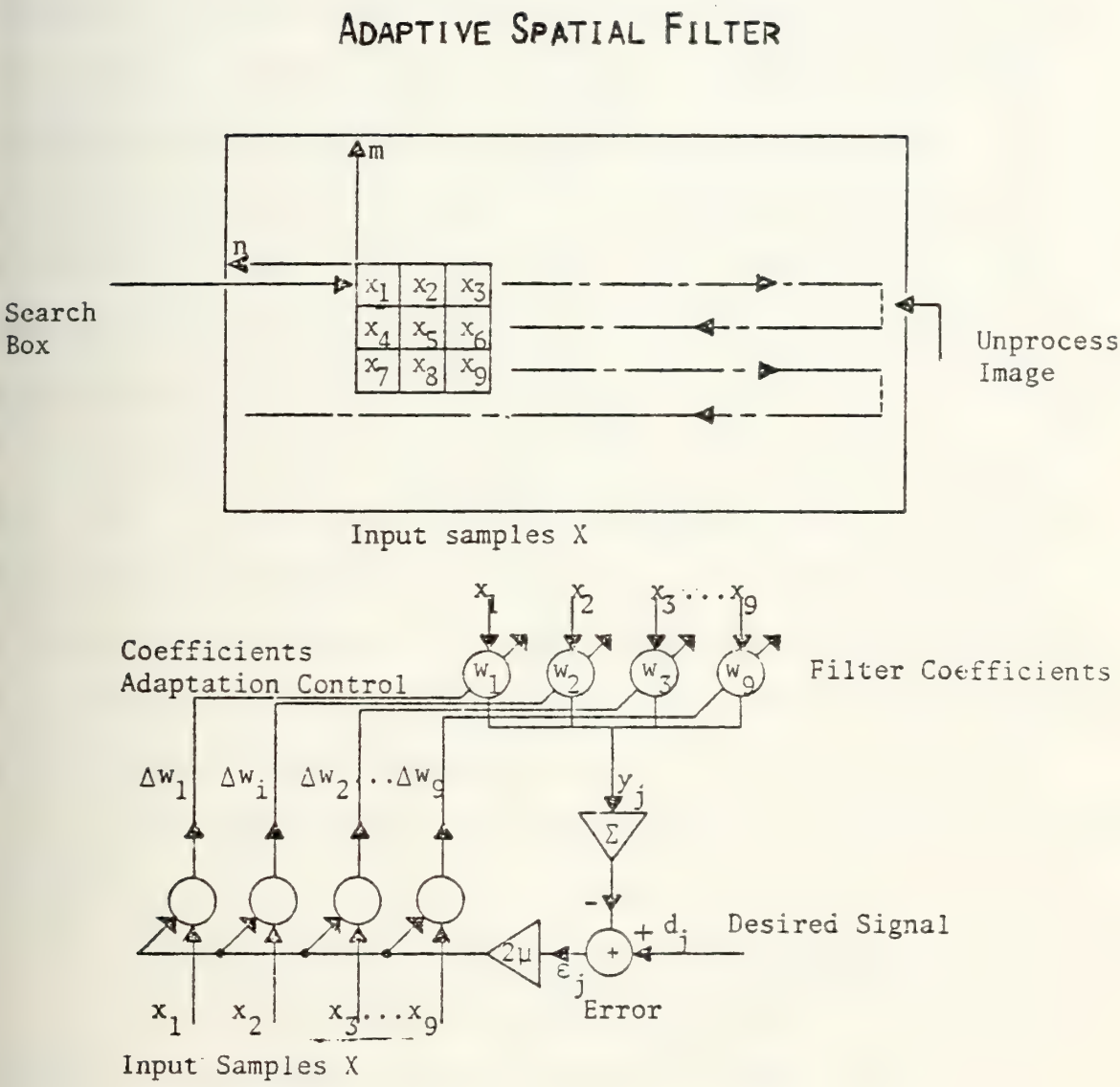

Figure 7-5 Configuration of Adaptive Two Dimensional Nonrecursive Spatial Filter.

signals, X, is read out and the adaptive filter process is repeated again. This adaptive process is repeatedly carried out according to the process described in Appendix C and based on the LMS adaptive algorithm, equation (C-42), until the steady state optimal solution is reached. The second difference of this adaptive spatial filter from the non-adaptive spatial filter is in the scanning pattern of the estimation pixel. It is not the conventional raster that the estimation pixel is moved back after the completion of each row and is always scanned in the same direction. Instead, after each row, the scan direction is reversed as shown in Fig. 7-5. The reason for this successive reversal of scan direction from one row to the next is to insure that the change of statistical characteristics of the clutter noise is minimized because in this new scan motion the estimation pixel is moved only by one pixel.

More details on the implementation of adaptive spatial filters will be developed in the next section.

2. Detailed Implementation of Adaptive Spatial Filter

Several aspects of adaptive spatial filter implementation are described in more detail in this section:

a. Image scanning pattern

b. Termination of filter coefficient adaptation

c. Derivation of desired reference d_j

d. Selection of adaptive loop gain μ

e. Required number of independent pixels to achieve adaptation

a. The Image Scanning Pattern

Several image scanning patterns were tested. Figure 7-6 presents two possible scanning alternatives. Comparing the scanning pattern of Fig. 7-6(a) to that of 7-6(b), it was found that using the pattern of Fig. 7-6(b) to adapt the filter did not yield the optimal filter coefficients. This scanning pattern introduced an artificial transition at the end of each row and therefore affected the adaptive process. On the other hand, the pattern of Fig. 7-6(a) offered a smooth adaptation without these artificial transitions and the resulting adapted filter coefficients were found to be the optimal.

b. Algorithm for Termination of Filter Adaptation

Several algorithms were tested for termination of filter adaptation. The selected algorithm is based on the following steps and its flow chart is presented in Fig. 7-7.

(1) Test the MSE at each $\underline{n}^*$ adaptation step.

(2) Keep track of the lowest MSE = $MSE_{min}(0)$ and its corresponding filter coefficients.

(3) Test every $\underline{N}^*$ ($\underline{N} >> \underline{n}$) adaptation step whether the new $MSE_{min} = MSE_{min}(1)$ is smaller than $MSE_{min}(0)$ by a

---

*n,N are constants that can be selected either by simulation or arbitrarily, as recommended later on.

Image Scanning Patterns

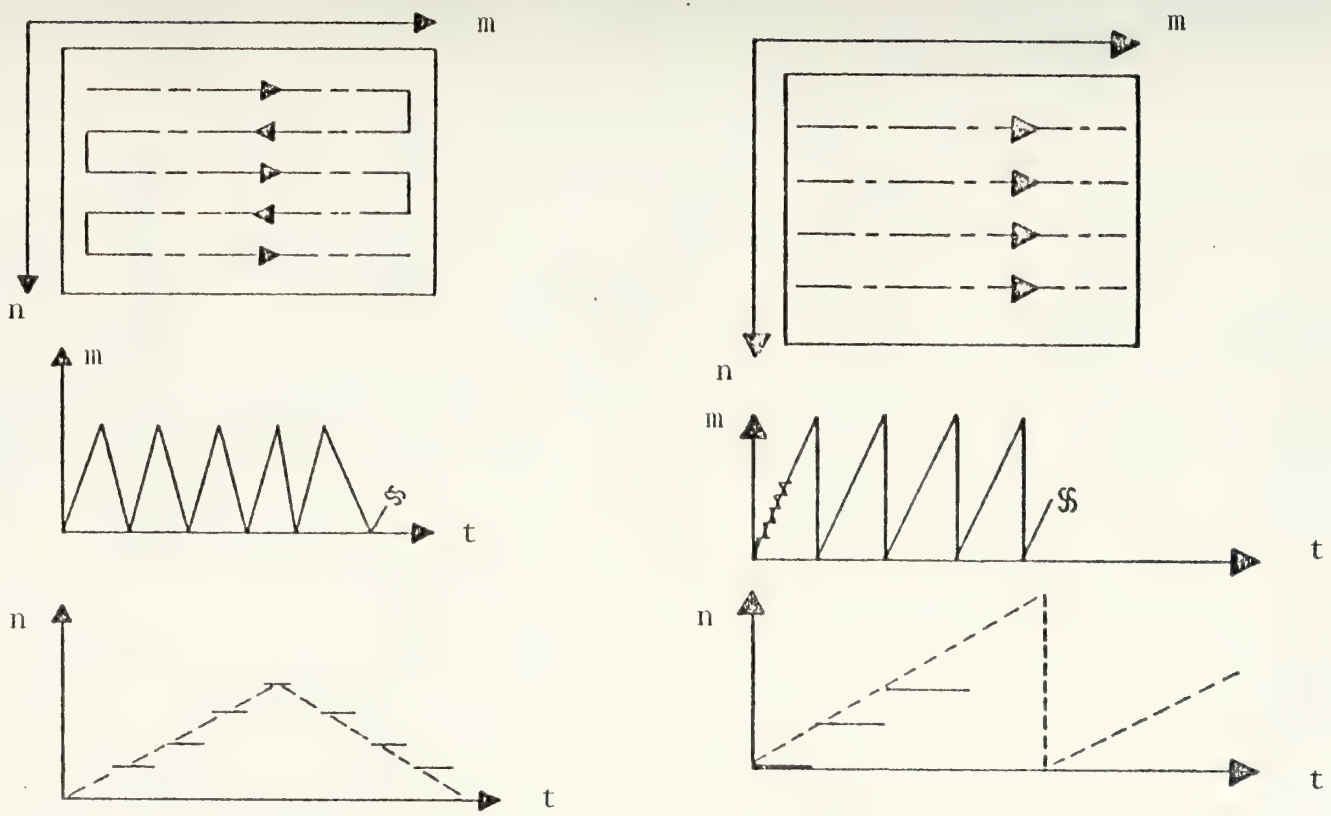

(a) Scanning pattern adequate for adaptation

(b) Scanning pattern not adequate for adaptation

Figure 7-6 Two Scanning Patterns for Performing Adaptive Spatial Filter.

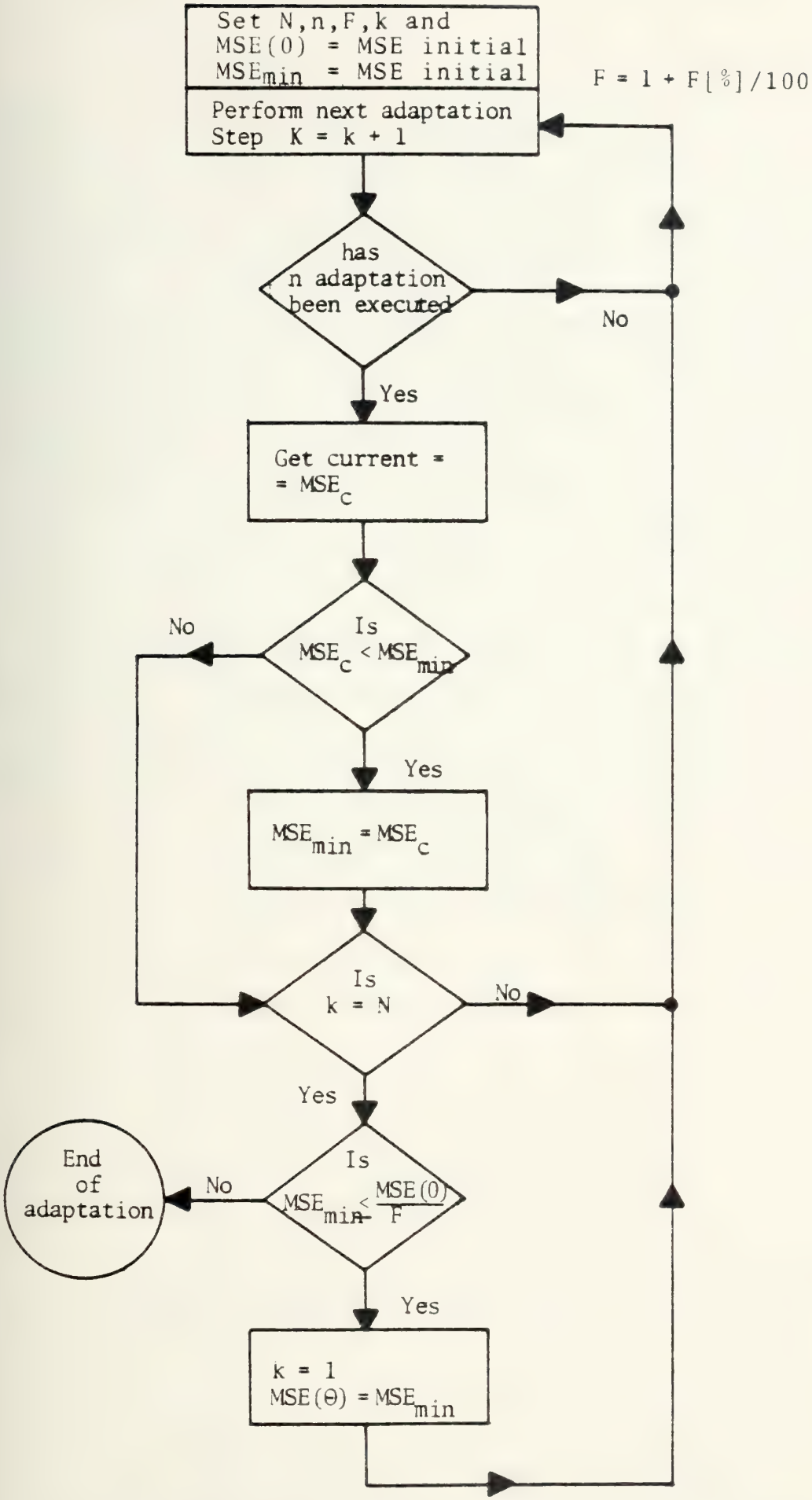

Figure 7-7. Software Algorithm to Terminate Filter Adaptation

certain factor F (say, 5%). If smaller, then continue, else terminate adaptation. Other algorithms based on monitoring the filter coefficients error or continuous tracking of MSE (short term observation) did not yield satisfactory results. The suggested algorithm was tested in various simulated images and it functioned well whenever the parameters F, N, n were selected properly. When absolutely no a priori knowledge of noise statistics is given, these parameters can be selected for the worst case: for example, n = 36; N = 360; F = 0.1%. When some statistical data is available, these parameters can be optimized to hield fastest indication of adaptation termination. The information about adaptation termination is necessary mainly for the following two purposes: (1) an attempt to filter the image before reaching the steady state solution will yield poor noise suppression; (2) in Chapter VIII a particular application of the adaptive filtering technique will be presented by dividing the image into many subimages and adapting a different filter to each subimage. Under such circumstances and when only one central processor is available, it is important to detect the adaptation termination in each subimage before moving to the next subimage.

c. The Derivation of the Designed Response, d_j

To derive the desired response, d_j, let us return to the LMS adaptation algorithm presented in eq. (C-42):

$$W_{j+1} = W_j + 2\mu\varepsilon_j \cdot X_j \qquad \text{or}$$

$$W_{j+1} - W_j = 2\mu\varepsilon_j \cdot X_j = \Delta W_j \tag{7-5}$$

where ΔW_j is the filter coefficients correction vector at adaption step j. Substitution of the error equation (C-2) into (7-5) will yield,

$$\Delta W_j = 2\mu(d_j - W^T \cdot X_j) \cdot X_j \qquad \text{or}$$

$$\Delta^* W = \frac{\Delta W_j}{2\mu} = (d_j - W^T \cdot X_j) \cdot X_j \tag{7-6}$$

Fig. 7-8 presents typical 3x3 spatial filter and the corresponding input samples for various target types.

Referring back to eq. (7-6), let us expand the matrix for the simple point target example of Fig. 7-8(a)

$$\begin{aligned}
\Delta^* w_1 &= x_1\{[x_1 w_1 + ..(x_5 + s)w_5 + \ldots x_9 w_9] - s\} \\
&\vdots \\
\Delta^* w_5 &= (x_5+s)\{[x_1 w_1 + \ldots(x_5 + s)w_5 + \ldots x_9 w_9] - s\} \\
&\vdots \\
\Delta^* w_9 &= x_9\{[x_1 w_1 + \ldots (x_5 + s)w_5 + \ldots x_9 w_9] - s\}
\end{aligned} \tag{7-7}$$

where s is used twice on this configuration - once as the desired response d_j, and once as an injected signal - injected artificially to sample x_5.

As mentioned earlier, the adaptive process acts as a low pass filter smoothing out equation (7-7) to yield its expected value:

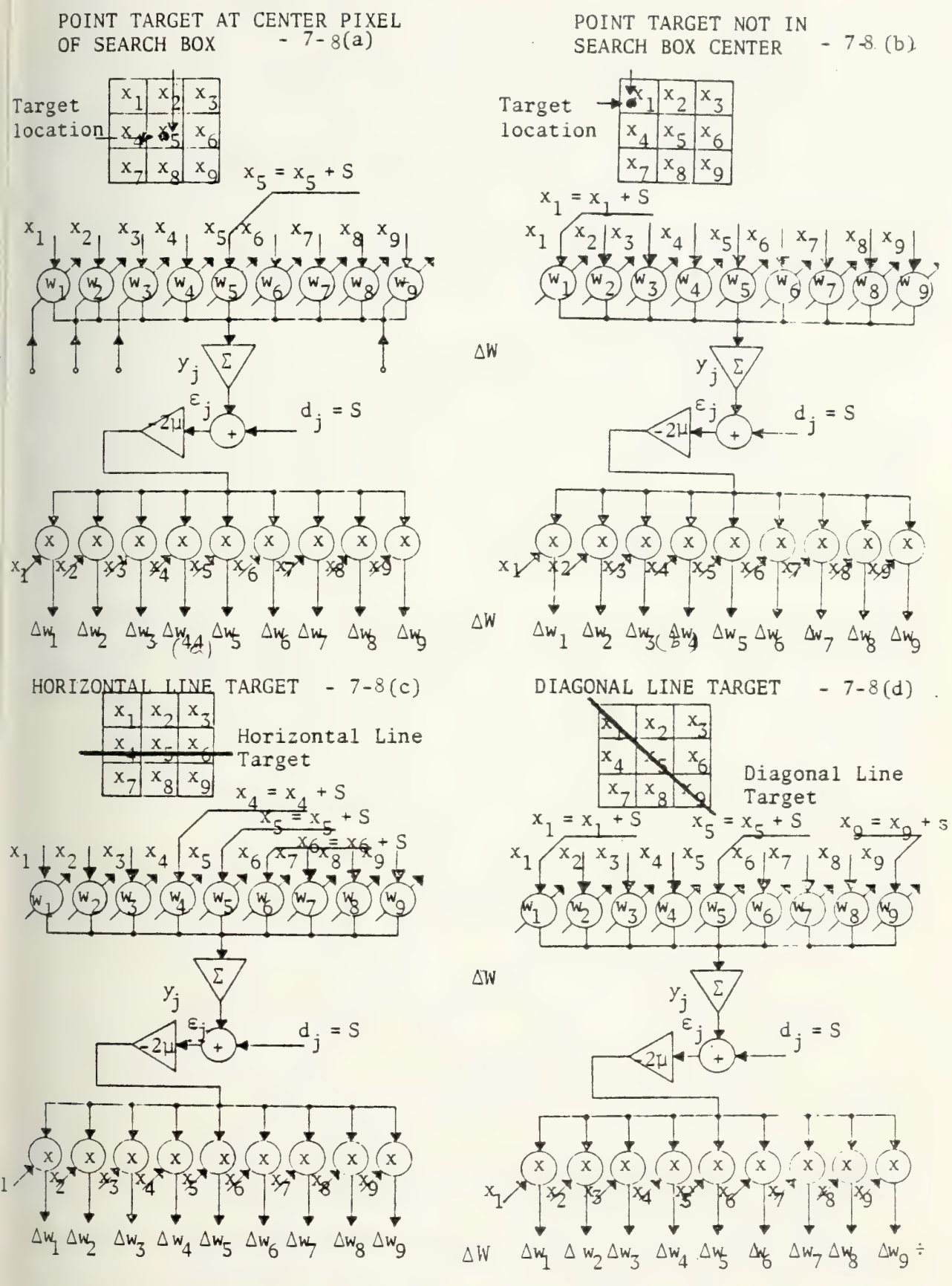
POINT TARGET AT CENTER PIXEL OF SEARCH BOX - 7-8(a)
POINT TARGET NOT IN SEARCH BOX CENTER - 7-8(b)
Target location
$x_5 = x_5 + S$
$x_1 = x_1 + S$
y_j
ε_j
$d_j = S$
-2μ
ΔW
Δw_1 Δw_2 Δw_3 Δw_4 Δw_5 Δw_6 Δw_7 Δw_8 Δw_9
HORIZONTAL LINE TARGET - 7-8(c)
Horizontal Line Target
$x_4 = x_4 + S$
$x_5 = x_5 + S$
$x_6 = x_6 + S$
DIAGONAL LINE TARGET - 7-8(d)
Diagonal Line Target
$x_1 = x_1 + S$
$x_5 = x_5 + S$
$x_9 = x_9 + S$

Figure 7-8 Operations for the Generation of Reference Input, d_j

$$E[\Delta^{*}w_1] = E[x_1x_1]\,w_1 \quad +.. E[x_1x_5]w_5 +.. E[x_1x_9]w_9$$

$$E[\Delta^{*}w_5] = E[x_5x_1]w_1 + E[x_5x_5]w_5 + E[x_5x_9]w_9$$

$$+ E[s\cdot s]w_5 - E[(x_5 + s)\cdot s]$$

$$E[\Delta^{*}w_9] = E[x_9x_1]w_1 + E[x_9x_5]w_5 + ..E[x_9x_9]w_9 \qquad (7\text{-}8)$$

Assuming the signal s and the noise samples X are uncorrelated. At steady state $E[\Delta W^{*}_i]i=1,2,...9$ will be zero and eq. (7-8) can be rewritten in the vector form,

$$[R_{NN} + R_{SS}]\ W = P \qquad (7\text{-}9)$$

Assuming the input samples X consist only of noise and the target is summed artificially to X.

R_{NN} = cov [noise]

R_{SS} = cov [target]

P = cross correlation vector given by eq. (C-5).

Eq. (7-9) is indeed the Wiener filter equation for a point target. We can proceed in a similar way to construct d_j for other simple type targets.

Let us summarize the steps of deriving the d_j in the spatial adaptive filter configuration:

1. The target shape should be drawn with respect to the search box dimension.

2. All the X vector locations through which the target will pass will be "marked" to establish a reference vector, $D = [d_1d_2...d_I]$. All the "marked" locations, d_m,

will be set to s ≡ signal desired level, and the remaining location will be set to zero according to the shape of the target of interest.

3. While adapting the filter coefficients, it is assumed that relatively few pixels contain the target. An even more reasonable assumption can be made for practical imaging systems, considering the total absence of the external target during the initial adaptation phase. Making this assumption will require a preliminary "learning" period prior to utilizing the filter. Under this assumption the referenced vector D may be summed together with the input sample vector, X. The resulting outcome will be applied to the filter to yield its output, y_j.

4. The output, y_j, will be subtracted from the referenced signal $d_j \equiv s \equiv$ signal level to yield the error signal.

5. The error signal multiplied by the loop gain, 2μ, will be thus multiplied by each of the input vector $(X + D)$ components to yield the correction vector, Δw.

6. At steady state after many adaptation steps, $E[\Delta W]$ will approach zero and the Wiener filter solution will be reached.

d. The Corresponding "Adaptive" Matched Filter

It was mentioned earlier in this work that the selected major goal is to detect point targets. It is interesting to note the correspondence between the adaptive Wiener filter for point target enhancement and its counterpart - the

matched filter. Referring back to eq. (7-8), let us select S to be extremely small compared to the input noise samples. Under this condition, eq. (7-9) will become

$$R_{NN} \cdot W = P \tag{7-10}$$

where the non-zero term of $R_{SS} = (S^2)$ is very small compared to $E[x_5 x_5]$. Recalling from matched filter derivation that the matched filter solution is given by

$$R_{NN} \cdot W = C \cdot S \tag{7-11}$$

where C is a constant and S is the signal vector. In the case of point targets, both P and S will be in the same form.

$$P = [0, \ldots s^2, \ldots 0]$$

$$S = [0, \ldots s, \ldots 0]$$

Since we can select the constant C arbitrarily, selecting C = S will cause eq. (7-11) to be identical to eq. (7-10).

A practical implementation method to adapt the corresponding matched filter was performed in this work as the following:

1. Select $d_j \equiv S \equiv 0$ to satisfy equation (7-10).
2. Since the constant C may be selected arbitrarily and likewise, one of the filter coefficients can be selected arbitrarily, the estimation point coefficient was selected to be 1.00. Resulting simulated adaptation plots will be presented in this chapter. This modified Wiener filter coefficients adaptation curve, when compared to the theoretical matched filter coefficients, shows excellent agreement.

To conclude the matched filter discussion, let us note that for the case of point target enhancement a modified adaptive Wiener filter will yield a corresponding matched filter. For targets other than point targets, in many practical cases we can find a corresponding matched filter counterpart. This issue is beyond the scope of this work and will not be pursued any further.

e. The Selection of the Adaptive Loop Gain, μ

Appendix C, section C. presented few factors related to the selection of the loop gain. The first is the misadjustment, given in eq. (C-63), and the second is the related convergence time constant given in eq. (C-64). A more crucial parameter related to μ, is the stability of the adaptive loop.

In Chapter VIII we subjected the processing algorithm to the assumption that no a priori knowledge is available. Based on this assumption, an appropriate automatic gain control ("AGC") was needed. Various gain control loops were tested and the selected configuration is presented in Fig. 7-9. The "AGC" loop major design requirements were:

1. Under all possible reasonable initialization of filter coefficients (W_o) loop stability has to be assured (selection of $W_o = 0$ should be avoided in any case).

2. For any external selection of loop gain constant, C, the loop should not diverge (avoid overflow).

3. The steady state misadjustment, independent of background noise statistics, should be the same and should be controlled externally.

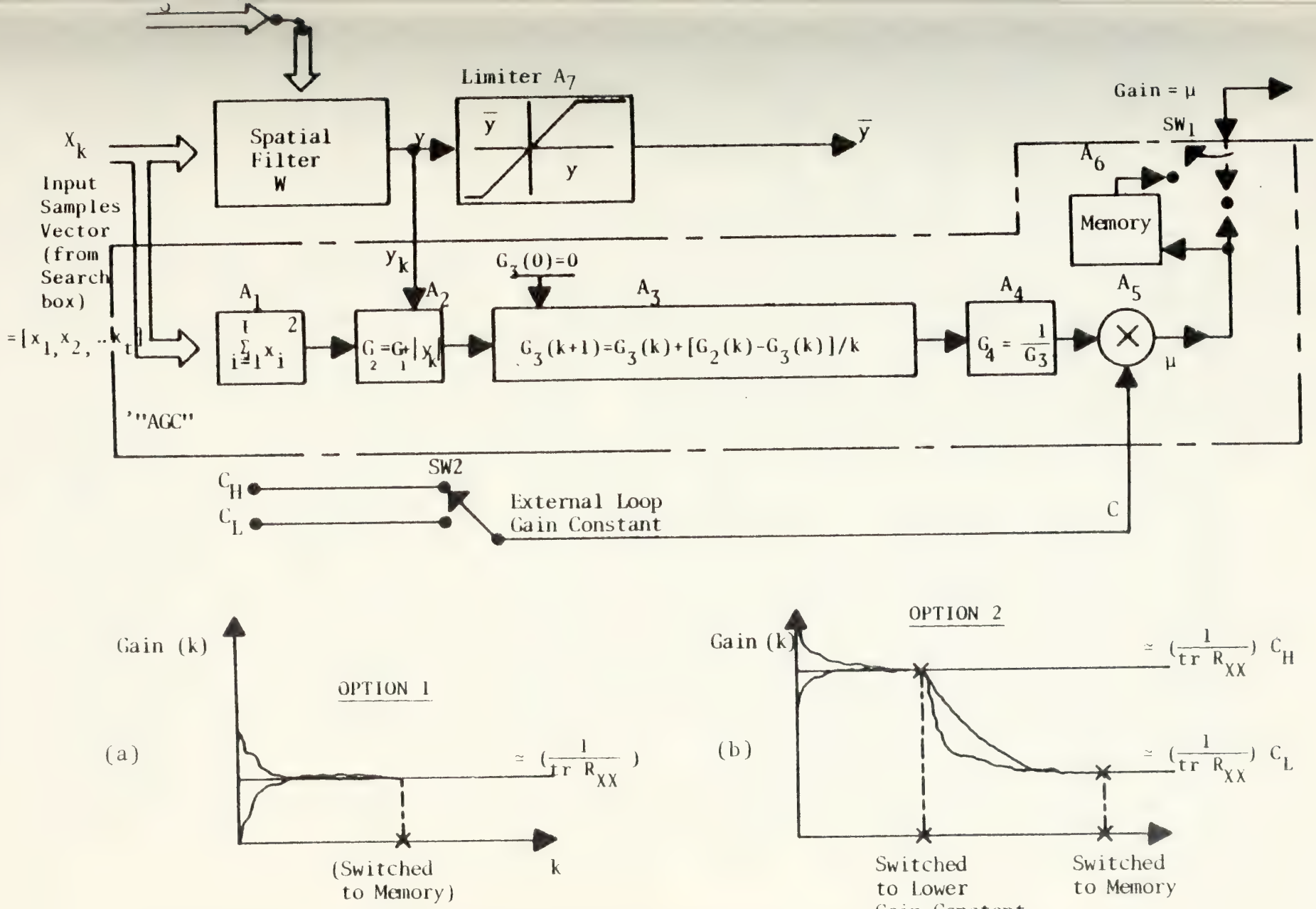

Figure 7-9 "AGC" Flow Diagram for Determining Adaptive Loop Gain, μ. Shown for the k-th Adaptation Step.

4. Subject to the above stated requirement, it is required to control the gain so as to yield the shortest adaptation time constant.

The following measures were taken to satisfy the listed requirements:

1. In order to avoid divergence of the filter output under any circumstances the output $y(m,n)$ is limited to a selected maximal value.

2. In order to assure a constant "misadjustment" the total input power in each input sample set, has to be calculated to get the estimate of $(\frac{1}{\text{trace } R_{XX}})$. This estimate is required since the misadjustment is given by:

$$M = \mu \cdot [\text{trace} \cdot R_{XX}] .$$

While estimating $(\frac{1}{\text{trace } R_{XX}})$ by A_1, A_2, A_3 in Fig. 7-9, an additional constraint is imposed on the trace measurement:

$$G_2(k) \stackrel{D}{=} \sum_{i=1} x_i^2 + |y(k)| \qquad (7\text{-}12)$$

As the filter adapts its coefficients, the output y becomes very small compared to $\sum_{i=1} x_i^2$ and, after a limited number of adaption steps, if indeed convergence is achieved,

$$G_2(k) \simeq \sum_{i=1} x_i^2 .$$

As indicated in Fig. 7-9, the gain constant C can be set externally. Therefore, in extreme cases when a high C is selected, by mistake or intentionally, the second term in

eq. (7-12), namely, $|y(k)|$, will assure the gain convergence, to prevent loop divergence.

As the filter converges, the trace estimate becomes less noisy due to the smoothing operation done by A_3. Eventually, after a few hundred adaption steps, the loop gain is stable and can be locked to its last value, as demonstrated in Fig. 7-9 by the memory, A_6, and the switch, SW1.

By utilizing the "AGC" configuration presented in Fig. 7-9, the misadjustment is indeed constant under all circumstances since the loop gain $\mu = C \frac{1}{tr\ R_{XX}}$ and the misadjustment given by (C-63) is $M = \mu \cdot tr\ R_{XX} = C$ (constant). Then, in Appendix C, section C, the adaption time constant was calculated as well and was given by (C-67) (for equal eigenvalues).

$$\tau_{mse} = \frac{I}{4\mu\ tr\ R_{XX}} = \frac{I}{4C}$$

For unequal eigenvalues, τ_{mse} is also related to $\frac{I}{C}$ but in a more complex form.

Therefore, this "AGC" configuration could yield the required performances, for a proper selection of the constant C. For example, a misadjustment of 10% can be assured by selection of $C = \frac{1}{10}$. Fixing C will result in a given adaptation time.

In order to accelerate the adaptation period, a gain switching option was tested such as demonstrated in Fig. 7-9 (b). In the gain switching case, an initial gain constant,

as high as possible, is selected to achieve a fast convergence toward steady state. After a certain number of adaptation steps, the gain constant is switched to a low value to assure the proper required misadjustment. When some a priori knowledge is available about background noise statistics, the gain switching point can further optimize the performance.

There is a clear trade-off that limits the utilization of the gain switching method. Whenever the initial guess, W_o (the initial filter coefficient) is close to the steady state solution, applying the gain switching technique will not be fruitful and sometimes will even be the worst. On the other hand, when initial guess of W is assumed to be far from the steady state solution, the gain switching technique will indeed shorten the adaptation time.

f. The Required Number of Independent Pixels to to Achieve Adaptation

Throughout all the preceding discussion the image statistics were assumed stationary. If one assumes that the stationarity is confined to limited image subzones, the adaptive filter input samples should be confined accordingly to a subzone. The question raised is, what is the minimum number of independent pixels sufficient to achieve filter adaptation? Intensive computer simulation indicated that for a 3x3 filter size a subimage of size 6x6 is sufficient to adapt filter coefficients. It was noticed that adaptation

rate is slowed down as the number of independent pixels is reduced. Simulation results for small size image filter adaptation will be presented at the end of this chapter.

E. COMPUTER SIMULATION RESULTS

1. Introduction

In this section typical computer simulation results will be presented. The type of filter selected to be presented is a spatial 3x3 size filter, optimized to enhance point targets and suppress correlated noise with variance $\sigma_{CN}^2 = 4.0$. The following plots will be shown:

1. The filter coefficients adaptation plots, compared to the theoretical coefficients.
2. The learning curve (MSE as a function of adaptation steps).
3. The gradient estimate curve as a function of adaptation steps.

The simulation procedure was conducted in the following way:

1. Generate the correlated noise image with specified statistical properties.
2. Adapt the filter coefficients.
3. Design a theoretical Wiener or matched filter based on the known statistical properties.
4. Plot the coefficients adaptation curve compared to the theoretically designed coefficients.

Three sets of adaption plots will be presented:

1. Adaption of the spatial filter to an image with first order Markov model statistics.
2. Adaption curves for second order Markov model clutter.
3. Small size image adaptation curves.

2. Adaption to First Order Markov Model

Fig. 7-10 presents the unprocessed clutter image generated by first order Markov process with correlation factor

$$\rho_H = \rho_V = 0.99$$

The theoretical filter coefficient and the steady state adaptive coefficients are shown as well in Fig. 7-10.

Fig. 7-11(a),(b),(c) presents the filter coefficients adaptation curves as a function of adaptation steps. The theoretical coefficients level is presented as well in each adaptation curve and it is seen that the adaptive filters coefficients come indeed very close to the theoretical value.

Fig. 7-12 is the learning curve and it shows the MSE at filter output as a function of adaptation steps.

Fig. 7-13 shows the sum of the absolute values of all coefficients correction signals.

3. Adaptation to Second Order Markov Model

Fig. 7-14 presents the unprocessed clutter image generated by second order Markov process with correlation factor

$$\rho_H = \rho_V = 0.95$$

and spatial frequency

$$\beta_H = \beta_V = 0.628$$

The theoretical and the steady state adaptive filter coefficients are shown as well in Fig. 7-14.

Fig. 7-15(a),(b),(c) are the filter coefficients adaptation curves. Fig. 7-16 is the learning curve and

The Unprocessed Image

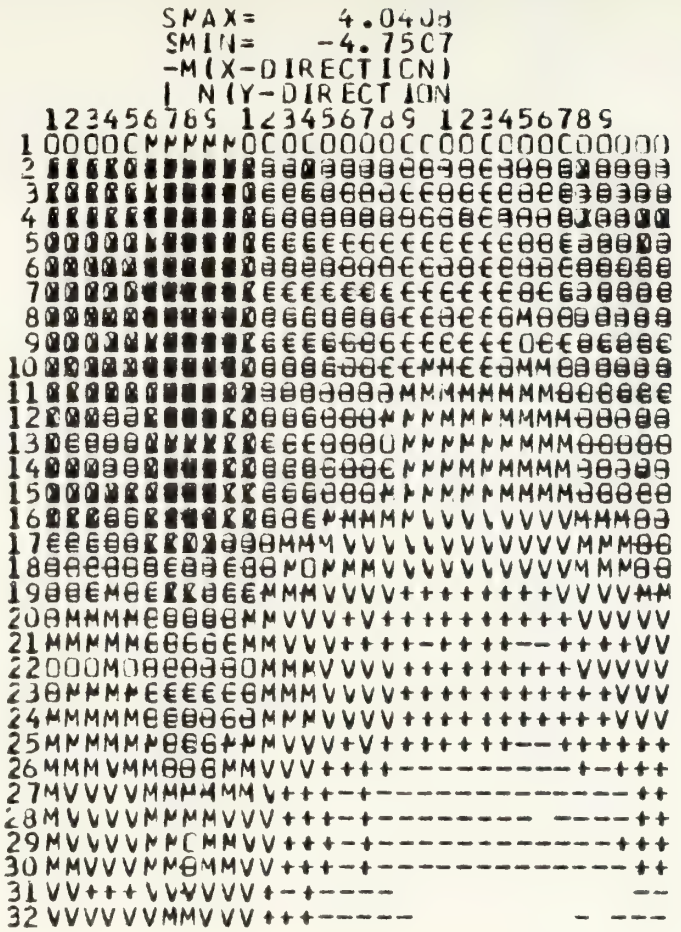

Filter Orientation

W(1)	W(2)	W(3)
W(4)	W(5)	W(6)
W(7)	W(8)	W(9)

∴ Gain constant
Fix Gain = 0.52

∴ Number of independent pixels: 26 x 26 x 676

Figure 7-10 Unprocessed Image and Filter Orientation

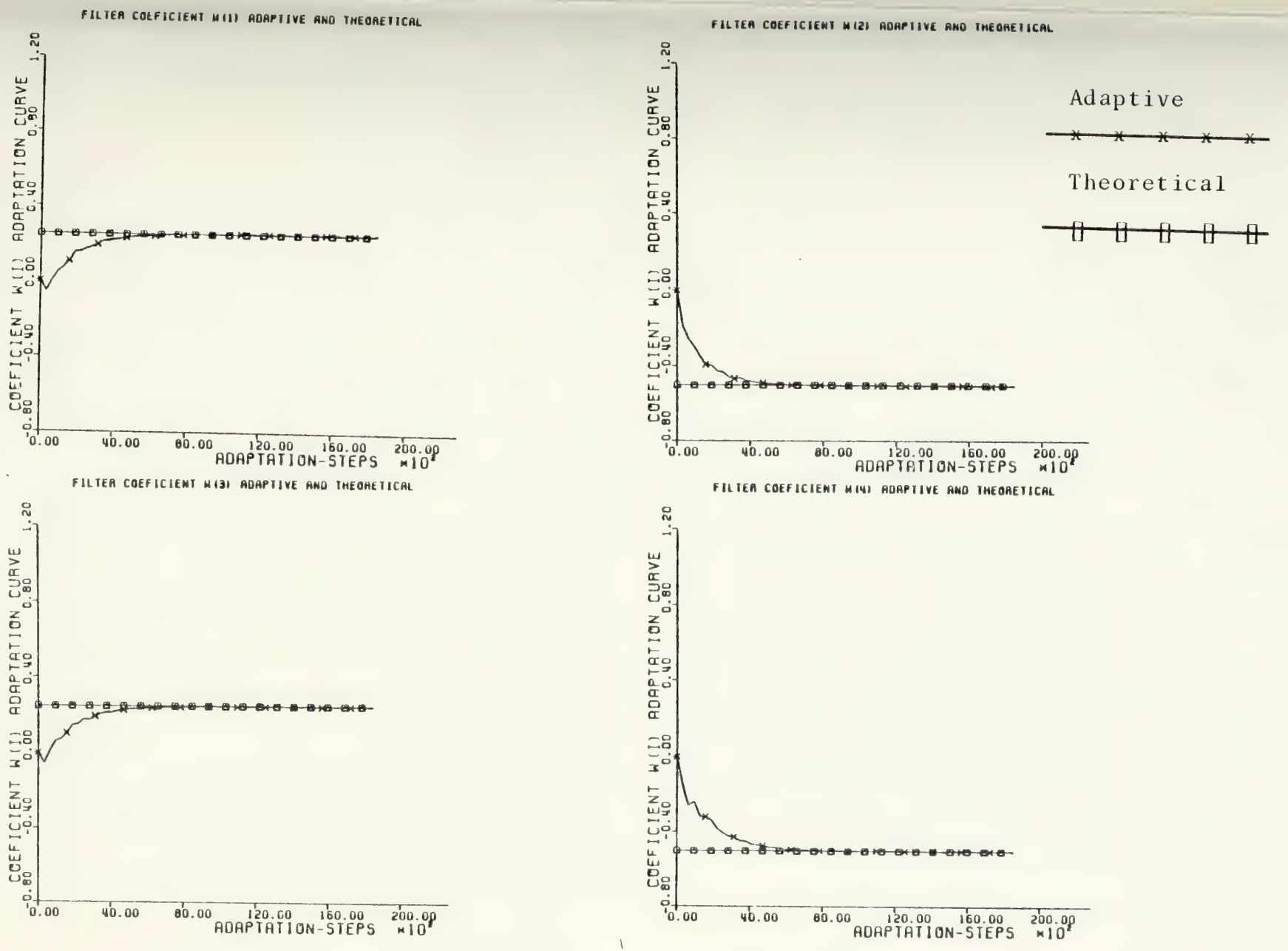

Figure 7-11(a) Coefficients Adaptation Plots

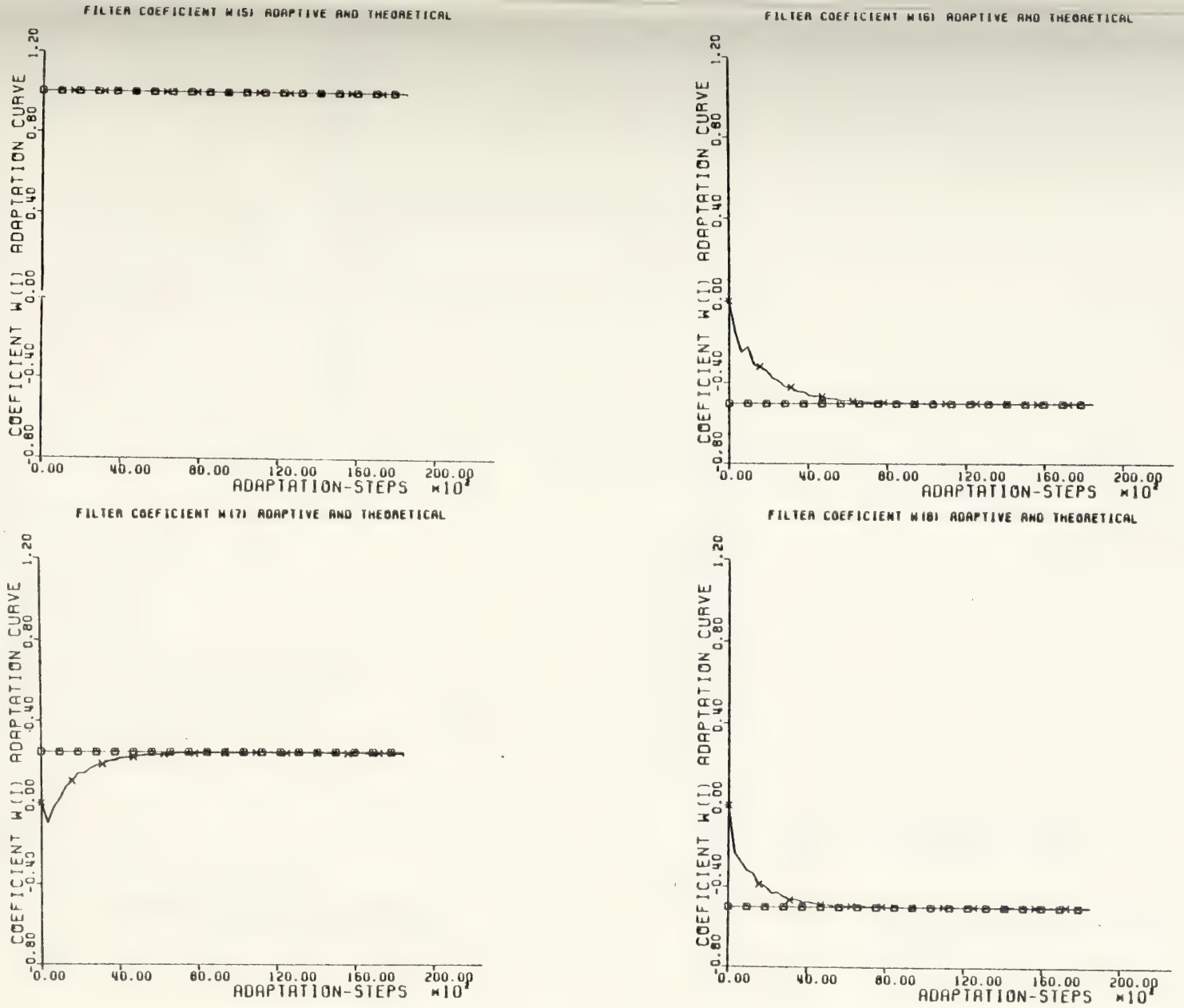

Figure 7-11(b) Coefficients Adaptation Plots

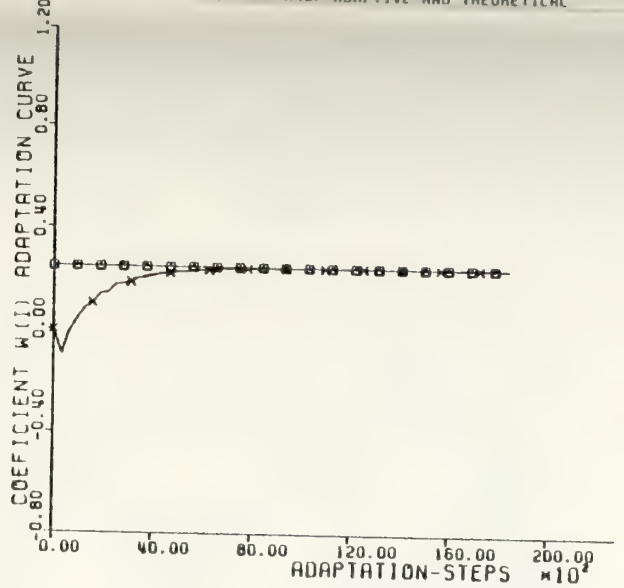

Figure 7-11(c)

Coefficients Adaptation Plots

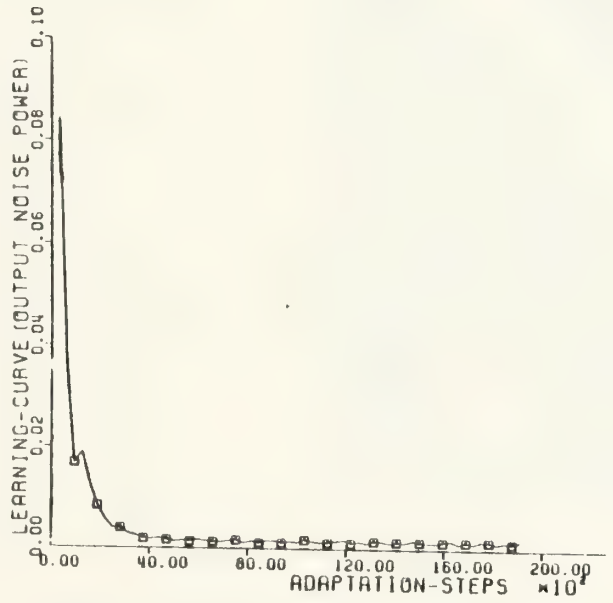

Figure 7-12 Learning Curve

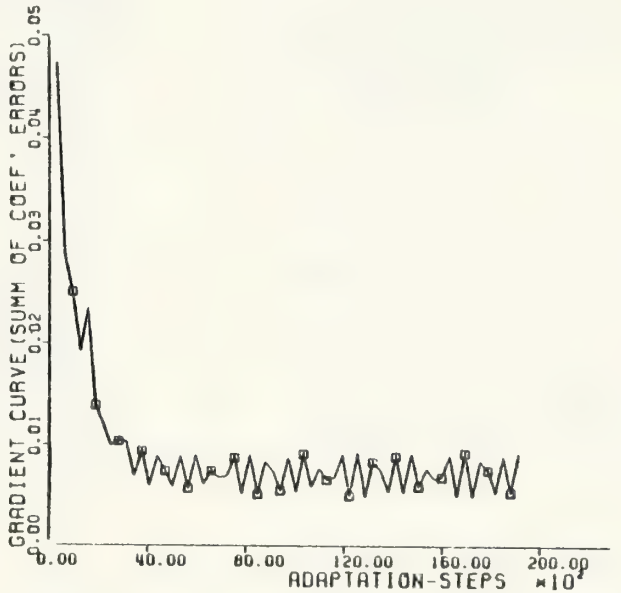

Figure 7-13 "Coefficients Error" Curve

The Unprocessed Image

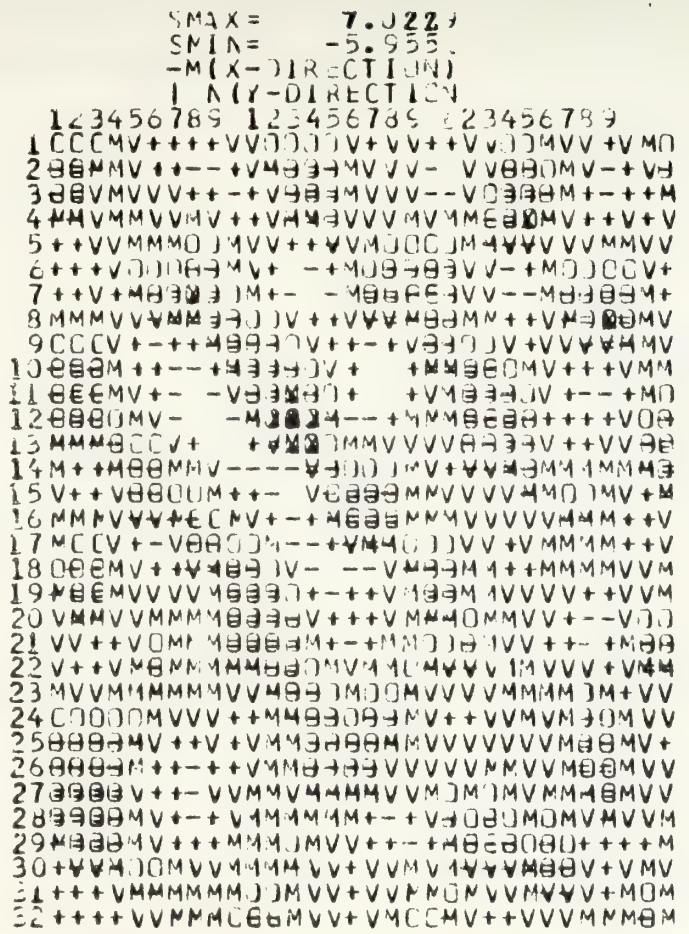

Filter Orientation

W(1)	W(2)	W(3)
W(4)	W(5)	W(6)
W(7)	W(8)	W(9)

∴ Gain constant

Gain switching 1.4/0.52

∴ Number of Independent Pixels: 26 = 26 = 676

Figure 7-14 Unprocessed Image and Filter Orientation

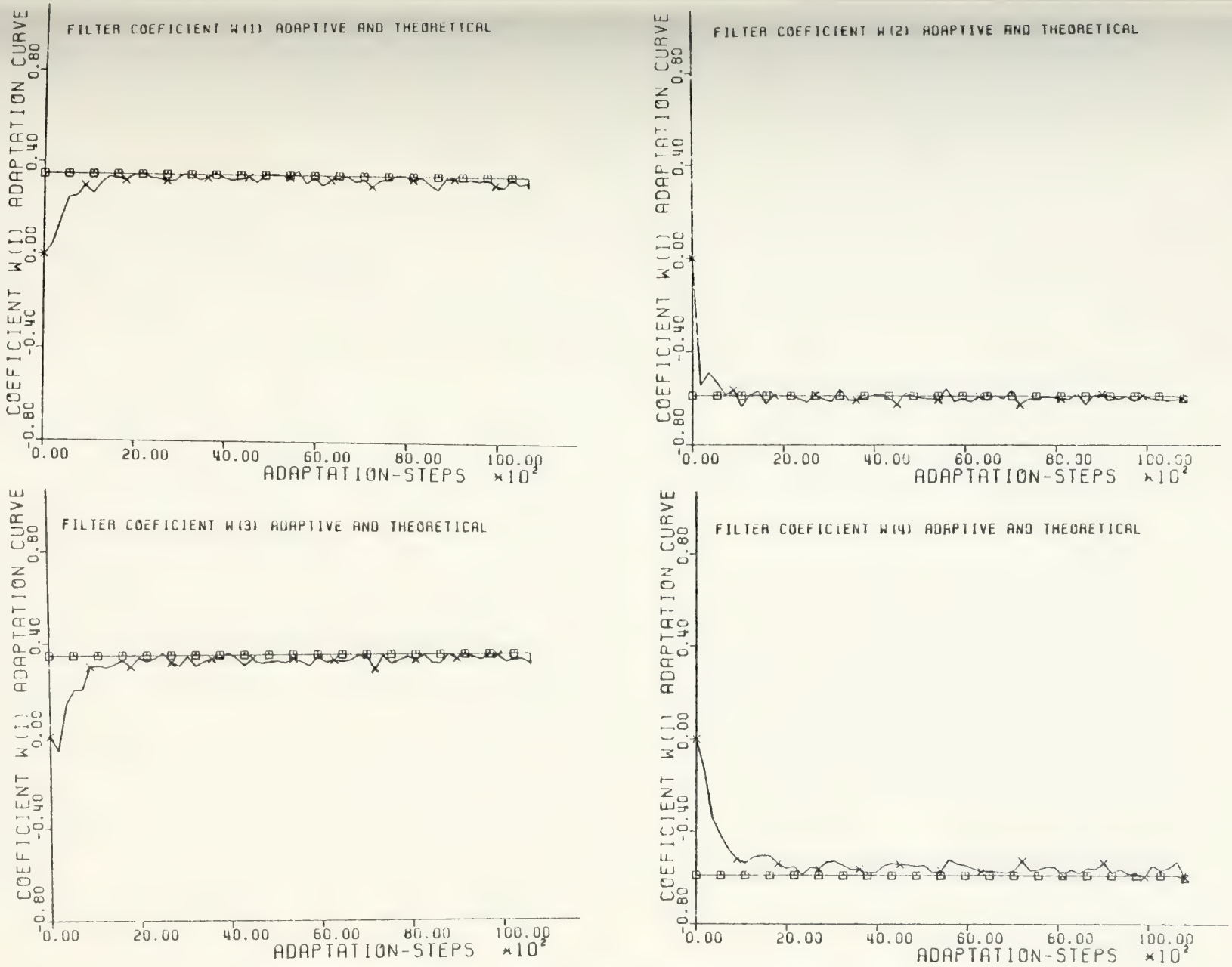

Figure 7-15a Coefficients Adaptation Plots

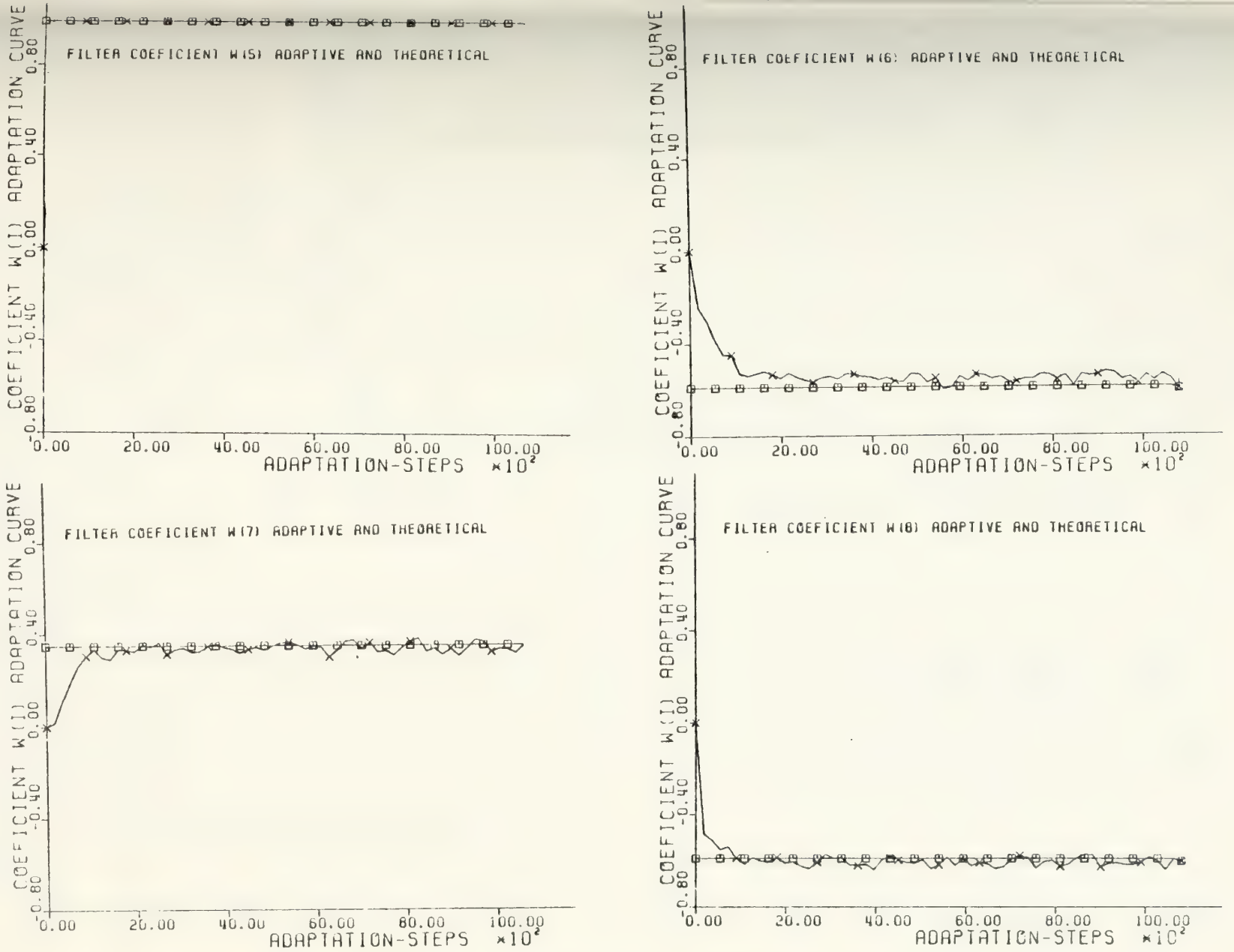

Figure 7-15(b) Coefficients Adaptation Plots

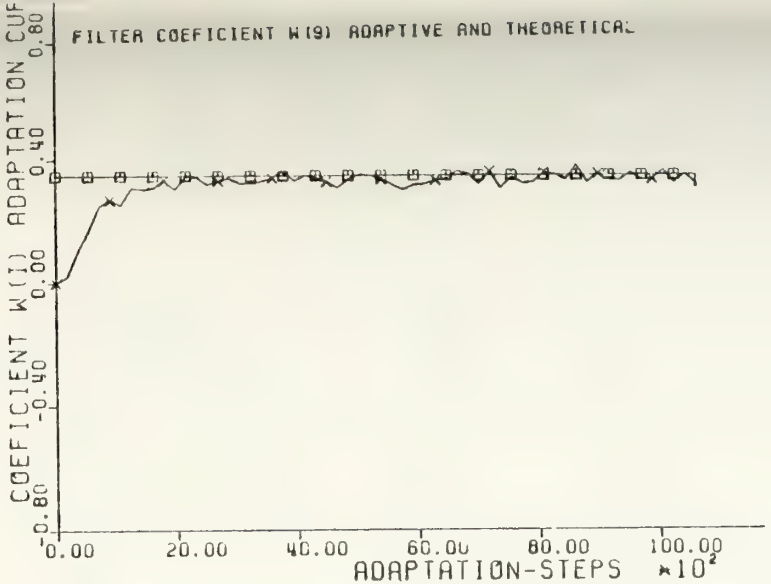

Figure 7-15(c)

Coefficients Adaptation Plots

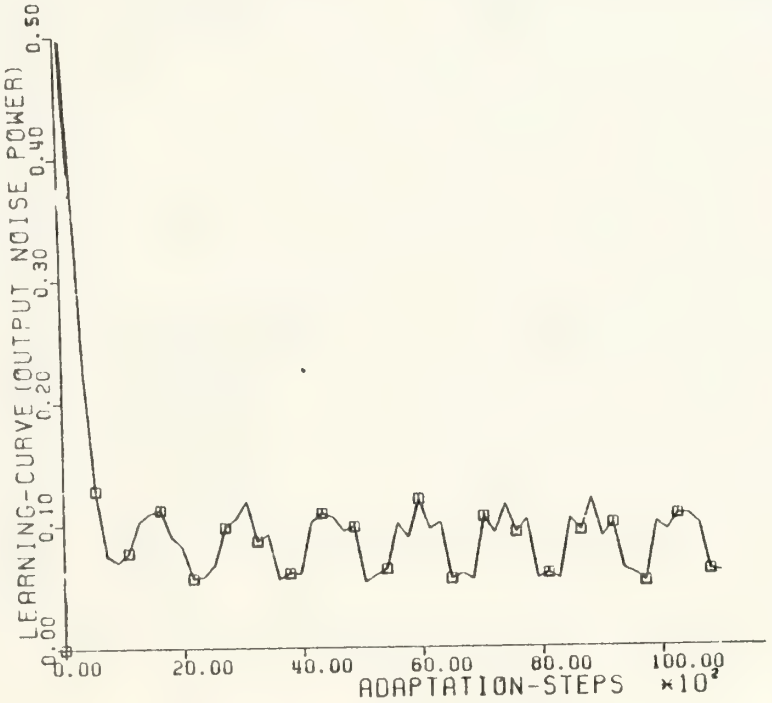

Figure 7-16 Learning Curve

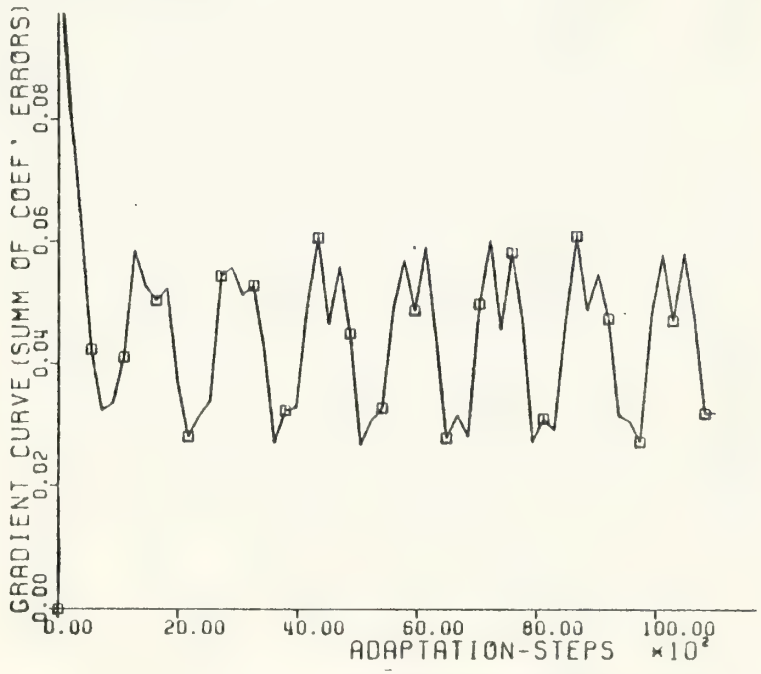

Figure 7-17 "Coefficients Error" Curve

Fig. 7-17 is the sum of the absolute values of all coefficients correction signals.

4. Adaptation to Small Size Image

Fig. 7-18 is the unprocessed first order Markov model clutter image. A section of 6x6 pixels is selected as shown in Fig. 7-18 to adapt the filter coefficients. The adaptive process is accomplished within this small size section. The resulting filter coefficients adaptation curves are shown in Fig. 7-19(a),(b),(c). The learning curve is shown in Fig. 7-20 and the sum of coefficients correction signals is shown in Fig. 7-21.

5. Simulation Results Conclusions

The major computer simulation results conclusions are described below.

- The adaptation rate decreases as correlation coefficient increases.

- An impirical relation was approximated to indicate the total number of adaptation steps N1(total), as a function of ρ_H or ρ_V and β_H or β_V.

- For the first order Markov process:

$$N1(\text{total}) \simeq k_1[1.0 - (\rho_{max})^2]$$

where ρ_{max} indicates the higher correlation coefficient (between ρ_H and ρ_V). Typically, $k_1 \simeq 250 - 500$, depending on loop gain constant.

- For second order Markov process, the following approximated empirical formula can be used:

The Unprocessed Image

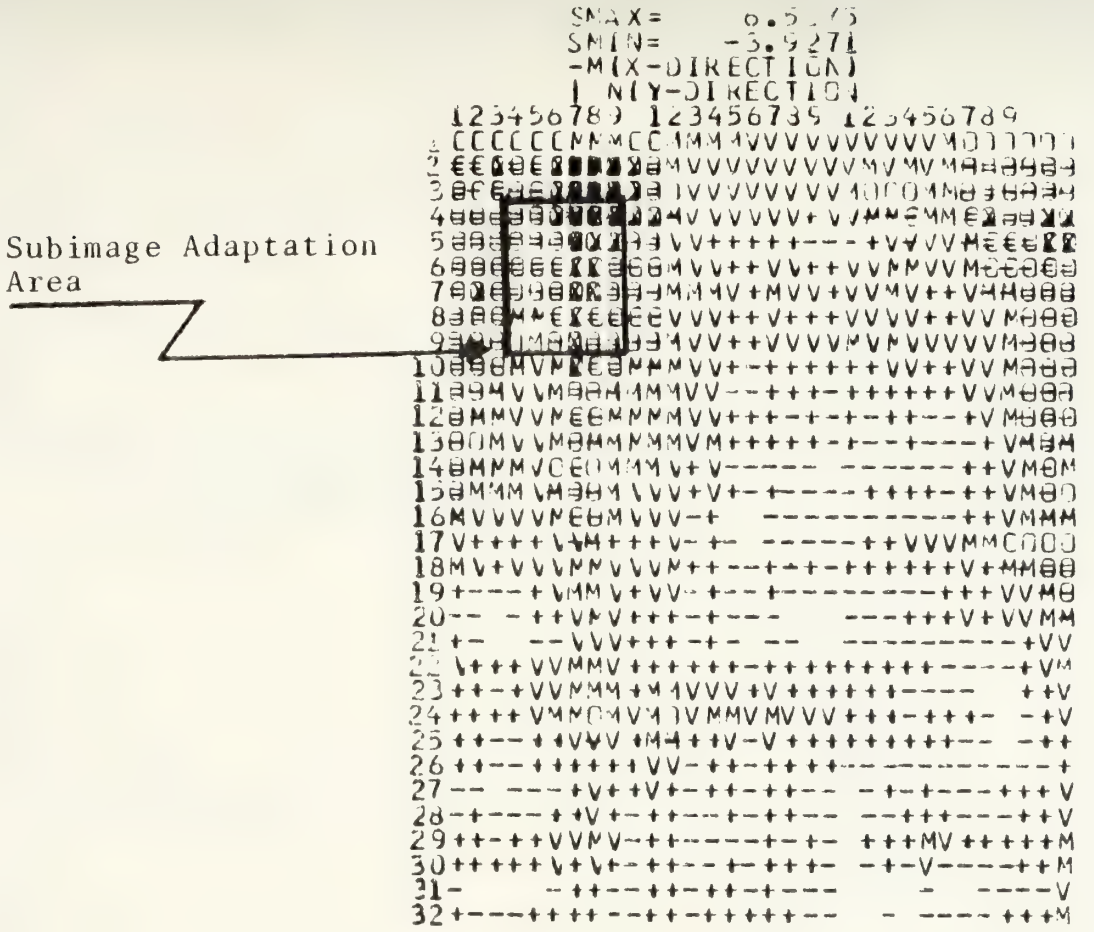

Filter Orientation

W(1)	W(2)	W(3)
W(4)	W(5)	W(6)
W(7)	W(8)	W(9)

Gain Constant

∴ Gain Switching 1.4/0.52

∴ Number of Independent pixels: 6 x 6 = 36

Figure 7-18 Unprocessed Image and Filter Orientation

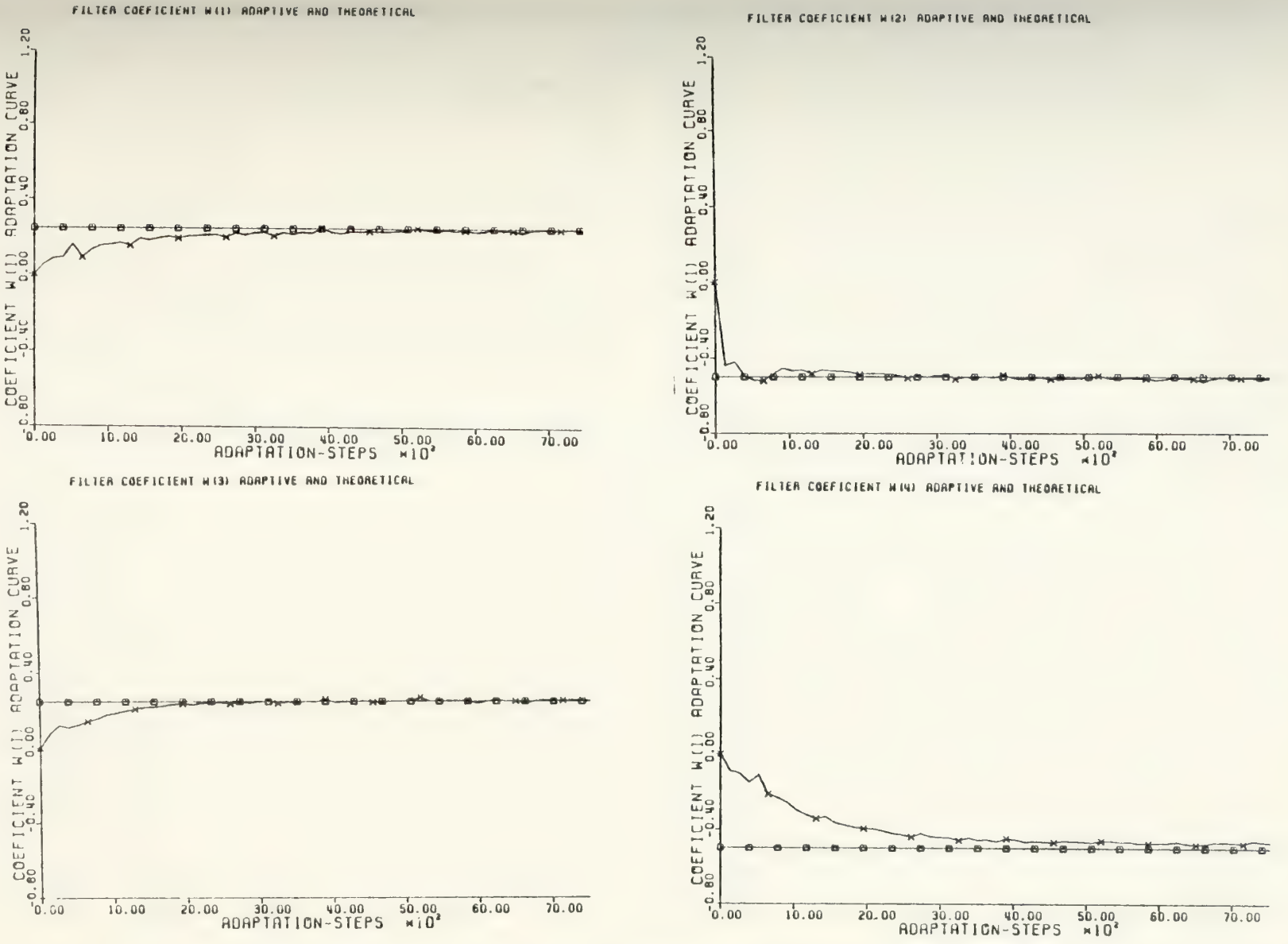

Figure 7-19(a) Coefficients Adaptation Plots

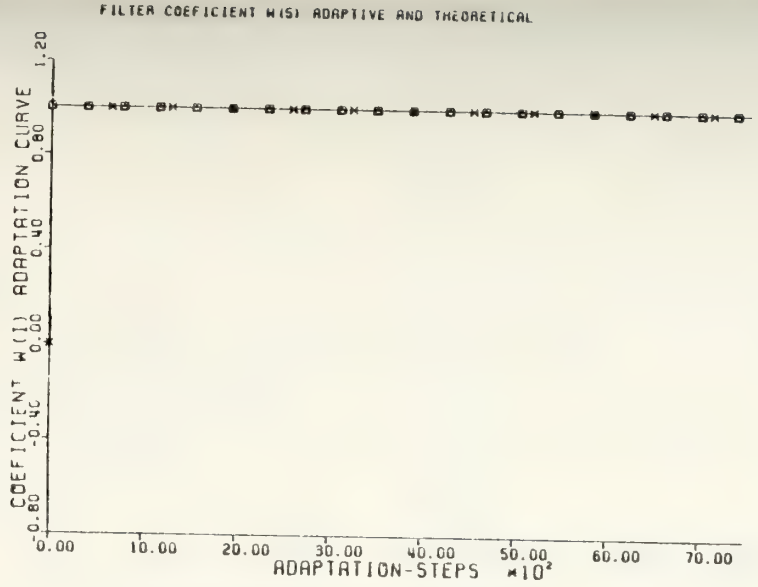

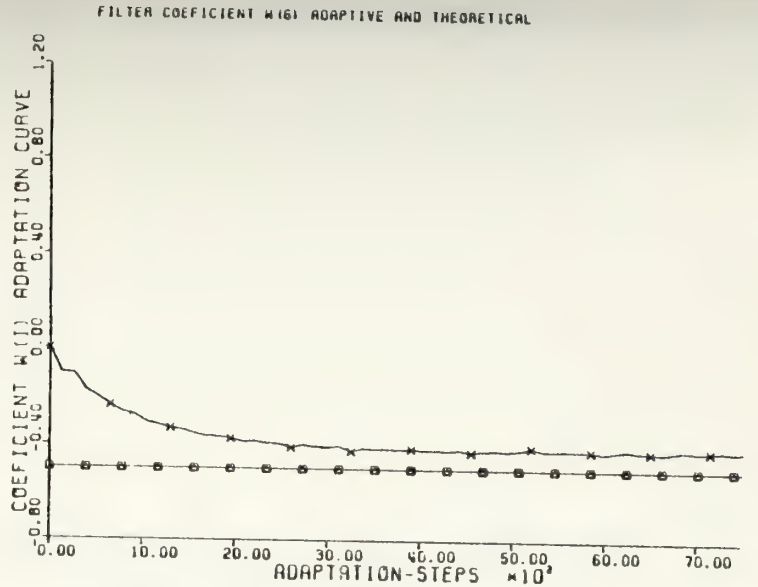

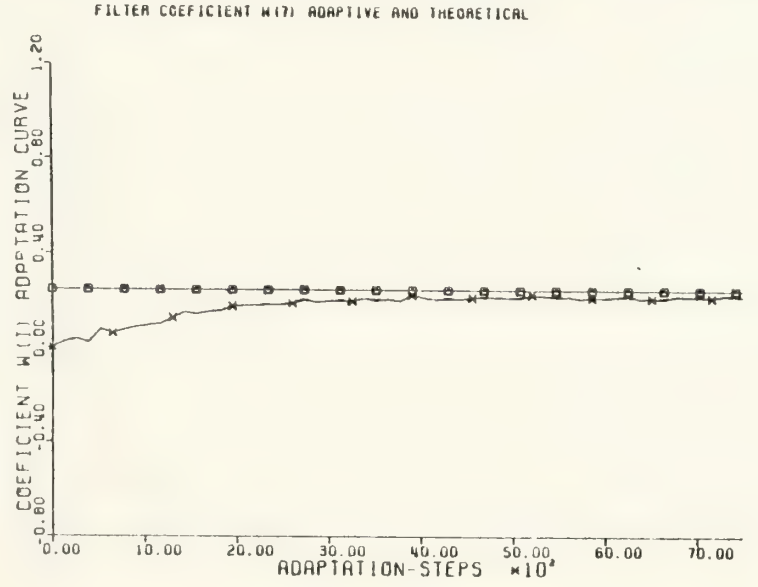

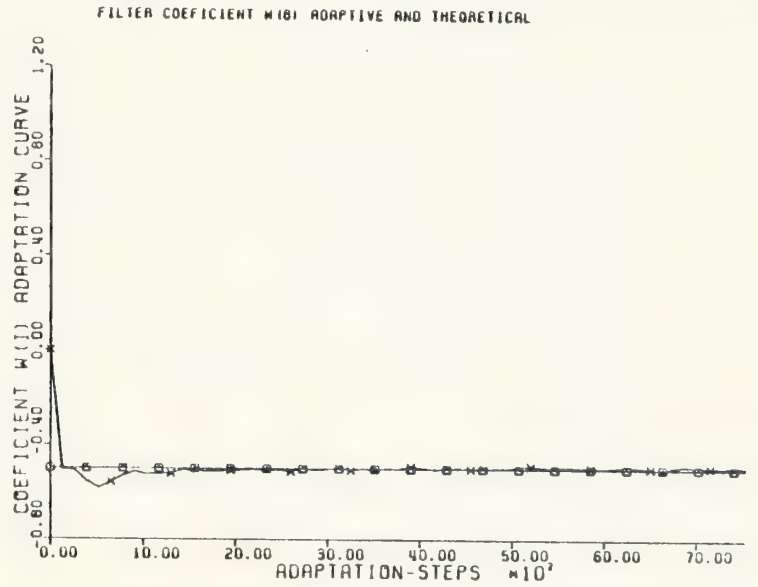

Figure 7-19(b) Coefficients Adaptation Plots

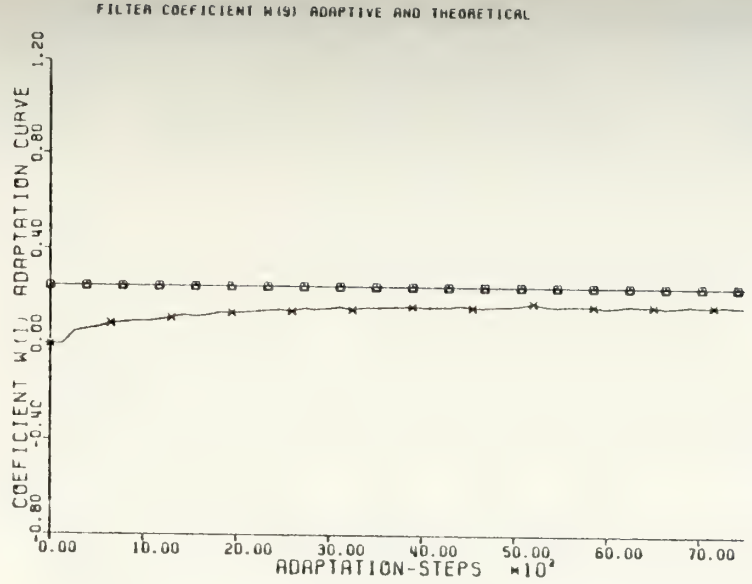

Figure 7-19(c)
Coefficients
Adaptation
Plots

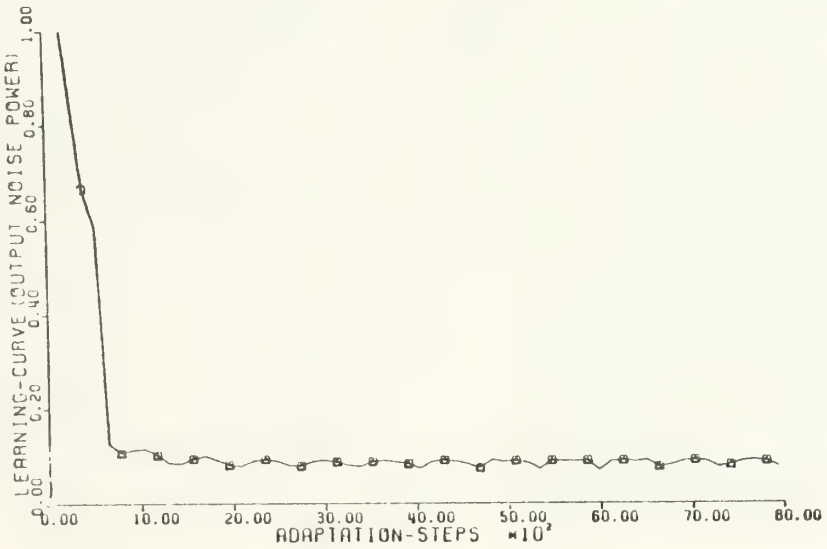

Figure 7-20 Learning Curve

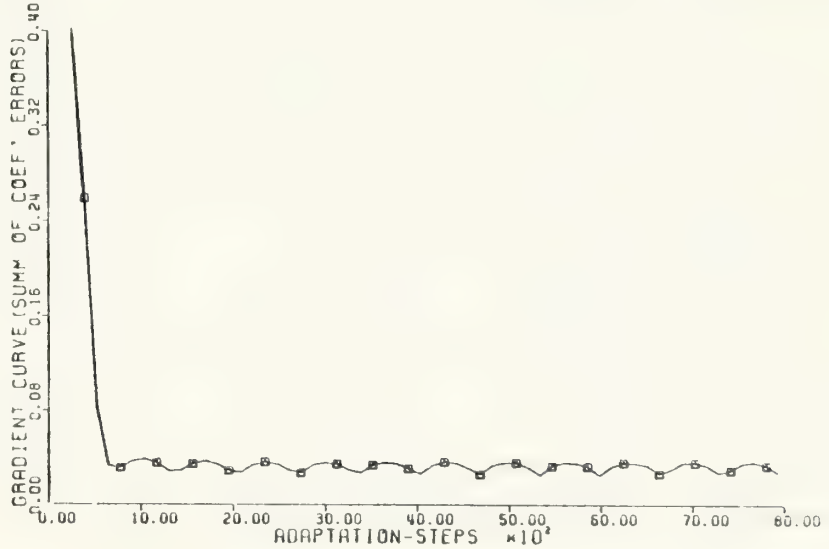

Figure 7-21 "Coefficients Error" Curve

$$N2(total) \approx N1(total)*[(1 + 1/\cos \beta_{max})]$$

β_{max} is the higher β.

- In general, it was noticed that the adaptation rate is slower in the second order Markov process than in the first order Markov process.

- The adaption time of a small sized image is slower compared to larged sized image (by large image it is meant that the image size is very large compared to the search box size).

- A complementary study with regard to suboptimal filters was carried out in the study phase presented in Chapter VI. One of the conclusions there was that a suboptimal filter designed to operate in the presence of highly correlated clutter is the preferred suboptimal filter. Combining this conclusion with the fact that adaptation time is slow in case of high correlation - it is always recommended to select the filter initial value as if it were designed to operate with the highest correlation factor.

F. SUMMARY

In this chapter a spatial adaptive filter concept was discussed and implemented. The adaptation method presented in the chapter is applicable for enhancement of targets of a given shape cluttered by highly correlated noise.

In addition, a practical method to modify a special Wiener filter - intended to detect point targets - into a matched filter was presented. This method enables a direct adaptation

of a matched filter in the case of point target. The suggested method was tested against simulated images and demonstrated the expected performance - namely, the adaptation of the filters into a steady state optimal solution.

Various practical implementation issues were mentioned in the chapter such as:

- The image scanning pattern
- The "desired response" derivation
- The adaptive loop gain setting
- The typical adaptation rates
- The required number of independent pixels.

This last issue will be utilized in the next chapter where nonstationary statistics will be assumed.

VIII. ADAPTIVE SPATIAL FILTER II - NONSTATIONARY CLUTTER STATISTICS

A. INTRODUCTION

In this chapter, an adaptive spatial filter technique capable of processing images having nonstationary clutter will be developed. Its basic idea is described in the following. More detailed explanations will be given in following sections.

The first assumption is that an image of nonstationary clutter statistics can be divided into subimages within which the clutter statistics are stationary.

A spatial filter will be assigned to each of these subimages. An adaptive algorithm is then applied to adapt the assigned filter to its optimal performance. An automatic procedure is applied to terminate the adaptation. The optimal filter is then applied to the subimage.

Following this, an optimal threshold will be determined and applied to the adaptively filtered subimage for target detection.

B. THEORETICAL DEVELOPMENT AND PRACTICAL CONSIDERATIONS

1. Subimage Division

In this thesis, a procedure of dividing the image into square shaped small subimages is developed. From the processing gain requirements, the smallest subimage size is

preferred because the chance is better to have "stationary" statistics in a small area. This makes possible the design of an optimal spatial filter. On the other hand, smaller subimage size requires more adaptive filters to cover a given image size and increases the computation load. A trade-off should be made for an optimum subimage size. The smallest size used is 6x6. Using this small size and simulated images containing Markov model correlated noise, it was found that the adaptive filter was able to converge to the optimal value in all cases tested.

2. Adaptive Spatial Filter

For each subimage, adaptive spatial filters developed in the last chapter can be used because we assume that the statistical properties in the subimage are stationary. Therefore, detailed explanation for the adaptive spatial filter will not be repeated here. Instead, only the important steps will be highlighted in the following.

a. Initialization of the Filter Coefficients

It can be started in two ways. We can assume a statistical characteristic and design a spatial filter accordingly. Alternatively, we can calculate the statistical characteristics of the image by ignoring the nonstationarity which might exist in the image and design a spatial filter accordingly and use it as the initial filter.

b. Selection of Adaptive Loop Gain

It was discussed in detail in Chapter VII, section G.4. In our computer simulation, a loop gain of 0.4 was used most frequently.

c. Termination of Adaptation

The procedure to terminate the adaptation was discussed in Chapter VII, section G.2. In our computer simulation, the following parameters are used:

$n = 36$, $N = 360$, $F = 5\%$

d. Adaptation Time

It depends on the following factors:

Filter initialization
Adaptive loop gain
Statistical characteristics of the image.

The last factor is beyond the control of the filter designer. However, design of the initialization and loop gain could have a significant effect on the adaptation time. It was found, from computer simulation, that using a loop gain in the range of $\frac{1}{4}$ to $\frac{1}{2}$, it took at most several thousand adaptive steps to reach the optimal filter in most cases.

C. COMPUTER SIMULATION RESULTS

1. Generation of Nonstationary Images

The nonstationary image used in this chapter is the same one introduced in Chapter VII, section G.4. It is an image of size 64 x 64 pixels, and consists of four quadrants, each of which has its own statistical properties.

They are separately shown in Figures 8-1 through 8-4, which include their statistical properties and optimal spatial filters together with the theoretical processing gain of these filters.

Fig. 8-1 Upper left quadrant
Fig. 8-2 Upper right quadrant
Fig. 8-3 Lower left quadrant
Fig. 8-4 Lower right quadrant

The composite nonstationary image is shown in Fig. 8-5(a) by a 9 gray level printout and in 8-5(b) by a 3-D plot.

2. Image Subdivision and Filter Adaptation

The image is divided into square shaped subimages of size 8x8 pixels, as shown in Fig. 8-6(a). An adaptive filter was assigned to each subimage and was adaptively changed until it reached the optimal performance. In Fig. 8-6(b) the adaptive filter coefficients of several selected subimages are shown and can be compared with the theoretical optimal filter. The resulting processing gain and optimal threshold are shown in 8-6(c). The threshold was determined by assuming Gaussian probability density function, and for a probability of false alarm in the range from $1 \times 10^{-1} \leq P_{FA} \leq 5 \times 10^{-3}$

3. Comparison of Filter Performance

The following figures of merits are used to evaluate the filter performance.

For clutter suppression:

a. Processing gain (P.G.)

CORRELATED NOISE
BAND PASS
R(M,N)=(SGMIMG**2)*(RH**|M|)*(RV**|N|)*COS(BH*M)*COS(BV*N)
BETAH= 0.628
BETAV= 0.063
RH= 0.950
RV= 0.950
SGMIMG= 2.000
SMEAN= 0.0

SMAX= 5.6955
SMIN= -4.3970
-M(X-DIRECTION)
| N(Y-DIRECTION)

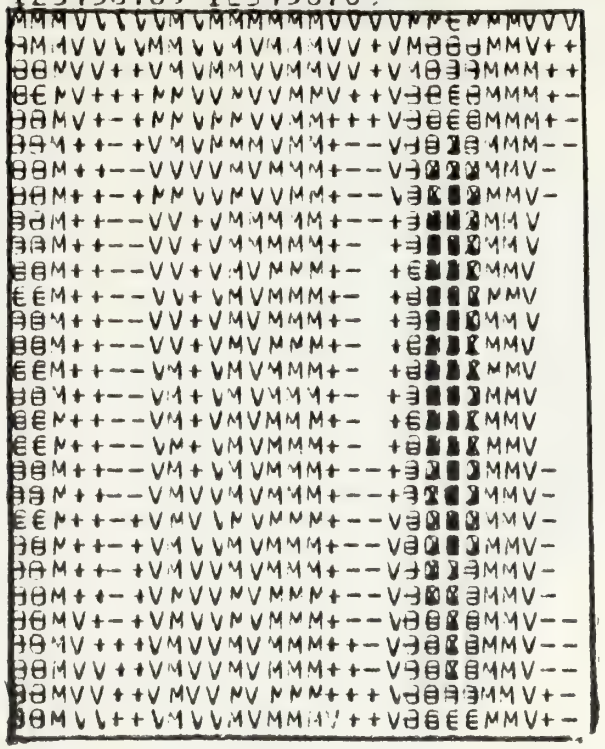

Estimation Point at the center

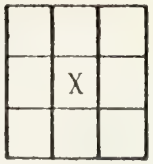

Corresponding filter coefficients:

.3	-.5	.3
-.6	1.0	-.6
.3	-.5	.3

Estimation point at upper left corner

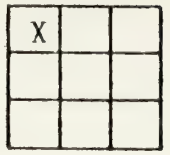

Corresponding filter coefficients

1.0	-1.35	.761
-.981	1.329	-.747
.035	-.047	.026

Estimation point at center of left edge

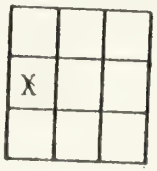

Corresponding filter coefficients

-.50	.677	-.381
1.0	-1.354	.761
-.5	.677	-.381

The noise covariance matrix R_{NN}

1	2	3	4	5	6	7	8	9
4.0000	3.0743	1.1156	3.7925	2.9148	1.0577	3.5815	2.7526	0.9983
3.0743	4.0000	3.0743	2.9148	3.7925	2.9148	2.7526	3.5815	2.7526
1.1156	3.0743	4.0000	1.0577	2.9148	3.7925	0.9983	2.7526	3.5815
3.7925	2.9148	1.0577	4.0000	3.0743	1.1156	3.7925	2.9148	1.0577
2.9148	3.7925	2.9148	3.0743	4.0000	3.0743	2.9148	3.7925	2.9148
1.0577	2.9148	3.7925	1.1156	3.0743	4.0000	1.0577	2.9143	3.7925
3.5815	2.7526	0.9988	3.7925	2.9143	1.0577	4.0000	3.0743	1.1156
2.7526	3.5815	2.7526	2.9148	3.7925	2.9148	3.0743	4.0000	3.0743
0.9983	2.7526	3.5815	1.0577	2.9148	3.7925	1.1156	3.0743	4.0000

Figure 8-a(a) Computer Print and Statistical Properties of Upper Left Quadrant Image and Its Optimally Designed Spatial Matched Filters.

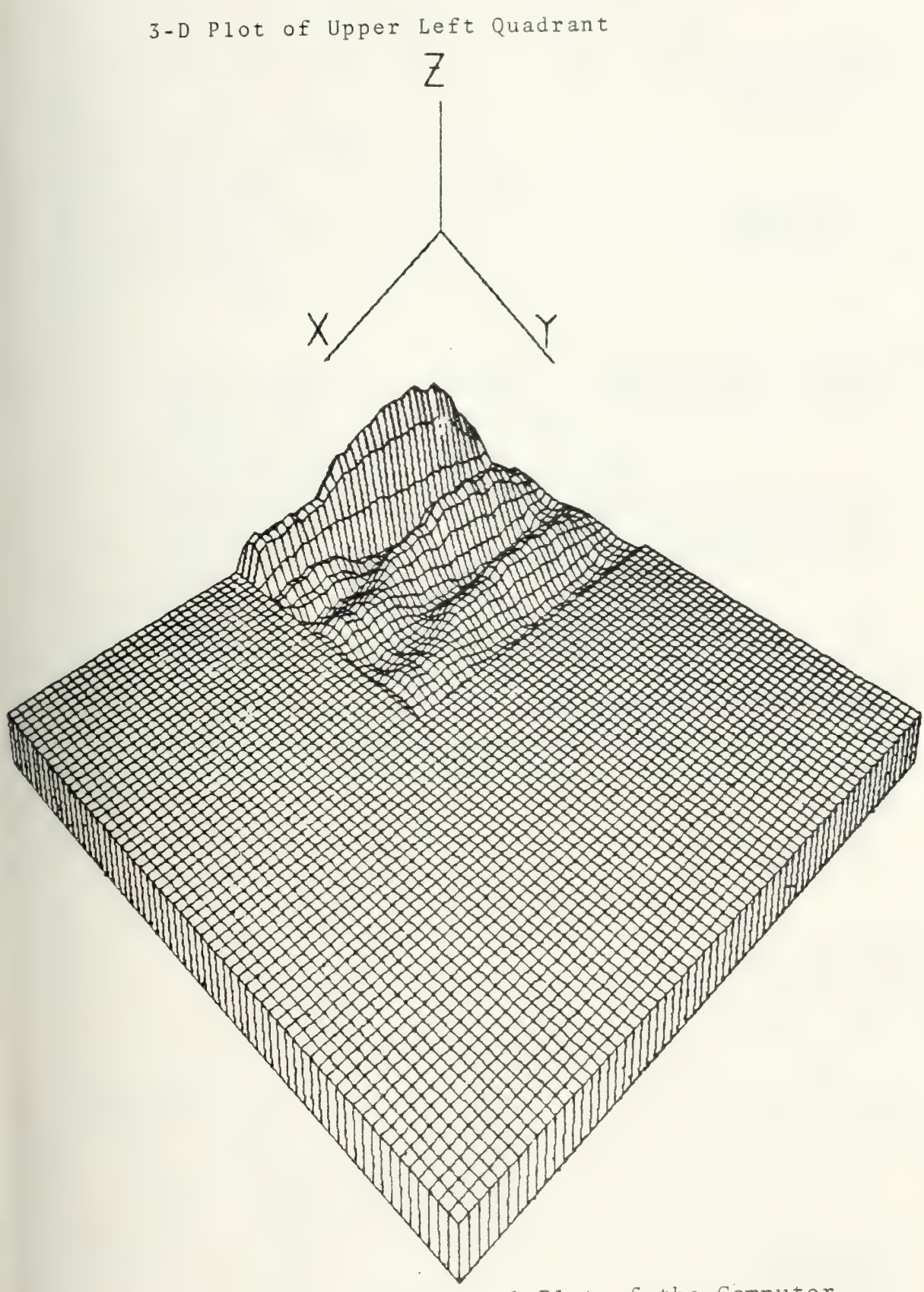

Figure 8-1(b) Three Dimensional Plot of the Computer Generated Upper Left Quadrant Image.

UPPER RIGHT QUADRANT

CORRELATED NOISE
BAND PASS
R(M,N)=(SGMIMG**2)*(RH**|M|)*(RV**|N|)*COS(BH*M)*COS(BV*N)
BETAH= 0.065
BETAV= 0.528
RH= 0.950
RV= 0.950
SGMIMG= 2.000
SMIDIM= 0.0

SMAX= 7.6776
SMIN= -3.6980
-M(X-DIRECTION)
| N(Y-DIRECTION

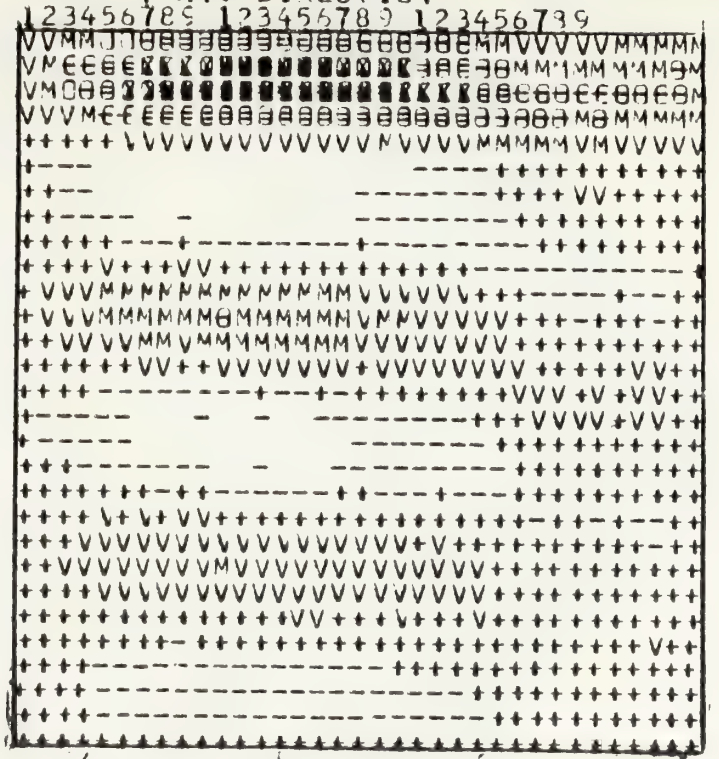

Estimation point at the center

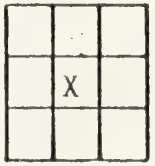

Corresponding filter coefficients:

.3	-.6	.3
-.5	1.0	-.5
.3	-.6	.3

The noise covariance matrix R_{NN}

1	2	3	4	5	6	7	8	9
4.0000	3.7925	3.5815	3.0743	2.9148	2.7526	1.1156	1.0577	0.9988
3.7925	4.0000	3.7925	2.9148	3.0743	2.9148	1.0577	1.1156	1.0577
3.5815	3.7925	4.0000	2.7526	2.9148	3.0743	0.9988	1.0577	1.1156
3.0743	2.9148	2.7526	4.0000	3.7925	3.5815	3.0743	2.9148	2.7526
2.9148	3.0743	2.9148	3.7925	4.0000	3.7925	2.9148	3.0743	2.9148
2.7526	2.9148	3.0743	3.5815	3.7925	4.0000	2.7526	2.9148	3.0743
1.1156	1.0577	0.9988	3.0743	2.9148	2.7526	4.0000	3.7925	3.5815
1.0577	1.1156	1.0577	2.9148	3.0743	2.9148	3.7925	4.0000	3.7925
0.9988	1.0577	1.1156	2.7526	2.9148	3.0743	3.5815	3.7925	4.0000

Estimation point at upper right corner

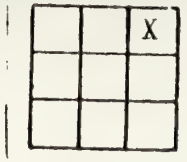

Corresponding filter coefficients

.035	-.981	1.0
-.047	1.329	-1.35
-.026	-.747	.761

Estimation point at center of right edge

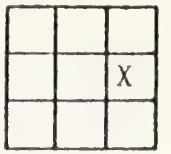

Corresponding filter coefficients

-.02	.589	.6
-.035	.981	1.0
-.02	.589	-.6

Figure 8-2(a) Computer Print and Statistical Properties of Upper Right Quadrant Image and Its Optimally Designed Spatial Matched Filters.

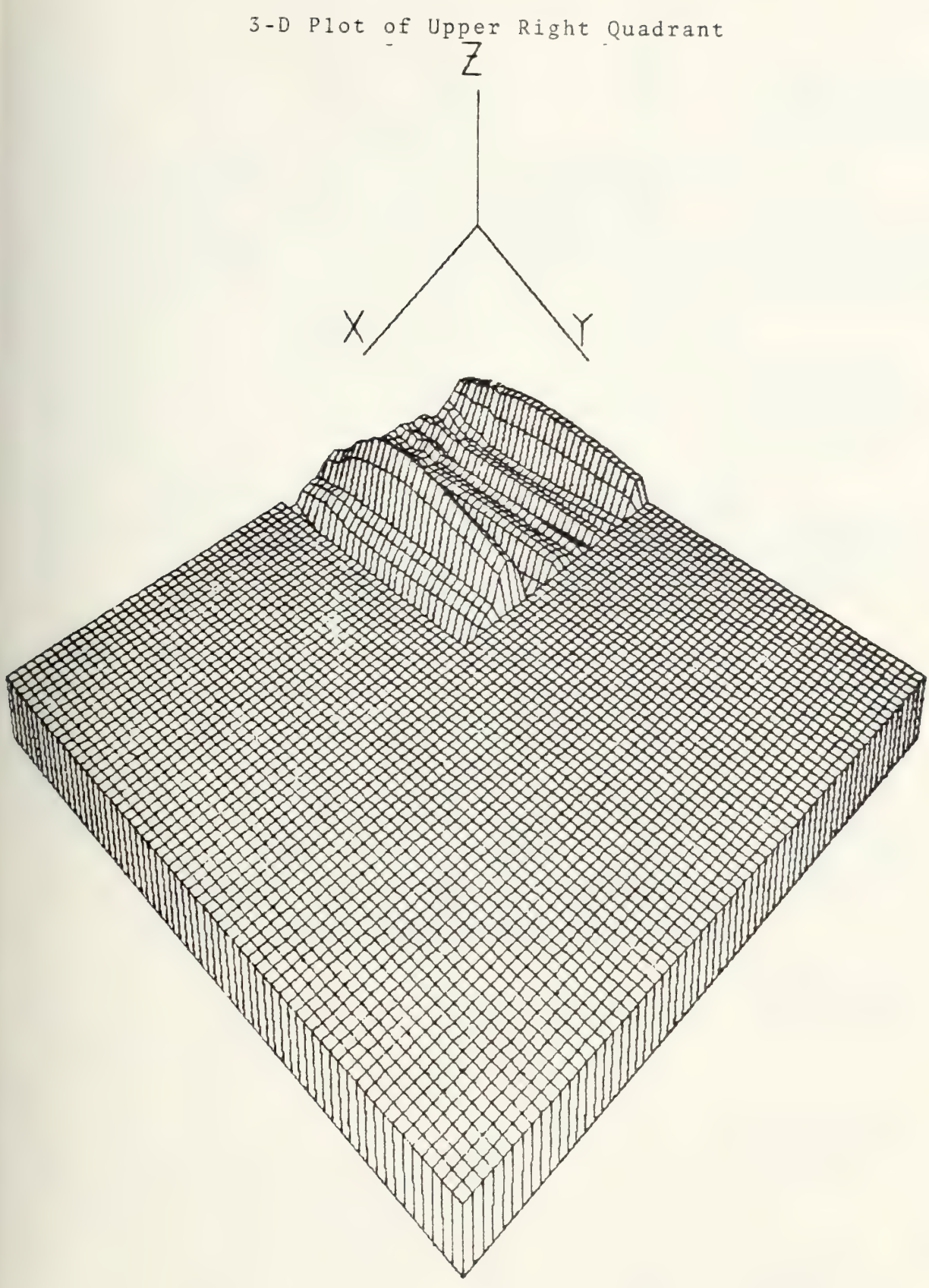

Figure 8-2(b) Three Dimensional Plot of the Computer Generated Upper Right Quadrant Image.

LOWER LEFT QUADRANT

CORRELATED NOISE
BAND PASS
R(M,N)=(SGMIMG**2)*(RH**|M|)*(RV**|N|)*COS(BH*M)*COS(BV*N)
BETAH= 0.628
BETAV= 0.628
RH= 0.950
RV= 0.950
SGMIMG= 2.000
SMEAN= 0.0

SMAX= 7.6954
SMIN= -3.2781
-M(X-DIRECTION)
| N(Y-DIRECTION

Estimation point at the center

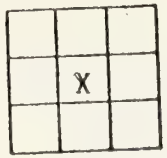

Corresponding filter coefficients

.33	-.6	.36
-.6	1.0	-.6
.36	-.6	.36

The noise covariance matrix R_{NN}

1	2	3	4	5	6	7	8	9
4.0000	3.0743	1.1156	3.0743	2.3628	0.8574	1.1156	0.8574	0.3111
3.0743	4.0000	3.0743	2.3628	3.0743	2.3628	0.8574	1.1156	0.8574
1.1156	3.0743	4.0000	0.8574	2.3628	3.0743	0.3111	0.8574	1.1156
3.0743	2.3628	0.8574	4.0000	3.0743	1.1156	3.0743	2.3628	0.8574
2.3628	3.0743	2.3628	3.0743	4.0000	3.0743	2.3628	3.0743	2.3628
0.8574	2.3628	3.0743	1.1156	3.0743	4.0000	0.8574	2.3628	3.0743
1.1156	0.8574	0.3111	3.0743	2.3628	0.8574	4.0000	3.0743	1.1156
0.8574	1.1156	0.8574	2.3628	3.0743	2.3628	3.0743	4.0000	3.0743
0.3111	0.8574	1.1156	0.8574	2.3628	3.0743	1.1156	3.0743	4.0000

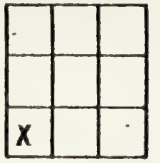

Corresponding filter coefficients

.761	-1.03	.58
-1.35	1.38	-1.03
1.0	-1.354	.761

Estimation point at center of left edge

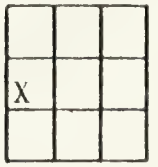

Corresponding filter coefficients

-.6	.81	-.45
1.0	-1.35	.76
-.6	.81	-.45

Figure 8-3(a) Computer Print and Statistical Properties of Lower Left Quadrant Image and Its Optimally Designed Spatial Matched Filters.

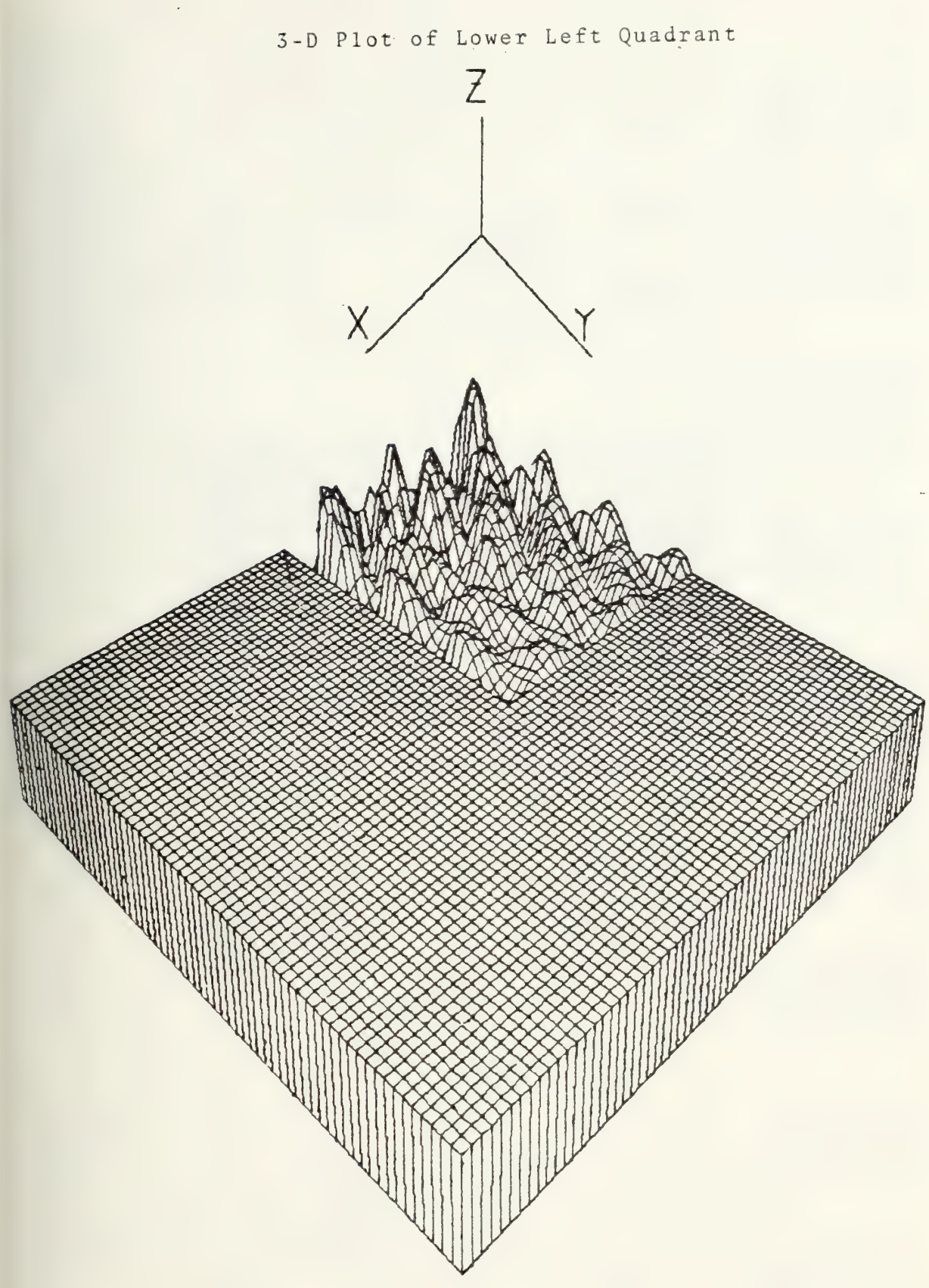

Figure 8-3(b) Three Dimensional Plot of Computer Generated Lower Left Quadrant Image.

CORRELATED NOISE
LOW PASS
R(M,N)=(SGMIMG**2)*(RH**|M|)*(RV**|N|)
RH= 0.990
RV= 0.800
SGMIMG= 2.000
SMEAN= 0.0

SMAX= 4.3797
SMIN= -5.8165
-M(X-DIRECTION)
| N(Y-DIRECTION

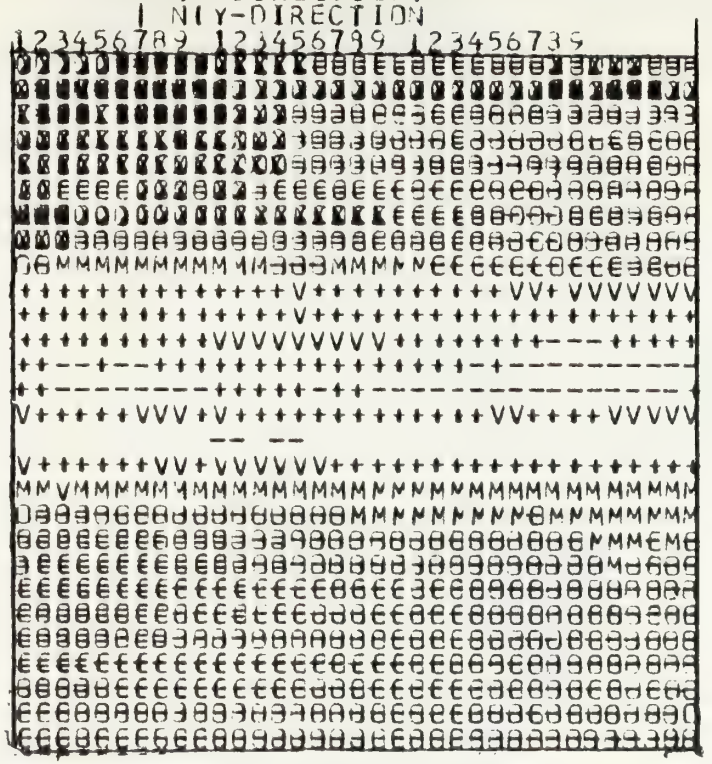

Estimation point at the center

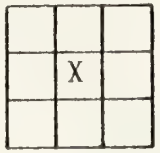

.24 -.487 .24
.499 1.0 .499
.243 -.487 .243

The noise covariance matrix R_{NN}

Estimation point at lower corner

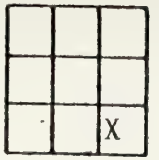

Corresponding filter coefficients

0.0 0.0 0.0
0.0 .792 -.8
0.0 .99 1.0

Estimation point at center of right edge

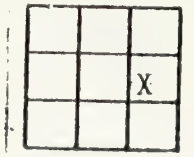

Corresponding filter coefficients

0.0 .482 -.487
0.0 -.99 1.0
0.0 .4829 -.487

1	2	3	4	5	6	7	8	9
4.0000	3.9600	3.9204	3.2000	3.1680	3.1363	2.5600	2.5344	2.5091
3.9600	4.0000	3.9600	3.1680	3.2000	3.1680	2.5344	2.5600	2.5344
3.9204	3.9600	4.0000	3.1363	3.1680	3.2000	2.5091	2.5344	2.5600
3.2000	3.1680	3.1363	4.0000	3.9600	3.9204	3.2000	3.1680	3.1363
3.1680	3.2000	3.1680	3.9600	4.0000	3.9600	3.1680	3.2000	3.1680
3.1363	3.1680	3.2000	3.9204	3.9600	4.0000	3.1363	3.1680	3.2000
2.5600	2.5344	2.5091	3.2000	3.1680	3.1363	4.0000	3.9600	3.9204
2.5344	2.5600	2.5344	3.1680	3.2000	3.1680	3.9600	4.0000	3.9600
2.5091	2.5344	2.5600	3.1363	3.1680	3.2000	3.9204	3.9600	4.0000

Figure 8-4(a) Computer Print and Statistical Properties of Lower Right Quadrant Image and Its Optimally Designed Spatial Matched Filters.

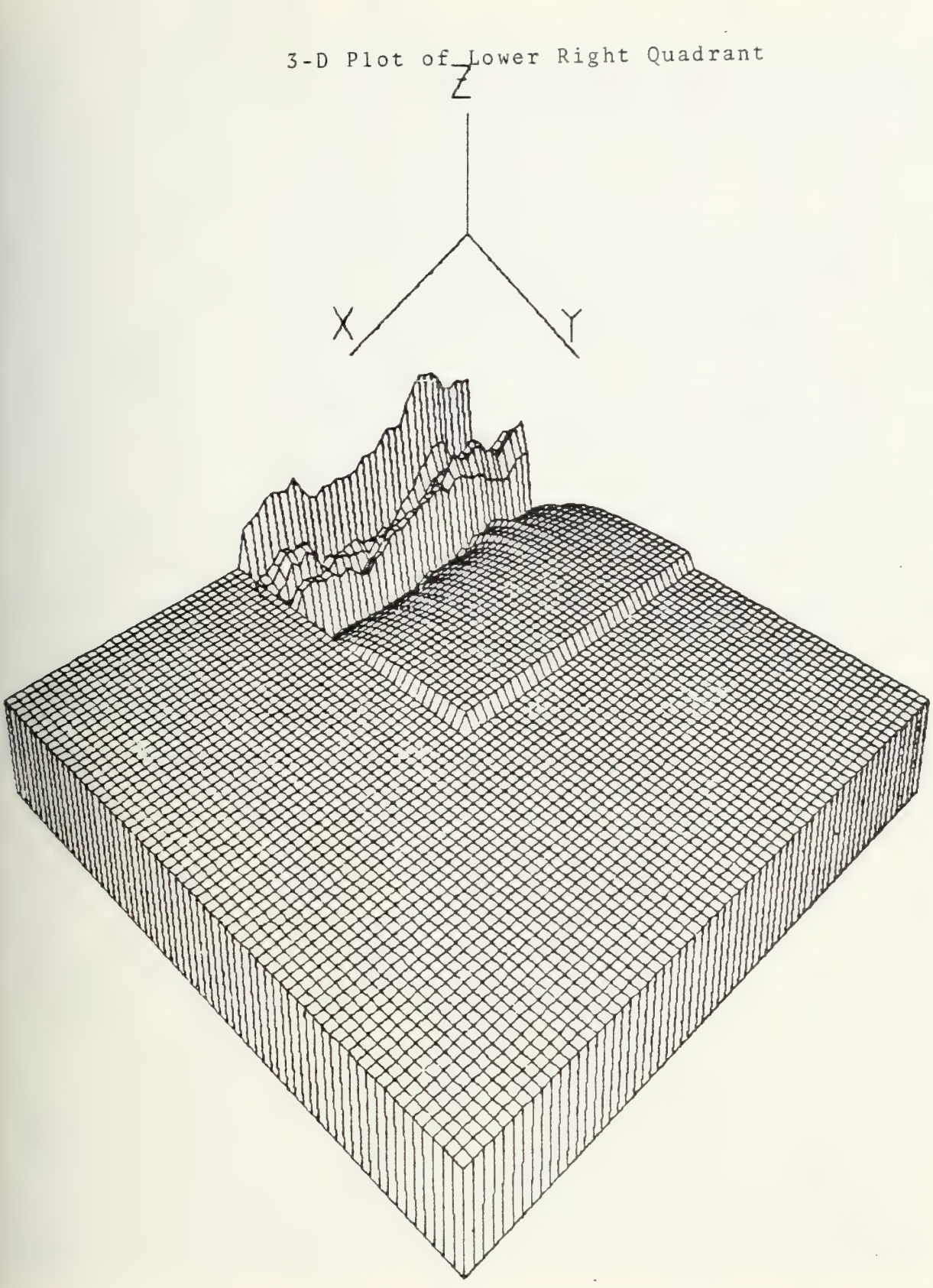

Figure 8-4(b) Three Dimensional Plot of Computer Generated Lower Right Quadrant Image

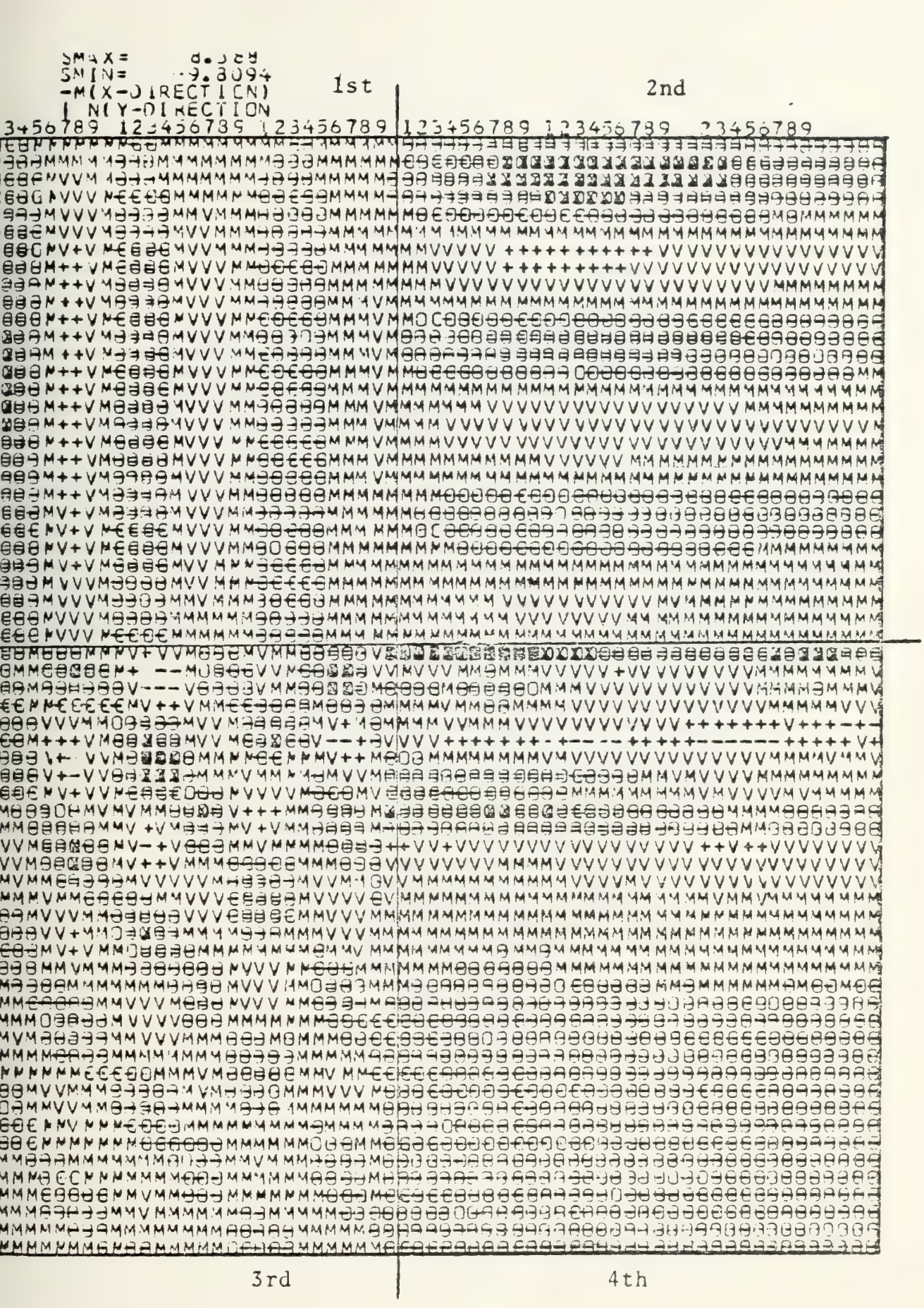

Figure 8-5(a) Nine Gray-level Computer Print of Four Quadrant "Nonstationary" Simulated Clutter Image.

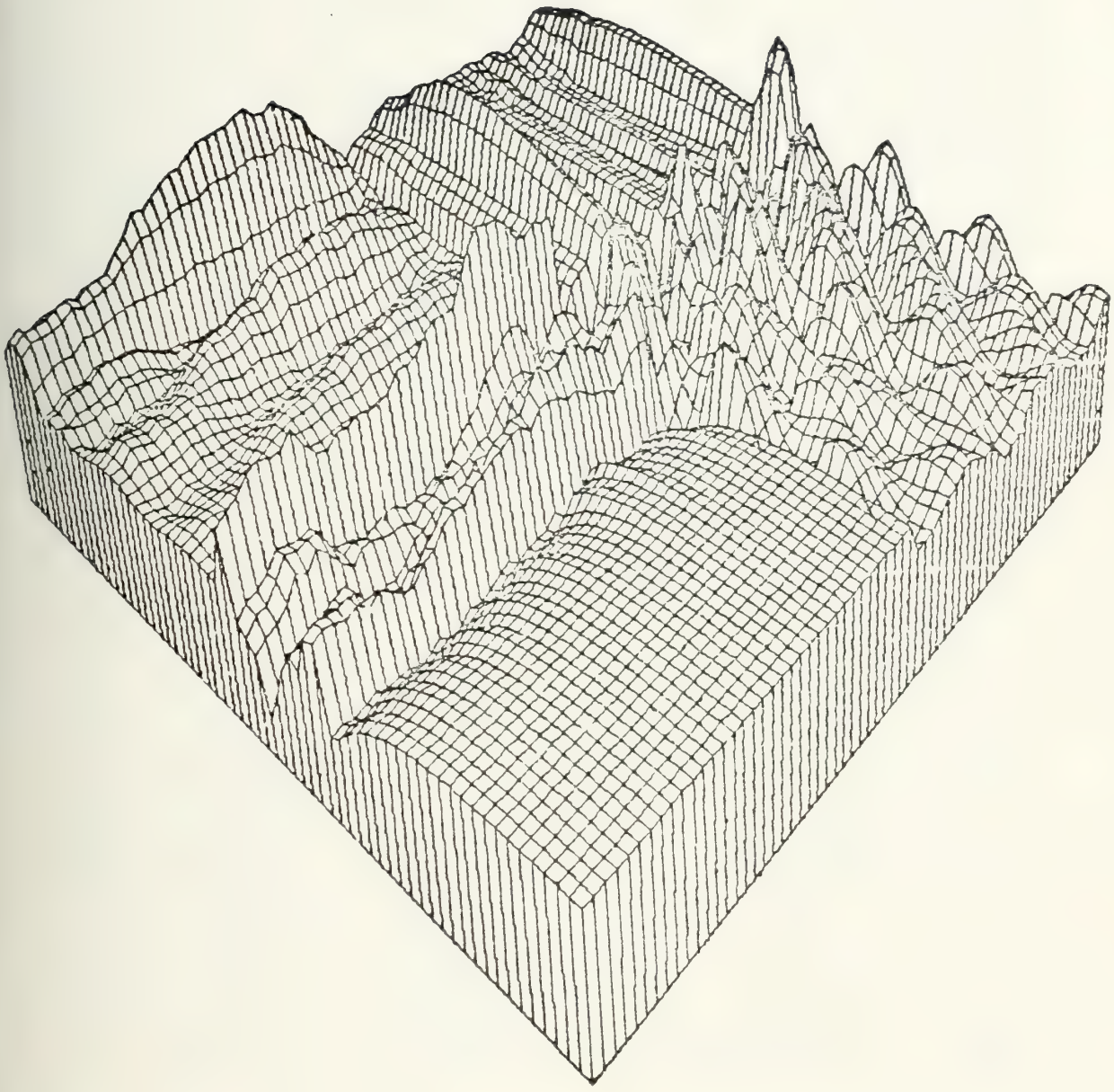

Figure 8-5(b) Three Dimensional Plot of "Four Quadrant" "Nonstationary" Simulated Clutter Image.

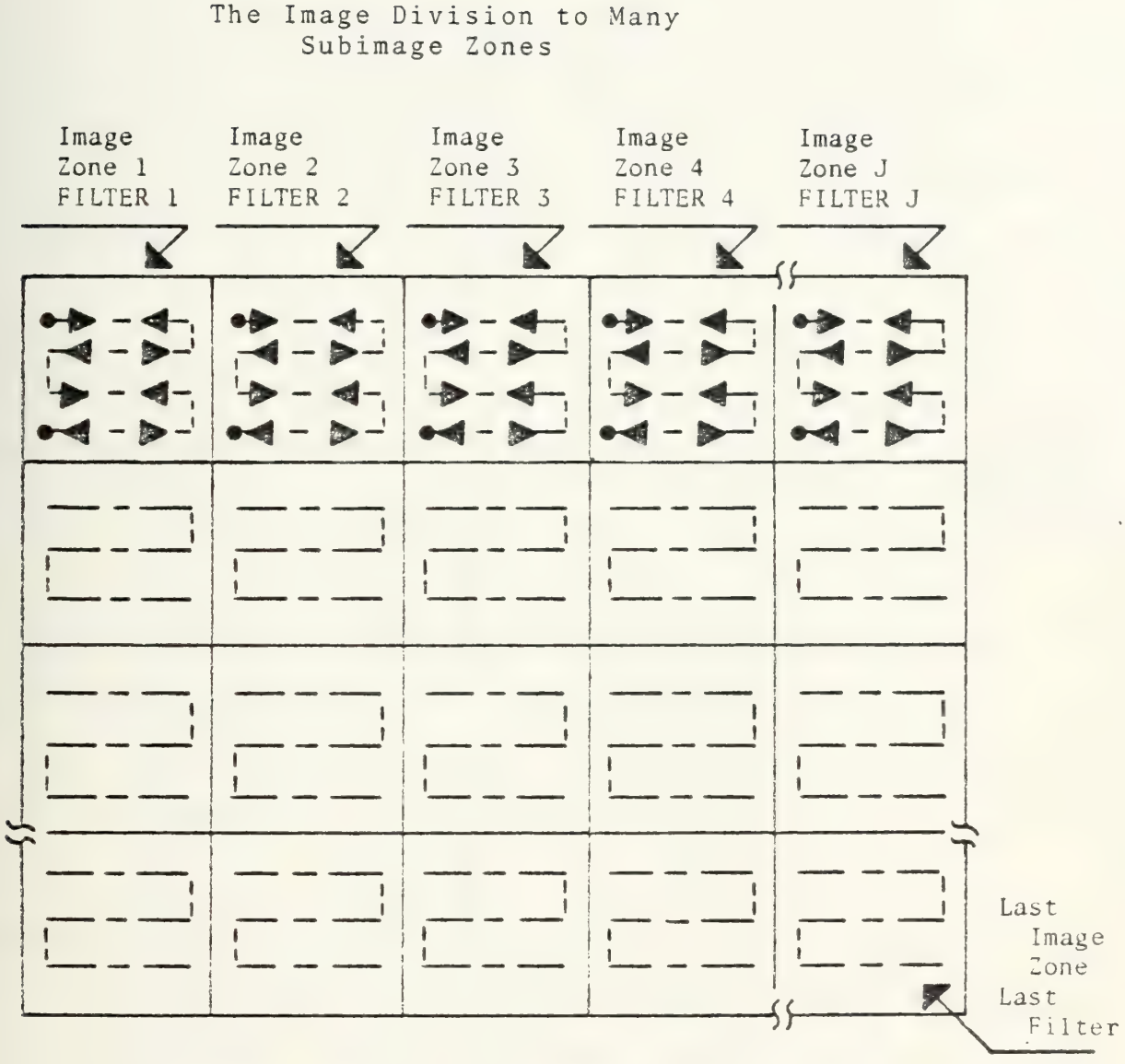

Figure 8-6(a) Division of a Given Image Into Subimage Zones for Performing Filter Adaptation.

1st Quadrant						2nd Quadrant					
1		8	9		24	32	33	55	56		64
1.0	-1.16	0.49	-0.54	1.0	-0.59	-.54 1.0 -.46	-.49	1.0 -.5	.22	-1.1	1.0
-1.21	1.09	-0.25	0.57	-1.08	0.56	.59 -1.15 .56	.57	-1.1 .54	.02	1.26	-1.52
0.29	-0.05	-0.17	-0.06	0.15	-0.01	-.08 .23 -.12	-.21	.39 -.19	-.29	-.46	.9
-0.5	0.53	-0.068	0.25	-0.5	0.25	.24 -.5 .25	.29	-.59 .29	-.03	.52	-.56
1.0	1.07	0.136	-0.5	1.0	-0.5	-.5 1.0 -.5	-.49	1.0 -.49	.15	-1.05	1.0
-0.5	0.536	-0.06	0.25	-0.5	0.25	.26 -.5 .25	.31	-.62 .31	-.04	.59	-.61
24											
25 -0.64	0.70	-0.39	0.25	-0.6	0.28	.08 -.46 .23	.21	-.61 .4	-.13	.31	-.28
1.0	-1.1	.55	-.44	1.0	-.5	-.42 1.0 -.46	-.48	1.0 -.5	.19	-1.0	1.0
-.54	.56	-.29	.27	-.58	.28	-.11 -.46 .06	.22	-.35 .06	-.08	.43	-.39
32											
33 -0.58	0.58	-0.67	0.27	-0.5	0.27	.25 -.57 .29	.21	-.46 .24	-.08	.5	.45
1.0	-.99	.11	-.46	1.0	.46	-.45 1.0 -.47	-.48	1.0 -.5	.14	-1.07	1.0
-.65	.64	-.07	.30	-.65	.30	.29 .59 .26	.27	-.52 .24	-.04	.55	-.54
55											
56 .7	-.86	.37	-.48	.82	-.44	-.37 .74 -.47	-.37	.729 -.485	-.02	.198	.174
-1.35	1.52	-.73	.81	-1.39	.755	.82 -1.56 .898	.82	-1.57 .889	-.19	1.09	-1.04
1.0	-1.08	.478	-.58	1.0	-.55	-.568 1.0 .526	-.52	1.0 -.48	.2	-1.05	1.0

3rd Quadrant 4th Quadrant

Figure 8-6(b) Adapted Spatial Filter Coefficients for Each 8 by 8 Pixels Adaptation Subimage Zone.

Processing Gain and Threshold Level in Each Subimage

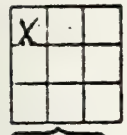

I

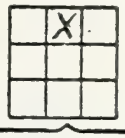

II

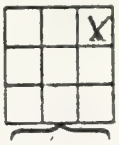

PG =	32.6	34	40	29.7	34	35	36	24
V_{TH} =	0.14	0.078	0.058	0.2	0.11	0.1	0.09	0.37
PG =	53	56	56	40	46	49	45	34
V_{TH} =	0.01	0.009	0.009	0.055	0.03	0.02	0.03	0.12
PG =	64	73	83	47	55	61	67	38
V_{TH} =	0.003	0.001	0.0004	0.026	0.01	0.005	0.002	0.077
PG =	13	15	16	5.4	20	20	20	11
V_{TH} =	1.3	1.07	0.9	3.2	0.6	0.6	0.6	1.7

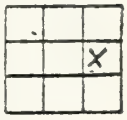

PG =	15	18.5	18.6	10.5	18.4	18.6	19	10.2
V_{TH} =	1.1	0.7	0.7	1.8	0.74	0.7	0.68	1.9
PG =	60	64	65	19.9	27.3	29.8	36	29
V_{TH} =	0.006	0.0037	0.0033	0.62	0.26	0.19	0.09	0.217
PG =	60	63.8	67	34	97	98	98	71
V_{TH} =	0.006	0.004	0.0027	0.11	0.0001	0.0001	0.0001	0.0016
PG =	22.7	25.6	29	26.4	59.8	59.6	57	24.7
V_{TH} =	0.5	0.29	0.21	0.095	0.006	0.0064	0.008	0.358

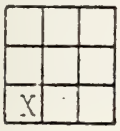

III

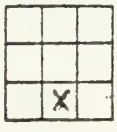

IV

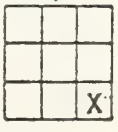

Estimation point in the inner sectors is in the search box center.

Figure 8-6(c) Processing Gain and Threshold Level for Each 8 by 8 Pixels Adaptation Subimage Zone.

For target detection:

b. Probability of detection (P_d)

c. Probability of false alarm (P_{FA})

Sets of comparisons will be presented.

a. For Background Clutter Suppression

The first set is to compare adaptive and non-adaptive filters in terms of background clutter suppression and probability of false alarm. It consists of five figures.

Fig. 8-7 shows the adaptively filtered and thresholded background clutter image, using a subimage size of 8x8 pixels. The resulting probability of false alarm is also listed in Fig. 8-7.

Fig. 8-8 shows nonadaptively filtered and thresholded background clutter image and consists of four figures. Fig. 8-8(a) is the result using the optimal spatial filter designed for the first quadrant. Figures 8-8(b), (c) and (d) are the corresponding results using spatial filters optimally designed for the second, third, and fourth quadrants respectively. Probabilities of false alarm for each case are also listed in these figures.

Comparing Fig. 8-7 and Fig. 8-8 revealed that the probability of false alarm of the adaptive filter case is about 22 times lower than that of the nonadaptive filter case.

The second set of comparisons is similar to the first set for comparing clutter suppression and P_{FA}. However, the adaptive spatial filter in this set used a large subimage size of 16 x 16 pixels. Only three figures are used.

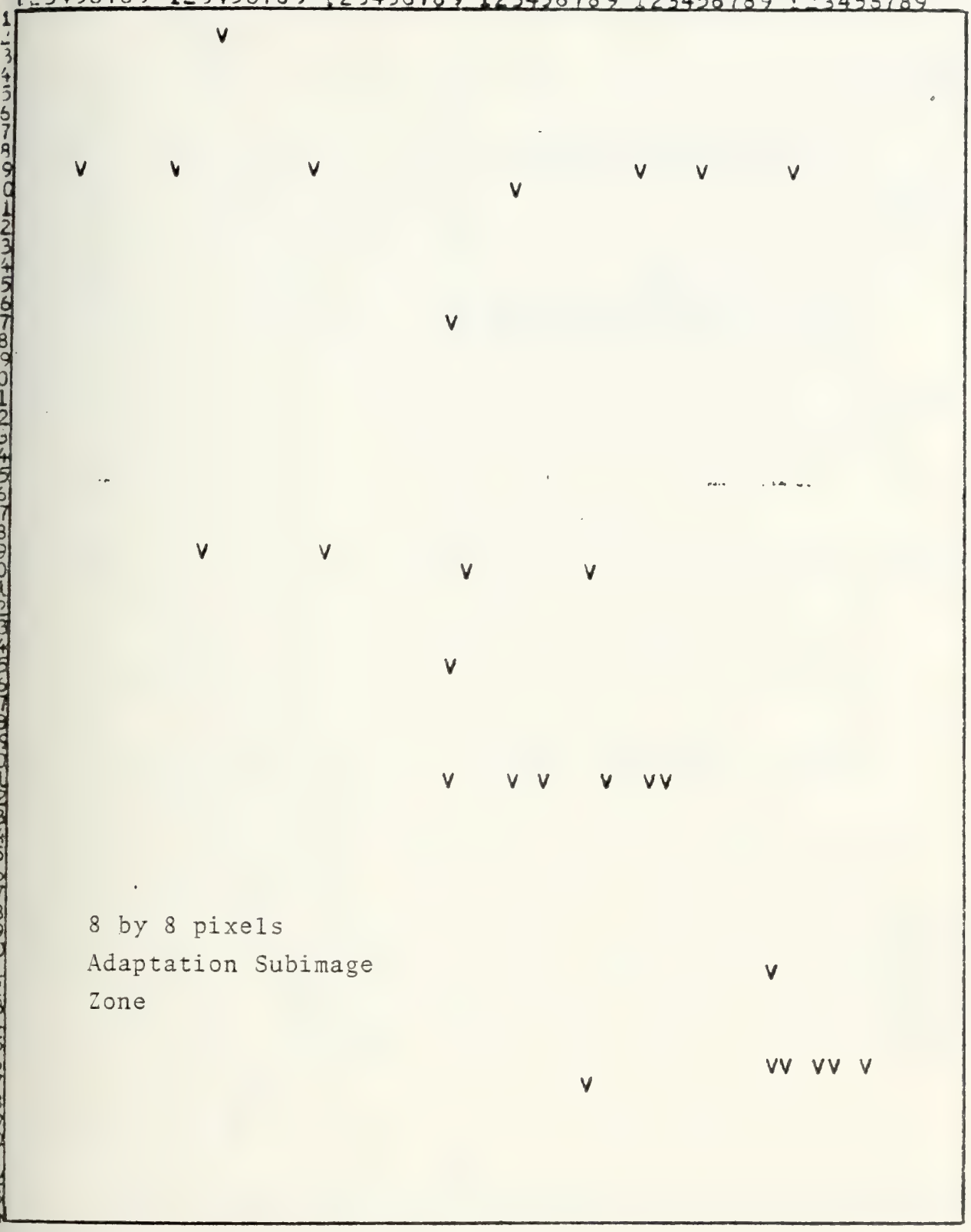

THE ADAPTIVELY FILTERED IMAGE

PROBABILITY OF FALSE ALARM IS 0.0066

Figure 8-7 Computer Print of False Alarms of Adaptively Filtered and Thresholded Four Quadrant "Nonstationary" Simulated Clutter Image.

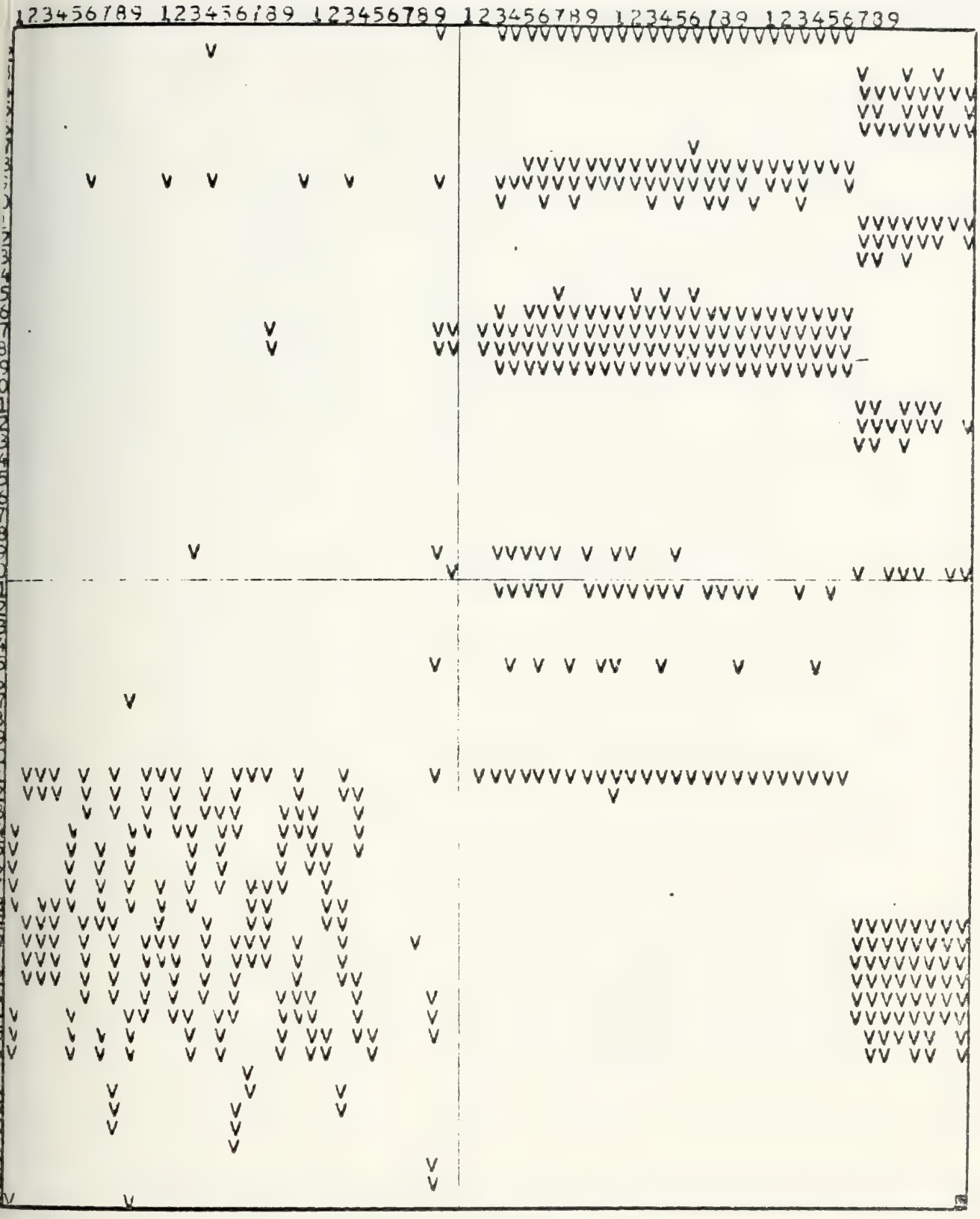

PROBABILITY OF FALSE ALARM IS 0.1431

Figure 8-8(a) Computer Print of False Alarms of Nonadaptively Filtered and Thresholded Four Quadrant "Non-stationary" Simulated Clutter Image Using Spatial Filter Optimally Designed for First Quadrant.

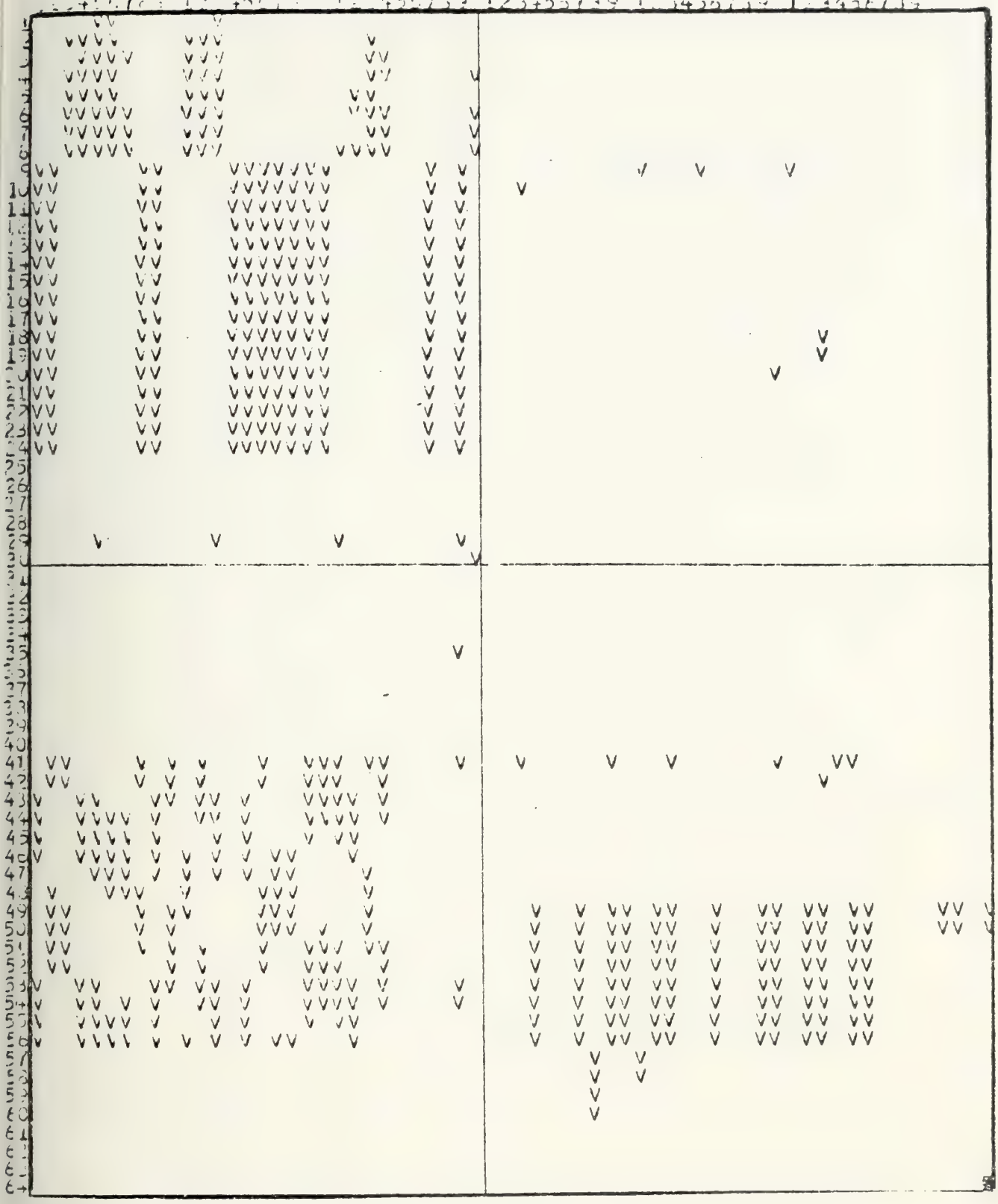

PROBABILITY OF FALSE ALARM IS 0.1462

Figure 8-8(b) Computer Print of False Alarms of Nonadaptively Filtered and Thresholded Four Quadrant "Non-stationary" Simulated Clutter Image Using Spatial Filter Optimally Designed for Second Quadrant.

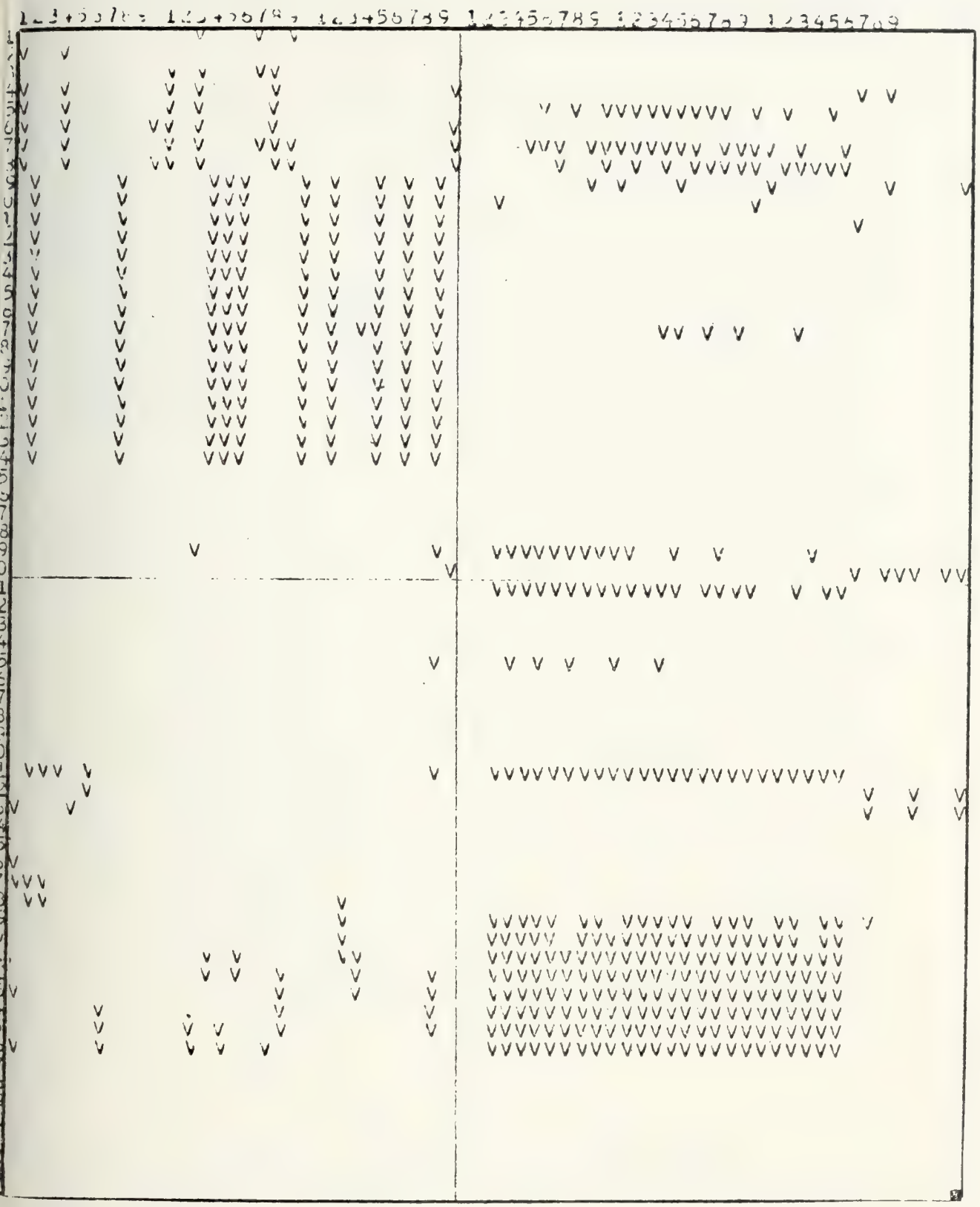

PROBABILITY OF FALSE ALARM IS 0.1396

Figure 8-8(c) Computer Print of False Alarms of Nonadaptively Filtered and Thresholded Four Quadrant "Non-stationary" Simulated Clutter Image Using Spatial Filter Optimally Designed for Third Quadrant.

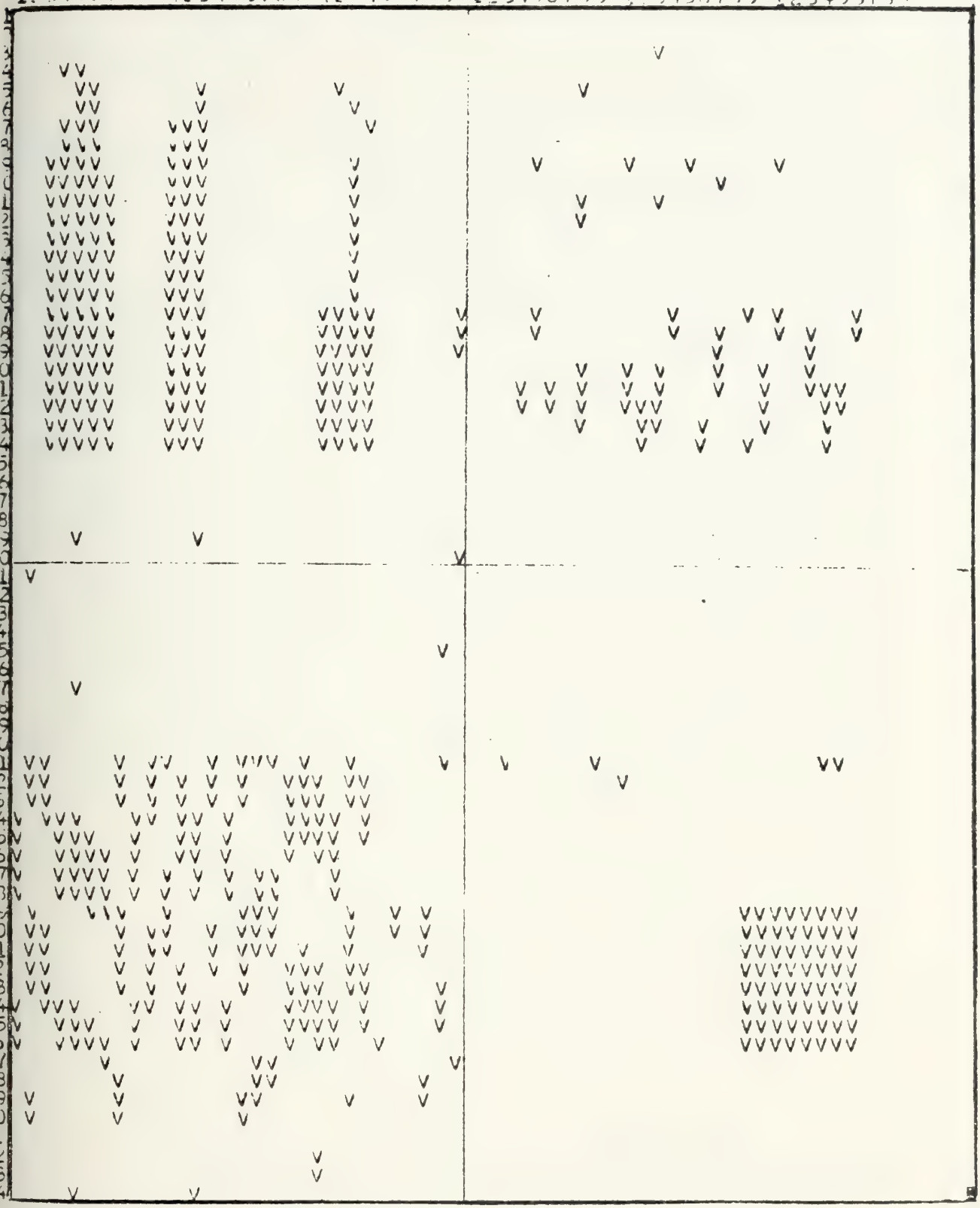

PROBABILITY OF FALSE ALARM IS 0.1335

Figure 8-8(d) Computer Print of False Alarms of Nonadaptively Filtered and Thresholded Four Quadrant "Non-stationary" Simulated Clutter Image Using Spatial Filter Designed Optimally for Fourth Quadrant.

Figure 8-9 shows the adaptively filtered and thresholded clutter image and its P_{FA}.

Figure 8-10 compares the performance of adaptive filters using 8 x 8 and 16 x 16 subimage areas. It can be seen that a smaller subimage size offers better results. Figure 8-10 indicates that in 7 out of 16 (43%) subimage areas of size 16 x 16 a transition in the statistical properties occurs inside the subimage area. On the other hand, Fig. 8-6(c) indicated that in the 8 x 8 subimage areas the transition in the statistical properties occurs only in 15 out of 64 (23%). This difference explains the improvement in the P_{FA} as subimage areas size is reduced.

Figure 8-11 shows the nonadaptive filtered and thresholded image using a spatial filter optimally designed for the lower right quadrant. The resulting P_{FA} is also listed in the figure.

Comparing figures 8-9 and 8-11 revealed that the P_{FA} of the adaptive filter case is about five times lower than that of the nonadaptive filter case. The difference is not as big as a factor of 22 for the smaller subimage size case shown in figures 8-7 and 8-8.

b. For Clutter Suppression and Target Detection

The third set of comparisons is for both clutter suppression and target detection. For this purpose, an ensemble of point targets shown in Fig. 8-12 are added to the clutter image. The resultant image is shown in Fig. 8-13.

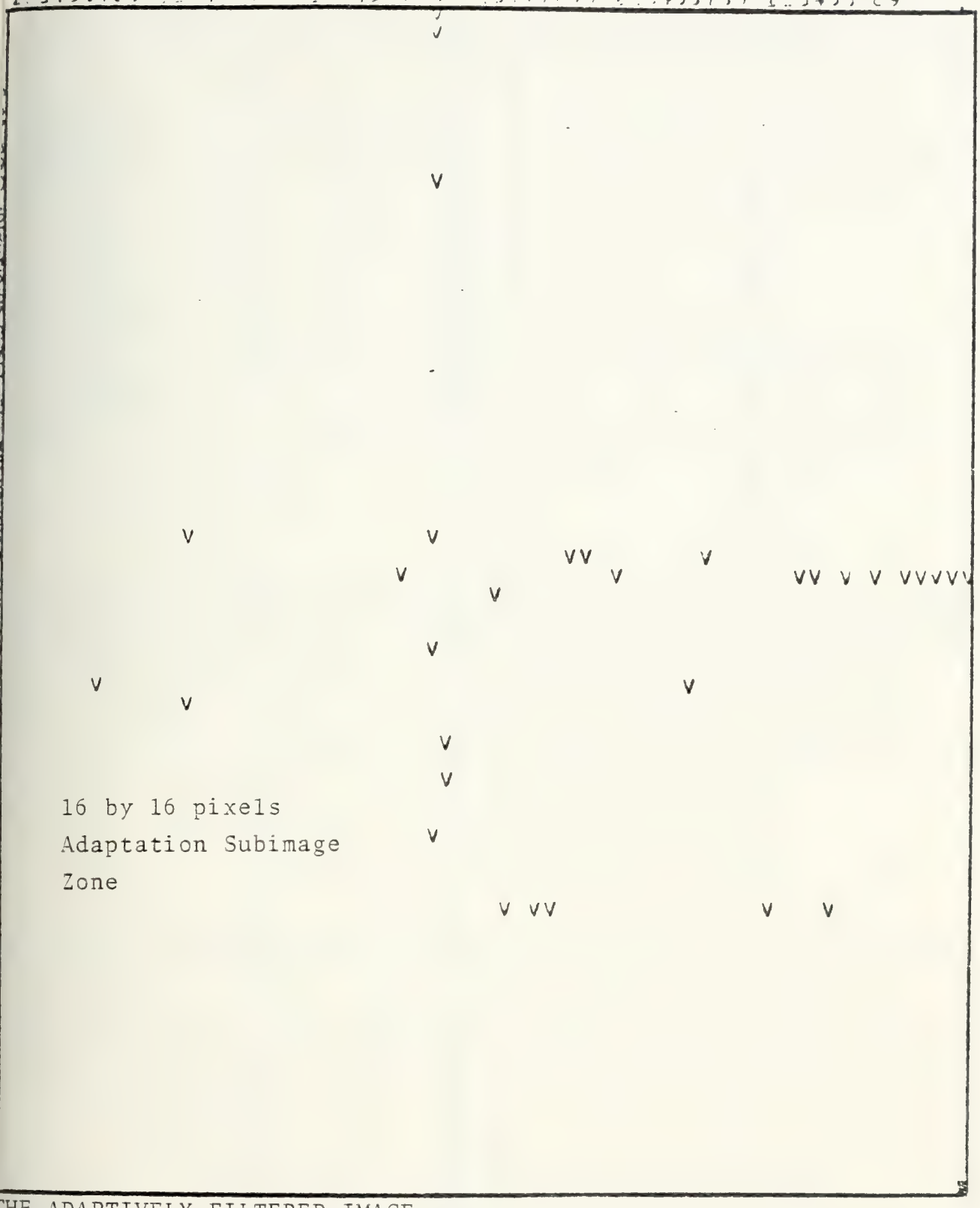

THE ADAPTIVELY FILTERED IMAGE
PROBABILITY OF FALSE ALARM IS 0.0078

Figure 8-9 Computer Print of False Alarms of Adaptively Filtered and Thresholded Four Quadrant "Nonstationary" Simulated Clutter Image.

PG = 30 V_{TH} = 0.19	PG = 33 V_{TH} = 0.13	PG = 35 V_{TH} = 0.1	PG = 27 V_{TH} = 0.27
PG = 14 V_{TH} = 1.25	PG = 17.6 V_{TH} = 0.8	PG = 32 V_{TH} = 0.15	PG = 13.8 V_{TH} = 1.25
PG = 18.2 V_{TH} = 0.75	PG = 17 V_{TH} = 0.8	PG = 25 V_{TH} = 0.31	PG = 14 V_{TH} = 1.2
PG = 18 V_{TH} = 0.74	PG = 23 V_{TH} = 0.43	PG = 40 V_{TH} = 0.056	PG = 30 V_{TH} = 0.19

Figure 8-10 Processing Gain and Threshold Level for Each 16 by 16 Pixels Adaptation Subimage Zone.

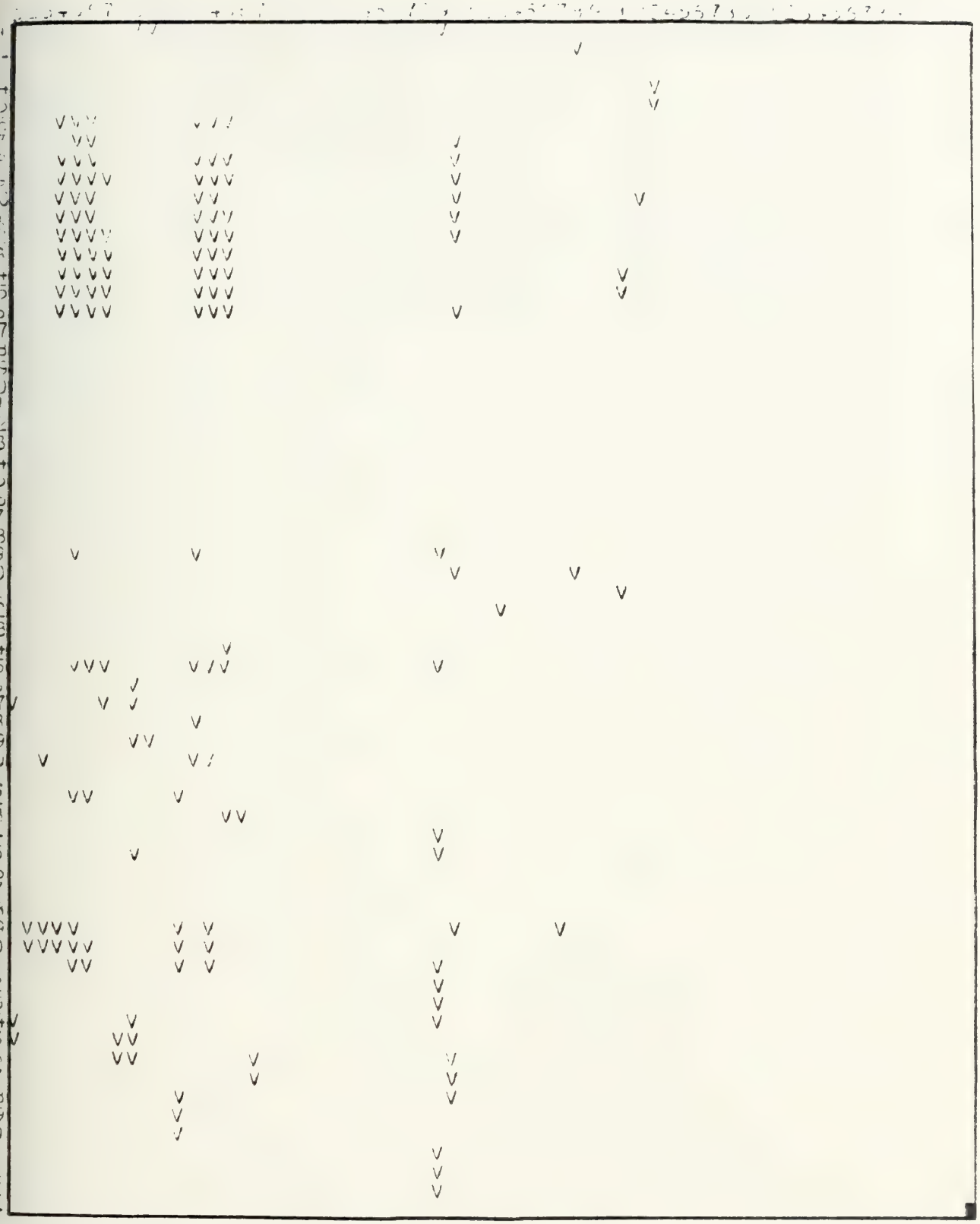

PROBABILITY OF FALSE ALARM IS 0.0383

Figure 8-11 Computer Print of False Alarms of Nonadaptively Filtered and Thresholded Four Quadrant "Non-stationary" Simulated Clutter Image Using Spatial Filter Designed Optimally for Fourth Quadrant.

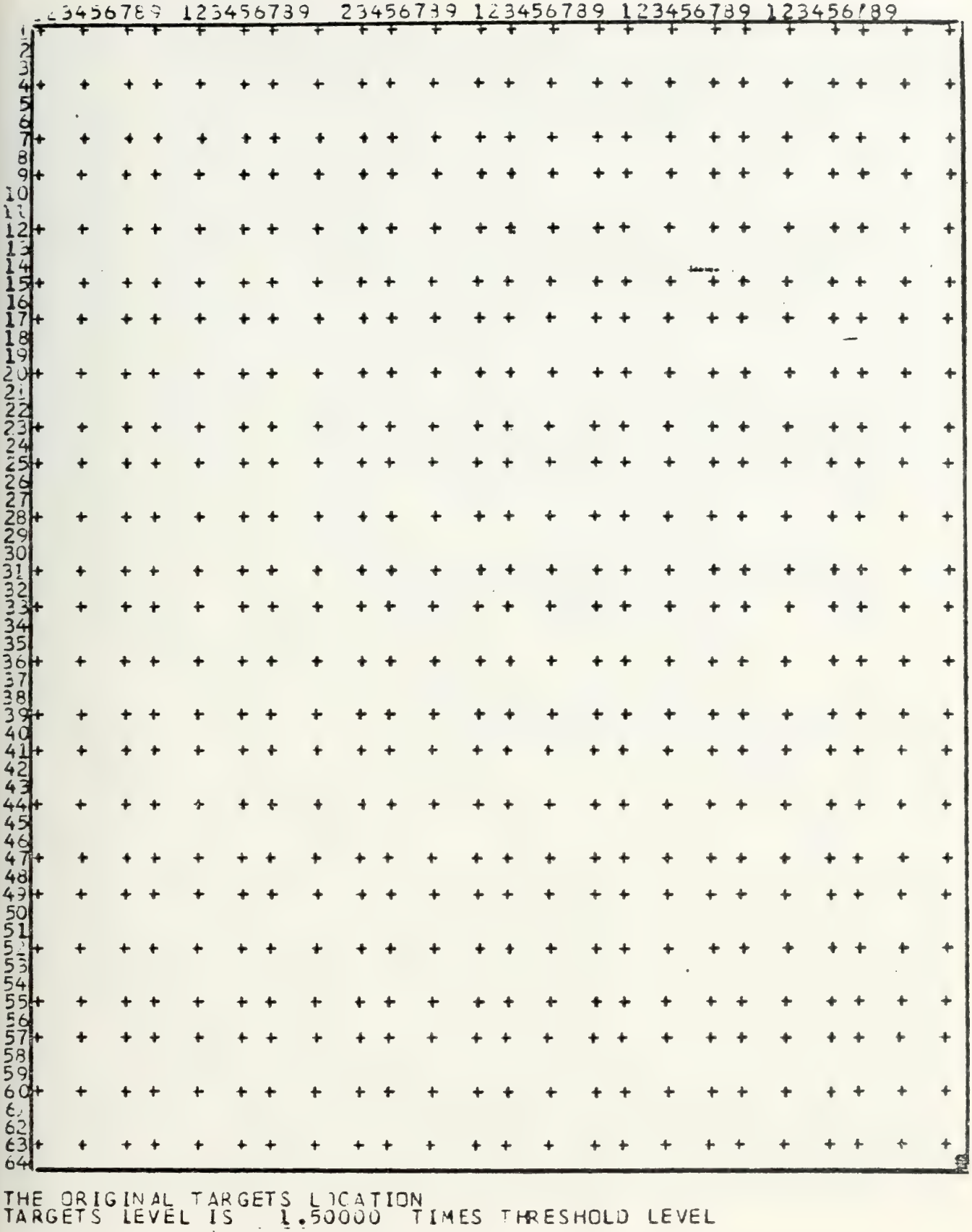

Figure 8-12 Locations of Point Targets Added to the Four Quadrant "Nonstationary" Simulated Clutter Image for Calculating Probability of Detection.

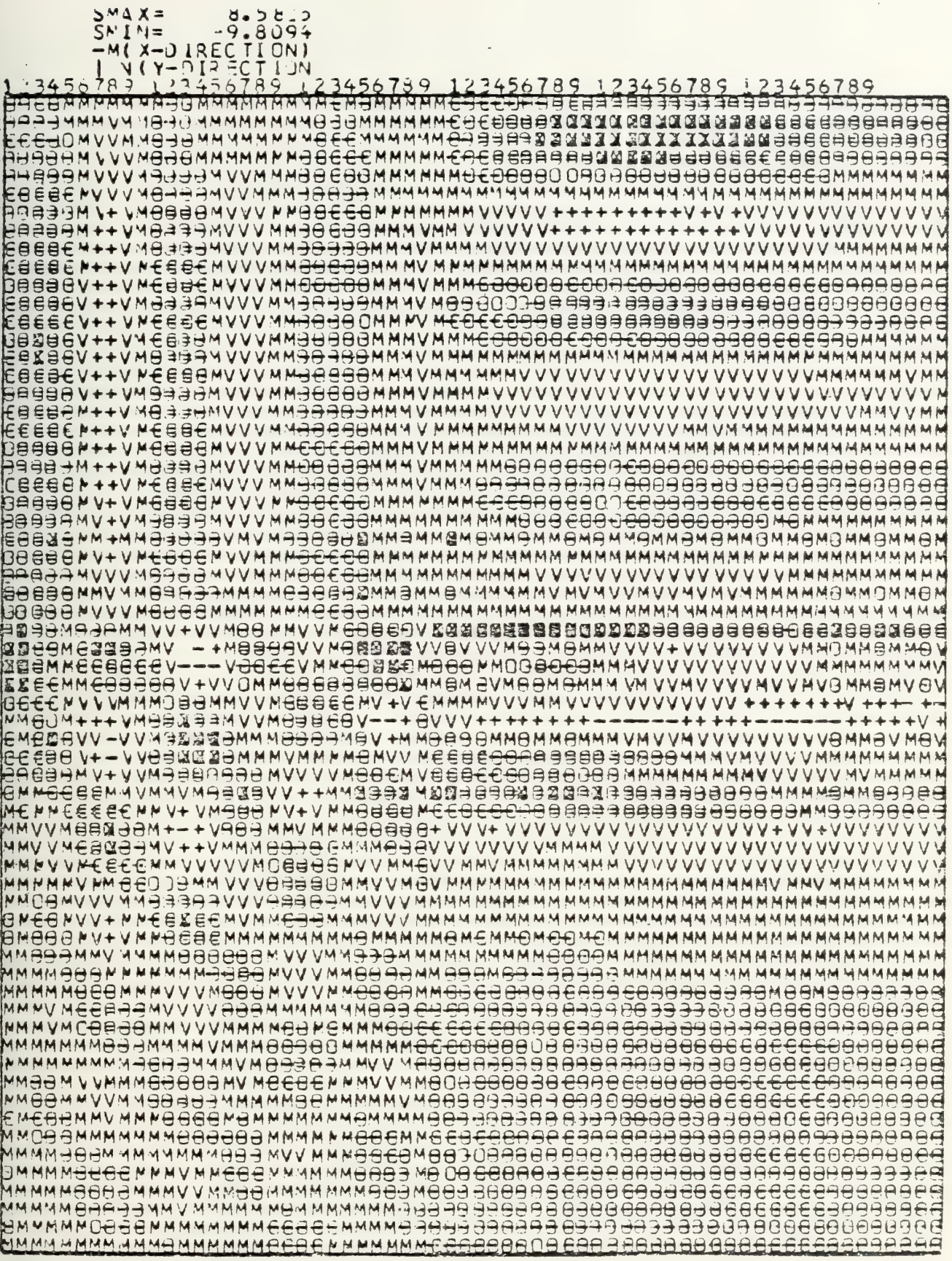

THE TARGETS TOGETHER WITH BACKGROUND NOISE

Figure 8-13 Computer Print of Four Quadrant "Nonstationary" Simulated Clutter Image Including Added Point Targets Shown in Figure 8-12.

The target intensity is proportional to the threshold level at each subimage zone.

Figure 8-14 presents the adaptively filtered and thresholded image in which all false alarms have been removed so that the probability of detection can be calculated. It is included in the figure.

Figure 8-15(a),(b),(c),(d) present the nonadaptively filtered and thresholded image using spatial filters designed optimally for first, second, third and fourth quadrants respectively. Resulting probability of detection for each case is included in corresponding figures.

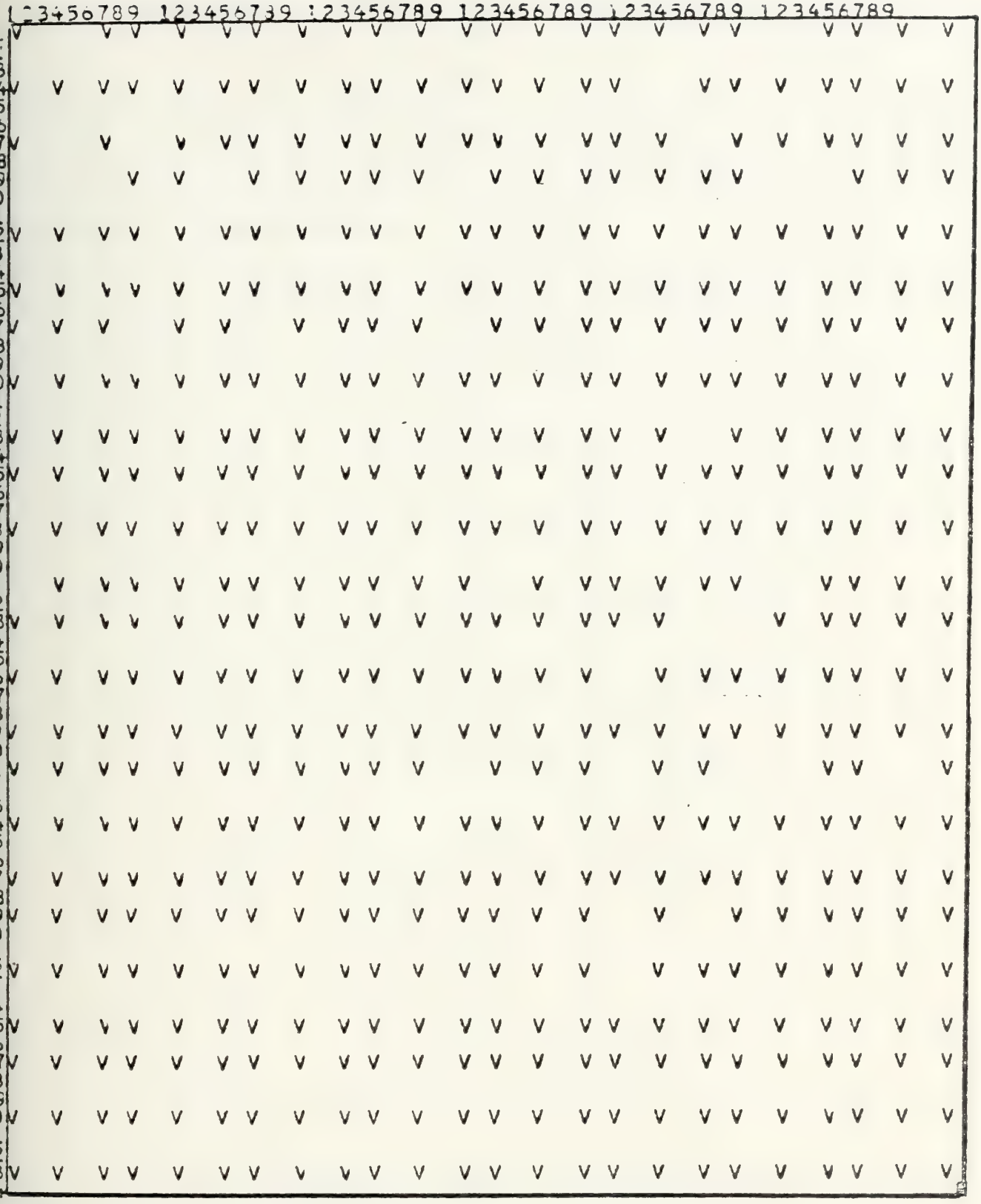

THE ADAPTIVELY FILTERED IMAGE

Figure 8-14 Computer Print of Adaptively Filtered and Thresholded Four Quadrant "Nonstationary" Simulated Clutter Image Including Added Point Targets.

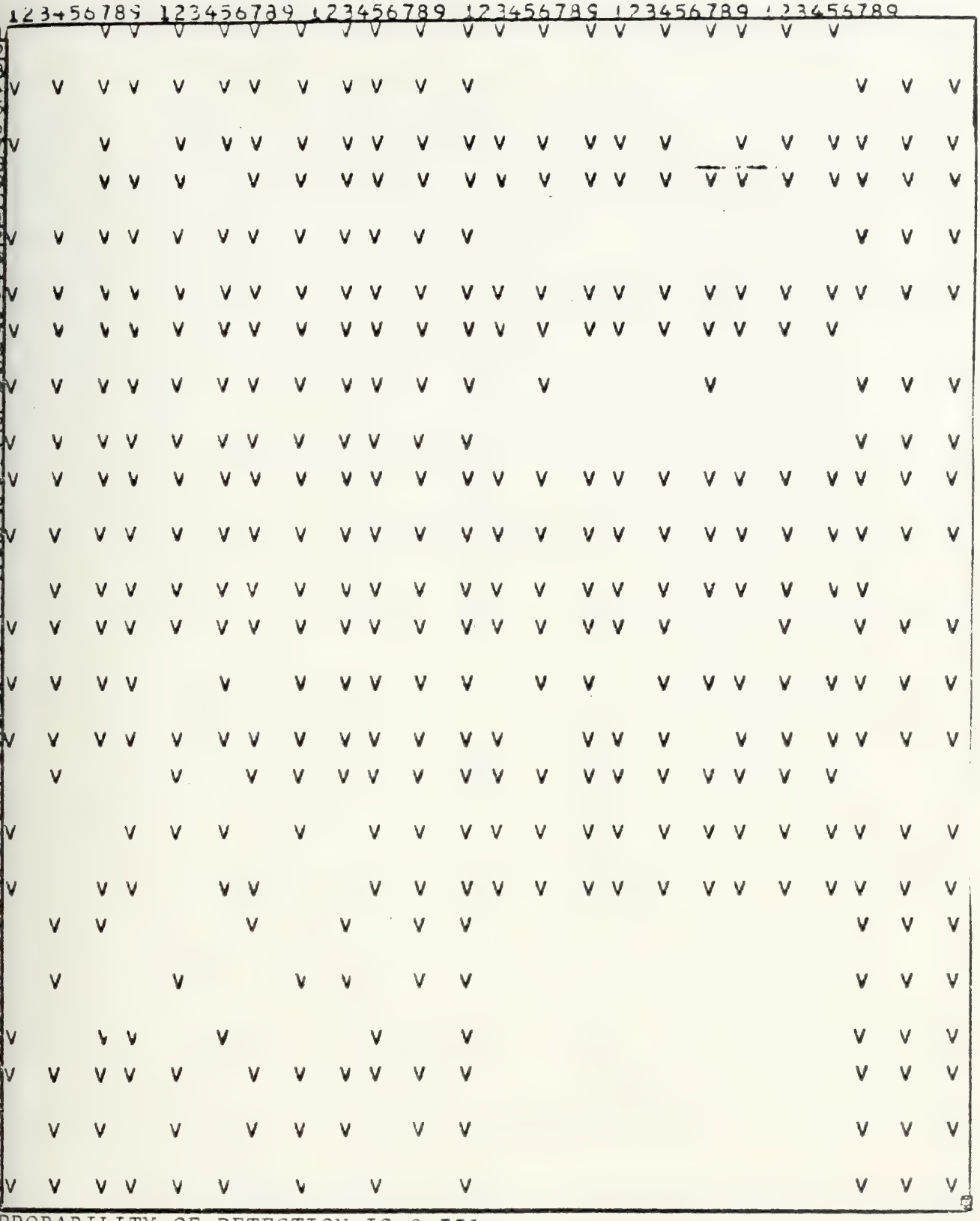

PROBABILITY OF DETECTION IS 0.731

Figure 8-15(a) Computer Print of Nonadaptively Filtered and Thresholded Four Quadrant "Nonstationary" Simulated Clutter Image. Spatial Filter Used was Designed Optimally for the First Quadrant.

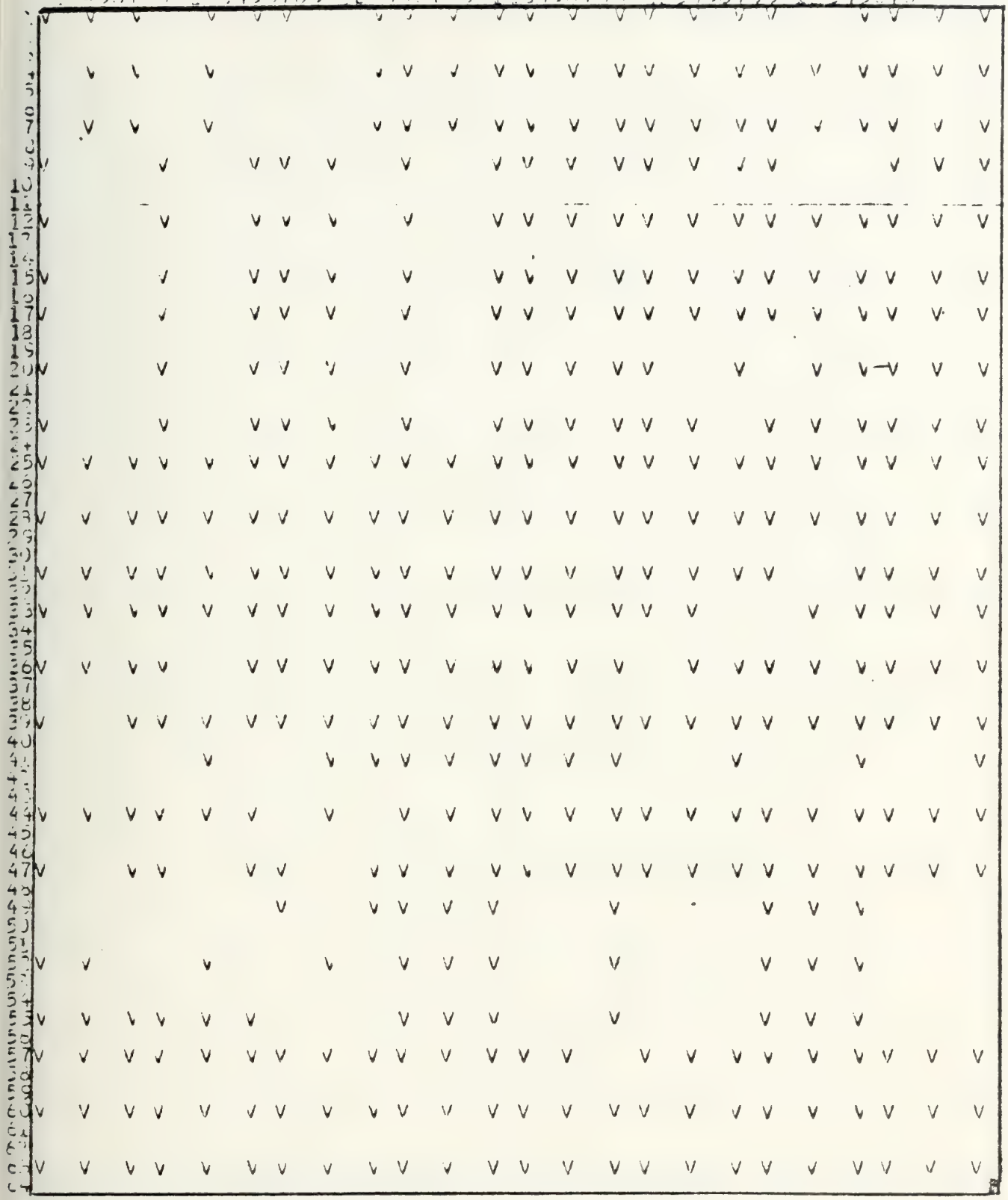

PROBABILITY OF DETECTION IS 0.807

Figure 8-15(b) Computer Print of Nonadaptively Filtered and Thresholded Four Quadrant "Nonstationary" Simulated Clutter Image. Spatial Filter Used was Designed Optimally for the Second Quadrant.

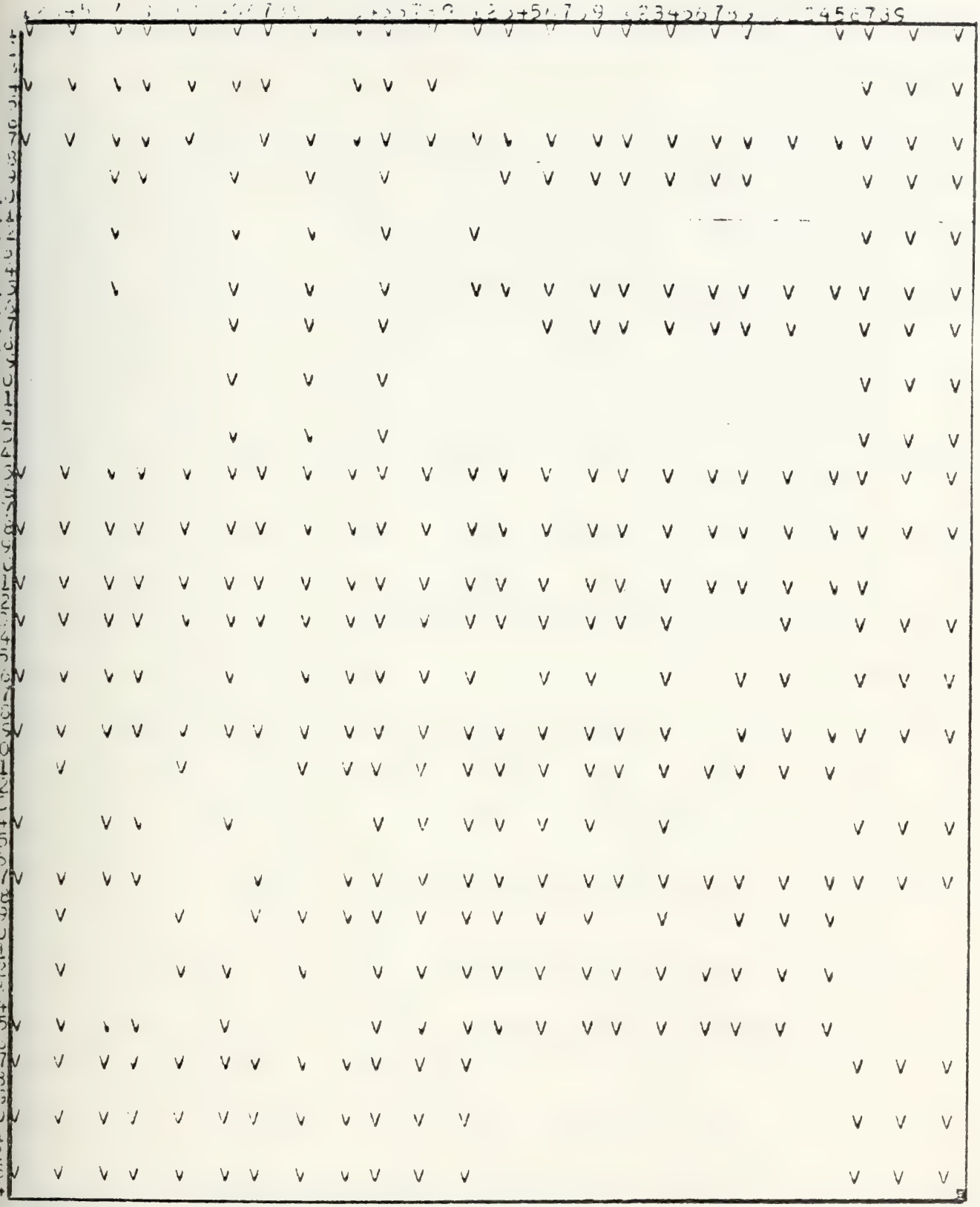

PROBABILITY OF DETECTION IS 0.694

Figure 8-15(c) Computer Print of Nonadaptively Filtered and Thresholded Four Quadrant "Nonstationary" Simulated Clutter Image. Spatial Filter Used was Designed Optimally for the Third Quadrant.

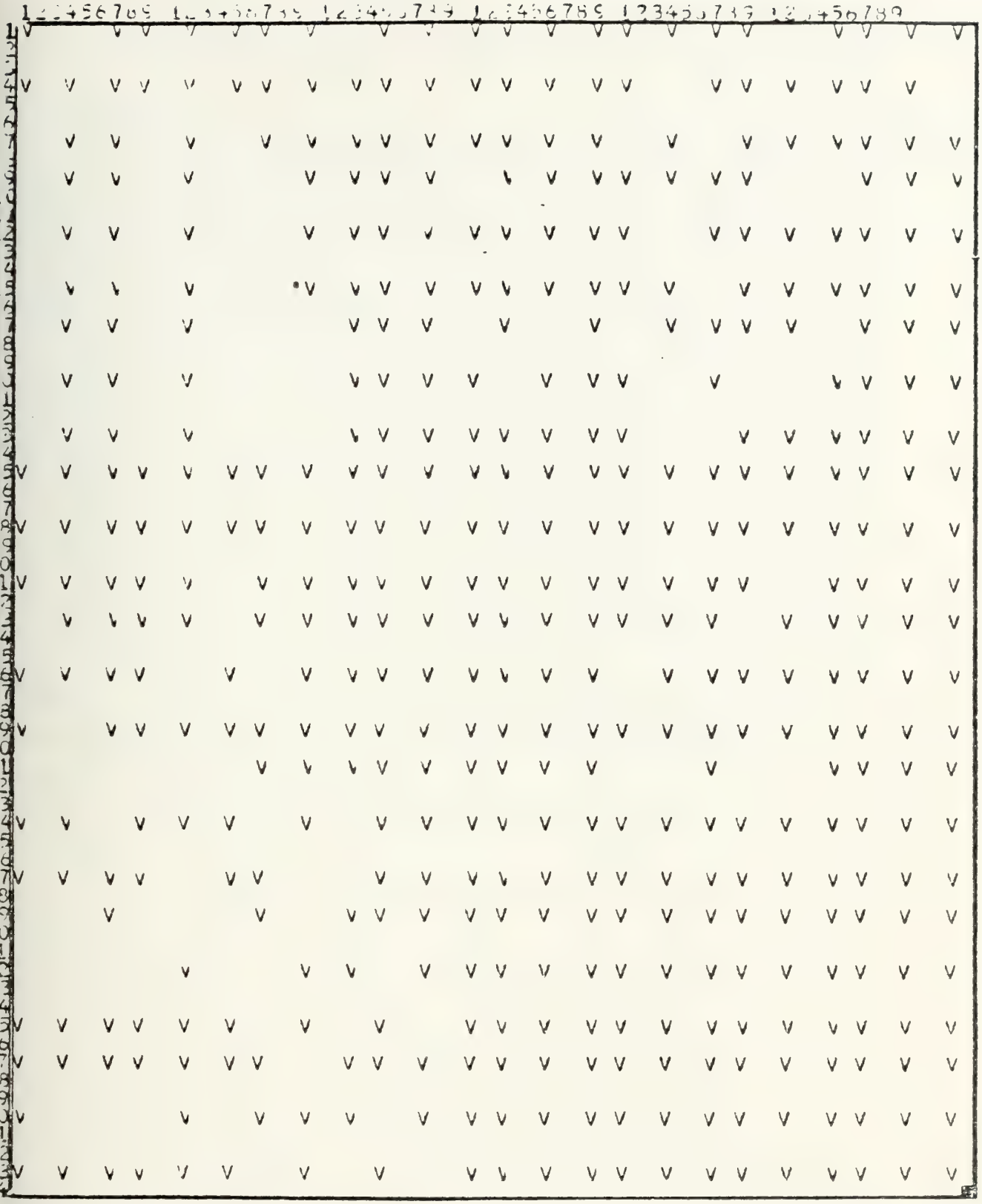

PROBABILITY OF DETECTION IS 0.823

Figure 8-15(d) Thresholded Four Quadrant "Nonstationary" Simulated Clutter Image. Spatial Filter Used was Designed Optimally for the Fourth Quadrant.

D. SUMMARY

An adaptive spatial filter algorithm based on least mean square criteria and using a steepest descent technique is shown to be effective in suppressing nonstationary clutter based on computer simulation of Markov model clutter noise.

The probability of false alarm of the adaptive filter case is lower than that of nonadaptive filter case by 5 to 22 times for the examples used in this study.

The probability of detection of the adaptive case is slightly better than that of the nonadaptive case when the threshold level is kept equal for both cases. It must be emphasized that P_{FA} for the nonadaptive case is 5 to 22 times higher. On the other hand, if a CFAR detection is applied by adjusting the threshold for the nonadaptive case, severe reduction of P_d will occur.

IX. SUMMARY AND CONCLUSIONS

A. SUMMARY

1. Introduction

New infrared surveillance and guidance systems using large mosaic detector array focal planes require the detection of targets deeply buried in background clutter noise by several tens of db's. New image processing techniques must be developed to accomplish these heretofore unachievable goals. They must also be relatively straightforward so that on-board implementation using moderate LSI signal processors is possible to meet real time processing requirements. They should also be flexible enough so that a focal plane processing algorithm is able to adapt itself to changing background scenes.

This thesis develops five focal plane processing procedures which consist of nonrecursive statistical filters for background clutter suppression followed by thresholding to initiate the target detection. Nonrecursive approaches are taken because they make extensive use of both the spatial and temporal behavior of the image signal in the neighborhood of the pixel of interest. On one frame of the image, signals of pixels all around the pixel of interest are used. In addition, signals at the same pixel location from other frames before and after the frame of interest are also used in the focal plane processing. New integrated circuit tapped delay

line devices may be used effectively for their hardware implementation. Statistical approaches are used because it is believed that a collective statistical description can be found for different background scenes if they belong to the same class of terrain, weather conditions, etc. Therefore, it is possible to design a statistical filter which is able to estimate a weak target buried in noise and is not limited to only a few background scenes.

The concept of using nonrecursive statistical filters for background clutter suppression was originated by Lt. D. Bar-Yehoshua [14] in his development of nonadaptive spatial filters based on the minimization of mean square error. This thesis made extensive extension and more thorough developments of four nonadaptive filters in both spatial and temporal domains. In addition, a new adaptive spatial filter is developed.

2. Nonadaptive Focal Plane Processing

In Chapter II, the basic concept of the nonrecursive statistical filter is expanded and generalized to include all nonadaptive and adaptive, spatial, temporal and mixed spatial-temporal or temporal-spatial filters. A unified processing concept is presented for clutter suppression based on the statistical spatial and temporal behaviors of the image in the neighborhood of the pixel of interest. Two statistical criteria for filter design are introduced. One is based on the minimization of mean square error criterion which leads to the MMSE filter or Wiener filter. The other is based on

the maximization of signal to noise ratio criterion which leads to the statistical matched filter.

Detailed developments of the principles, configurations, and design procedures for the filters are developed in Chapter III for spatial filters using a single image frame and in Chapter IV for sequential spatial-temporal filters using several frames of images. These three dimensional statistical filters are useful in situations when multiple frames of images are available, either when the surveillance and guidance systems are already in their tracking modes after the targets have been acquired or when the fields of view of the systems are stabilized to cover an area for a number of frames.

In Chapter V, the thresholding procedure for a two dimensional image is developed for the initialization of target detection. Two CFAR (constant false alarm rate) procedures to set the threshold level are developed. One is for Gaussian probability density functions. The other is for the more general non-Gaussian PDF.

In Chapter VI, the background clutter suppression filters and thresholding are combined together in four non-adaptive focal plane processing procedures. Their properties and performance are studied in detail, using two types of images. One type is a set of twenty frames of real world infrared images with 10% uniform drift between frames. The second type is computer generated images which use two Markov

processes to model the correlated noise which is assumed to be a good simulation of the real world background clutter. It has recently been brought to our attention that the Markov model was found to be an acceptable simulation of the background clutter based on recent work on a tactical infrared hostile weapon location system.* With the computer generated model, a wide variety of images with varying statistical properties can be generated with ease.

Both background clutter suppression performance and target detection performance are evaluated by computer simulation using both types of images. Using the real world infrared images, a background clutter suppression of 27 db is achieved by a single frame spatial filter. Using a five frame spatial-temporal filter, a suppression of 87 db is achieved. These results are the most important testimony of the practical usefulness of the nonadaptive statistical filters because they have been used by other research groups and considered as one of the "standard" test scenes. Comparison with results of other groups is difficult in this unclassified study because the absolute calibration of the image signal is a classified number and was not made available. It should be acknowledged that the real world infrared image test described by figures 6-11 to 6-18 was made by Captain D. Hilmers and was reported originally in Ref. 30.

*J. Otazo, MIT Lincoln Laboratory, private communication, and to be presented in the SPIE 1979 symposium, Washington, D.C., April 17-18, 1979.

3. Adaptive Focal Plane Processing

In Chapters VII and VIII, adaptive statistical spatial filters based on the minimization of mean square error criteria are developed for clutter suppression. In Chapter VII, the adaptive procedure is developed using computer generated "stationary" images whose statistical spatial correlation properties are uniform. In the following chapter, the procedure is applied to computer generated "nonstationary" images which have four different statistical spatial correlation properties in a given image. It is found that using a small adaptive array of 8x8 pixels, better clutter suppression can be achieved compared with nonadaptive statistical spatial filters. Using the adaptive approach, the resulting probability of false alarm (P_{FA}) of the adaptively filtered and thresholded image was found to be more than twenty times better than that of the four possible nonadaptive filters.

B. CONCLUSION

In conclusion, five nonrecursive statistical focal plane processors have been developed. The usefulness of this new concept of clutter suppression has been demonstrated by applying these nonadaptive filters to a set of real world infrared images. Although the adaptive spatial filters have been tested on computer generated images, it is believed that good clutter suppression can also be achieved on real world images.

Neither the concepts of nonrecursive filters nor that of statistical estimation are new. However, the combination of these two concepts to process two and three dimensional images of very low signal to noise ratio for suppression of "colored" clutter noise and for substantial enhancement of target signal to noise ratio up to several ten's of db's has not been reported before. The contributions of this thesis to the advancement of focal plane processing techniques for the enhancement of point/line targets and the suppression of clutter are highlighted in the following.

1. Nonadaptive Focal Plane Processing

a. One dimensional statistical estimation techniques based on the minimization of mean square error criterion (Wiener filter) and the maximization of signal to noise ratio criterion (matched filter) are extended to two dimensions for a single frame and to three dimensions for multiple frame focal plane processing. They are different from other multiple dimensional image processing studies because special emphasis is given to the suppression of clutter which is modeled by correlated noise. Furthermore, target signals several ten's of db's below clutter noise are considered. Images of such low signal to noise ratio have not been considered until motivated by the recent interest in smart sensor systems.

b. The clutter suppression is accomplished by performing an estimate of the target. This is different from

other approaches which first estimate the clutter and then suppress it by subtraction from the estimate of the target signal.

2. Adaptive Focal Plane Processing

a. One dimensional nonrecursive adaptive filter techniques based on the least mean square criterion are extended to two dimensional single frame focal plane processing with special emphasis on the suppression of correlated clutter noise several ten's of db's higher than the signal of interest.

b. A procedure to derive the desired response corresponding to different types of target signals is developed which is used in the adaptive process as the optimal response.

c. The adaptive loop gain is set by an "automatic gain control" procedure which includes several requirements simultaneously to yield constant misadjustment for varying statistical properties of the clutter, to prevent overflow and to assure adaptive convergence.

d. A procedure for dividing images whose statistical properties are nonstationary and unknown a priori, into subimage zones for filter adaptation is developed which minimizes the degree of nonstationarity and improves the performance of adaptation.

APPENDIX A [Ref. 14]

GENERATION (MODELING) OF TWO-DIMENSIONAL RANDOM FIELDS*

A. INTRODUCTION

Any monochromatic image can be modeled by specifying its value (gray level) f(m,n) at each spatial coordinate (m,n). An ensemble of such images can be modeled by interpreting f(m,n) as a random field. A class of images with particular spatial correlation can be modeled by a random field with the same autocorrelation function.

When spectral factorization in two dimensions is possible [Ref. 36], the autocorrelation function of a random field is related to the transfer function of a system that generates the random field from a set of uncorrelated variates. Then, specifying a class of images by their autocorrelation function specifies a dynamic model representation for these images.

For a discrete random-field, the dynamic model is a partial difference equation that can be represented by a two dimensional recursive relation. The problem in this Appendix is to find a linear equation that represents a given random field. A discrete two dimensional random process with two kinds of autocorrelation functions will be considered.

The presented method uses the spatial frequency domain to generate the requested random field.

---

*Excerpt from thesis by D. Bar-Yehoshua, "Two Dimensional Nonrecursive Filter for Estimation and Detection of Targets," Naval Postgraduate School, June 1974 [14].

B. SPATIAL FREQUENCY DOMAIN METHOD (TRANSFER FUNCTION)

1. Introduction

The discrete power transfer relation, for linear filtering of random signals, is useful for designing signal processors. If we like to generate a random field with given autocorrelation function, we can find a transfer function through which an uncorrelated random field at the input (white noise), will give a defined discrete power spectrum density at the output.

Figure A-1 shows the relationship between a white noise input signal passing through a linear filter and the resulting output. In this case, the discrete power density of the input is the 2-D unity function, and the discrete power density of the output equal to the absolute square of the filter transfer function.

The transfer function method procedure can be written as follows:

a. From the autocorrelation function of the random field to be modeled, find the discrete power spectral density using z transform.

$$S(z_1, z_2) = Z\{R(m,n)\} \qquad \text{(A-1)}$$

b. Assume that the discrete power spectral density is:

$$S(z_1, z_2) = |H(z_1, z_2)|^2 = H(z_1, z_2) \cdot H(z_1^{-1}, z_2^{-1}) \qquad \text{(A-2)}$$

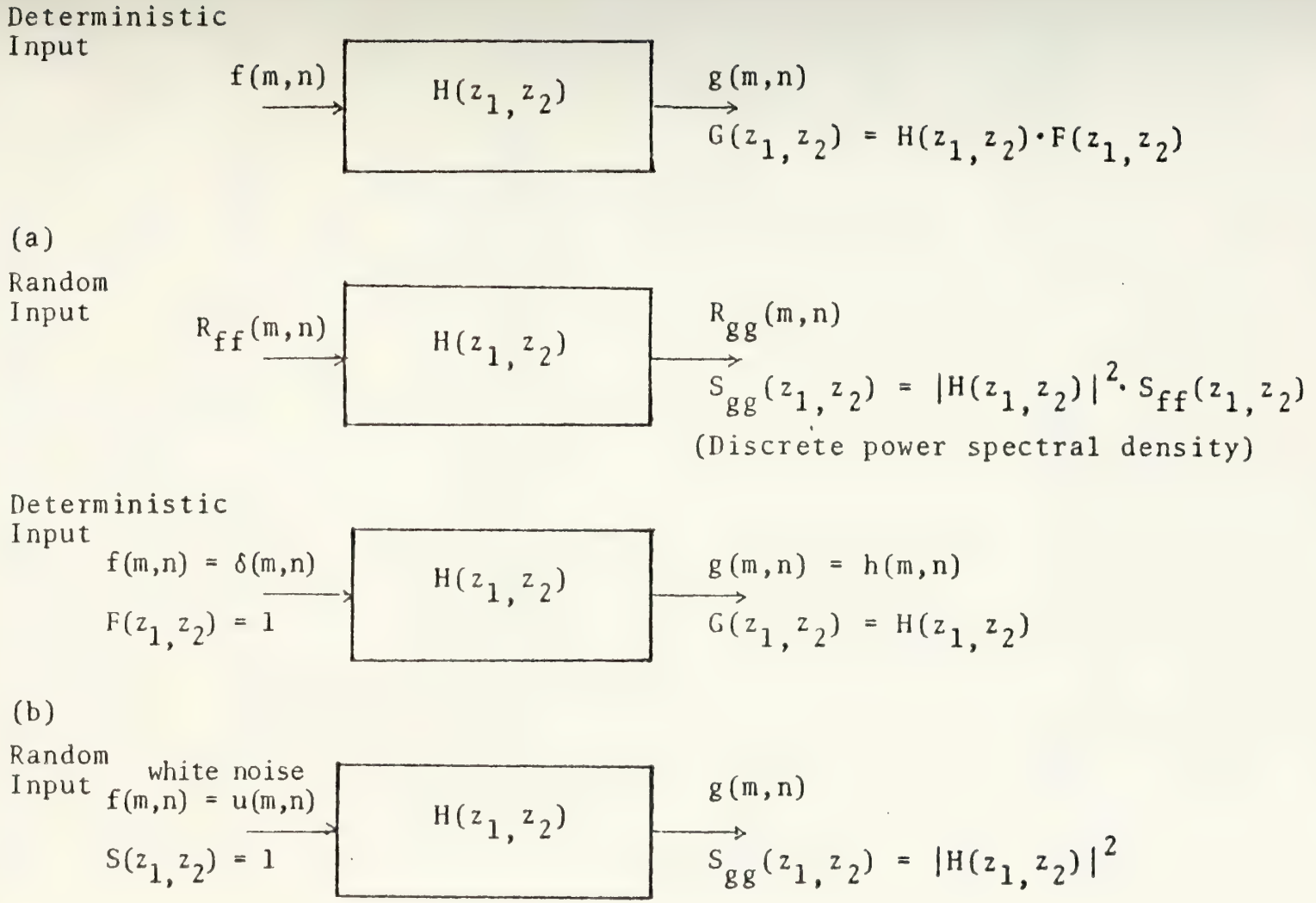

Figure A-1. A filter with deterministic and random inputs (a) a general case, (b) with impulse and white noise inputs.

Try to separate $S(z_1, z_2)$ in order to get $H(z_1, z_2)$ as a transfer function of the random field model, according to eq. A-2.

c. Using an uncorrelated random field as an input to $H(z_1, z_2)$, find the dynamic model of the designed random field in the z domain.

$$G(z_1, z_2) = H(z_1, z_2) \cdot u(z_1, z_2) \tag{A-3}$$

where $u(z_1, z_2)$ is a random white noise signal.

d. Convert the dynamic model to a spatial model by inverse z transform. In this process it is assumed that the random field is stationary and ergodic. In this section the dynamic model for two autocorrelation functions will be considered.

2. Dynamic Model of One-Dimensional Autocorrelation Function $R(\tau) = \sigma_R^2 \rho^{|\tau|}$

Given the autocorrelation function of one-dimensional random signal as:

$$R(m) = \sigma_R^2 \cdot \rho^{|m|} \tag{A-4}$$

The discrete power spectral density will be:

$$S(z) = \frac{\sigma_R^2 \cdot (1-\rho^2)}{(1-\rho z) \cdot (1 - \rho z^{-1})} \tag{A-5}$$

$$= \frac{\sigma_R \cdot \sqrt{1 - \rho^2}}{1 - \rho z} \cdot \frac{\sigma_R \cdot \sqrt{1 - \rho^2}}{1 - \rho z^{-1}} = H(z)\ H(z^{-1})$$

So, the transfer function will be

$$H(z) = \frac{\sigma_R \cdot \sqrt{1 - \rho^2}}{1 - \rho z^{-1}} \tag{A-6}$$

and the output for such transfer function:

$$g(z) = H(z) \cdot F(z) = \frac{\sigma_R \sqrt{1-\rho^2}}{1-\rho z^{-1}} \cdot F(z)$$

If we replace the input by white noise, we will get the dynamic model in z domain:

$$g(z) = \rho z^{-1} \cdot g(z) + \sigma_R \sqrt{1-\rho^2} \cdot u(z) \qquad (A-7)$$

or in time domain:

$$g(n) = \rho g(n-1) + \sigma_R \sqrt{1-\rho^2} \cdot u(n) \qquad (A-8)$$

where $u(n)$ is a white noise with variance $\sigma_u = 1$.

Eq. (A-8) represents a dynamic model for a one-dimensional first order Markov process.

3. Dynamic Model of One-dimensional Autocelleration Function $R(n) = \sigma_R^2 \rho^{|n|} \cdot \cos(\omega \cdot n)$

Given the autocorrelation function:

$$R(n) = \sigma_R^2 \cdot \rho^{|n|} \cdot \cos(\omega \cdot n) \qquad (A-9)$$

The discrete power spectral density will be:

$$S(z) = \sigma_R^2 \cdot (1-\rho^2) \cdot \frac{a + bz}{(1 - 2\rho \cdot \cos \omega z + \rho^2 \cdot z^2)} \cdot \frac{a + bz^{-1}}{(1 - 2\rho \cdot \cos \omega z^{-1} + \rho^2 \cdot z^{-2})} \qquad (A-10)$$

where

$$a = \frac{\sqrt{1 - 2\rho \cdot \cos \omega + \rho^2} + \sqrt{1 + 2\rho \cdot \cos \omega + \rho^2}}{2}$$

$$b = \frac{\sqrt{1 - 2\rho \cdot \cos \omega + \rho^2} - \sqrt{1 + 2\rho \cos \omega + \rho^2}}{2} \qquad (A-11)$$

Note: $1 - 2 \cos \omega + \rho^2 \geq 0$ for $0 \leq \rho \leq 1$.

Separating $S(z)$ to $H(z)\cdot H(z^{-1})$, we get:

$$H(z) = \sigma_R \cdot \sqrt{1-\rho^2} \cdot \frac{a + bz - 1}{1 - 2\rho\cdot\cos\omega z^{-1} + \rho^2 z^{-2}} \qquad \text{(A-12)}$$

There are two ways to represent the dynamic model of such transfer function.

a. First way:

$$G(z) = H(z) \cdot F(z)$$

Substitute $H(z)$ from eq. (A-12) and represent f as a white noise, we will get:

$$G(z) = 2\rho\cdot\cos\omega\cdot z^{-1}\cdot F(z) - \rho^2 z^{-2}\cdot F(z) + \sigma_R\sqrt{1-\rho^2}\cdot[a + bz^{-1}]\cdot u(z) \qquad \text{(A-13)}$$

The dynamic model in time domain will be:

$$g(n) = 2\rho\cdot\cos\omega\cdot g(n-1) - \rho^2 g(n-2) + R\cdot\sqrt{1-\rho^2}\cdot[a\cdot u(n) + b\cdot u(n-1)] \qquad n > 3 \qquad \text{(A-14)}$$

where $u(n)$ is a random white noise.

The initial condition will be:

assume $g(-1) = g(0) = u(0) = 0$

we will get:

$$g(1) = \sigma_R\cdot u(1)$$

$$g(2) = 2\rho\cdot\cos\omega\cdot g(1) + \sigma_R\sqrt{1-\rho^2}\cdot[au(2) + bu(1)]. \qquad \text{(A-15)}$$

b. Second way - state variable representation

Let us define:

$$F'(z) = \sigma_R\cdot\sqrt{1-\rho^2}\cdot(a + bz^{-1})\cdot z\cdot F(z) \qquad \text{(A-16)}$$

so that:

$$G(z) = H(z)\cdot z^{-1}\cdot F'(z) = \frac{z^{-1}\cdot F'(z)}{1-2\rho\cdot\cos\omega z^{-1}+\rho^2 z^{-2}} \qquad (A\text{-}17)$$

or

$$G(z) = 2\cdot\rho\cdot\cos\omega\cdot z^{-1}\cdot G(z) - \rho^2 z^{-2} G(z) + z^{-1}\cdot F'(z) \qquad (A\text{-}18)$$

Let us define:

$$p_1(z) \stackrel{D}{=} G(z)$$

$$p_2(z) \stackrel{D}{=} \rho^2\cdot z^{-1}\cdot G(z) \qquad (A\text{-}19)$$

From eq. (A-18) and eq. (A-19), we get:

$$p_1(z) = 2\rho\cdot\cos\omega\cdot z^{-1}\cdot p_1(z) - z^{-1}\cdot p_2(z) + z^{-1}\cdot F'(z)$$

$$p_2(z) = \rho^2 z^{-1}\cdot p_1(z)$$

Its expression in the time domain is:

$$p_1(n) = 2\rho\cdot\cos\omega\cdot p_1(n-1) - p_2(n-1) + f'(n-1)$$

$$p_2(n) = \rho^2\cdot p_1(n-1) \qquad (A\text{-}20)$$

Expressing eq. (A-20) in the state variable form, we have:

$$\begin{bmatrix} p_1(n) \\ p_2(n) \end{bmatrix} = \begin{bmatrix} 2\rho\cdot\cos\omega & -1 \\ \rho^2 & 0 \end{bmatrix}\cdot\begin{bmatrix} p_1(n-1) \\ p_2(n-1) \end{bmatrix} + \begin{bmatrix} 1 \\ 0 \end{bmatrix}\cdot f'(n-1)$$

for $n > 1$ (A-21)

where the output is defined as:

$$g(n) = [1 \quad 0]\cdot\begin{bmatrix} p_1(n) \\ p_2(n) \end{bmatrix} \qquad (A\text{-}22)$$

and $f'(n-1) = \sigma_R\sqrt{1-\rho^2}\cdot[au(n) + bu(n-1)]$

where $u(n)$ is a white noise.

The initial condition is:

$$\begin{bmatrix} p_1(1) \\ p_2(1) \end{bmatrix} = \begin{bmatrix} 1 \\ 0 \end{bmatrix} \cdot \sigma_R \cdot u(1)$$

4. Dynamic Model of Two-dimensional Autocorrelation Function $R(m,n) = \sigma_R^2 \cdot \rho_h^{|m|} \cdot \rho_v^{|n|}$

Given the autocorrelation function

$$R(m,n) = \sigma_R^2 \cdot \rho_h^{|m|} \cdot \rho_v^{|n|} \qquad \text{(A-23)}$$

the discrete power spectral density is (using eq. A-5):

$$S(z_1,z_2) = S_1(z_1) \cdot S_2(z_2) =$$

$$= \frac{\sigma_R^2 \cdot (1-\rho_h^2) \cdot (1-\rho_v^2)}{(1-\rho_h \cdot z_1) \cdot (1-\rho_h \cdot z_1^{-1}) \cdot (1-\rho_v \cdot z_2) \cdot (1-\rho_v \cdot z_2^{-1})} \qquad \text{(A-24)}$$

Separating $S(z_1,z_2)$ to $H(z_1,z_2) \cdot H(z_1^{-1},z_2^{-1})$ gives:

$$H(z_1,z_2) = \frac{\sigma_R \cdot \sqrt{(1-\rho_h^2) \cdot (1-\rho_v^2)}}{(1-\rho_h \cdot z_1^{-1}) \cdot (1-\rho_v z_2^{-1})} \qquad \text{(A-25)}$$

and the output of such transfer function:

$$G(z_1,z_2) = H(z_1,z_2) \cdot u(z_1,z_2)$$

yields the following recursive equation:

$$G(z_1,z_2) = \rho_h \cdot z_1^{-1} \cdot G(z_1,z_2) - \rho_h \cdot \rho_v \cdot z_1^{-1} \cdot z_2^{-1} \cdot G(z_1,z_2)$$

$$+ \rho_v \cdot z_2^{-1} \cdot G(z_1,z_2) + \sigma_R \sqrt{(1-\rho_h^2) \cdot (1-\rho_v^2)} \cdot u(z_1,z_2)$$

(A-26)

The dynamic model in spatial domain will be:

$$g(m,n) = \rho_h \cdot g(m-1,n) - \rho_h \cdot \rho_v \cdot g(m-1,n-1) + \rho_v \cdot g(m,n-1) + \sigma_R \cdot \sqrt{(1-\rho_h^2)\cdot(1-\rho_v^2)} \cdot u(m,n) \qquad \text{(A-27)}$$

$$\text{for } m,n > 1$$

Equation (A-27) is a two dimensional first order Markov process representation.

The initial condition will be:

$$g(1,1) = \sigma_R \cdot u(1,1) \qquad \text{(A-27)}$$

$$g(m,1) = \rho_h \cdot g(m-1,1) + \sigma_R \cdot \sqrt{1-\rho_h^2} \cdot u(m,1) \qquad m > 1$$

$$g(1,n) = \rho_v \cdot g(1,n-1) + \sigma_R \cdot \sqrt{1-\rho_v^2} \cdot u(1,n) \qquad n > 1$$

where u(m,n) is white noise with variance 1.

This dynamic model was used by Habibi [Ref. 17] and can be characterized in a state space structure [Ref. 18] by:

$$\begin{bmatrix} r(m+1,n) \\ s(m,n+1) \end{bmatrix} = \left[\begin{array}{c|c} \rho_h & 1 \\ \hline 0 & \rho_v \end{array}\right] \cdot \begin{bmatrix} r(m,n) \\ s(m,n) \end{bmatrix} + \begin{bmatrix} 0 \\ \sigma_R \cdot \sqrt{1-\rho_h^2)\cdot(1-\rho_v^2} \end{bmatrix} \cdot u(m,n) \qquad \text{(A-29)}$$

$$g(m,n) = \begin{bmatrix} 1 & 0 \end{bmatrix} \cdot \begin{bmatrix} r(m,n) \\ s(m,n) \end{bmatrix}$$

5. Dynamic Model of Two-dimensional Autocorrelation Function $R(m,n)$ =

$$\sigma_R^2 \cdot \rho_h^{|m|} \cdot \rho_v^{|n|} \cdot \cos(\omega_h \cdot m) \cos(\omega_v \cdot n)$$

Given the autocorrelation function:

$$R(m,n) = \sigma_R^2 \cdot \rho_h^{|m|} \cdot \rho_v^{|n|} \cdot \cos(\omega_h \cdot m) \cdot \cos(\omega_v \cdot n) \qquad \text{(A-30)}$$

The discrete power spectral density (using eq. A-10) is:

$$S(z_1, z_2) = S(z_1) \cdot S(z_2) =$$

$$= H_1(z_1) \cdot H_1(z_1^{-1}) \cdot H_2(z_2) \cdot H_2(z_2^{-1}) \qquad \text{(A-31)}$$

where

$$H(z_1^{-1}, z_2^{-1}) = H_1(z_1^{-1}) \cdot H_2(z_2^{-1})$$

$$= \sigma_R \sqrt{(1-\rho_h^2) \cdot (1-\rho_v^2)}$$

$$\cdot \frac{(a_h + b_h \cdot z_1^{-1}) \cdot (a_v + b_v \cdot z_2^{-1})}{(1 - 2\rho_h \cdot \cos\omega_h \cdot z_1^{-1} + \rho_h^2 \cdot z_1^{-2}) \cdot (1 - 2\rho_v \cdot \cos\omega_v \cdot z_2^{-1} + \rho_v^2 \cdot z_2^{-2})}$$

(A-32)

where

$$a_h = \frac{\sqrt{1 - 2\rho_h \cdot \cos\omega_h + \rho_h^2} + \sqrt{1 + 2\rho_h \cdot \cos\omega_h + \rho_h^2}}{2}$$

$$b_h = \frac{\sqrt{1 - 2\rho_h \cdot \cos\omega_h + \rho_h^2} - \sqrt{1 + 2\rho_h \cdot \cos\omega_h + \rho_h^2}}{2}$$

$$a_v = \frac{\sqrt{1 - 2\rho_v \cdot \cos\omega_v + \rho_v^2} + \sqrt{1 + 2\rho_v \cdot \cos\omega_v + \rho_v^2}}{2} \qquad \text{(A-33)}$$

$$b_v = \frac{\sqrt{1 - 2\rho_v \cdot \cos\omega_v + \rho_v^2} - \sqrt{1 + 2\rho_v \cdot \cos\omega_v + \rho_v^2}}{2}$$

The output of the transfer function of eq. (A-32) is:

$$G(z_1, z_2) = H(z_1, z_2) \cdot U(z_1, z_2)$$

Calculate $G(z_1, z_2)$ and make the two-dimensional inverse z transform, the dynamic model in spatial domain will be:

$$\begin{aligned} g(m,n) = {} & C_v \cdot g(m,n-1) - \rho_v^2 \cdot g(m,n-2) \\ & + C_h \cdot g(m-1,n) - C_h \cdot C_v \cdot g(m-1,n-1) + C_h \cdot \rho_v^2 \cdot g(m-1,n-2) \\ & - \rho_h^2 \cdot g(m-2,n) + \rho_h^2 \cdot C_v \cdot g(m-2,n-1) - \rho^2{}_h \cdot \rho_v^2 g(m-2,n-2) \\ & + \sigma_R \cdot \sqrt{(1-\rho_h^2)\cdot(1-\rho_v^2)} \cdot [a_h \cdot a_v \cdot u(m,n) + a_h \cdot a_v \cdot u(m,n-1) \\ & + a_v \cdot b_h \cdot u(m-1,n) + b_h \cdot b_v \cdot u(m-1,n-1)] \end{aligned} \qquad \text{(A-34)}$$

for $m,n > 2$

where $C_h \overset{D}{=} 2 \cdot \rho_h \cdot \cos \omega_h$

$C_v \overset{D}{=} 2 \cdot \rho_v \cdot \cos \omega_v$

and $u(m,n)$ is an uncorrelated random field (white noise).

The initial condition is:

a. $g(i,j) = u(i,j) = 0$ when i or $j < 1$ (A-35)

b. $g(1,1) = \sigma_R \cdot u(1,1)$

$g(m,1)$ - for $m > 1$ - use eq. (A-34)

with $\rho_v = 0$ and $\omega_v = 0$ and (eq. A-35)

$g(1,n)$ - for $n > 1$ - use eq. (A-34)

with $\rho_h = 0$ and $\omega_h = 0$ and eq. (A-35).

Equation (A-34) is a two dimensional second order Markov process representation.

An example of an image 100 x 100 in size, formed by equation (A-34), representing the given autocorrelation function eq. (A-30) is shown in Fig. A-1. In this picture we used $\rho_h = \rho_v = 0.99$ and $\sigma_R = 1$ and $\omega_h = \omega_v = 0.143$. Comparison of the correlation function R(m,n) of the simulated image to the given image yielded an average error of the correlation factor around 1%.

The state space structure can be found as follows:

Let us define:

$$u^1(z_1,z_2) = z_1^2 \cdot z_2 \cdot u(z_1,z_2) + \sigma_R \sqrt{(1-\rho_h^2)(1-\rho_v^2)} \cdot (a_h + b_h \cdot z_1^{-1}) \cdot (a_v + b_v \cdot z_2^{-2}) \tag{A-36}$$

we get:

$$G(z_1,z_2) = \frac{z_1^{-2}}{(1-2\rho_h \cdot \cos\omega_h + \rho_h^2 \cdot z_1^{-2}} \cdot \frac{z_2^{-1} \cdot u^1(z_1,z_2)}{(1-2\rho_v \cdot \cos\omega_v + \rho_v^2 \cdot z_2^{-2})} \tag{A-37}$$

By using the following definition:

$$p_1(z_1,z_2) \overset{D}{=} -z_1^{-1} \cdot \rho_h^2 \cdot p_2(z_1,z_2) + z_1^{-1} \cdot p_4(z_1,z_2) \tag{A-38}$$

$$p_2(z_1,z_2) \overset{D}{=} \frac{z_1^{-2} \cdot p_4(z_1,z_2)}{(1-2 \cdot z_1^{-1} \cdot \rho_h \cdot \cos\omega_h + \rho_h^2 \cdot z_1^{-2})} \tag{A-39}$$

$$p_3(z_1,z_2) \overset{D}{=} -\rho_v^2 \cdot z_2^{-1} \cdot p_4(z_1,z_2) \tag{A-40}$$

$$p_4(z_1,z_2) \overset{D}{=} \frac{z_2^{-1} \cdot u^1(z_1,z_2)}{(1-2 \cdot \rho_v \cdot \cos\omega_v \cdot z_2^{-1} + \rho_v^2 \cdot z_2^{-2})} \tag{A-41}$$

$$G(z_1,z_2) \overset{D}{=} p_2(z_1,z_2) \tag{A-42}$$

Figure A-2 - A random field given by the auto-correlation function $R_{ff}(m,n) = \sigma_R^2 \cdot \rho_h^{|m|} \cdot \rho_v^{|n|} \cdot \cos(\omega_m \cdot m) \cos(\omega_n \cdot n)$ forming computer, using the dynamic model of eq. (A-30). (The picture is presented by 9 level gray scale).

Eq. (A-37) can be represented as:

$$
\begin{aligned}
P_1(z_1,z_2) &= -z_1^{-1}\cdot\rho_h^{2}\cdot P_2(z_1,z_2) + z_1^{-1}\cdot P_4(z_1,z_2)\\
P_2(z_1,z_2) &= 2\rho_h\cdot\cos\omega_h\cdot z_1^{-1}\cdot P_2(z_1,z_2) + z_1^{-1}\cdot P_1(z_1,z_2)\\
P_3(z_1,z_2) &= -\rho_v^{2}\cdot z_2^{-1}\cdot P_4(z_1,z_2) \qquad\qquad (A\text{-}43)\\
P_4(z_1,z_2) &= 2\rho_v\cos\omega_v\cdot z_2^{-1}\cdot P_4(z_1,z_2) + z_2^{-1}\cdot P_3(z_1,z_2)\\
&\quad + z_2^{-1}\cdot u^1(z_1,z_2)
\end{aligned}
$$

Converting eq. (A-43) to spatial domain and putting in state variables form, we get:

$$
\begin{bmatrix} p_1(m+1,n)\\ p_2(m+1,n)\\ p_3(m,n+1)\\ p_4(m,n+1)\end{bmatrix} = \left[\begin{array}{c|c|c|c} 0 & -\rho_h^{2} & 0 & 1\\ \hline 1 & 2\rho_h\cdot\cos\omega_h & 0 & 0\\ \hline 0 & 0 & 0 & -\rho_v^{2}\\ \hline 0 & 0 & 1 & 2\rho_v\cdot\cos\omega_v\end{array}\right]\cdot\begin{bmatrix} p_1(m,n)\\ p_2(m,n)\\ p_3(m,n)\\ p_4(m,n)\end{bmatrix}
$$

$$
+ \begin{bmatrix} 0\\ 0\\ 0\\ 1\end{bmatrix}\cdot u^1(m,n) \qquad (A\text{-}44)
$$

where

$$
g(m,n) = [0 \quad 1 \quad 0 \quad 0]\cdot\begin{bmatrix} p_1(m,n)\\ p_2(m,n)\\ p_3(m,n)\\ p_4(m,n)\end{bmatrix}
$$

and $u^1(m,n)$ is an uncorrelated random field given by:

$$u^1(m,n) = \alpha_R \cdot \sqrt{(1-\rho_h^2)(1-\rho_v^2)} \cdot [a_h \cdot a_v \cdot u(m,n) + \qquad \text{(A-45)}$$

$$+ a_h \cdot b_v \cdot u(m,n-1) + a_v \cdot b_h \cdot u(m-1,n) + b_h \cdot b_v \cdot u(m-1,n-1)]$$

APPENDIX B

BAYES CRITERION

A. REVIEW OF ONE DIMENSIONAL CRITERION [32]

In this appendix, a threshold setting algorithm will be presented, similar (but not identical) to the Bayes decision algorithm. First, the basic decision model in one dimension will be reviewed.

- Given a measurement sample x -

$$x = s + n$$

s = desired signal

n = noise

- There is an unknown parameter Θ related to the measurement. Example:

Given a pixel containing noise and "possible" signal, as in Fig. B-1(a) -

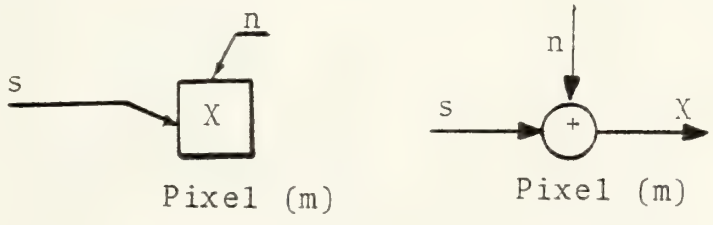

Fig. B-1(a)

The "possible signal that has to be detected in pixel (m) is shown in Fig. B-1(b) -

Signal = $s(m) = \begin{Bmatrix} s_1 \\ \text{or} \\ s_0 \end{Bmatrix}$

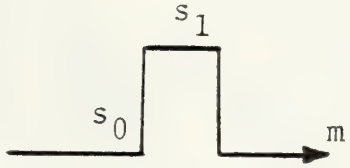

Pixel (m)

Fig. B-1(b)

The resulting signal plus noise samples are shown in Fig. B-1(c) -

Measurement samples = x(m)

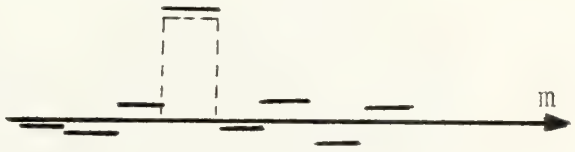

Pixel (m)

Fig. B-1(c)

The unknown parameter ("event") Θ -

$$\Theta = \begin{cases} s_1 = \Theta_1 \\ \quad \text{or} \\ s_0 = \Theta_0 \end{cases}$$

Given the conditional PDF's

$P[x/\Theta_0]$ $P[x/\Theta_1]$

such as shown in Fig. B-2 -

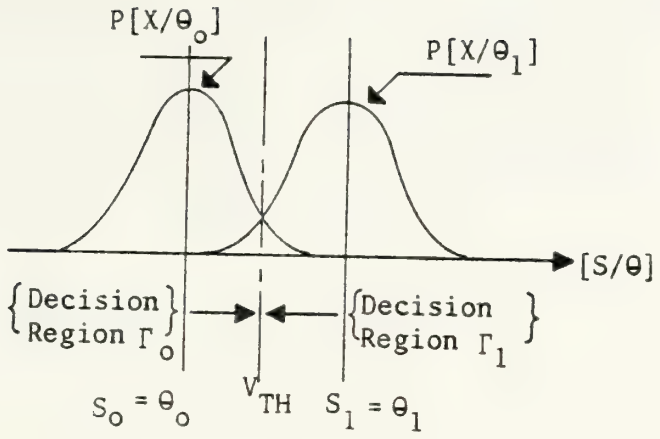

Fig. B-2

In order to determine whether the signal in pixel (m) is s_0 or s_1, the following definitions have to be made:

- Define the following decision errors:

$\alpha \equiv$ Reject when correct

$$\alpha = \int_{\Gamma_1} P[X/\theta_1]dx$$

$\beta \equiv$ Accept when false

$$\beta = \int_{\Gamma_1} P[X/\theta]dx$$

- Define the following costs:

$C_M \triangleq$ Cost of deciding "s_0" when not true

$\triangleq$ Cost of miss

$C_{FA} \triangleq$ Cost of deciding "s_1" when not true

$\triangleq$ Cost of false alarm.

(In the Bayes solution there are two additional cost terms which are not required here.)

- Define the risks:

$$C_M \cdot \beta = R_0$$

$$C_{FA} \cdot \alpha = R_1$$

- Given the probability of "event" $\Theta_0 \Rightarrow g_0$ ("event" of no target)
- Given the probability of "event" $\Theta_1 \Rightarrow g_1 = 1-g_0$ ("event" of target present)
- The total risk can be found by combining all the definitions above and is given by:

$$R = g_0 \cdot R_0 + g_1 \cdot R_1$$

$$R = g_0 \cdot C_M \beta + g_1 \cdot C_{FA} \alpha \qquad \text{(B-1)}$$

$$= g_0 \cdot C_M \cdot \int_{-\infty}^{V_{TH}} P[X|\Theta_0]dx + g_1 C_{FA} \cdot \int_{V_{TH}}^{\infty} P[X|\Theta_1]dx$$

- Minimizing R with respect to V_{TH} ($\frac{dR}{dV_{TH}} = 0$) yields the following threshold equation:

$$g_0 C_M P[V_{TH}/\Theta_0] = g_1 C_{FA} P[V_{TH}/\Theta_1] \qquad \text{(B-2)}$$

When all the parameters are known, we can solve (B-2) for the threshold level. The following two definitions are useful:

$$\frac{P[X|\theta_1]}{P[X|\theta_o]} = \Lambda(X) \qquad \text{(B-3)}$$

$\Lambda(X) \triangleq$ likelihood ratio

$$\frac{g_o C_M}{g_1 C_{FA}} = k \qquad \text{(B-4)}$$

$k \triangleq$ threshold ratio

Example

Given a measurement X that can belong either to X_o or X_1 where -

$X_o = N(0, \sigma^2)$	$X_1 = N(\mu, \sigma^2)$
g_o, $\theta_o = 0$	$g_1 = 1-g_o$; $\theta_1 = \mu$

N is normal PDF.

Decide whether X belongs to X_o or X_1.

- Decision method:

$$P[X_o/0] = \frac{1}{\sqrt{2\pi}\sigma} e^{-X^2/2\sigma^2}$$

$$P[X_1/\mu] = \frac{1}{\sqrt{2\pi}\sigma} e^{-\frac{(X-\mu)^2}{2\sigma^2}}$$

$$k = \frac{g_o C_M}{g_1 C_{FA}}$$

C_M, C_{FA}, g_o, g_1 assumed to be specified.

The likelihood ratio is:

$$\Lambda(X) = \frac{e^{-(X-\mu)^2/2\sigma^2}}{e^{-X^2/2\sigma^2}} \Bigg|_{X=V_{TH}} = K$$

The threshold level is:

$$V_{TH} = \frac{\mu}{2} + \frac{\sigma^2}{\mu} \ln K \qquad (B-5)$$

The decision algorithm:

when $X > V_{TH}$ X belong to X_1

when $X < V_{TH}$ X belong to X_0

c. Extension to Two Dimensional Multivariable Criteria

Following the one dimensional case, we can define the signal to be a vector rather than a scalar.

The signal is $S = [s_1, s_2, \ldots s_I]$.

The noise is $N = [n_1, n_2, \ldots n_I]$.

The measurement is $X = [x_1, x_2, \ldots x_I]$.

$$X^T = S^T + N^T$$

For the multivariable normal PDF, the Bayes solution requires that the vector X will be filtered first by a matched filter and then compared with a given threshold.

- This conclusion can be demonstrated as follows:

The multivariable normal PDF is:

$$P(N) = \frac{1}{(2\pi)^{i/2}|R_{NN}|^{1/2}} \cdot \text{Exp}[-\tfrac{1}{2} N R_{NN}^{-1} N^T] \qquad (B\text{-}6)$$

$P(N) \equiv$ multivariate normal PDF

$R_{NN} \equiv$ covariance matrix of the noise

$\equiv E[N^T N]$ (assuming $E[N] = 0$)

The noise vector can be presented as follows:

$$N^T = (X^T - S^T) = \begin{cases} (X^T - S_1^T) \\ \qquad\qquad \text{or} \\ (X^T - S_0^T) \end{cases}$$

A point target can be expressed as:

$$S_1 = [0,0,\ldots\ S(m,n),0] = S$$

$$S_0 = [0,0,\ldots 0 \ldots 0] = 0$$

The likelihood ratio is given by:

$$\Lambda(X) = \frac{\text{Exp}[-\frac{1}{2}(X - S_1) R_{NN}^{-1} (X - S_1)^T]}{\text{Exp}[-\frac{1}{2}(X - S_0) R_{NN}^{-1} (X - S_0)^T]} = k \qquad (B\text{-}7)$$

Taking the natural log of (B-7) will yield the required conclusion:

$$\ln k = -\tfrac{1}{2}(X - S) R_{NN}^{-1} (X - S)^T + \tfrac{1}{2} X R_{NN} X^T$$

$$= X \cdot R_{NN}^{-1} \cdot S - C_1 \qquad (B\text{-}8)$$

where

$$C_1 = \tfrac{1}{2} S R_{NN}^{-1} S^T$$

$$= \left\{ \begin{matrix} \text{Input} \\ \text{vector} \end{matrix} \right\} * \left\{ \begin{matrix} \text{Matched} \\ \text{filter} \end{matrix} \right\} \begin{matrix} < \ln k + C_1 \Rightarrow S_0 \\ > \ln k + C_1 \Rightarrow S_1 \end{matrix}$$

as described in Fig. B-3.

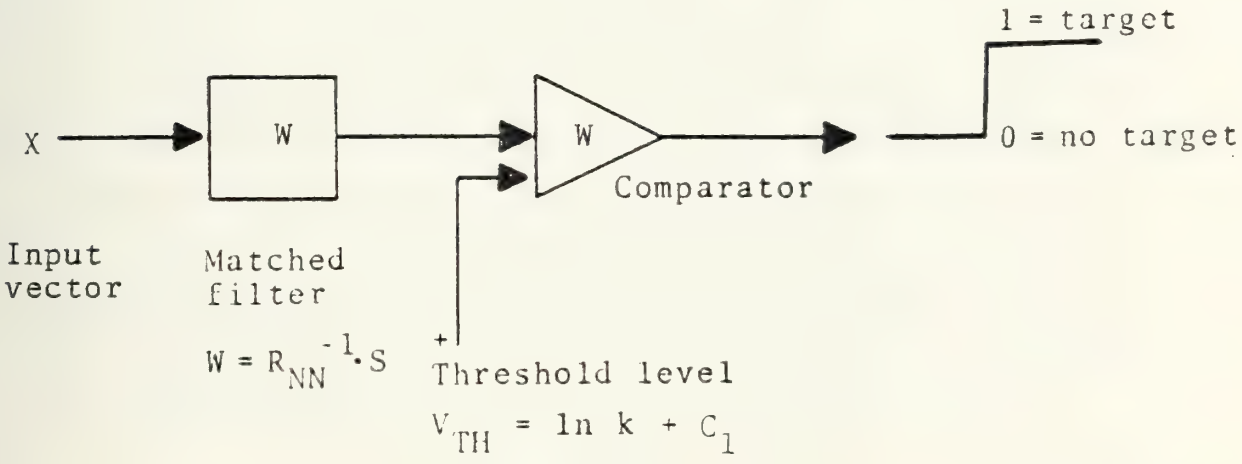

Figure B-3

APPENDIX C

DERIVATION OF ADAPTIVE FILTER ALGORITHM*

A. ALGORITHM DERIVATION

At a given pixel, the output of the filter is

$$y_j = X_j^T W = W^T X_j \tag{C-1}$$

Let us select a desirable reference performance, d_j, which we seek to achieve at the steady state. For example, in the case of point target detection (or estimation), we seek to achieve the best estimate of a point target while suppressing the background clutter noise as much as possible.

Let us define the error ε_j at pixel location j to be

$$\varepsilon_j = d_j - y_j = d_j - W^T X_j \tag{C-2}$$

It is the purpose of the adaptive process to adjust the weighting coefficients of the linear adaptive filter to minimize the mean square error, ε_j.

The derivation of the adaptive algorithm is started by considering the k-th step of adaptive iteration. The mean square error is given by

$$\varepsilon_j^2 = d_j^2 - 2d_j X_j^T W_k + W_k^T X_j X_j^T W_k \tag{C-3}$$

Its statistical expected value is obtained by averaging (C-3) over an ensemble of identical adaptive filters.

---

*This appendix is based on the original derivation of B. Widrow [21,22].

$$E[\varepsilon_j^2]_{w=wk} = E[d_j^2] - 2E[d_j X_j^T]W_k + W_k^T E[X_j \cdot X_j^T]W_k \quad (C\text{-}4)$$

Let us define a vector P as the crosscorrelation between the desired response and the X- vector.

$$P^T = E[d_j X_j^T] = E[d_j X_{1_j}, d_j X_{2_j}, \ldots d_j X_{I_j}] \quad (C\text{-}5)$$

The input correlation matrix R_{xx} is defined in terms of the ensemble average

$$R = R_{xx} \triangleq E[X_j X_j^T] = \begin{bmatrix} (x_{1_j} x_{1_j})(x_{1_j} x_{2_j}) \ldots \\ (x_{2_j} x_{1_j}) \ldots \\ \\ (x_{I_j} x_{I_j}) \end{bmatrix} \quad (C\text{-}6)$$

The mean square error ξ_k can be expressed as

$$\xi_k = E[d_j^2] - 2P^T W_k + W_k^T R \; W_k \quad (C\text{-}7)$$

It is a quadratic function of the coefficients. Adjusting the coefficients involves descending along a concave hyperparaboloidal surface with the objective of reaching its minima. Gradient method is commonly used for this purpose. The gradient ∇_k of the mean square error function at $W = W_k$ is obtained by differentiating (C-7)

$$\nabla_k = \begin{bmatrix} \frac{\partial E[\varepsilon_j^2]}{\partial w_1} \\ \frac{\partial E[\varepsilon_j^2]}{\partial w_2} \\ \frac{\partial E[\varepsilon_j^2]}{\partial w_I} \end{bmatrix}_{w = wk} = -2P + 2R \cdot W_k \quad (C\text{-}8)$$

The optimal filter W*, generally called the Wiener filter, is obtained by setting the gradient to zero and is:

$$\boxed{W^* = R_{xx}^{-1} p} \qquad (C\text{-}9)$$

For some of the subsequent analysis, it is convenient to express the mean square error ξ_k (C-7) and the gradient function (C-8) in another form to be derived as follows:

Substituting (C-9) into (C-7) will yield:

$$\xi_{min} = E[d_j^2] - W^{*T} p \qquad (C\text{-}10)$$

Recombining (C-10) with (C-7) and (C-9) will yield:

$$\xi_k = \xi_{min} + V_k^T R \cdot V_k \qquad (C\text{-}11)$$

where $V_k \triangleq W_k - W^*$, (C-12)

and the gradient becomes

$$\nabla_k = 2RV_k \qquad (C\text{-}13)$$

Since R is the correlation matrix, it is positive definite, and may be expressed in normal form as follows:

$$R = Q \Lambda Q^{-1} \qquad (C\text{-}14)$$

where Λ is a diagonal matrix of the eigenvalues of R. If Q is constructed to be orthonormal, then $Q^{-1} = Q^T$ and then (C-15)

$$R^{-1} = Q \Lambda^{-1} Q^{-1} \qquad (C\text{-}16)$$

and the mean square error may be expressed as:

$$\xi_k = \xi_{min} + V_k^T Q \Lambda Q^T V_k \qquad (C\text{-}17)$$

A new set of coordinates may now be defined as

$$V' = Q^T V = Q^{-1} V \qquad (C\text{-}18)$$

$$V'^T = V^T Q \qquad (C\text{-}19)$$

and

$$\xi_k = \xi_{min} + V_k'^T \Lambda V_k' \qquad (C\text{-}20)$$

This transformation projects V into prime coordinates. Since Λ is diagonal, the prime coordinate must comprise the principal axes of the quadratic mean square error performance surface. The gradient expressed in primed coordinates becomes

$$\nabla_k' = 2\Lambda V_k' \qquad (C\text{-}21)$$

B. THE METHOD OF STEEPEST DESCENT

The objective of the adaptive process is to find a solution to (C-9). It should be noted that (C-9) has exactly the same form as the equation in Chapter III for designing the spatial MMSE filter.

In that chapter, nonadaptive filters were developed. Solution of (C-9) required a two step process by first calculating the statistical properties of the image and of the targets, then followed by a solution of a set of linear equations.

In this chapter, adaptive filters are being developed. An alternative approach is used, based on the steepest descent adaptive method.

The adaption in this method starts with an initial value assigned to the filter $-W_o$. The gradient of the mean square error is measured and the filter coefficients are modified accordingly. This procedure, when repetitively applied, causes the error to reduce successively until the filter approaches the optimal value. This method can be described by the following relation.

$$\boxed{W_{k+1} = W_k + \mu(-\nabla_k)} \qquad (C\text{-}22)$$

where μ is a parameter (loop gain) that controls stability and convergence rate, ∇_k is the value of the gradient at a point on the error surface corresponding to $W = W_k$.

An expression for ∇_k is given by (C-13). Substituting (C-13) into (C-22) will yield

$$W_{k+1} = W_k - 2\mu R V_k \qquad (C\text{-}23)$$

Subtracting W* from both sides of (C-23) will yield

$$V_{k+1} = V_k - 2\mu R V_k = (I - 2\mu R) V_k \qquad (C\text{-}24)$$

Equation (C-24) is a linear homogenous vector difference equation whose solution characterizes the dynamic behavior of the adaptive filter. The solution to (C-24) is:

$$V_k = (I - 2\mu R)^k V_o \qquad (C\text{-}25)$$

It is stable if

$$\lim_{k\to\infty} (I - 2\mu R)^k = 0 \qquad \text{(C-26)}$$

Since $$(I - 2\mu R) = Q(I - 2\mu\Lambda)Q^{-1} \qquad \text{(C-27)}$$

and $$(I - 2\mu R)^k = Q(I - 2\mu\Lambda)^k Q^{-1} \qquad \text{(C-28)}$$

condition (C-26) will be satisfied if

$$\lim_{k\to\infty} (I - 2\mu\Lambda)^k = 0 \qquad \text{(C-29)}$$

Condition (C-29) will be satisfied if

$$|1 - 2\mu\lambda_p| < 1 \qquad \text{(C-30)}$$

for $p = 1, 2 \ldots I$

or $$\frac{1}{\lambda_{max}} > \mu > 0 \qquad \text{(C-31)}$$

where λ_{max} is the largest eigenvalue of R_{xx}.

Equation (C-31) gives the stable range for μ.

It can be seen that in primed coordinates, the coefficient equation given by

$$V'_{k+1} = (I - 2\mu\Lambda)V'_k \qquad \text{(C-32)}$$

with the solution

$$V'_k = (I - 2\mu\Lambda)^k V_o \qquad \text{(C-33)}$$

For the p-th coordinate we may write

$$v'_{pk} = (1 - 2\mu\lambda_p)^k v'_{po} \qquad \text{(C-34)}$$

Eq. (C-34) represents a geometrical progression for v'_{pk} starting from the initial condition v'_{po}.

The geometric ratio of the p coordinate is:

$$r_p = (1 - 2\mu\lambda_p) . \qquad (C-35)$$

Since we prefer to talk usually in terms of exponential progression, we can fit an exponential envelope to (C-33) with time constant, τ_p. If the unit of time is one iteration cycle, then

$$r_p = \exp(^{-1}/\tau_p) = 1 - \frac{1}{\tau_p} + \frac{1}{2!\tau_p^2} - \ldots \qquad (C-36)$$

In practical applications, μ is selected so that $\tau_p >> 1$ and (C-36) can be approximated by the first two terms only. Combining (C-36) and (C-35) gives the formula for the p-th time constant

$$r_p = 1 - 2\mu\lambda_p = 1 - \frac{1}{\tau_p}$$

$$\tau_p = \frac{1}{2\mu\lambda_p} \qquad (C-37)$$

Therefore, we can summarize that the transients in the coefficients of "filter V" are geometric sequences with an approximate time constant, τ_p. In the filter W (not in prime coordinates) the transients will consist of sum of geometric sequences, with the total number of time constants typically equal to the number of coefficients.

Similarly, while the coefficients are varying, the mean square error (MSE) varies as well. Substitution of (C-33) into (C-20) will yield the "learning curve" - the MSE as a function of k:

$$\xi_k = \xi_{min} + V_o'^T (I - 2\mu\Lambda)^{2k} \Lambda \cdot V_o' \qquad (C\text{-}38)$$

As long as condition (C-34) and (C-31) are met, the adaptive process will converge on the minimum point of the MSE surface.

$$\lim_{k\to\infty} \xi_k = \xi_{min} \qquad (C\text{-}39)$$

Here again, the relaxation process is a sum of geometric sequences where the p-th mode has a geometric ratio of $(1 - 2\mu\lambda_p)^2$ resulting in a time constant

$$\tau_{p_{mse}} = \frac{1}{4\mu\lambda_p} = \frac{\tau_p}{2} \qquad (C\text{-}42)$$

To accomplish the coefficient's adaptation, we have to measure or estimate the gradient at each iteration. Reference [21] suggested two methods to obtain the gradient estimate. The first method uses differentiation and requires that finite perturbations be made on the filter coefficients. The second, so-called LMS method, obtains gradient estimates directly and without perturbing the nominal coefficients adjustment.

In this work, the second method was selected, based on two reasons.

1. Practical implementation and utilization of this method is simpler, compared to the other alternative.

2. Reference [21] demonstrated the superiority of the LMS algorithm with regard to convergence time and mean square error, compared to the other candidate.

C. THE LMS ADAPTATION ALGORITHM

The LMS algorithm is an implementation of the steepest descent method that employs an efficient gradient estimation technique. This method was found applicable to the two dimensional filtering configuration presented earlier in Fig. 7-3.

1. Gradient Estimation, Convergence and Time Constants

The error, ε_j, of a filter such as shown in Fig. 7-2 is given by (C-2). A gradient estimate may be obtained by squaring the single value of ε_j and differentiating it as if it were the mean square error:

$$\hat{\nabla}_j = \begin{bmatrix} \frac{\partial \varepsilon_j^2}{\partial w_1} \\ \vdots \\ \frac{\partial \varepsilon_j^2}{\partial w_I} \end{bmatrix} = 2\varepsilon_j \begin{bmatrix} \frac{\partial \varepsilon_j}{\partial w_1} \\ \vdots \\ \frac{\partial \varepsilon_j}{\partial w_I} \end{bmatrix} = -2\varepsilon_j X_j \qquad \text{(C-41)}$$

since $\varepsilon_j = d_j - W^T X_j$ and $\frac{\partial \varepsilon_j}{\partial w} = -X_j$.

Substituting (C-41) into (C-42) will yield the LMS algorithm

$$\boxed{W_{j+1} = W_j + 2\mu\varepsilon_j X_j} \qquad \text{(C-42)}$$

where the index k is replaced by j since we perform an adaptation step for each new input vector, i.e., a new set of data samples.

The gradient estimate of (C-41) may be implemented in a practical system without further squaring or averaging and is simple and elegant. All components of the gradient vector are obtained from one input data set X. Since the estimate is obtained without averaging, it contains a large component of noise. The noise, however, is averaged and attenuated by the adaptive process, which acts as a low pass filter in this respect.

It is important to note also that for a fixed value of W, the estimate is unbiased, which can be shown as follows:

$$E[\hat{\nabla}_j] = -2E[\varepsilon_j X_j] = -2E[d_j X_j - X_j X_j^T W] \qquad (C\text{-}43)$$

From (C-8), this expression can be rewritten as

$$E[\hat{\nabla}_j] = -2(P - RW) = \nabla \qquad (C\text{-}44)$$

recalling that ∇ is approaching zero at steady state.

2. Convergence of the Mean of Filter Coefficients

Let us now show that the mean value of the filter coefficient instead converges to a steady state when the LMS algorithm is implemented. Taking the expected value of (C-42), we obtain the following:

$$E[W_{j+1}] = E[W_j] - 2\mu E\{X_j[d_j - X_j^T W_j]\} =$$

$$= [I + 2\mu R] \cdot E[W_j] - 2\mu P \qquad (C\text{-}45)$$

In obtaining (C-45), we assumed that W and X are uncorrelated. It will be shown later that proper selection

of the adaptation loop gain μ will cause the filter coefficients to vary very slowly compared with the value of the noise (X) correlation coefficients.

$$E[x^T w] \simeq E[x^T] \cdot W$$

where W is considered almost as a constant relative to $E[x^T]$. Under these assumptions, $E[x^T \cdot w] \simeq E[x^T] \cdot E[w]$, i.e., X and W can be considered uncorrelated.

Referring back to equation (C-45), with an initial filter coefficient, W_o, j + 1 iterations of equation (C-45) yield

$$E[w_{j+1}] = [I + 2\mu R_{xx}]^{j+1} W_o - 2\mu \sum_{i=o}^{j} [I + 2\mu \cdot R_{xx}]^i P \qquad (C\text{-}46)$$

Eq. (C-46) may be put in diagonal form by using the normal expansion of R_{xx}, that is,

$$R_{xx} = Q^{-1} \Lambda Q$$

The eigenvalues are all positive, since R_{xx} is positive definite. Equation (C-46) may now be expressed as

$$E[w_{j+1}] = [I + 2\mu Q^{-1} \Lambda Q]^{j+1} W_o - 2\mu \sum_{i=o}^{j} [I + 2 Q^{-1} \Lambda Q]^i P =$$

$$= Q^{-1} [I + 2\mu\Lambda]^{j+1} Q \cdot W_o - 2\mu Q^{-1} \sum_{i=o}^{j} [I + 2\mu \Lambda]^i Q \cdot P \qquad (C\text{-}47)$$

Consider the diagonal matrix $[I + 2\mu \Lambda]$. As long as its diagonal terms are all of magnitude less than unity

$$\lim_{j \to \infty} [I + 2\mu\Lambda]^{j+1} \to 0$$

and the first term of (C-47) vanishes as $j \to \infty$.

The second term in (C-47) converges to a non-zero limit. The summation factor -

$$\sum_{i=o}^{j} [I + 2\mu\Lambda]^i$$

becomes $$\lim_{j\to\infty} \sum_{i=o}^{j} [I + 2\mu\Lambda]^i = - \frac{1}{2\mu} \Lambda^{-1}$$

where the formula for the sum of the geometric series has been used, that is:

$$\sum_{i=o}^{\infty} (1 + 2\mu\lambda_p)^i = \frac{1}{1-(1+2\mu\lambda_p)} = \frac{-1}{2\mu\lambda_p}$$

Thus, on the limit, equation (7-49) becomes

$$\lim_{j\to\infty} E[w_{j+1}] = Q^{-1}\Lambda Q \cdot P = R_{xx} \cdot P$$

Comparison of this result with (C-9) shows that as the number of iterations increases without limit, the expected value of the filter coefficient converges to the coefficients of the Wiener filter.

The convergence is assured if, and only if, μ is set within certain bounds. Since the diagonal terms of $[I + 2\mu\Lambda]$ must all have magnitude less than unity, and since all eigenvalues in Λ are positive, the bounds, on μ, are given by

$$|1 + 2\mu\lambda_{max}| < 1$$

$$\frac{-1}{\lambda_{max}} < \mu < 0$$

where λmax is the maximum eigenvalue of R_{xx}. This convergence condition can be related to the total input signal power as follows:

$$\lambda \max < \text{trace } R_{xx} \tag{C-48}$$

$$\text{trace } [R_{xx}] \triangleq E[X_j^T X_j] = \sum_{i=1}^{I} E[x_i^2] \triangleq \text{total input power.}$$

Therefore, the bounds for satisfactory convergence are

$$\frac{-1}{\sum_{i=1}^{I} E[x_i^2]} < \mu < 0 .$$

In practical applications, when precise adaptation is required, μ is usually selected such that

$$\boxed{\frac{1}{\sum_{i=1}^{I} E[x_i^2]} >> \mu} \tag{C-49}$$

3. The Noise of Gradient Estimation

Let it be assumed that the adaptive process, using a small loop gain μ, has converged to a steady state near the minimum of the MSE (ξ). The gradient estimation noise of the LMS algorithm at the minimum, where the true gradient is zero, is the gradient estimate itself:

$$N_j = \hat{\nabla}_j = -2\varepsilon_j X_j \tag{C-50}$$

since $\hat{\nabla}_j = \nabla_j + N_j$

where ∇_j = the true gradient

N_j = gradient noise vector.

The covariance of this noise is given by

$$\text{cov}[N_j] = E[N_j N_j^T] = 4E[\varepsilon_j^2 x_j x_j^T] \qquad \text{(C-51)}$$

It is known from Wiener filter theory that when $W_j = W^*$ [the optimal filter] the error ε_j is uncorrelated with the input vector x_j. If one assumes that ε_j and x_j are Gaussian, they will be independent, as well, at the minimum. Under these conditions (C-51) becomes

$$\text{cov}[N_j] = 4E[\varepsilon_j^2] \cdot E[X_j X_j^T] = 4\xi_{min} R_{xx} \qquad \text{(C-52)}$$

In primed coordinates, the covariance is

$$\text{cov}[N'_j] = Q^{-1} \text{cov}[N_j] Q = 4\xi_{min} \Lambda \qquad \text{(C-53)}$$

4. Noise in Filter Coefficients

Adaptation based on noisy gradient estimates results in noise in the filter coefficients. The method of steepest descent with ideal gradients is represented by (C-29). With estimated gradients, this equation may be rewritten as:

$$V_{j+1} = V_j + u(-\hat{\nabla}_j) = V_j + (-\hat{\nabla}_j - N_j) \qquad \text{(C-54)}$$

where the estimated gradient is $\hat{\nabla}_j \triangleq \nabla_j + N_j$.

Substituting (C-13) and combining terms yields

$$V_{j+1} = (I - 2\mu R_{xx}) V_j - \mu N_j \qquad \text{(C-55)}$$

This is a first order difference equation with a stochastic driving function of $-\mu N_j$. Projection into primed coordinates

may be accomplished by premultiplying both sides of (C-55) by Q^{-1}.

$$V'_{j+1} = (1 - 2\mu\Lambda)V'_j - \mu N'_j \qquad \text{(C-56)}$$

In steady state, after initial adaptive transients have died out, V_j' undergoes a stationary random process in response to the stationary driving function, $-\mu N_j'$. Since there is no cross coupling between terms and the components of N_j' are mutually uncorrelated, the components of V_j' will also be mutually uncorrelated, and the covariance matrix of N'_j will be diagonal. To find the matrix, one first multiplies both sides of (C-56) by their transposes.

$$V'_{j+1} V_{j+1}^T = (I - 2\mu\Lambda)V_j'V_j'^T(I - 2\mu\Lambda) + \mu^2 N'_j N_j'^T - \mu(I - 2\mu\Lambda)V_j'N'^T_j - \mu N_j'V_j'^T(I - 2\mu\Lambda) \qquad \text{(C-57)}$$

Taking expected values of both sides yields

$$\text{cov}[V'_j] = (I - 2\mu\Lambda)\text{cov}[V_j'](I - 2\mu\Lambda) + \mu^2\text{cov}[N_j'] \qquad \text{(C-58)}$$

(Note that V_j' N_j' are uncorrelated since V_j is affected only by gradient noise from previous adaptive cycles.)

Combining terms further yields:

$$\text{cov}[V_j'] = \mu^2(4\mu\Lambda - 4\mu^2\Lambda^2)^{-1}\text{cov}[N'_j] \qquad \text{(C-59)}$$

In practical applications, when μ is small,

$$\mu\Lambda << I$$

Neglecting the squared terms in (C-59)

$$\text{cov}[V_j'] = \frac{\mu}{4}\Lambda^{-1}\text{cov}[N_j']$$

Combining (C-59) with (C-52), one may write

$$\text{cov}[V_j'] = \frac{\mu}{4}\Lambda^{-1}(4\xi_{min}\Lambda) = \mu\xi_{min} I \qquad \text{(C-60)}$$

The covariance of V_j can be obtained from (C-60) by using (C-16) and (C-18).

$$\text{cov}[V_j] = E[QV_j' V_j'^T Q^{-1}] = Q\cdot\mu\xi_{min} I Q^{-1} = \mu\xi_{min}\cdot I \qquad \text{(C-61)}$$

5. Misadjustment

Without noise in the weighting vector, adaptation by the method of steepest descent would converge to a steady-state solution at the minimum point of the MSE surface. The MSE and the minimum will be ξ_{min}. Noise on the weighting vector, however, tends to cause the steady-state solution to vary randomly about the minimum. The result is an excess mean square error, a mean square that is greater than ξ_{min}.

An expression for mean square error in terms of V' is given by (C-20), where the excess mean square error is $V_j'^T \Lambda V_j'$, The average excess mean square error is

$$E[V_j'^T \Lambda V_j'] = \sum_{p=1}^{I} \lambda_p E[v_{p_j}'^2] = \mu\xi_{min} \sum_{p=1}^{I} \lambda p$$

where, according to (C-61),

$$E[(v'_{p_j})^2] = \mu\xi_{min} \text{ for all } P$$

A useful parameter in the design of adaptive processes is the misadjustment M, which is defined as the average excess mean square error divided by the minimum mean square error.

$$M \triangleq \frac{E[V'^T_j \Lambda V_j]}{\xi_{min}} \tag{C-62}$$

The misadjustment is a dimensionless measure of the difference between adaptive performance and optimal Wiener performance as a result of gradient noise. The misadjustment is thus given by

$$\boxed{M = \mu \text{ tr } R_{xx}} \tag{C-63}$$

This useful formula may be re-expressed in a manner that allows one to perceive the relationship between misadjustment and rate of adaptation. According to (7-42) one may write

$$\mu \text{ tr } R_{xx} = \frac{1}{4} \sum_{p=1}^{I} \frac{1}{\tau_{p_{mse}}} = \frac{I}{4} \left(\frac{1}{\tau_{p_{mse}}}\right)_{av} \tag{C-64}$$

The misadjustment may thus be written

$$M = \frac{I}{4} \left(\frac{1}{\tau_{p_{mse}}}\right)_{av} \tag{C-65}$$

where I is the number of filter coefficients and $\tau_{p_{mse}}$ is the MSE time constant, related to the learning curve. When the eigenvalues are equal,

$$M = \frac{I}{4} \left(\frac{1}{\tau_{mse}}\right) \tag{C-66}$$

Since trace R_{XX} is the total power of the input vector X, which is generally known, one can use (C-63) in choosing a value of that will produce a desired value of M. Combining (C-66) with (C-63) will yield a general formula for the time constant of the learning curve with equal eigenvalues.

$$\tau_{mse} = \frac{I}{4\mu \text{ tr } R_{XX}} \qquad \text{(C-67)}$$

This formula is also a good approximation in many cases when the eigenvalues of R_{XX} are unequal.

BIBLIOGRAPHY

1. Barbe, D. "Advanced Infrared Focal Plane Concepts." Electro-Optical Systems Design, Vol. 9, p. 50-58, April 1977.

2. Barbe, D. "Time Delayed Integration Image Sensors." Solid State Imaging Systems, Jaspers, P.G., Vandewiele, F., White, M., editors. NATO Advanced Study, E-Applied Science No. 16. Nordhoff-Layden, Belguim, 1976, p. 659-671.

3. Barbe, D. "Solid State Infrared Imaging." Solid State Imaging Systems, Jaspers, P.G., Vandewwiele, F., White, M., editors. NATO Advanced Study, E-Applied Science No. 16. Nordhoff-Layden, Belguim, 1976, p. 673-683.

4. Nummendal, K. "CCD Read Out of HgCdTe Detectors." Proceedings of 1974 National Infrared Information Symposium (IRIS).

5. McIver, G. TRW Systems, Redondo Beach, California. Private communication.

6. French, D. "Use of CCD in IR Sensor Systems." Proceedings of SPIE Symposium, Vol. 62.

7. Oppenheim, A.V., editor. Application of Digital Signal Processing. Prentice-Hall, 1978.

8. Skolnik, M. Introduction to Radar Systems. McGraw-Hill, 1962.

9. Parenti, R.R. and Bus, H.M. "Analytic Technique for Evaluating Autonomous Acquisition Methods." Proceedings of 26th National Infrared Information Symposium, May 1978.

10. Unpublished Progress Reports by Rockwell International, Hughes Aircraft Company and Grumman for DARPA HALO Project from Spring 1977.

11. Unpublished Progress Reports by Rockwell International for DARPA HALO Project, August 1978.

12. Barry, P.E., Gran, R. and Waters, C.R. "State Variable Techniques in Optimal Image Processing." Proceedings of 10th Asilomar Conference on Circuits, Systems and Computers, p. 169-174, 1976.

13. Shachar, M. and Titus, H.A. "Optimal Recursive Estimation of Two Dimensional Random Fields." Proceedings of 10th Asilomar Conference on Circuits, Systems and Computers, 1976, p. 598-609.

14. Bar-Yehoshua, D. Two Dimensional Nonrecursive Filter for Estimation and Detection of Target. Naval Postgraduate School thesis, June 1977.

15. Liang, A.C. "A Technique for Infrared Background Suppression." Proceedings of 22nd SPIE Symposium on "Modern Utilization of Infrared Technology," 1975, p. 1-8.

16. Schwartz, M. and Shaw, L. Signal Processing: Discrete Spectral Analysis Detection and Estimation. McGraw-Hill, 1975, p. 277-286 and 251-260.

17. Pratt, W.K. Digital Image Restoration, Chapter 19, Sections 2,3. Prentice Hall, 1978.

18. Mitra, S.K. and Ekstrom, M.R., editors. Two Dimensional Digital Signal Processing. Dowdon Hutchinson & Ross, Inc., 1978, p. 174-177.

19. Rosenfeld, A. and Kak, A.C. Digital Picture Processing. Academic Press, 1976, p. 216-222 and 238-249.

20. Widrow, B. et al. "Adaptive Noise Cancelling: Principles and Applications." Proceedings, IEEE, December 1975.

21. Widrow, B. and McCool, J. "A Comparison of Adaptive Algorithms Based on the Methods of Steepest Descent and Random Search." IEEE Transaction on Antennas and Propagation, Vol. AP-24, No. 5, September 1976.

22. Widrow, B. "Adaptive Filters." Aspects of Network and System Theory, R.E. Kalman and N. Declaris, editors. New York: Holt, Reinhart and Winston, 1970.

23. Helstrom, C.W. "Image Restoration by the Method of Least Squares," J. Opt. Soc. Amer., Vol. 57(3), p. 297-303, 1967.

24. Pratt, W.K. "Generalized Wiener Filtering Computation Techniques," IEEE Trans. Computers, Vol. C-21(7), p. 636-641, 1972.

25. Ekstrom, M.P. and Algazi, V.R. "Optimum Design of Two Dimensional Nonrecursive Digital Filters." Proceedings of IV Asilomar Conference on Circuits and Systems, p. 707-712, 1970.

26. Andrew, H.C. and Hunt, B.R. "Digital Image Restoration, Prentice-Hall, p. 147-151, 1977.

27. Turin, G.L. "An Introduction to Digital Matched Filters." Proceedings of the IEEE, Vol. 64, No. 7, p. 1092-1112, July 1976.

28. Papoulis, A. Signal Analysis, McGraw-Hill, p. 325-329, 1977.

29. Applebaum, S. "Adaptive Arrays," IEEE Transactions on Antennas and Propagation, Vol. AP-24, No. 5, September 1976.

30. Hilmers, D.C. Spatial-Temporal Filter for Clutter Suppression and Target Detection of Real World Infrared Images, Engineer Thesis, Naval Postgraduate School, December 1978.

31. Van Trees, H.L. Detection, Estimation and Modulation Theory, John Wiley and Sons, p. 23-39, 1968.

32. Van Trees, H.L. Detection, Estimation and Modulation Theory, John Wiley and Sons, p. 40-65, 1968.

33. Melsa, J.L. and Cohn D.L. Decision and Estimation Theory, McGraw-Hill, 1978.

34. Soon Ju, Ko. An Adaptive Recursive Filter. Naval Postgraduate School thesis, December 1977.

35. Shachar, M. Modeling and Recursive Estimation of Two Dimensional Random Fields and Applications to Target Detection, Engineer Thesis, Naval Postgraduate School, June 1977.

36. Habibi, G.A. "Two Dimensional Bayesian Estimation of Images," Proceedings of IEEE, Vol. 60, No. 7, p. 878-883, July 1972.

INITIAL DISTRIBUTION LIST

		No. Copies
1.	Defense Documentation Center Cameron Station Alexandria, Virginia 22314	2
2.	Library, Code 0142 Naval Postgraduate School Monterey, California 93940	2
3.	Department Chairman, Code 62 Department of Electrical Engineering Naval Postgraduate School Monterey, California 93490	1
4.	Professor T. F. Tao, Code 62Tv Department of Electrical Engineering Naval Postgraduate School Monterey, California 93940	10
5.	Professor D. E. Kirk, Code 62 Department of Electrical Engineering Naval Postgraduate School Monterey, California 93940	1
6.	Professor E. C. Crittenden, Jr., Code 61 Ct Department of Physics and Chemistry Naval Postgraduate School Monterey, California 93940	1
7.	Professor U. Kodres, Code 52 Kr Department of Computer Science Naval Postgraduate School Monterey, California 93940	1
8.	Professor H. Titus, Code 62 Ts Department of Electrical Engineering Naval Postgraduate School Monterey, California 93940	1
9.	Professor S. R. Parker, Code 62 Px Department of Electrical Engineering Naval Postgraduate School Monterey, California 93940	1
10.	LCDR B. Even-or Israeli Navy, c/o Embassy of Israel 1621 N.W. 22nd Street Washington, D.C. 20008	6

11. Lt. Zach Shlomo 1
Israeli Navy, c/o Embassy of Israel
1621 N.W. 22nd Street
Washington, D.C. 20008

12. Lt. Amir Haim 1
SMC 2641
Naval Postgraduate School
Monterey, California 93940

13. CDR Ehud Ben-Dor 1
c/o Embassy of Israel
1621 N.W. 22nd Street
Washington, D.C. 20008

14. LCDR Uzi Ben-Yakov 1
SMC 1664
Naval Postgraduate School
Monterey, California 93940

15. LCDR Shmuel Shelef 1
SMC 1165
Naval Postgraduate School
Monterey, California 93940

Thesis 184624
E77965 Even-or
c.1 Statistical nonrecursive spatial-temporal focal plane processing for background clutter suppression and target detection.

thesE77965
Statistical nonrecursive spatial-tempora
3 2768 000 98487 6
DUDLEY KNOX LIBRARY